A navigation strategy for mobile robots in a manufacturing environment.

Ko, Wen-Shen

A NAVIGATION STRATEGY FOR MOBILE ROBOTS IN A MANUFACTURING ENVIRONMENT

A thesis for the degree of

Doctor of Philosophy

in the

Faculty of Engineering

University of London

by

Wen-Shen Ko

Department of Mechanical Engineering

King's College London

University of London

February 1996

ABSTRACT

The aim of the project is to develop a feasible navigation strategy for a mobile robot working in a manufacturing factory environment. General-purpose and off-the-shelf systems are used as hardware elements, a mobile robot, an articulated robot, ultrasonic sensors, a vision camera and a personal computer, integrated to construct a working system, capable of performing the principal functions of material transportation. A triangulation based navigation strategy is proposed, which at the planning stage generates a collision-free navigational route, and at the executing stage, system behaviours are co-ordinated to perform the planned navigational route.

The planning stage is sequentially divided into a global journey step and a local route step. The global journey step carries out operations for spatial reasoning and graph mapping. Within the free space is constructed a triangulation graph. A node of the triangulation graph represents a triangular partition of the free space, and an edge represents the topological connectivity of two triangular partitions (nodes). The triangulation graph is searched to produce a solution graph path. This path is a space channel bounded by physical objects, and represents a global journey (trend) for a mobile robot towards the given destination. A variety of navigational routes, for the mobile robot to follow, are included in the solution space channel. The final navigational route is locally determined according to criterion, such as cost requirement and unexpected obstruction.

The local route planning step only works on the space channel produced by the global journey planning step. The space channel is a sub-set of the overall free space of the mobile robot, and only searching efforts relevant to the final navigational route need to be carried out. A navigational route thus planned is always within the free space of the mobile robot, and, therefore, collision free.

The executing stage of the navigation strategy is to manage operations of motion co-ordinating and sensing. Since the final navigational route to be followed is designed to

keep a clearance distance from obstacles and to be parallel to the environment boundary, ultrasonic sensors are integrated to generate reliable observations for monitoring the navigation. Implementations of the planned navigational route in computational graphical simulation environments, and experimental simulation systems, including using the manipulative robot, are presented.

It is shown that the developed triangulation based navigation strategy provides a safe, flexible and efficient solution for mobile robots carrying out material transportation in a manufacturing environment. Given more sophisticated sensors and means for handling unexpectations, further implementations, towards completely autonomous performance, can be accomplished.

ACKNOWLEDGEMENTS

I am grateful to many people who have helped me in numerous ways during my studying at King's College London.

First, I wish to express my sincere thanks and gratitude to Professor S. W. E. Earles, my supervisor, for guidance and constructive advise throughout the research and the preparation of this thesis. To Dr. L. D. Seneviratne, my joint supervisor, for valuable inspiration during the project and for introducing me to robotics research conferences. To Ms. S.-L. Choong, the departmental secretary, and Mr. M. Harrington, the departmental superintendent, for their help on administrative matters. To Dr. K. Jiang, Dr. U. Sezgin, Dr. H. Yu, Mr. A. Ngmoh, Mr. Y. Zhu and Mr. A. Macleod, my research colleagues, for their useful discussions and enjoyable conversations with me. And to SUNUP Co. Ltd. and HOTAI Co. Ltd. for their financial support.

I also want to thank my host family, Mr. and Mrs. Stoner in Crowborough, for always offering me a warm place in the cold weather. To my friends, Dr. Yao-Nan Shieh, Dr. Wen-Chi Tsai, Mr. and Mrs. Chien-Liang Yeh, Mr. and Mrs. Hsi-Yao Wang, Ms. Yu-Shan Chang, Mr. and Mrs. Ying-Cheng Wu, Ms. I-Chien Wu, Mr. Kuan-Chu Chen, Dr. Ming-Der Su, Ms. Mei-Hsing Wang, Ms. Chi-Lin Yeh, and many others, for their company and sharing experiences with me.

Finally, this thesis is dedicated to my parents and family, many thanks for their constant support and encouragement during the five and half years of study. And to a peaceful Britain and a fearless Taiwan.

CONTENTS

LIST OF FIGURES

LIST OF TABLES

LIST OF PLATES

CHAPTER ONE

INTRODUCTION

The world has become smaller with the result of intensive and free trading activities across continents. Competing for the global market is a world-wide challenge worthy for all manufacturers. Declining productivity has been diagnosed by many as one of the problems of lacking world competitiveness. According to [1], productivity may be defined as output per worker-hour, and is usually expressed as units manufactured per worker-hour invested in the manufacturing industry. To meet the steady increase in labour and over-head costs [2][3], the introduction of automation provides a prospective direction to improving manufacturing productivity. Through the efficient and innovative investment in automation, productivity can be raised.

1.1. MANUFACTURING ENVIRONMENT

Automation in manufacturing environments, factory automation, is defined as "the automatically controlled manufacturing operation of an apparatus, process or system in the factory by mechanical or electronic devices that take the place of human observation, effort and decision" [4]. Considerations for improving productivity by factory automation

are focused on reducing costs per unit of product and increasing quality by using automated and computerised machines and tools.

1.1.1. Factory Automation

At the early stage of factory automation, hard automation [5][6][7] was the central issue, and factory mechanisation and machinery automation to acquire fixed, special purposed automation were discussed. Higher output rate per shift can be achieved through full scale widespread use of industrial robots and automatic machines. However, hard automation is confined to the philosophy of conventional mass production methods, which perform a series of tasks on a very narrow range of products by dedicated machinery and particular plant construction. It may necessitate holding large inventories of raw materials and finished parts when production runs are extended. High volumes are required in order to be cost-effective.

Nowadays the typical life cycle of products is generally shorter than before. Hard automation can well outlive the product for which it was developed, and equally the dedicated machinery can become obsolete early in the product life. In order to quickly respond to diversified market demands, the production process and manufacturing environment have to be adjusted, even re-configured, often and rapidly. Flexible automation [5][6][7] is thus introduced. Increasingly in the future there are likely to be more flexible manufacturing systems (FMS) deployed, capable of handling different products in a flexible order within the same manufacturing environment.

1.1.2. Flexible Manufacturing System

A FMS may be described as programming and reprogramming a manufacturing system in its broadest scene, dealing with high level distributed data processing and automated material flow, using highly flexible, computer controlled material and information processors within an integrated, multi-layered feedback control architecture [4][5][8].

Usually, a FMS is a co-ordinated arrangement of manufacturing cells, or work stations, interconnected by a material transport system and controlled by a master computer.

A manufacturing cell [4] is a stand alone functional unit, designed using group technology [9], within a factory in which computers, robots, numerical control machines, material transport systems and auxiliary devices work together in a production group and perform a set of integrated product-oriented operations. It is the place where manufacturing tasks are performed. There is usually a communications network associated with the machines contained so that they can exchange data and inform other machines of their current states. A typical work station is shown in Plate 1.1.

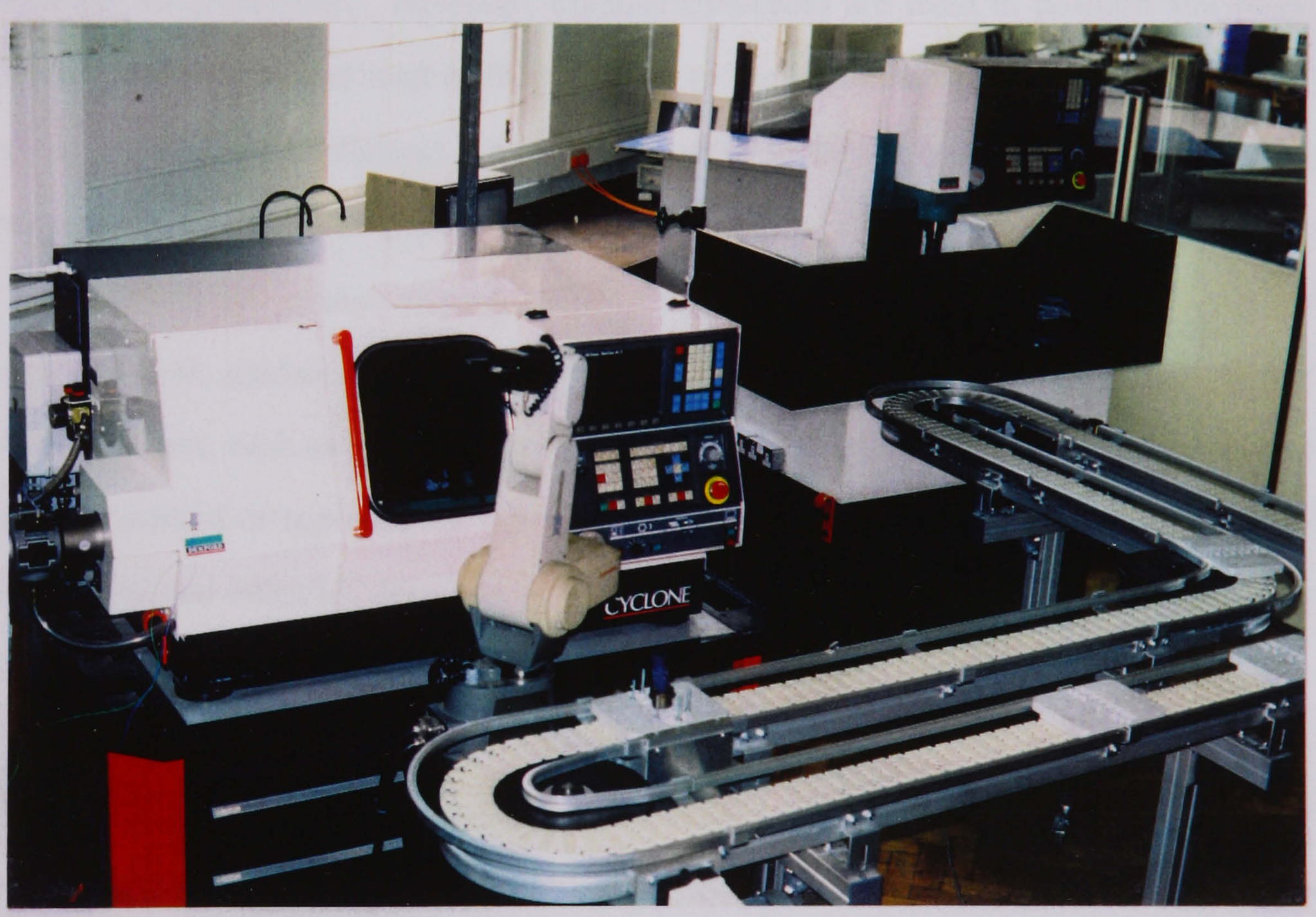

Plate 1.1. A typical work station. King's College Robotics Laboratory.

The main advantage of flexible manufacturing systems is their flexibility. A FMS normally allows a variety of items to be manufactured in the same plant by collaborating material flow control with the minimum re-configuration of its manufacturing cells.

Through planning an efficient processing sequence and corresponding material flow according to customer orders, low volume, versatile manufacturing can be achieved. As a result, material transport systems, which link manufacturing cells and are responsible for the sequence and flow of material being processed, are crucial to flexible automation. Conveyors and automated guided vehicles are two automated material transport systems at present.

1.1.3. Material Transportation

The conveyor method [10], also shown in Plate 1.1, provides a high and steady flow of materials for production. However, because conveyors are fixed in position and route, they are obstructive and tend to block access to the connected manufacturing cells, and can not be easily re-configured. In addition, conveyors normally may only be used for the machines to which they are connected, and consume space.

An automated guided vehicle, AGV, is, in general, a driverless wheeled vehicle equipped with guidance equipment for automatically following a network of explicit physical routes, such as electrical cables laid beneath the floor and optically reflective lines painted, marked or taped on the floor [10][11]. Using AGVs can overcome some of the obstructive and inflexible drawbacks of conveyors. However, AGVs are restricted to a network of explicit routes, which may easily wear away or be covered over.

Automation of material transportation by means of conveyors and AGVs is most suitable for the regular movement of large quantities of materials along fixed paths. The maximum advantage from these systems can only be derived when the goods handled are in standardised units. Also, conveyors and automated guided vehicles are restrictive and inflexible in relation to route layouts. Therefore, the use of flexible material transport systems to cope with diversifying distribution and product range in market change is required. Flexible material transport systems with reliable and flexible guidance capabilities, which allow automated operations without explicit physical routes, and can be

easily set up for varied production schemes, have to be developed for manufacturing environments.

Potential candidates for flexible material transportation are free ranging automated guided vehicles [12][13], able to navigate freely without explicit physical route guidance, and mobile robot systems [11][14][15] which are, in general, combinations of manipulators and free ranging automated guided vehicles. Automated guided vehicles and free ranging automated guided vehicle are both included in the context of mobile robot systems.

1.2. MOBILE ROBOT SYSTEMS

Mobile robotics has attracted the attention of researchers from many engineering areas, and has become a fast growing field because of the potential applications.

1.2.1. Definition

The British Robot Association, in a 1985 report, defined an industrial robot as a re-programmable device designed to both manipulate and transport parts, tools or specialised manufacturing implements through variable programmed motions for the performance of specific manufacturing tasks [14]. At the IFR (International Federation of Robotics) meeting held in October 1990 during the 21st IRIS (International Symposium on Industrial Robot) period, mobile robots were included as a type of industrial robot with locomotive function in place of manipulation. Although an universal agreement on what should be contained in a mobile robot has not yet been reached, "an automatically controlled, re-programmable, multipurpose, locomotive machine" [16], has been widely recognised as the basic content of mobile robots. The term 'mobile robot system' is normally used to describe a system combining a mobile robot with other functional mechanisms, such as a manipulative robot and sensor systems.

To independently and autonomously complete a material transportation task, a mobile robot system basically needs four functions; mobility, manipulation, perception and control. Hardware modules to carry out these functions are mobile robots, manipulative robots, sensors and computers respectively. Further, as in the nervous system transmitting signals inside a human body, and activating reflex and cognitive behaviours, a function to harmonise the four modules is necessary. Communications channels, together with control and supervision software, construct the required function.

1.2.2. General Survey

Since the first reported mobile robot system, Shakey [18], was introduced, researchers in related fields have continuously contributed efforts to the study. A general survey on existing and developing technologies for mobile robot systems is conducted.

(a) Mobility. The locomotive mechanism of a mobile robot system has three functional features; supporting, driving, and steering. Six types of mobility are being used, or under development:

(a.1) Gantry mechanism. The first step in mobility was the gantry robot introduced by Olivetti in 1975 [14, P.190]. In a gantry robot, such as Kawasaki Unimate and Cincinnati Milacron [17, P.20-21], the base moves along rails, allowing the working envelope of the manipulative robot to be expanded.

(a.2) Wheeled mechanism. A wheeled mobile robot is the primary type in use since it applies the simplest method of mobility. Besides, it performs well and has good traction if the terrain is smooth and level, or has only a limited slope. Three basic ways of steering a wheeled mechanism are:

(a.2.1) all-wheel steering, such as KRA by Cybermation [14, P.194] and B12 developed in Massachusetts Institute of Technology and produced by Real World Interface [19], allowing the mobile robot to rotate about its central axis and move omni-directionally,

(a.2.2) differential steering, such as FRAGV developed in Imperial College [12][13] and Shakey by Stanford University [18], using two side wheels revolving differently for steering, and also allowing rotation on a spot,

(a.2.3) car-like steering, such as Seeing-eye mel dog from MITI Ibaraki [17, P.213], applying the method used by cars and bicycles, and turning around in a confined space using back-and-forth manoeuvring.

(a.3) Tracked mechanism. A tracked mobile robot, such as Explosive Ordinance Disposal EOD robot from OAO Corporation [17, P.181], is well-suited for outdoor, off-road applications, since its mobility mechanism can climb over obstacles lower than the height of the track ramp. Differential steering is normally used for turning.

(a.4) Legged mechanism. A legged mobile robot, such as Savannah River walking robot from Odetics Inc. [17, P.189], has the greatest capability of going over different types of terrain and climbing stairs. A smooth ride may be achieved even on a very rough ground surface. However, building a legged mobile robot able to walk or run in a satisfactorily stable manner is still very difficult.

(a.5) Special mechanism. In addition to the solo-mobile mechanisms, some special arrangements/combinations, such as TO-ROVER designed by University of Tokyo and Mars rover produced by Jet Propulsion Laboratory, have been constructed to extend the wandering capability in special applications.

The mobile mechanisms above may be called land surface vehicles [11], since they are constrained to the supporting ground surface. To attain more degrees of mobility, mobile mechanisms which can move through a medium have also been developed.

(a.6) Air and water cushioned mechanism. An aerial mobile robot, such as the one in the University of Southern California, consists of a flying machine. Georgia Tech's Heliquad [20] can fly over barriers to execute the shortest route. A submarine mobile robot, such as French Epaulard capable of autonomous underwater operations, has also been proposed for naval applications. Since aerial and submarine mobile robots either fly

or float in a three dimensional medium, three translational and three rotational degrees of freedom need to be controlled. The stability and balance issues are important.

(b) Manipulation. The manipulative mechanism of a mobile robot system is a polyarticular structure made up of joints, limbs and an end effector, or segments and articulations [21]. Joints are designed to move with two basic types of motion; linear and angular. The work envelop [4] of a manipulative mechanism is the collective space its end effector can achieve. Most manipulative robots at present have three or four major joints (more than three axes) to define their work envelopes. Five types of movement pattern, subject to the co-ordinate system, are currently available:

(b.1) Cartesian movement. A Cartesian type manipulative robot, such as KUKA IR400 from KUKA Inc. [11, P.23], has three linear joints moving in the X, Y and Z directions to reach its target, ensuring that the motion of the end-effector is in Cartesian co-ordinates.

(b.2) Cylindrical movement. A cylindrical type manipulative robot, such as Prab E from Prab Robots Inc. [7, P.33], has two linear joints, one for in-and-out and the other for up-and-down movement, and one angular joint with rotational axis normal to the base plane. The resulting work envelope is a cylinder.

(b.3) Polar movement. A polar type manipulative robot, such as Unite 2000 from Unimation Inc. [1, P.56], has three operational axes. Using two angular joints, one with its rotational axis normal to the base plane and the other with its rotational axis parallel to the base plane, and a linear joint for in-and-out movement, a polar mechanism may sweep in a spherical movement pattern.

(b.4) Articulated movement. An articulated type manipulative robot, such as PUMA from Unimation Inc. [8, P.15] and MOVEMASTER-EX from Mitsubishi Inc., is descriptive of a jointed system. It uses the anthropomorphic arm structure, having all angular joints, to produce a greater degree of flexibility.

(b.5) Special movement. Special movement pattern are also available. For instance, a SCARA (Selective Compliance Assembly Robot Arm) type manipulative robot, such as IBM 7537 [1, P.57], has two angular joints, one with its rotational axis normal to the base plane and the other's parallel to the first rotational axis, and one linear joint attached to the terminal limb, performing rigidly vertical movement. Another example is the Spine manipulator [11, P.125] designed to offer very flexible movement by stacking many identical joints in series.

A collection of manipulative robots and their manufacturers are detailed in [7].

(c) Perception. Mobile robot systems use sensors for perception. A sensor [4] is a measurement device, consisting of a transducer, which can detect characteristics of physical phenomena through some form of interaction with them. A transducer [22] is a device that converts different forms of energy. To supply information about a mobile robot system to its electrical controllers for interpretation, transducers converting non-electrical energy into electrical signals are usually used.

Sensors implemented in mobile robot systems may be classified in different ways. For instance, external sensors are primarily used to learn the working environment and objects being manipulated, and internal sensors inform a mobile robot system of its internal states. Sensors may also be classified as remote and contact according to technologies used. A remote sensor measures the response of its target to some forms of electromagnetic radiation such as visible light (camera), X-ray, infrared (IR beacon scanner), laser (laser range finder), acoustic (sonar), and electric or magnetic radiation. A contact sensor measures the response of its target to some forms of physical contact, such as touch, force, torque, pressure and tactility.

As the types and number of sensors implemented increase, so does the capability of a mobile robot system to perform complicated operations. However, the complexity of the sensor fusion problem also increases.

(d) Control. Since the tasks a mobile robot system may perform are described more in software than in hardware, computers which accommodate and execute the corresponding control software are important. Computers used in mobile robot systems may be functionally classified as dedicated controllers and general purpose computers.

A dedicated controller is one devoted to a specific application. It is normally invisible to the user of a mobile robot system in which it is located. Typically, a dedicated controller contains only the components strictly necessary for executing its allocated tasks. Most mobile robots, manipulative robots and sensor systems have their own dedicated controllers only for processing commands and driving mechanisms. A general purpose computer has sufficient memory and peripherals to handle a wide range of applications. It always has facilities for expansion, thereby enabling users to add more memory or peripherals later. For example, IBM personal computers, and their compatibles, can be used for programming, word processing and remote device controlling.

In addition, control languages must be established between human users and computer-based robotics systems so that the users can direct the systems to perform desired tasks. Table 1.1 is a list of robotics languages with the high-level languages they are based on or similar to.

Assembly language	**FORTRAN**	**Algol**	**BASIC**	**Pascal**	**PL/1**	**Lisp**	**Numerical control**
T^3	RCL	AL	VAL	HELP	Maple	MINI	Anorad
Emily	RPL		VAL-II	JARS	Autopass	RPL	APT
SIGLA	MCL			AML		AML	
ML	RAPT			RAIL			
				Karel			

Table 1.1. Robotics languages [14]

(e) Communications. The communications problem arises when a group of systems need to exchange data and to interface with others. For example, the fetched sensor

information must be fed back to the controller of a mobile robot system. Communications in mobile robot systems are done in two methods, parallel and serial.

(e.1) Parallel communications. Since microprocessors handle internal binary signals simultaneously in parallel formats, the most natural pattern of data transmission is parallel communications [23][24].

(e.1.1) When various single board controllers have to be interconnected compactly to share data, system bus boards are normally used. At least 35 different bus structures are currently being manufactured [25, P.72], but only a few of them are supported by peripheral single board microcomputers from different manufacturers. For example, LSI-11, Multibus, STD bus, S-100 bus, STE bus, VME bus, Multibus, Q-bus and G-64 bus are some of the most commonly used system bus boards [26].

(e.1.2) When data signals have to be transmitted from a system to a remote peripheral, data exchange through an external way is required. By using a multi-channel passage, such as a group of wires and connectors or bandwidth in radio media, parallel communications can be achieved. For example, 24-pin IEEE-488, 86-conductor CAMAC (Computer Automated Measurement And Control), 36-pin Centronics and 25-pin IBM parallel configurations are some widely recognised industrial interface standards [23]. However, an important disadvantage is that the distance for parallel communications is usually limited due to the distortion of data signals (synchronisation), caused by the finite and variable speed of data bits in each channel.

(e.2) Serial communications. When digital data have to be exchanged over a long distance, serial communications, transmitting (or receiving) binary data sequentially and one bit at a time through one channel, alleviates the synchronisation problem. The serial data bits can be sent over any electrical path, such as a pair of wires, a coaxial cable, telephone lines, or with a proper interface media such as radio, microwave, light, infrared or sound. Since data to and from a microprocessor are in parallel format, parallel-to-serial and serial-to-parallel data conversion is necessary. The universal asynchronous receiver

transmitter (UART) circuitry [25][27] is usually used to accomplish this task. Some serial standards commonly used with microprocessor based systems are TTY, RS-232 and RS-449 [27].

Appropriate communications software which fully supports parallel or serial data transmission is also important.

(f) Operational Modes. To run a mobile robot system, operational software is required as well as hardware construction. Many control programs have been developed, which enable mobile robot systems to behave in either tele-operated or autonomous modes.

A tele-operated mobile robot system or telechiric machine [28] works under direct human user instruction. In addition to being disability assistants, tele-operated mobile robot systems usually work in remote or hazardous environments, where direct human access to the working sites is restricted. For example, the surveillance and sampling tasks in outer space exploration and maintenance jobs in nuclear plants [17, P.186] may be taken over by tele-operated mobile robot systems. Information feedback from on-board sensors is important for users to understand the working sites.

An autonomous mobile robot system is commanded by intelligent robotics control programs [29] to perform tasks through program execution. No direct human interference is required. Computers and appropriate control software take the equivalent place of human operators in tele-operated systems, and are directly in charge of running the mobile robot systems. Although programs in some artificial intelligence fields, such as planning, decision making and sensing, have been incorporated into real mobile robot systems, a control program for universal tasks has not yet been attained.

(g) Projects. Many universities and laboratories have studied mobile robot systems. Manufacturers are also interested in the commercial applications. Only few mobile robot systems are, so far, mature enough for the real world environment. Among other robotics

research institutions of University of London, which have projects involving mobile robot systems, Queen Mary and Westfield College has tele-operated walking robots [30, P.62], and Imperial College has Free Ranging AGVs [12][13]. For commercial applications, Denning Sentry robot [17, P.206] from Denning Mobile Robotics is for warehouses, prisons and office buildings, and Hero [17, P.219] from Heathkit is for household tasks. The Transitions Research Corp. has Helpmate [17, P.136] that delivers meals in hospitals.

Mobile Robot	**Research Institute**	**Sensor on Board**
BUZZ	Georgia Institute of Technology	Sonar, camera, infrared range finder
CARMEL	U. of Michigan	Sonar, camera, bumper detectors
CHIP	U. of Chicago	Infrared range finder, sonar, colour camera, bumper detector
Crowley	J. L. Crowley	sonar, tactile sensor
DARPA	FMC	Colour camera, sonic sensor, laser range finder
FLAKEY	SRI International	Laser, sonar
Ground Surveillance Robot	Scott Y. Harmon	Acoustic sensor, laser range finder, colour camera, grey level camera
Hermies IIB	CESAR	CCD camera, sonar, laser range finder
HILARE	LAAS	Contact sensor, sonar, laser range finder, vision
HUEY	Brown U.	Sonar
HUMVEE	National Institute of Standards & Technology	Cameras
ICAGV	Imperial College	Sonar, bumper switch, camera
IPAMAR	Fraunhofer Institute	Sonar, optical range finder, tactile bumper
Mark 5	Queen Mary College	Sonar, Infrared sensor, camera
NAVLAB	Carnegie Mellon U.	Colour camera, laser range finder, sonar
ODYSSEUS	Carnegie Mellon U.	Sonar, two cameras
Robuster	Oxford U.	Sonar
SCARECROW	David Miller	Bumper detectors
SHAKY	Stanford U.	TV camera, tactile sensor, optical range finder
SODA-PUP	Johnson Space Centre	Sonar, infrared rang finder, colour camera, bumper detector
Stanford	Stanford	Laser range finder, stereo vision, sonar, tactile sensor
T.J.	IBM T.J. Watson Centre	Sonar, infrared range finder, compass, camera
UNCLE BOB	Mitre Corp.	Sonar, infrared range finder, laser
Yamabiko	Tsukuba U.	Sonar

Table 1.2. Mobile robot systems [12][15][16][17][20]

A list of some mobile robot projects are shown in Table 1.2. A mobile robot system with a full range of flexible and universal human features and behaviours is the ultimate goal of mobile robotics researches. However, such a system is still at the research stage. Most mobile robot systems only combine necessary functions for dedicated applications.

1.3. NAVIGATION METHODS

To accomplish a task, a mobile robot system has to move independently in its working environment. A fundamental behaviour required is autonomous navigation. A successful and feasible navigation method is crucial to controlling a mobile robot system. Three types of navigation are currently used or being investigated for applications in manufacturing environments; explicit network following, fixed beacon guiding and free ranging navigating.

The easiest navigation method for a mobile robot system is to follow a network of explicit routes. This method is well-studied, and has been widely used in many manufacturing applications. Although such a mobile robot system has little ability to go around objects when following explicit routes, it can still do useful work autonomously in an industrial setting, without direct human instructions. However, the explicit network following method is too rigid and not flexible enough to handle applications requiring wide-ranging mobility.

An improvement in flexibility over the explicit network following method is to fix guiding beacons around the working environment. Information, such as position or job assignment, specific to each beacon is sent out continuously to be detected and used in locating, configuring or instructing the mobile robot system [31][32]. The construction cost, for fully covering a large working environment with beacon signals, may be very

high. Also, signal free zones, where the beacon information is blocked by objects or can not be received due to poor relative receiving angles, have to be carefully considered.

Another step towards flexibility is the free ranging navigation method. Planning paths by space reasoning techniques, in co-operation with perceived natural features of the working environment [33][34][35], a free ranging type of mobile robot system can greatly expand its working territory. However, only a few simple manipulations, such as wall following [15], have been implemented in the real world since many aspects of the free ranging method are still immature.

1.4. KING'S COLLEGE MOBILE ROBOT PROJECT

It is envisaged that in future factory automation most of the operations of a manufacturing environment will be under automatic process control, linked together by flexible material flows and information channels. The King's College mobile robot project is to develop a mobile robot system as a flexible material transport system for factory automation.

1.4.1. Operational Domain

As mentioned earlier, flexible manufacturing systems are a possibility in coping with changing uncertain market demands. To achieve the maximal flexibility, the project is to study applications where a FMS is integrated with other computer tools to form a computer aided flexible manufacturing system. By linking computer aided design, CAD, with a material transport system, two levels of flexibility may be incorporated into the design of manufacturing schemes:

(a) Process level. Process level flexibility describesthe planning and designing of production processes, based on the current spatial arrangement of manufacturing cells.

All component machines and equipment remain at their positions. At this level, the material transport system has to deliver materials according to a variety of planned manufacturing schemes and material flows in the same factory layout.

(b) Plant level. Plant level flexibility describes the re-locating of the manufacturing cells in a factory. To fabricate a new series of products, a different machine allocation inside the factory may be necessary. A new spatial arrangement of the component machines is thus planned using a CAD design tool. The material transport system has to be fitted into the manufacturing system, and work appropriately again in the new plant layout with the least possible delay.

In addition to the changeable material flow and variable floor layout, the operational domain of the project, in which the mobile robot system works, may be characterised as:

(1) There is a consistent information flow for all systems in the environment.

(2) The configurations and locations of all contained machines are completely known.

(3) There may be unexpected events occurring.

1.4.2. System Construction

The mobile robot project is to build a working flexible material transport system, consisting of a mobile robot, manipulative robot, sensor devices and control computers. The mobile robot is cylindrical. It has an omni-directional three wheel synchronic drive mechanism, equipped with optical encoders. Six ultrasonic sensors are installed for on-board perception. The manipulative robot is of the articulated type, with five joints and a gripper. A vision system, consisting of a CCD type camera, monitor screen and dedicated processing boards, is also used.

The central computer of the mobile robot system is a personal computer. Since the flexible material transport system is designed to work efficiently under a centralised

control scheme [36][37], all levels of control calculations and intelligent activities are performed by the central personal computer. Communication channels together with interface and control programs, connecting the personal computer with the mobile robot, ultrasonic sensors, manipulative robot and vision system, are also constructed.

1.4.3. Navigation Strategy

The developed navigation strategy is basically divided into planning and executing stages. At the planning stage, a practicable route with collision tolerance space between obstacles and the mobile robot is planned. At the executing stage, the planned route is followed according to the physical specifications of the mobile robot. Since the route planning approach is developed to accommodate minor errors from the mobile robot and models [38], the planned route is feasible. During the navigation, knowledge about the manufacturing environment is updated with information from sensors. If the planned route can not be executed successfully, unexpected event handlers will be activated to divert the original route or re-plan a new one. These actions are performed until the completion of the navigational task, or some pre-defined conditions of the mobile robot system, subject to failures, are reached.

1.5. STRUCTURE OF THE THESIS

The thesis addresses several parts of the mobile robot project: system construction, theoretical development of a navigation strategy, implementation techniques, experimental conclusions and future directions. It is organised in six chapters.

The project is to construct a flexible material transport system for factory automation. Problem definition, operational domain, project motivation and goals to attain have been introduced in chapter one. A general survey of existing mobile robot systems is also conducted.

In chapter two, construction of the flexible material transport system is discussed in detail. Physical features of the · hardware components, and communications methods, are described. To make the system work, control programs for environment modelling, route planning, obstacle avoiding, sensing, motion executing and unexpected event handling are necessary. The structure of these programs is also previewed.

In chapter three, applied mathematical tools and theories are described. The formulation of polygonal triangulation and related mathematical results are discussed. Computational algorithms for achieving polygonal triangulation are proposed.

After discussing other path planning methods, chapter four describes an environment model based on the proposed triangulation algorithms. A feasible route planning approach based on the model is developed for mobile robots. An unexpected event handling approach is also proposed. Once a route has been planned, the execution of the route is discussed.

In chapter five, considerations for sensing and motion co-ordinating in accordance with the planned route are discussed. Implementation techniques and experimental results are described, which demonstrate the feasibility and practicability of the triangulation based route planning approach.

Chapter six finally concludes the mobile robot project, and addresses some directions for further development.

CHAPTER TWO

THE PROJECT: A MOBILE ROBOT SYSTEM

The mobile robot project is to construct a working flexible material transport system, and particularly to develop a feasible navigation strategy, for factory automation. Since a complete system built from specialised components is likely to cost more to achieve the same purpose, the philosophy of the project is to use general-purpose and off-the-shelf hardware elements to 'assemble' the flexible material transport system. In this chapter, industrial robots and standardised devices, as hardware components, are integrated into the system, capable of performing the principal functions of material transportation. The structural design of the system, and the physical specifications with operational features of the hardware components, are discussed. A navigation strategy, allowing the mobile robot to freely and safely move in a manufacturing environment, is also introduced.

2.1. STRUCTURAL ORGANISATION

Material transportation in manufacturing applications is to deliver work pieces from one location to another inside factories and warehouses. Four interrelated fundamental functions, required to accomplish a delivery task, are material handling, material

transporting, on-line sensing and decision making. In other words, the constructed system should embody together manipulation, mobility, perception and intelligence in an autonomous mode. Since the project uses general-purpose off-the-shelf systems and devices instead of specialised components, the corresponding modules to perform those functions are a manipulative robot, mobile robot, sensor systems and microcomputers.

In order to exchange data among these off-the-shelf general-purpose component systems, communications channels together with interface and control programs for data/signal transmission are constructed. Also, supervision programs, enabling all component systems to work as a whole, are developed. The communications channels physically connect the manipulative robot, mobile robot and sensor systems to controllers and microcomputers, and transfer signals among them. The transmission and supervision programs, running on microcomputers, co-operatively activate these component systems to do jobs properly as an integrated flexible material transport system. Figure 2.1 illustrates the structural organisation of the flexible material transport system.

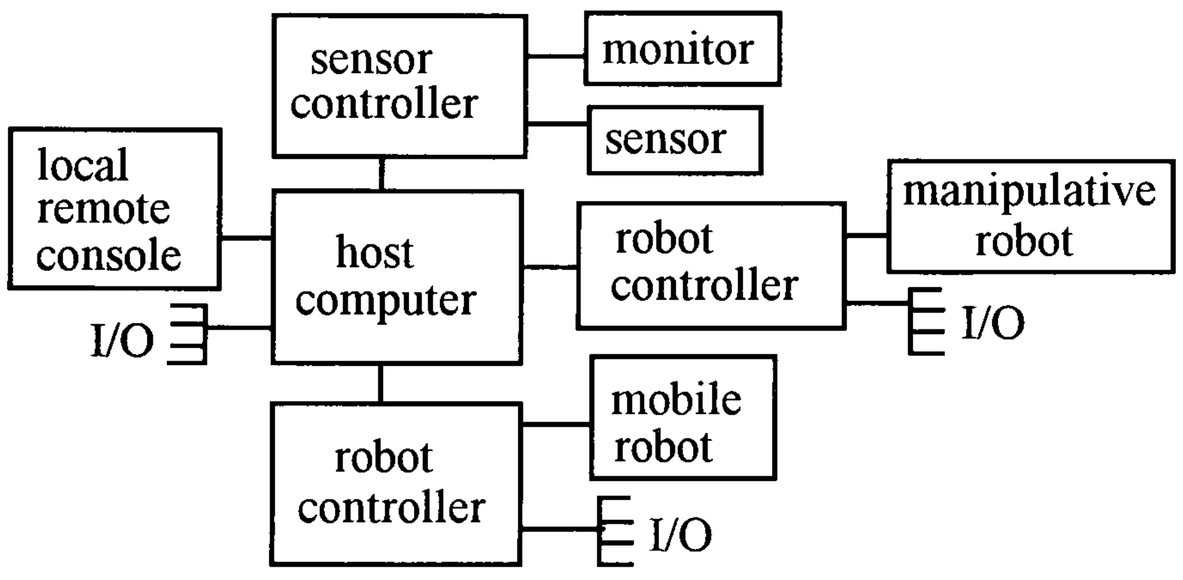

Figure 2.1 Structural proposal of system

2.2. PROJECT WORKING ENVIRONMENT

A 319cm by 319cm fenced, level and solid platform has been constructed to simulate a manufacturing environment. Various machines, objects and work stations in a manufacturing environment are represented by polyhedral obstacles, constructed using

cardboards. The layout re-arrangement on the platform can thus be achieved easily. Docking sites are settled in the manufacturing environment for the material transport agent (mobile robot) to load and unload materials, standby or re-charge energy. The manipulative robot is designed to reside aside a docking site to work with the mobile robot. Figure 2.2 shows an example layout of a working environment.

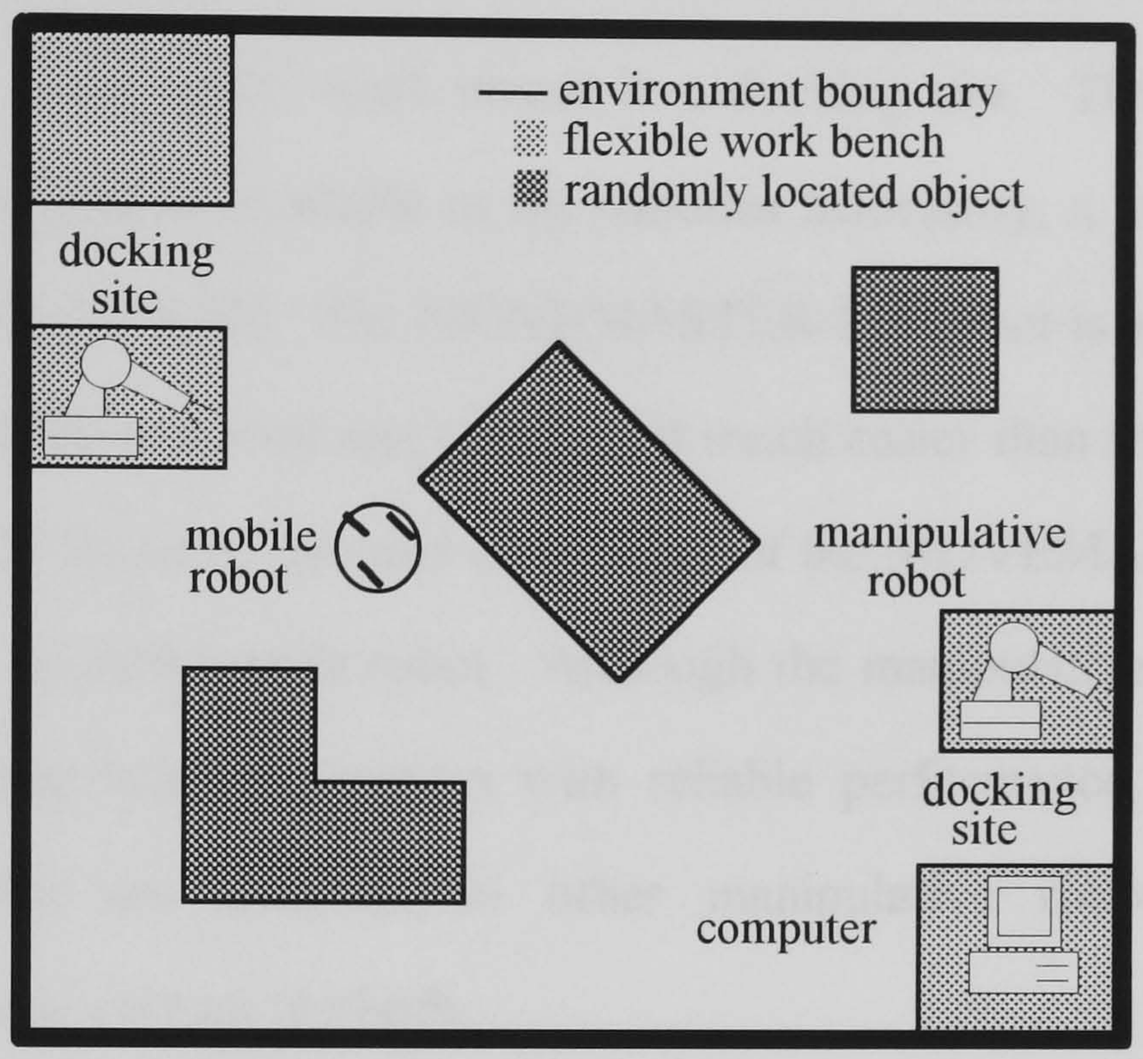

Figure 2.2. Example layout of working environment

The geometrical features of the working environment, with contained machines and objects, are known a priori. However, machines, objects and docking sites forming the plant layout are likely to be re-located and re-arranged after a period of manufacture. Humans, other robot systems or unknown objects may unexpectedly enter the working environment. Therefore, the flexible material transport system has to deliver work pieces subject to production processes and plant layouts, and cope with unexpected events during a material transportation task.

2.3. SYSTEM HARDWARE

The hardware components of the developed mobile robot system are introduced in this section.

2.3.1. Manipulative Robot

The function of the manipulative robot in the flexible material transport system is to help the mobile robot to handle work pieces in a docking site. There are two electric-actuated manipulative robots available in the robotics laboratory, a MOVEMASTER-EX [39][40] and a PUMA [41][42]. The MOVEMASTER-EX robot is applied in the project mainly because it can be removed and re-installed much easier than the PUMA one, if the layout is re-designed. Besides, size and capabilities of the MOVEMASTER-EX robot are compatible with the applied mobile robot. Although the manipulative robot is an off-the-shelf and ready-to-use industrial system with reliable performance, two main inherent features exist, which are common to other manipulative robots with articulated mechanisms and similar control methods.

(a) Position repeatability. The load-free position repeatability, relative to the robot base to which the mechanism is positioned, is 0.3mm [39], statically measured at the roll centre of the wrist tool surface. However, the position repeatability is much worse when the system is dynamically operated. The position repeatability is also affected by applications, load, and mechanical maintenance.

(b) Line-following difficulty. Due to the movement restrictions of articulated mechanisms, this manipulative robot can only achieve the line-following function, (straight or curve path for the wrist tool surface or the gripper), by dividing the travel distance and the angular positions, between the two end configurations, into a number of intermediate points according to the path accuracy required. Each intermediate point is sequentially

executed by linear articulated interpolation. The greater the number of intermediate points, the smoother the movement path, and the closer it will be to the desired performance. But more time will be consumed by the calculation. Nevertheless, an ideal line-following performance is hard to attain precisely.

Plate 2.1 shows the MOVEMASTER-EX manipulative robot; nomenclature and specifications are described in Appendix A.

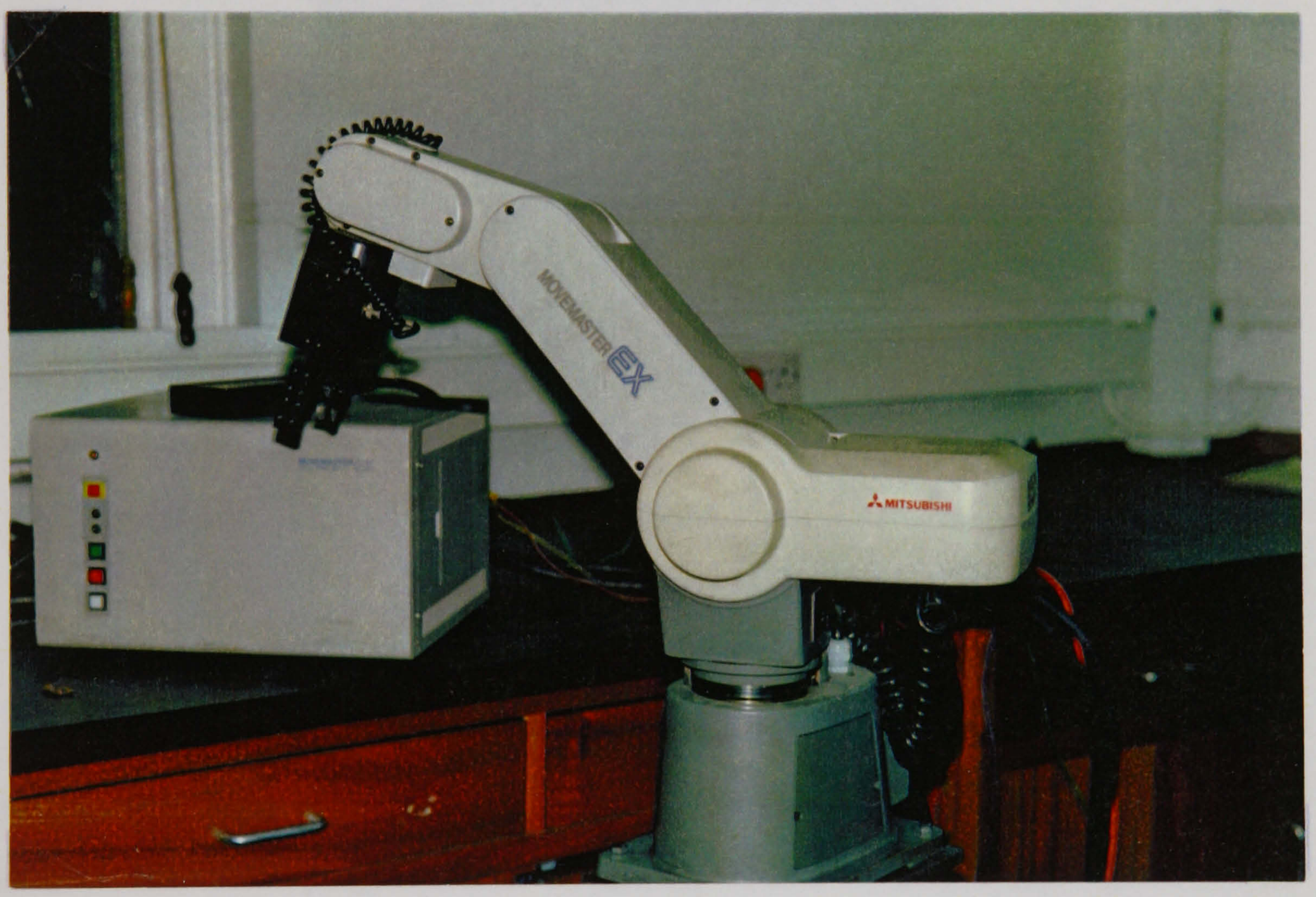

Plate 2.1. MOVEMASTER-EX manipulative robot

2.3.2. Mobile Robot

The functional component of the flexible material transport system, providing mobility, is a B12 mobile robot manufactured by Real World Interface Inc. [19][43]. The circular-shaped, three-wheeled mobile robot is a self-contained system, consisting of motors, power amplifiers, batteries, optical encoders, and microprocessor-based control

boards with supporting operational software. Plate 2.2 shows the B12 mobile robot. Specifications of this mobile robot are described in Appendix B.

Plate 2.2. Outlook of B12 mobile robot

The mobile robot has independent translation and rotation transmission systems to achieve omni-directional movement. Through the synchronous driving mechanism, the mobile robot can be programmed to navigate in discrete or continuous modes. By de-coupling the translation and rotation motions, the mobile robot can move forward and backward, and turn about its central axis to achieve discrete navigation. This discrete navigation is simply characterised by a sequence of move-stop-turn movements. Continuous navigation is the result of precisely controlling two servo loops simultaneously, according to the given route which the mobile robot has to follow. Curve trajectories are possible in continuous navigation.

Similar to the manipulative robot, operational (navigational) errors of the mobile robot in location, orientation, and motion (velocity and acceleration) are likely when a planned route is performed in the actual scene.

(a) Internal error. Although the mobile robot has optical shaft encoders providing feedback information for closed-loop control, because of internal reasons, mainly from the mechanical structure, mechanism accuracy and control accuracy, errors occur. Internal error sources, such as gear backlash, timing belt slippage, mechanism resolution, mechanical wear, control resolution, inertia, and calculation and conversion resolution, are inherent to the mobile robot. Compared with external errors, internal errors have minor effects on the performance of the mobile robot.

(b) External error. The seriousness of external errors on the mobile robot behaviour is highly dependent on the working environment. The resulting performance affected by external errors varies from one application to another. External error sources such as wheel slippage, friction, wheel wear, and vibration are mainly caused by the features (roughness, ramp and slope) of the ground surface. In the worst cases when the mobile robot is navigating in an outdoor off-road working environment, the navigational behaviour is unpredictable and uncontrollable.

(c) Error multiplication and cumulation. Although the translation and rotation transmission systems can be operated independently, they contribute vibrations affecting each other. Errors of the overall performance are usually a multiplying function of the steering and driving errors. Without adjustment or correction, the mobile robot navigation will be cumulatively diverted from the desired route.

2.3.3. Sensors

To self-control adaptively to variations in working environments, a flexible material transport system needs self-supporting and compliant functions with perception [44][45]. In this project, the use of ultrasonic sensors, compasses and vision camera is discussed, and efforts are concentrated on integrating these sensors into the developed navigation strategy.

(a) Ultrasonic Sensor. Similar to animal sonar systems, ultrasonic sensors are designed for measurement of distance and detection of objects [46]. They work on the principle of either sending a single sound pulse or emitting a continuous-wave signal, where the pulse displacement is measured between the transmission and the return of the signal. The interest in ultrasonics as a sensing technique in robotics has been growing steadily, and may be classified into three main areas: ranging and navigation for mobile robots [47][48][49][50], gripper-mounted sensors [51], and imaging methods [52][53][54]. In this project, ultrasonic sensors are used to support the ranging and navigation of the mobile robot.

A ring of six ultrasonic ranging sensors, manufactured by Polaroid Inc. [55][56], are mounted around the mobile robot; each device embodying together a transmitter and a receiver. Having a dedicated drive card, each sensor is individually addressable by connecting to one of the four 8-bit analogy/digital converters on a sensor control board. The sensor control board is based on a Motorola 68HC11 microprocessor, and is equipped with 32 kbyte of ROM and 32 kbyte of RAM to support sensor operations. Communications with the sensor control board can be achieved through the serial port, compatible with the EIA-RS232C standard, or the bus connector conforming to the G-64 bus interface configuration. An on-board 4-pin plug accepts 5-volt power input for operating in a stand-alone mode.

In general, ultrasonic sensors are low-cost and easy to use, which explains their widespread use. However, ultrasonic sensors suffer from low measurement rate, and measurement results are notoriously difficult to interpret correctly. Hence, there is a tendency to limit the use of ultrasonic sensors only to obstacle avoidance in the immediate neighbourhood of the mobile robot [57][58][59].

(b) Compass. A compass is an instrument for showing the direction of magnetic north and bearing from it. Although compasses have contributed to marine navigation, there are very few reports, with unsatisfactory results, of applying them to the navigation of mobile robots in a manufacturing environment. From the experimental results acquired, compasses are found not suitable for use in indoor manufacturing applications, because of following reasons:

(b.1) Manufacturing environments are always full of electromagnetic fields, caused by running machines and high iron materials, which seriously affect the compass performance.

(b.2) Time for stabilisation of the compass may lag far behind the requirement for rapid mobile robot response.

(b.3) It is important that the compass be elevated from the floor due to the structural steel in the concrete and the platform.

Compasses operate by tracking the earth's natural magnetic fields. They are inevitably thrown off by any stray magnetic field, such as a machine made with steel parts. To use compasses successfully in a manufacturing environment, magnetic sensor technologies have to be employed to calibrate the devices, by gauging the 'artificial' magnetic effect and eliminating it from the overall reading. A similar experience is also suggested by [37].

(c) Vision camera. The Automated Vision Association defines machine vision as "a device used for optical non-contact sensing to receive and interpret automatically an image of a real scene in order to obtain information and/or to control machines or processes". A

great advantage of the use of vision cameras is that a vast amount of data can be collected and processed at a glance, and so provides plentiful information to initiate corrective actions before the system goes out of control [60][61][62].

The applied vision system, from Data Translation Inc. [63], has a CCD (Charged Coupled Device) solid-state camera. The vision system is currently being investigated, by a research colleague, as an independent project for efficient algorithms on image acquisition and analysis, and pattern recognition. Reliable integration of the vision system into the working control scheme, especially robust sensor fusion approaches, will be further investigated.

2.3.4. Computers and Control Language

In the architecture design of the flexible material transport system, a centralised control scheme [64][65] is used. All calculations of task-level intelligent activities, such as supervising, decision making, planning, modelling, scheduling, module co-ordinating and exception handling, are carried out by a host computer. An IBM compatible personal computer, equipped with an Intel 80386SX-16Mhz microprocessor based mother board, is used for the purpose. In addition, a Gespac MPL-4080 single board computer [66], manufactured by MPL AG Elektronikunternehmen and based on a Motorola 68HC000-8MHz microprocessor, is equipped on the mobile robot to deal with general action-level activities on the remote moving platform. This single board computer connects the mobile robot and the ultrasonic sensor system through a G-64 passive system bus board. Appendix C describes the specifications of the computers.

As to the control language for system control and user interface, commercial programming languages can be used, instead of developing system specific language sets, since the proposed flexible material transport system has a personal computer as its central controller. Languages providing functions for controlling external input/output of the personal computer are appropriate. Among the available language packages, Microsoft

Visual BASIC [67], based on the BASIC language, is selected for programming the flexible material transport system, because of its well-written, English-like statements and mathematical notations, as well as its support for handling string data. The communications among the host computer and all stand-alone component systems use ASCII (American Standards Code for Information Interchange) codes, and many command parameters are in hexadecimal notations. Data interchanges have to be interpreted often, by some decoding programs, into their string formats. BASIC has many build-in routines and commands for manipulating strings. These string handling capabilities are not as easy in C, Pascal, COBOL, or FORTRAN as they are in BASIC [68][69][70].

2.4. COMMUNICATIONS CHANNELS

The input/output interface function of a system is to carry message signals between systems, and to prevent the system from damage when connecting to a dissimilar environment. Two cables, one for parallel communications and one for serial communications, are produced, in the project, to link the host computer with the manipulative robot and the mobile robot respectively.

2.4.1. Parallel Communications Channel

In the application environment, the host computer is located aside the base docking site, and is in close proximity to the manipulative robot. Since the distance of signal transmission is short and fixed, the IEC-625 (International Electrotechnical Commission) compatible 25-pin IBM parallel port of the host computer links through a cable with the Centronics compatible 36-pin parallel port of the manipulative robot's control unit [39][71]. Figure 2.3 illustrates the produced connection cable. An important feature is

that data signals are only transmitted in one direction, from the personal computer to the manipulative robot, in this parallel communication.

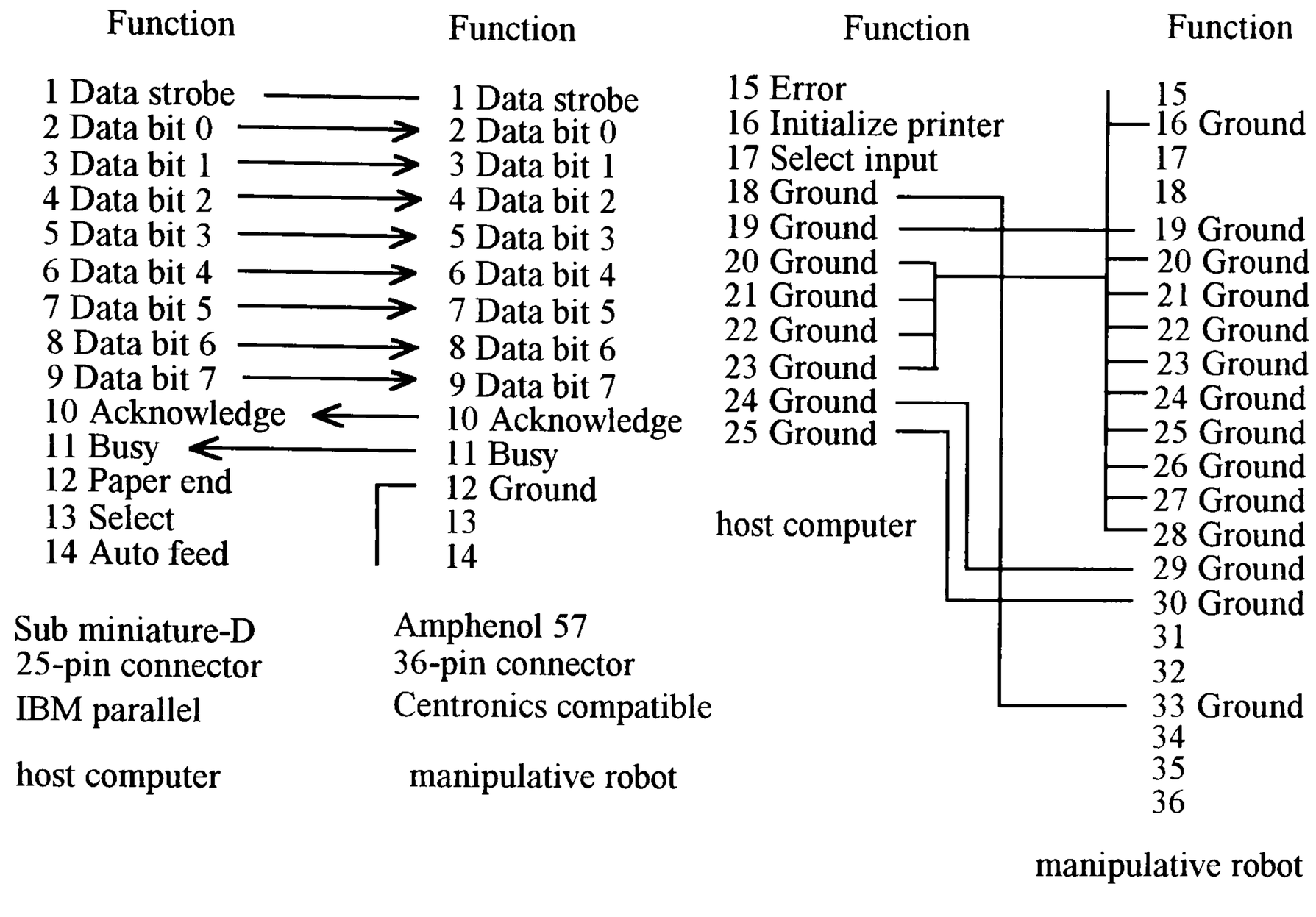

Figure 2.3. Parallel cable arrangement
(subject to IEEE-488 or IEC-625 standard)

2.4.2. Serial Communications Channel

A serial communications cable, confining to the EIA-RS232C standard [71][72], is produced to link the host computer and the mobile robot. This serial cable links the 9-pin sub-miniature D connector of the mobile robot with the 9-pin sub-miniature D connector of the host computer, using a transmission protocol configured as 8 data bits, 1 stop bit, none parity check and 9600 Baud Rate.

Since the serial communications interface on the mobile robot does not support the handshaking signals for Data Carrier Detect, Data Terminal Ready, Data Set Ready and Clear To Send [19], pins 1, 4, 6, 8 of the 9-pin sub-miniature D connectors (or 5, 6, 8, and 20 pins of a DB25 connector) at the host computer end of the cable are shorted together. Figure 2.4 illustrates the cable arrangement.

Through the serial communications cable, the mobile robot can be operated as a full duplex terminal through the host computer. All characters are echoed, and a carriage return (enter) is expanded into a carriage return plus a linefeed. A command can be edited with the backspace key or the delete key on the keyboard.

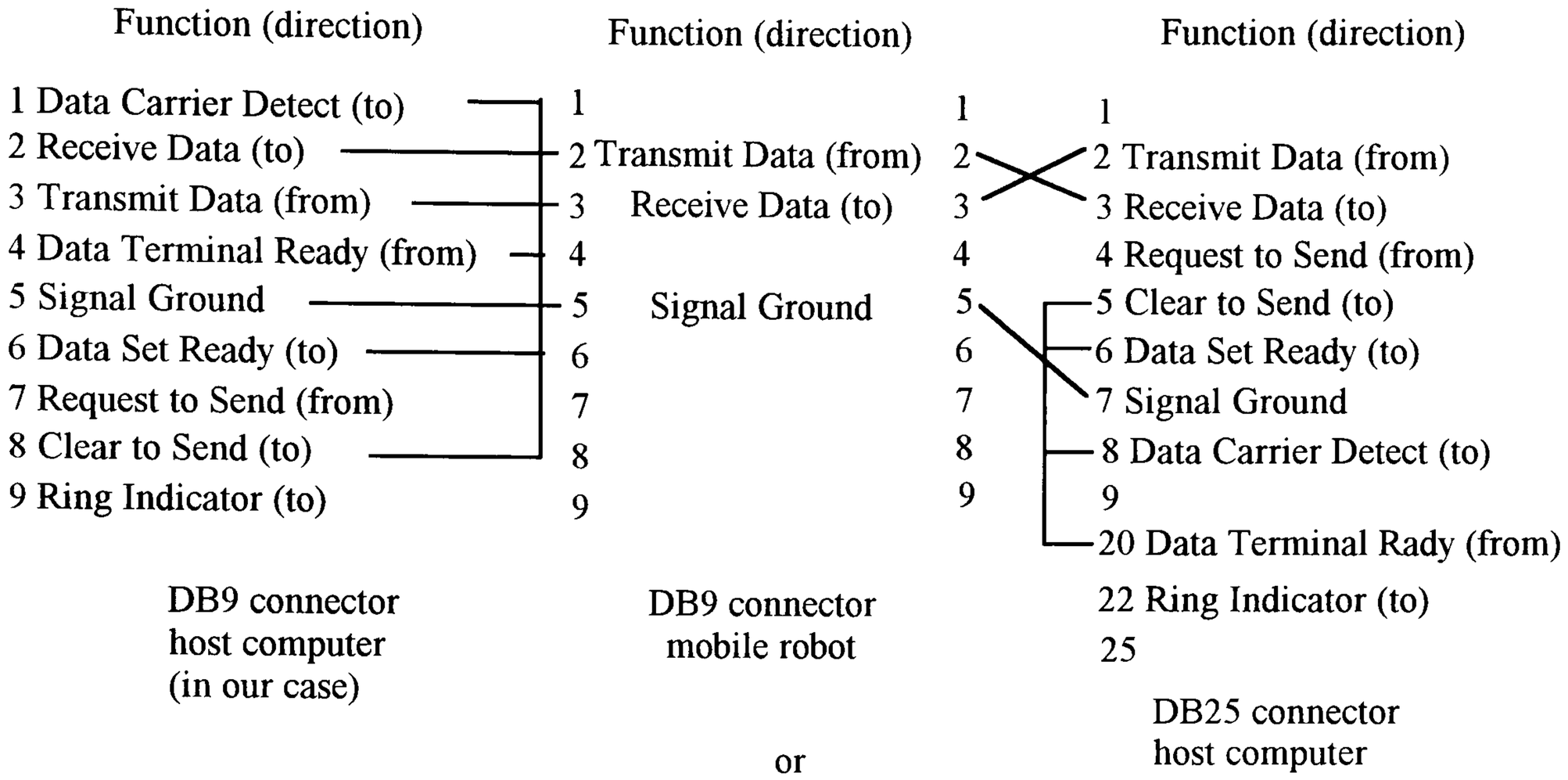

Figure 2.4. Serial cable arrangement (subject to EIA-RS232C standard)

2.5. PREVIEW OF THE NAVIGATION STRATEGY

The flexible navigation ability of a mobile robot is an important issue. Dealing with uncertainties and errors in practical scenes is also crucial to successful navigation. In this project, a triangulation based navigation strategy for mobile robots is developed, which proposes an error-tolerant solution to the navigation problem. This navigation strategy works in two stages; planning and executing.

A navigation is error-tolerant if a mobile robot will not come to harm if it makes a small deviation from the intended navigation. Due to errors and uncertainties in position, orientation and motion, a mobile robot is never able to exactly execute a planned navigation, even with the aid of sensors (sensors also have uncertainty problems). A

possible solution to error tolerance is a route that maintains a prescribed minimum clearance from obstacles. The prescribed-clearance formulation also addresses the fact that a mobile robot is a physical entity with physical dimensions. Because a mobile robot occupies a finite space in the working environment, the minimum-cost navigation of zero width, that is computed by shortest-path algorithms [73][74][75], is not feasible without modification. In addition, the optimum navigation for a mobile robot of width D1 can not be obtained by simply widening or narrowing the optimum navigation for a mobile robot of width D2. The proposed navigation strategy, at the planning stage, is to develop error-tolerant navigation with clearance, which can be performed at the executing stage without much difficulty.

2.5.1 Planning Stage

The proposed triangulation based strategy plans a navigation in two steps: journey searching and route finding. In the journey searching step, the working environment is first modelled as a topological graph by triangulation. Searching on this topological graph produces a solution graph path, which is equivalent to a continuous obstruction-free space containing the start and the goal of the navigation. Then comes the route finding step. A feasible route, maintaining clearance spaces from obstacles, is planned inside the obstruction-free space, based on a particular boundary-parallel and maximum-clearance strategy. The planned route thus reflects the boundary layout of the obstruction-free space, or the solution graph path. This route also facilitates the ultrasonic sensors to fetch information along it. In addition, an unexpected-event handling function is used to divert the navigation, in case of any unexpected event. In the worst case, a new route is re-planned.

2.5.2. Executing Stage

The navigation strategy at the executing stage is to carry out the route from the planning stage. Practical actions considered at the executing stage are system specific

[76][77][78][79], including de-coupling servo mechanisms to move along the route and triggering system sensors accordingly. Mobile robots with different mobility mechanisms require different servo control schemes to trace the same route. Once a solution route has been planned, a set of servo control schemes are derived, enabling the mobile robot to execute the route. Integration of the system sensors into the mobile robot control schemes is also considered to ensure successful performance, mainly for obstacle detection and error correction at present. Finally, if events beyond the prescribed navigation plans are detected, the unexpected-event handling functions will be activated, and the control will be transferred back to the planning stage.

2.5.3. Structure

After the theoretical analyses of the principle navigation functions, synthesising all functional programs in an efficient structure is another important issue [80][81]. The triangulation based navigation strategy is organised as a three-layer structure.

On the top of the structure is the strategy layer. Functions contained in this layer are mainly for computations of high-level intelligence, including data organising and updating, modelling, triangulating, graph searching, routing, and unexpected event handling. The bottom layer is the operation layer comprising functional programs for driving all component systems and mechanisms, and interpreting the perceived information. The middle management layer consists of an interactive user interface, and a central linker connecting programs of the other two layers. The linker program manages files and information sources, directs data flow in the structure, and activates programs at the right moment. In short, the interface between the top and the bottom layers is a route description in one way and posture feedback in the other. Figure 2.5 shows the structure of the navigation scheme.

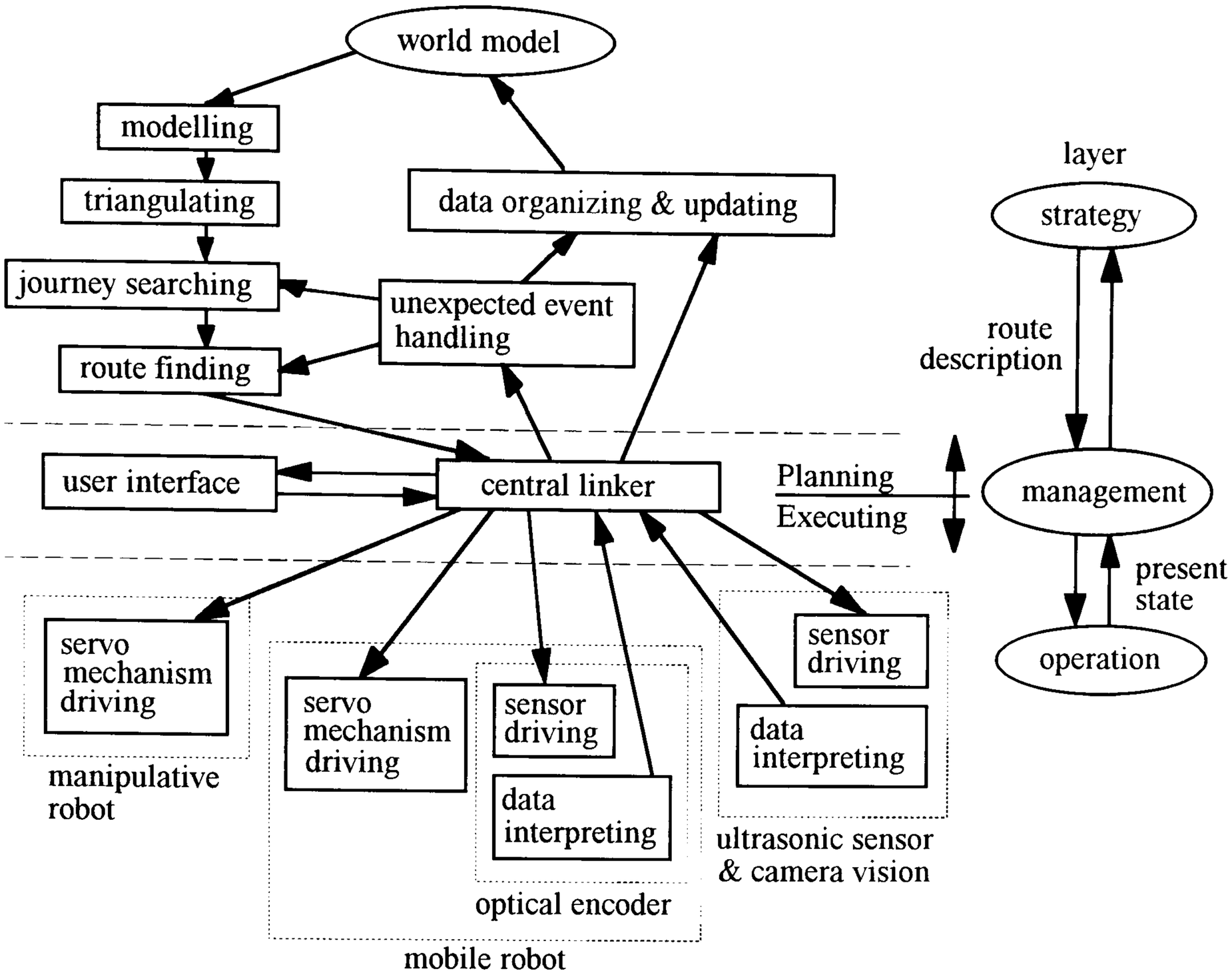

Figure 2.5. Program structure of the navigation strategy

2.6. SUMMARY

The project is to construct a working flexible material transport system, using general-purpose and off-the-shelf hardware components. Figure 2.6 and Plate 2.3 show the constructed system, which consists of a personal computer, dedicated computer, manipulative robot, mobile robot, vision camera and ultrasonic sensors. To exchange/share data among these hardware components, communications channels together with interface and control programs for signal transmission are composed. Programs enabling the host personal computer to drive the hardware components are also developed. Then, a triangulation based navigation strategy is introduced, which will be shown to have the advantages of simplicity and efficiency. In addition, having clearance

space to tolerate errors and uncertainties, the planned navigation is able to be executed by the mobile robot without difficulty.

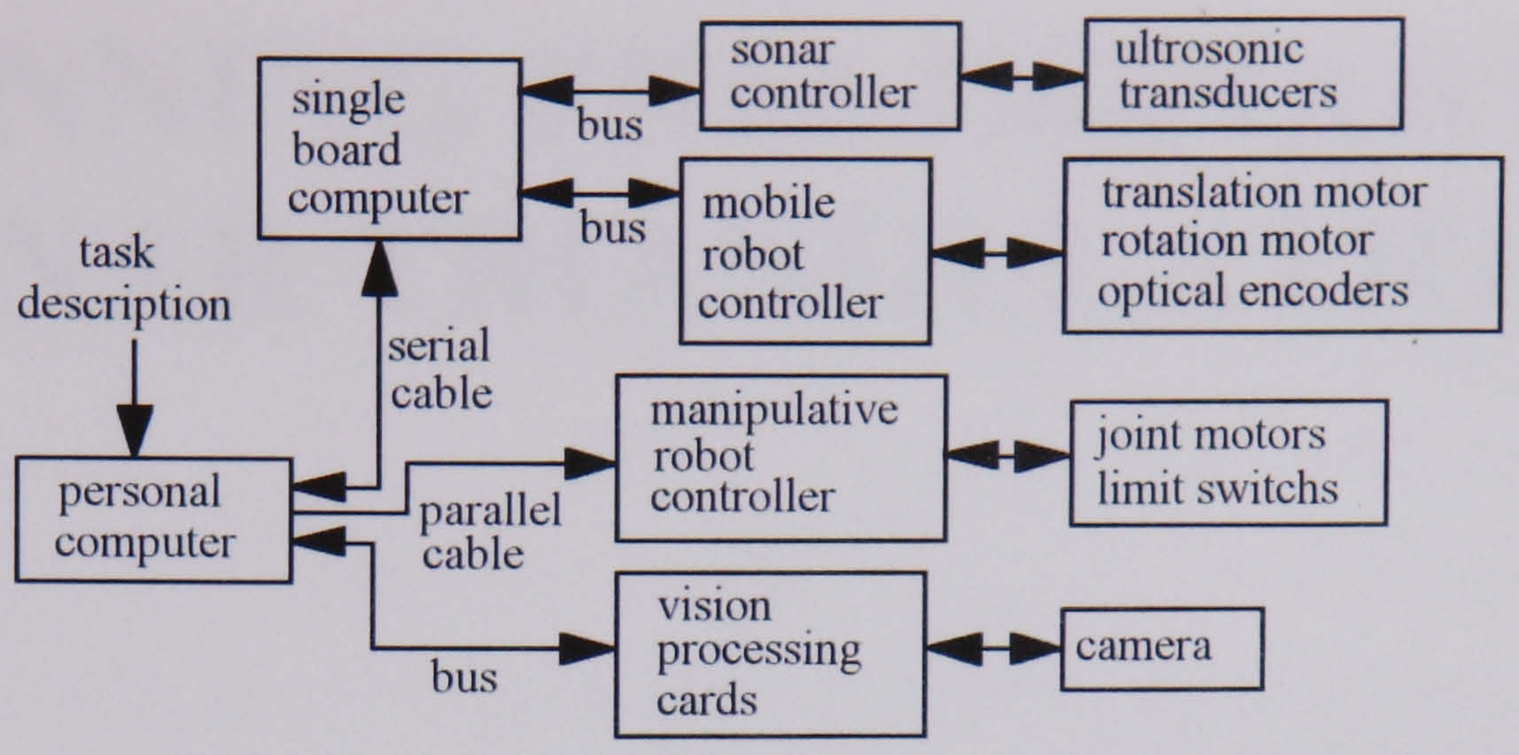

Figure 2.6. Flexible material transport system & information flow

Plate 2.3. The flexible material transport system

CHAPTER THREE

PLANNING PRELIMINARY: PLANAR TRIANGULATION

The problem statement to a mobile robot's navigational controller normally only specifies the desired task in general terms, e.g. move the mobile robot from work station *A* to docking site *B*. In order to use computers to plan (calculate) a feasible navigation, a preliminary task is to "computerise" the domain and the statement of the physical navigation problem. In other words, the problem has to be translated into (modelled as) a collection of mathematical objects , such as values, symbols, expressions, etc., which are structured to represent the environmental states with corresponding initial and final postures of the mobile robot. Then, appropriate computational algorithms [82][83][84] are implemented to produce a series of intermediate environmental states, transforming the initial state to the final state. The given mobile robot navigation problem is consequently computed and planned.

In practice, geometric descriptions are used to model the mobile robot and the environment. Therefore, a navigation strategy, consisting of a series of computational algorithms for achieving the geometric input/output transformation of the mobile robot navigation problem, will be developed. Since this strategy will use the planar polygonal

triangulation as a fundamental mathematical tool, the computational algorithms for carrying out the triangulation processes are developed in this chapter.

3.1. TRIANGULATION AND NAVIGATION STRATEGY

The proposed navigation strategy is based on the planar polygonal triangulation of computational geometry [85][86], which uses computational algorithms to decompose a polygonal region into triangular components.

At the planning stage, this navigation strategy first partitions the 'free' working environment of the mobile robot, a simple closed polygonal boundary with interior polygonal obstacles, into a set of non-overlapping triangular regions. These triangular regions together cover the part of the working environment where the mobile robot can move without collision. To process the triangulation, a pre-processing algorithm, bridge building, is proposed. This bridge-building pre-processing reduces the problem to a regular polygonal triangulation, so that existing triangulation algorithms can be implemented.

From the produced triangle set, a graph, called the triangulation graph, is constructed to represent the topological connectivity of the free working environment by a graph building algorithm. Every point of the free working environment can be retracted (mapped) onto a corresponding point on the triangulation graph. Initial and final locations of the mobile robot are also mapped onto the triangulation graph by a point location algorithm. Using general graph searching algorithms on the triangulation graph yields an optimal solution graph path. A physically feasible route for the mobile robot is then planned by resolving the solution graph path with an interpretation algorithm.

To complete the navigation task, the mobile robot must move itself in a co-ordinated fashion along that prescribed route. At the executing stage, a series of conversion

algorithms, converting the planned route to motor and sensor control profiles, are finally carried out to perform the route.

3.2. TERMINOLOGY AND NOTATION

Since the planar polygonal triangulation is fundamental to the development of the navigation strategy, a thorough discussion and related definitions applied will be specified. Also, notations used in computational geometry to quantitatively express efficiency, size, and complexity of a computational algorithm are described.

3.2.1. Co-ordinate System

The objects considered in computational geometry are sets of points and their combination in Euclidean space. A reference co-ordinate system has to be defined first so that each point can be represented as a combination of co-ordinates, or a vector with appropriate dimension from the system's reference origin.

Definition 3.1. The d-dimensional Euclidean space, denoted by E^d, is the space of d-tuples $(x_1,\ldots,x_d)$ of real numbers x_i, $i = 1,\ldots,d$ with metric $\left(\sum_{i=1}^{d} x_i^2 \right)^{1/2}$

Definition 3.2. A d-tuple $(x_1,\ldots,x_d)$ denotes a point P of E^d. This point may also be interpreted as a d-component vector applied to a reference origin of E^d, whose free terminus is the point P.

Definition 3.3. If a point P_1 has co-ordinates (x_1,x_2,x_3), P_2 has co-ordinates (y_4,y_5,y_6), and α is a real number, then the sum of points P_1 and P_2, P_1+P_2, is the point with co-ordinates $(x_1+y_1,x_2+y_2,x_3+y_3)$, and the product of α and point P_1, αP_1, is the point with co-ordinates $(\alpha x_1,\alpha x_2,\alpha x_3)$.

Definition 3.4. Given two distinct points P_1 and P_2 in E^d, the linear combination $L(P_1,P_2)$ expresses the straight line passing through P_1 and P_2:

$$L(P_1,P_2)=\{P|P=\alpha P_1+(1-\alpha)P_2,\ \alpha\in\boldsymbol{R}\}$$

Definition 3.5. Given two distinct points P_1 and P_2 in E^d, the set $R[P_1,P_2)$ represents the oriented ray from P_1 to P_2:

$$R[P_1,P_2)=\{P|P=(1-\alpha)P_1+\alpha P_2,\ \alpha\geq 0\}$$

Definition 3.6. Given two distinct points P_1 and P_2 in E^d, the parameter combination $S(P_1,P_2)$ describes the open straight-line segment joining points P_1 and P_2:

$$S(P_1,P_2)=\{P|P=\alpha P_1+(1-\alpha)P_2,\ 0<\alpha<1\}$$

$$S(P_1,P_2]=S(P_1,P_2)\cup\{P_2\}$$

$$S[P_1,P_2)=S(P_1,P_2)\cup\{P_1\}$$

$$S[P_1,P_2]=S(P_1,P_2)\cup\{P_1,P_2\}$$

Definition 3.7. A domain D in E^d is convex if, for any two points P_1 and P_2 in D, the segment $S[P_1,P_2]$ is entirely contained in D. That is, $P_1,P_2\in D$ implies $S[P_1,P_2]\subset D$.

Definition 3.8. The convex hull of a set of points **P** in E^d is the boundary of the smallest convex domain in E^d containing **P**. The number of elements of set **P**, or size of **P**, is called the cardinality of **P**, and is denoted by $|\mathbf{P}|$.

Although the definitions above can be applied to any d-dimensional Euclidean space, the reference system used in this thesis is confined to the Cartesian co-ordinate system (two $\boldsymbol{R}^2$ or three $\boldsymbol{R}^3$ dimensions) with Euclidean metrics. Axes of the Cartesian co-ordinate system, usually represented by **X**, **Y** (and **Z**), are perpendicular to each other.

3.2.2. Polygon

Once a co-ordinate system is specified, properties of polygons which are the objects to be manipulated can be defined:

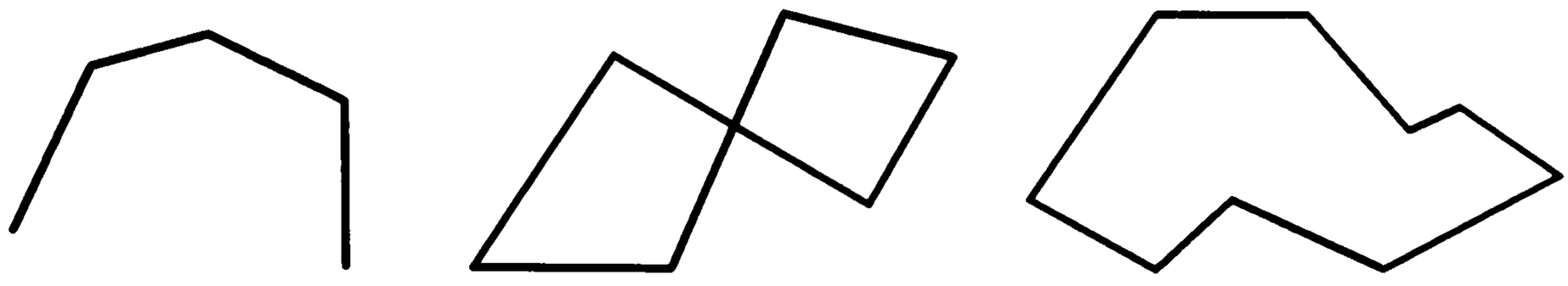

(a) Open (b) Closed (c) Closed and simple

Figure 3.1. Polygons

Definition 3.9. A closed polygon (usually simplified as a polygon) is a finite set of straight-line segments, that each segment extreme is shared by exactly two segments and no subset of the segments has the same property. The straight-line segments are the sides, and their extremes are the vertices of the polygon. The numbers of sides and vertices of a closed polygon are identical.

Definition 3.10. A closed polygon is simple, as illustrated in Fig. 3.1, if there is no pair of non-consecutive sides sharing the same point (intersecting each other). A n-vertex closed simple polygon is usually called a n-gone.

Definition 3.11. A graph G is a pair (V,E), where V is a finite set and E is a binary relation on V. The set V is called the node set of G, and its elements are called nodes. The set E is called the edge set of G, and its elements are called edges.

Graph theory [87] has many applications. However, a graph is mentioned in this chapter merely to represent the union of a point set and an edge set, that an edge is a straight-line segment connecting elements of the point set.

Definition 3.12. A graph is planar if it can be drawn in a plane so that its edges intersect only in the nodes of the graph. A planar graph has no crossing edges and determines a partition of the host plane called planar subdivision or map.

Although non-planar graphs are also included in definitions 3.9 and 3.10, discussions afterwards in this chapter will be focused only on planar graphs in the Euclidean space, that is all elements involved are co-planar. Let **P** be a closed simple polygon with n vertices in a plane. **P** is usually expressed by its vertices in a consecutive order, $v_1v_2...v_n$, that is these vertices in sequence are maintained as a linked circular list. Each vertex v_i, $i=1,2,...,n$, $n\geq 3$, is represented by its **X** and **Y** (and **Z**) co-ordinates.

$$\mathbf{P}=v_1v_2...v_n=\{P|P\in\bigcup_{i=1}^{n}S[v_i,v_{i+1}], \text{ where } v_{n+1}=v_1\}$$

$$\forall\ S(v_i,v_{i+1}),\ S(v_j,v_{j+1})\subset\mathbf{P},$$

$$1\leq i<j\leq n\wedge j\neq i+1\wedge\{i,j\}\neq\{1,n\}\Rightarrow S(v_i,v_{i+1})\cap S(v_j,v_{j+1})=\varnothing.$$

Definition 3.13. The left-side half plane of a straight line $L(P_1,P_2)$ or a straight-line segment $S(P_1,P_2)$ is the union of points P that ray $R[P_1,P)$ can be turned to ray $R[P_1,P_2)$ by a clockwise rotation of less than $180°$.

Definition 3.14. A polygonal region is the union of a closed simple polygon **P** with its interior, where the interior, represented as $In(\mathbf{P})$, is defined as the intersection of the open left-side half planes of every sides of the polygon while the sequence of straight-line sides and vertices are traversed in counter-clockwise manner. The closed simple polygon is also called the boundary of its polygonal region.

Definition 3.15. A triangle formed by three non-collinear points O, P, and Q is defined as an union set $\Delta OPQ=S[O,P]\cup S[P,Q]\cup S[Q,O]$. A triangle is the smallest simple polygon, and a triangular region is the union of a triangle and its interior.

From the above definitions, a closed simple polygon consists of a sequence of sides and vertices that form a closed loop with no two non-consecutive sides intersecting. Starting from a vertex and traversing the boundary of a polygonal region in counter-clockwise order, all sides and vertices will be passed over only once, and the interior lies to the left of the boundary. A closed simple polygon partitions the residing Euclidean plane into two

disjoint regions, the bounded interior and the unbounded exterior (Jordan curve theorem) [88].

In addition, it can be derived that a polygonal region $\Pi \subseteq \boldsymbol{R}^2$ is convex if and only if the internal angles measuring at all vertices of its boundary, **P**, are less than $180°$. Otherwise, any straight-line segment connecting elements of sides of the non-convex (concave) vertices will lie in the exterior of **P**, which contradicts with definition 3.7.

3.2.3. Planar Triangulation

Although triangulation problems are many and varied, planar triangulation only concerns planar graphs. Rigorous descriptions of the planar triangulation which decomposes polygonal regions into triangular regions in an Euclidean plane are given.

Definition 3.16. Let $P=\{P_1,P_2,P_3\ldots,P_n \mid n \text{ is an integer}\}$ be a set of n points. A triangulation of P, $T(P)$, is a maximum set of non-intersecting straight-line segments connecting elements of P:

$$\forall\ S(P_i,P_j),\ S(P_k,P_l) \in T(P),$$

$$S(P_i,P_j) \neq S(P_k,P_l) \Rightarrow S(P_i,P_j) \cap S(P_k,P_l) = \varnothing.$$

Triangulation of a set of points is not unique. There may be a variety of ways of triangulating a point set. However, in many cases the point triangulation problem may be of a constrained nature. For example, a set of triangulation straight-line segments may be pre-specified in the problem statement. The problem becomes triangulating a given set of points P with a set of non-intersecting straight-line segments on P (the constraints), and that these non-intersecting straight-line segments must appear in the triangulation. This is the polygonal triangulation.

Typically, the most-studied polygonal triangulation is the case when the interior of a closed simple polygon is required to be triangulated. The previous convention of triangulating a point set must be modified.

Definition 3.17. Let $\mathbf{P} \subseteq R^2$ be a closed simple polygon and Π be its polygonal region, a diagonal of $\mathbf{P}$ or Π is an open straight-line segment joining two non-adjacent vertices of $\mathbf{P}$ such that the open straight-line segment lies entirely in the interior of $\mathbf{P}$:

$$\forall\ v_i, v_j \in \mathbf{P},\ v_i, v_j \text{ are distinct vertices of } \mathbf{P},$$

$$S(v_i, v_j) \text{ is a diagonal of } \mathbf{P} \Leftrightarrow S(v_i, v_j) \cap \Pi = S(v_i, v_j) \wedge S(v_i, v_j) \cap \mathbf{P} = \varnothing.$$

Since two end points of a diagonal, v_i, v_j, are vertices of $\mathbf{P}$, a diagonal partitions the interior of $\mathbf{P}$ into two adjacent parts. For a convex polygon, any straight-line segment joining two non-adjacent vertices must be a diagonal of the polygon.

Definition 3.18. The triangulation of a polygonal region Π, $T(\Pi)$, is a triangulation of its vertices such that all triangulating straight-line segments are diagonals of Π:

$$S(v_i, v_j),\ S(v_k, v_l) \in T(\Pi) \Rightarrow S(v_i, v_j),\ S(v_k, v_l) \subset In(\mathbf{P})$$

$$S(v_i, v_j) \neq S(v_k, v_l) \Rightarrow S(v_i, v_j) \cap S(v_k, v_l) = \varnothing.$$

In other words, the polygon-triangulation problem is to find a maximum set of non-intersecting diagonals partitioning the interior of the polygon into a maximum set of non-overlapping regions whose union covers the whole polygonal region. Through the following theorem, the conclusion that the set of disjoint regions is a set a triangular regions can be attained.

Theorem 3.1. A polygonal region with n vertices can be decomposed (triangulated) by at most n-3 non-intersecting diagonals into a set of n-2 triangular regions whose vertices are vertices of the polygonal region.

Proof: This theorem can be proved using mathematical induction on the number of sides (vertices) of the polygonal region. Set a two-dimensional Cartesian co-ordinate system as the reference, let Π represent a polygonal region with n vertices, and $\mathbf{P}=v_1v_2...v_n$ be its boundary (n-gone). Also, let the vertices be labelled counter-clockwise, and v_1 be the vertex with the minimum y co-ordinate. Figure 3.2 illustrates the case.

When n=3, the cardinality (size) of the set of triangular regions decomposed is $|T(\Pi)_T|=n-2=3-2=1$, and the cardinality of the set of triangulating diagonals is $|T(\Pi)_D|=n-3=3-3=0$. The theorem is true for the simplest polygonal region n=3, and no diagonal is needed to produce the only triangular region.

Suppose the theorem is true for all polygonal regions having no more than $n=m$ sides, where m is a positive integer greater than 3.

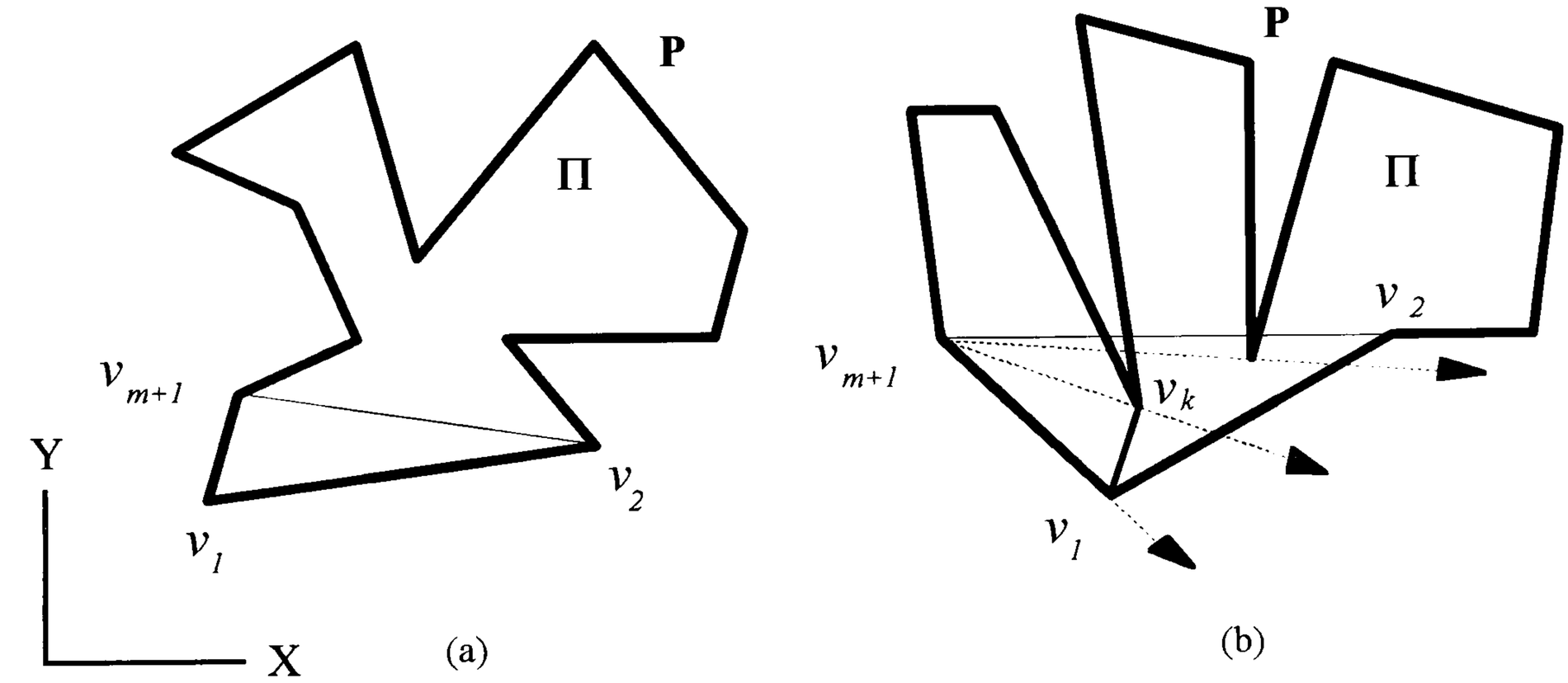

Figure 3.2. Illustration of theorem 3.1.

When $n=m+1$, the polygon is $\mathbf{P}=v_1v_2...v_{m+1}$.

If no vertex lies inside $\Delta v_{m+1}v_1v_2$, as in Fig. 3.2(a), then $\Pi=\Pi'\cup\Pi''$, where $\mathbf{P}'=\Delta v_{m+1}v_1v_2$ and $\mathbf{P}''=v_2v_3...v_mv_{m+1}$. Since Π'' has m sides, Π'' can be decomposed into a set of $|T(\Pi'')_T|=m-2$ triangular regions by $|T(\Pi'')_D|=m-3$ triangulating diagonals by the induction hypothesis. It follows that $\Pi=\Pi'\cup\Pi''$ can be decomposed into $|T(\Pi)_T|=|T(\Pi')_T|+|T(\Pi'')_T|$

$=1+(m-2)=(m+1)-2$ triangular regions. The set of triangulating diagonals is $S(v_{m+1},v_2)$ plus triangulating diagonals of Π'', thus $|T(\Pi)_D|=1+|T(\Pi'')_D|=1+(m-3)=(m+1)-3$.

If $\Delta v_{m+1}v_1v_2$ contains vertices of **P** within its interior, as in Fig. 3.2(b), let v_k be such a vertex that the measure of $\angle v_kv_{m+1}v_1$ is the minimum for these vertices. Then no vertex of **P** is in $\Delta v_kv_{m+1}v_1$, and v_k, v_{m+1} and v_1 form a triangular region. Segment $S(v_1,v_k)$ is a diagonal of **P** which partitioning Π into two regions Π' and Π'', where $\Pi=\Pi'\cup\Pi''$, $\mathbf{P}'=v_1v_2...v_{k-1}v_k$ has k sides, and $\mathbf{P}''=v_1v_kv_{k+1}...v_mv_{m+1}$ has $m-k+3$ sides. Since $3\le k\le m$ implies $3\le m-k+3\le m$, both $\mathbf{P}'$ and $\mathbf{P}''$ have no more than m sides. By the induction hypothesis, Π' can be decomposed into a set of $|T(\Pi')_T|=k-2$ triangular regions by $|T(\Pi')_D|=k-3$ triangulating diagonals, and Π'' can be similarly decomposed into a set of $|T(\Pi'')_T|=(m-k+3)-2=m-k+1$ triangular regions by $|T(\Pi'')_D|=(m-k+3)-3=m-k$ triangulating diagonals. Therefore, Π can be decomposed into a set of $|T(\Pi)_T|=|T(\Pi')_T|+|T(\Pi'')_T|=(k-2)+(m-k+1)=m-1=(m+1)-2$ triangular regions. The triangulating diagonals of Π is the union of triangulating diagonals of Π' and Π'' plus $S(v_1,v_k)$, therefore $|T(\Pi)_D|=|T(\Pi')_D|+|T(\Pi'')_D|+1=(k-3)+(m-k)+1=m-2=(m+1)-3$.

The theorem is true for $n=m+1$.

Proof is completed and theorem 3.1 is true for all polygonal regions. □

Correctness of Theorem 3.1 can also be confirmed by that it satisfies the Euler's formula V-E+F=χ [89][90], where V, E and F are the numbers of vertices, edges, and facets of a topology object respectively. Objects having the common Euler characteristic expressed as the invariant χ are classified in the same topology-equivalent group. Any closed simple polygon on an Euclidean plane is a planar graph, and can be deformed (shrunk) to a point by topology means. A polygonal region is, hence, topology-equivalent to a topology disk [91] on the surface of a sphere, that the genus (Euler characteristic) of this topology-equivalent class (polygonal regions) is $\chi=2$. For a map (planar subdivision) formed by a triangulated n-vertex polygonal region, the number of vertices is n, the number of edges is n sides plus $n-3$ triangulating diagonals, and the number of regions is n-2 triangular regions plus the planar region outside the polygon boundary:

$$V=n,\ E=n+(n-3),\ F=(n-2)+1,\ \therefore \text{Euler's formula } V-E+F=2$$

According to theorem 3.1, it follows that any polygonal region Π having n vertices can be decomposed by n-3 non-intersecting diagonals into a set of n-2 triangular regions which intersect only on their sides (i.e. diagonals of Π) and whose vertices are vertices of Π. The triangulation of a polygonal region can be concluded as:

> Triangulation of a simple polygon (or polygonal region) with n vertices is to find a set of non-intersecting n-3 diagonals that n-2 non-overlapping triangular regions are formed.

After triangulating a polygonal region Π, the sides of the produced triangular regions may fall into two groups: diagonal sides which are identical to the triangulating diagonals, and boundary sides which are identical to the sides of the polygonal region. Hence, the produced triangular regions of Π can be classified into four types: type I triangular region consisting of three diagonal sides, type II triangular region having two diagonal sides and one boundary side, type III triangular region consisting of one diagonal side and two boundary sides, and type IV triangular region having three boundary sides. Figure 3.3 is the illustration. However, type IV triangular region is rarely included in the discussions.

Theorem 3.2. Every side of a polygonal region except the vertices occurs in one and only one triangular region in any triangulation of the polygonal region.

Proof: Since triangulating operations are performed only on the vertices in any triangulation of a polygonal region, vertices of the set of decomposed triangular regions must be vertices of the polygonal region. When a side of the polygonal region is shared by more than one triangular regions in a triangulation as illustrated in Fig. 3.4, it is obvious that there must be additional vertices on this side. This is a contradiction to the definition of triangulating a polygonal region. Proof is completed and theorem 3.2 is true. □

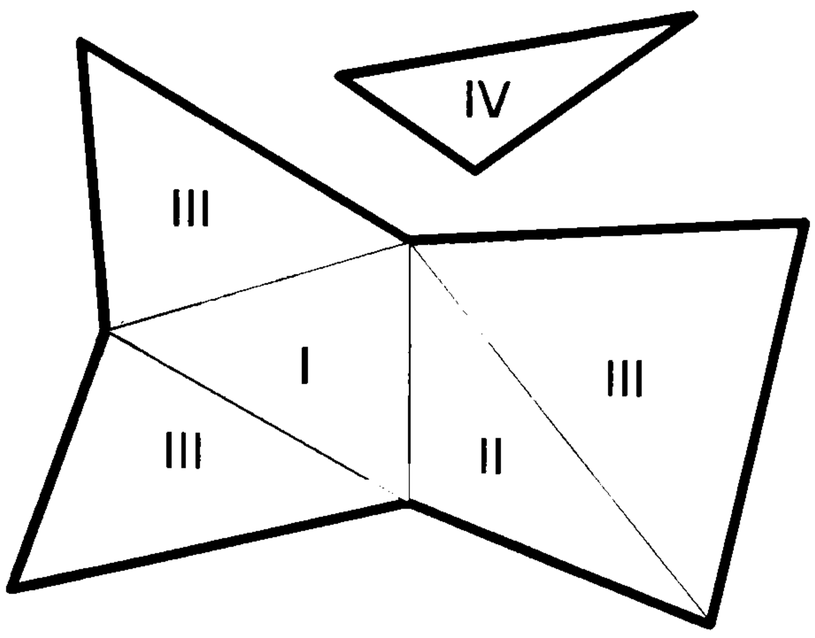

Figure 3.3. Four types of triangular region

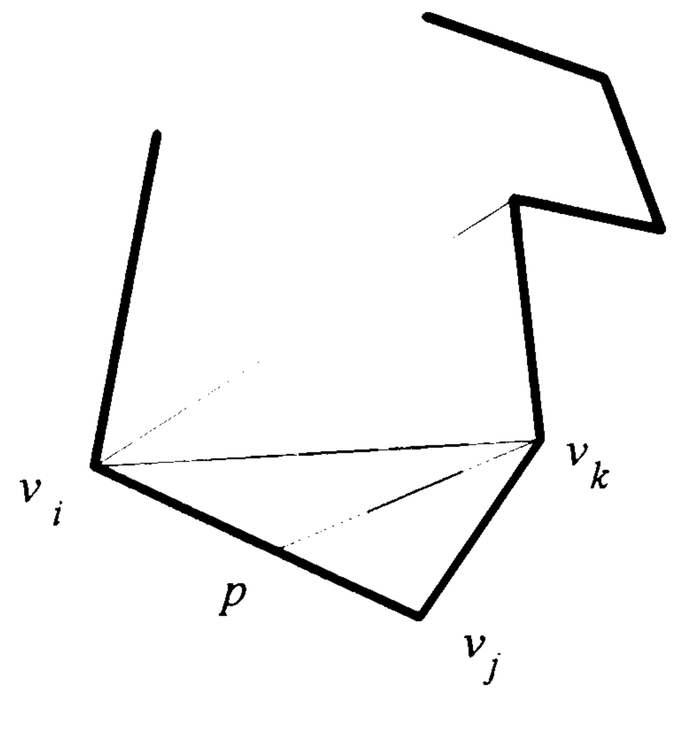

Figure 3.4. Theorem 3.2

From the above discussions, only vertices of the polygonal region are involved in its planar triangulation and additional points on the boundary are not considered. Nevertheless, some particular applications do not restrict the triangle-decomposing to be performed on the vertices of polygonal region, because the usage of additional points on the boundary may increase the processing speed and facilitate the decomposition.

3.2.4. Steiner Point

To decompose a polygonal region into a set of triangular components (regions) by introducing additional vertices on the boundary, so called Steiner points [11], theorem 3.3 is to be proved to provide the required theoretical support.

Theorem 3.3. Any polygonal region can be expressed as the union of a finite set of triangular components which intersect only on their sides if they intersect at all.

Proof: This theorem can also be proved by using mathematical induction on the number of sides (vertices) of the polygonal region. Let Π represent a polygonal region, n be the number of its sides (vertices), and $\mathbf{P}=v_1v_2...v_n$ be the n-gone (boundary). Also, assume that the vertices have been labelled counter-clockwise so that v_1 has the minimum y co-ordinate of the two-dimensional Cartesian reference system among all vertices. The notations are illustrated in Fig. 3.5.

When n=3, the theorem is true for a triangular region, the smallest polygonal region.

Suppose the theorem is true for all polygonal regions with less than $n=k$ sides, where k is a positive integer.

When $n=k+1$, the polygon is $\mathbf{P}=v_1v_2\ldots v_{k+1}$.
If **P** is convex, theorem 3.1 applies. Linking any two non-adjacent vertices v_i and v_j makes a diagonal $S(v_i,v_j)$ which partitions Π into two parts Π' and Π'', and $\Pi=\Pi'\cup\Pi''$. Since Π' and Π'' are both polygonal regions with no more than k vertices, the theorem is true for Π' and Π''. According to the induction hypothesis, the theorem is true for Π.

If **P** is not convex, let v_e be one of the concave vertices whose internal angle is larger than $180°$, $v_e\neq v_1$. Side $S(v_{e-1},v_e)$ is adjacent to side $S(v_e,v_{e+1})$. When ray $R[v_{e-1},v_e)$ is emitted into Π, it will encounter a set of points of **P**. Let v_f be the first intersection of $R[v_{e-1},v_e)$ with **P** other than $S[v_{e-1},v_e]$, i.e. v_f is the projection of $R[v_{e-1},v_e)$ onto **P** and $S(v_e,v_f)\subset\Pi$. Point v_f is either a vertex or a non-vertex element of **P**. If v_f is a vertex of **P**, $S(v_e,v_f)$ is a diagonal of **P**. Diagonal $S(v_e,v_f)$ partitions Π into Π' and Π'' two parts, that $\Pi=\Pi'\cup\Pi''$. Since both Π' and Π'' have no more than k vertices, by the induction hypothesis and theorem 3.1, Π, Π' and Π'' all satisfy the theorem. If v_f is a non-vertex element of boundary **P**, let v_f be on a side $S(v_i,v_j)$ of **P** so that $v_f\in S(v_i,v_j)$. Segment $S(v_e,v_f)$ also partitions Π into Π' and Π'' two parts, making Π the union of Π' and Π''. Since Π' and Π'' are polygonal regions formed by polygons $\mathbf{P}'=v_fv_ev_{e+1}\ldots v_{i-1}v_i$ and $\mathbf{P}''=v_fv_jv_{j+1}\ldots v_{e-1}v_e$ respectively, both Π' and Π'' have no more than k vertices. By the induction hypothesis and theorem 3.1, the theorem is true for Π, Π' and Π''.
Therefore, the theorem is true when $n=k+1$.

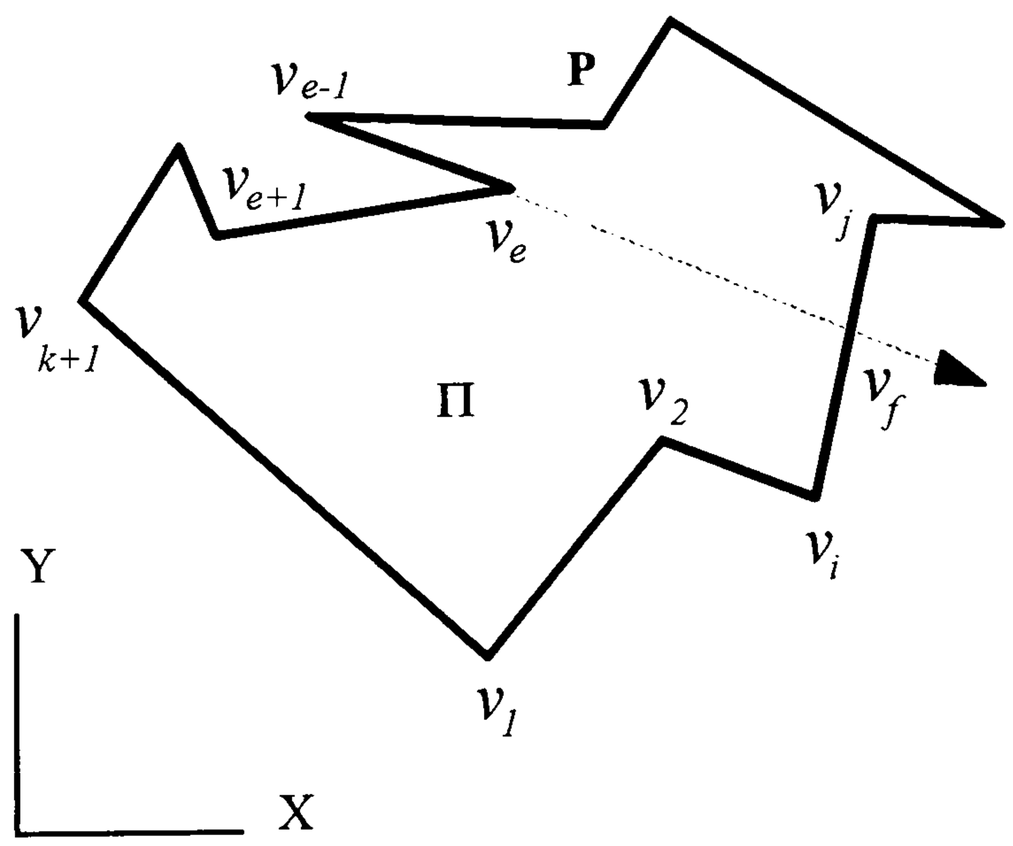

Figure 3.5. Theorem 3.3

Proof is completed and theorem 3.3 is true for all polygonal regions. □

Adding Steiner points to the boundary of a polygonal region, n applications where formal triangulation is not required, may facilitate the decomposition. This triangle-decomposition (instead of triangulation) can be viewed as applying the polygonal triangulation to the new set of vertices with the existing sides. However, the triangle-decomposition is likely to produce a set of irregular triangular partitions, whose features are to predict , since there are many ways of adding Steiner points. The triangulation applied to the mobile robot navigation is without Steiner points.

3.2.5. Computational Complexity

An algorithm is usually implemented as an instructing program and carried out by a computer. Analysing a computer algorithm means predicting the resources the algorithm requires, which mostly include storage space (or memory occupied) and computational time (or number of primitive operations or steps executed). These resources taken by an algorithm normally grow with the number of items (size) of the input. When computer instructions of an algorithm are executed one after another in the computational model of single-processor-random-access machine (serial not parallel machine) without operations being performed concurrently, it is rather natural to describe the computational complexity [93][94] of the algorithm as a function of the size of the input.

Notations used to describe the order of growth of the resource requirements (computational complexity) for executing an algorithm, such as running time and storage space, are expressed as functions of the input size of the algorithm:

(1) $\Theta(f(N))$ denotes the set of all functions $g(N)$ such that there exist positive constants C_1, C_2, and N_o with $C_1 f(N) \le g(N) \le C_2 f(N)$ for all $N \ge N_o$. $\Theta(f(N))$ is an asymptotically tight bound for $g(N)$.

(2) $O(f(N))$ denotes the set of all functions $g(N)$ such that there exist positive constants C and N_o with $0 \leq g(N) \leq Cf(N)$ for all $N \geq N_o$. $O(f(N))$ is an asymptotically upper bound for $g(N)$, $\Theta(f(N)) \subseteq O(f(N))$.

(3) $\Omega(f(N))$ denotes the set of all functions $g(N)$ such that there exist positive constants C and N_o with $0 \leq Cf(N) \leq g(N)$ for all $N \geq N_o$. $\Omega(f(N))$ is an asymptotically lower bound for $g(N)$. $\Theta(f(N)) \subseteq \Omega(f(N))$.

(4) $o(f(N))$ denotes the set of all functions $g(N)$ such that for all positive constants C there is a positive constant N_o with $0 \leq g(N) \leq Cf(N)$ for all $N \geq N_o$. $o(f(N))$ in the notation is just an upper bound that is not asymptotically tight. Equivalently, $g(N)$ becomes insignificant relative to $f(N)$ as N approaches infinity, i.e. $\lim_{N \to \infty} \frac{g(N)}{f(N)} = 0$.

(5) $\omega(f(N))$ denotes the set of all functions $g(N)$ such that for all positive constants C there is a positive constant N_o with $0 \leq Cf(N) \leq g(N)$ for all $N \geq N_o$. $\omega(f(N))$ in the notation is merely an lower bound that is not asymptotically tight. Equivalently, $g(N)$ becomes arbitrarily large relative to $f(N)$ as N approaches infinity, i.e. $\lim_{N \to \infty} \frac{g(N)}{f(N)} = \infty$.

These notations require that the range of every $f(N)$ be asymptotically non-negative, since the computational complexity of an algorithm expressed as functions of the input size should be always non-negative. That is, $f(N)$ is non-negative whenever N is sufficiently large. In general, the notations, $O(f(N))$ for example, are used to evaluate the rate of growth or order of growth in determining the computational efficiency of an algorithm, denoted by $g(N)$, for an input of large enough size N. Describing computational complexity by these notations is dependent on neither the computer hardware nor the languages used, because it is assumed that all algorithms analysed are executed on computing machines of the same serial computational model.

Although there are three basic types of analysis: best-case analysis, average-case analysis and worst-case analysis, this thesis concentrates on the worst-case analysis since the worst-case behaviour of an algorithm is an upper bound on evaluating resource requirements for any input to the algorithm. An algorithm is generally thought to be more efficient than another if its evaluation in worst-case analysis has a lower order of growth, although the evaluation may be in error for some particular inputs. For example, to solve the same problem, an algorithm with $O(n^2)$ worst-case running time will run more quickly than another with $O(n^3)$ worst-case running time, since the former performs much less steps of calculation than the latter does for large enough inputs. Also, an $O(n^2)$ algorithm may only use $\Theta(n)$ running time if the input is arranged in a good order.

3.3. TRIANGULATING POLYGONAL REGION

In computational geometry, many interesting subjects regarding decomposition of an object into simple elements [95] have been discussed. Most notable are the decomposition of polygonal region into convex parts [96][97] and monotone parts [98], the triangulation of a set of points [99][100], the triangulation of planar region [101][102][103], the triangulation of simple polygon [104][105][106], the decomposition of simple polygon into star-shaped polygons [107], and the trapezoidization of simple polygon [108].

The motivation for studying these decomposition subjects, beyond their theoretical interest, is that further processing in practical applications such as CAD, computer graphics and pattern recognition, especially for surface interpolation, is usually easier on the produced simple elements. Moreover, it is expected that the simplification will offset the increase in storage and processing time due to the large number of elements caused by the decomposition. For example, for the purposes of computer graphical display and for calculations in numerical analysis, it is often essential to manipulate only convex polygon, trapezoids, or triangles [109][110][111] for speed and simplicity of hardware

implementation. In pattern recognition, the decomposition of a polygonal region into simpler components allows easier classification and analysis [112]. Triangles, in particular, are helpful for applications requiring interpolating two-dimensional functions whose ranges are independent of the orientation of the triangles.

In our applications, triangulation algorithms are fundamental to the spatial reasoning operation [113] at the planning stage of the mobile robot navigation strategy. Since triangles are easier to handle compared with other simple elements, it is believe that spatial reasoning of this nature should facilitate the computational tasks required to navigate the mobile robot. Algorithms either with or without Steiner points can all be implemented depending on the requirements of the application scenes, and will be developed in this section. Above all, problem formulation and input/output format have to be specified:

> Given the n vertices of a polygonal region sequentially in counter-clockwise order, develop a triangulation algorithm which produces n-2 triangular regions and n-3 triangulating diagonals.

3.3.1. Triangulation Algorithm without Steiner point

As to the triangulation without Steiner points, it is to decompose a polygonal region into a set of non-overlapping triangular regions (except their boundaries) without using additional vertices on the boundary when manipulating the polygonal region.

(a) Algorithm. A very straightforward algorithm which merely uses a routine recursively to examine intersection between two straight-line segments can produce a triangulation. For each of the n vertices of a polygonal region, there are at most n-2 candidate vertices (except two adjacent vertices) which can be linked to form a diagonal. Each of the potential diagonals has to be examined, by a checking routine, that is its intersection with

every side of the boundary and with every diagonal already produced. So, the intersection-checking routine is to be performed $\Theta(n)$ times before a diagonal can be verified. Since there are n vertices and a routing checking intersection between two straight-line segments only takes a constant running time $O(1)$, the overall running time is bounded by $\Theta(n^3)$. This algorithm is straightforward but time-consuming.

An algorithm is developed here which takes advantage of some characteristics of triangulation, using neither Steiner points nor pre-conditioning of data structure, and taking less computational time:

Subject: Triangulation of Simple Polygonal Region Π by Trimming Ear
Input: Boundary of Π: $Bo(\Pi)=v_1v_2...v_{n-1}v_n$ in a counter-clockwise sequence
Output: $T(\Pi)_T=\{\Delta(k) \mid k=1 \text{ to } n-2\}$, $T(\Pi)_D=\{D(k) \mid k=1 \text{ to } n-3\}$
Algorithm:

1. $|T_D|\leftarrow 0$
2. $i\leftarrow 0$
3. $j\leftarrow 0$
4. **while** $|T_D|<n-3$
5. **do if** $j\geq 3$ and $\angle u_{j-2}u_{j-1}u_j<180°$
6. **then** TEST$\leftarrow$(Concave vertex of $Bo(\Pi)\cap\Delta u_{j-2}u_{j-1}u_j$): Inclusion Test
7. **if** TEST$=\varnothing$
8. **then** $|T_D|\leftarrow|T_D|+1$
9. $\Delta(|T_D|)\leftarrow\Delta u_{j-2}u_{j-1}u_j$
10. $D(|T_D|)\leftarrow S(u_{j-2},u_j)$
11. $u_{j-1}\leftarrow u_j$
12. $j\leftarrow j-1$
13. **else** $j\leftarrow j+1$
14. $i\leftarrow i+1$
15. $u_j\leftarrow v_i$
16. **else** $j\leftarrow j+1$
17. $i\leftarrow i+1$
18. $u_j\leftarrow v_i$
19. $\Delta(|T_D|+1)\leftarrow\Delta u_{j-2}u_{j-1}u_j$
20. **end**

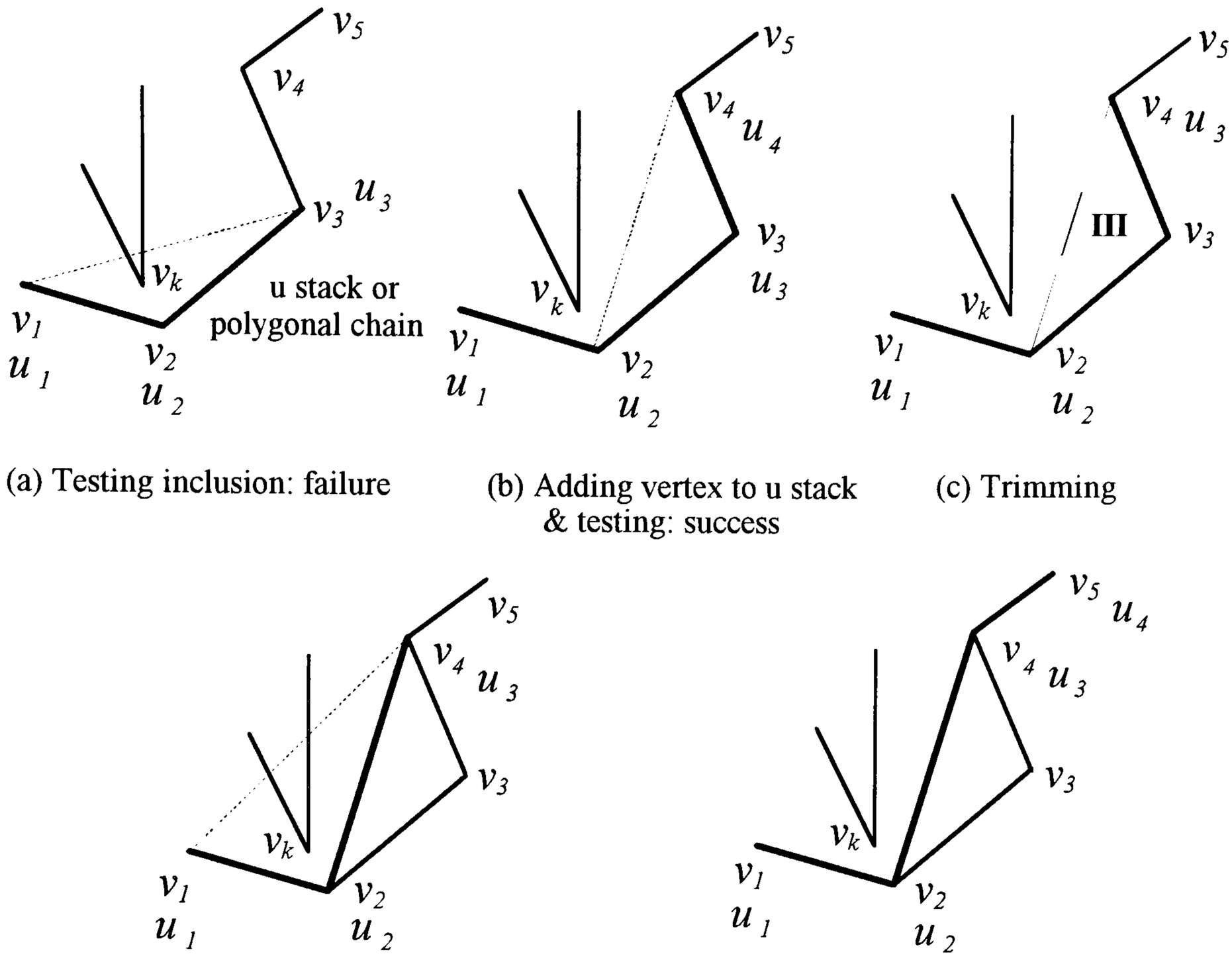

(a) Testing inclusion: failure

(b) Adding vertex to u stack & testing: success

(c) Trimming

(d) Test new chain: failure

(e) Adding vertex

Figure 3.6 Triangulation algorithm by trimming Type III region

This algorithm is illustrated in Fig. 3.6. Three consecutive vertices v_i, v_{i+1} and v_{i+2} are said to form an ear at v_{i+1} if $S(v_i, v_{i+2})$ is a diagonal of the polygonal region. A stack of u vertices are maintained by the algorithm, which dynamically represent a polygonal chain. New v vertices are added to the u stack at steps 16 to 18 until conditions 4 and 5 are satisfied. Then the latest three vertices u_j, u_{j-1} and u_{j-2} of the stack are examined by steps 6 and 7 to decide whether they form a type III triangular region (ear) or not. In other words, the idea of the algorithm is to find a type III triangular region from the current u stack, and to trim the ear from the polygonal region to produce a new and smaller polygonal region. By recursively doing the operation, the ear-trimming algorithm finally

converges to a triangulation solution. During processing, this algorithm always makes the locally optimal choice, at the moment, to produce a triangulating diagonal.

(b) Correctness. The correctness of the algorithm is based on the assumption that there are always type III triangular regions produced after triangulating an n-vertex polygonal region except for $n=3$. This assumption is to be proved in theorem 3.4.

Theorem 3.4. Any triangulation of a polygonal region has at least two type III triangular regions.

Proof: Let Π represent an n-vertex polygonal region, $n \leq 4$, whose boundary is a closed simple polygon denoted by **P**. Assuming that the numbers of triangular region type I, II and III produced after triangulating Π are x, y and z respectively. First, the total number of triangular regions is $n-2$: (1) $x+y+z=n-2$. Second, the sum of numbers of boundary sides of these triangular regions is the number of sides of **P**: (2) $0x+y+2z=n$. Third, the sum of numbers of diagonal sides of triangular regions is two times the number of triangulating diagonals of **P** because each triangulating diagonal is shared by two triangular regions: (3) $3x+2y+z=2(n-3)$. Therefore, equality $z=x+2$ can be achieved from (1)(2)(3). Since $x \geq 0$, thus $z \geq 2$. That is, at least two type III triangular regions will be produced in any triangulation of a polygonal region. Proof is completed. □

(c) Complexity analysis. Regarding the computational complexity of the algorithm for an input polygonal region with n vertices, a collection of lists v_i, u_j, $\Delta(k)$ and $D(k)$ are regularly maintained. Since v_i, $\Delta(k)$ and $D(k)$ have n, $n-2$, $n-3$ elements respectively, all are in $\Theta(n)$, and there are at most n elements in u_j which is in $O(n)$, the overall storage requirement of the algorithm is thus a polynomial upper-bounded by $O(n)$.

As to the running time analysis, steps 4 to 18 construct a recurrent loop. Operations for calculating conditions 4, 5 and 6, 7 take $O(1)$ constant and $O(n)$ running time respectively. If conditions 4, 5 are not satisfied, a new vertex v_i, or a side $S(v_i,u_{j-1})$ of Π, is added to the u chain at steps 16, 17, 18 that $O(1)$ operations are required. Otherwise,

steps 6, 7 will be taken. When condition step 7 can not be satisfied, the algorithm goes to steps 13, 14, 15 to add another new vertex to the u stack. Else, a diagonal $S(v_i,u_{j-2})$ and a triangular region (ear) $\Delta v_i u_{j-1} u_{j-2}$ are produced at steps 8, 9, 10, and the ear is trimmed from the polygonal chain at steps 11 and 12.

After trimming the ear, steps 4, 5, 6, 7 are to be executed again to examine the newly formed but shorter polygonal chain containing diagonal $S(v_i,u_{j-2})$. As the tracing-back examinations along the u stack continue, the loop is performed recursively. Each of the examinations produces a diagonal and a triangular region until the conditions are no longer satisfied. In other words, whenever a new polygonal chain is formed, i.e. the relation (edge) between the latest two consecutive elements of the u stack is changed, steps 4, 5, 6, 7 with $O(n)$ total running time will be executed once. A new u stack is only formed by either adding a new vertex v_i to the polygonal chain or by linking a triangulating diagonal which changes the u stack. Since the input polygonal region Π has an n-side boundary, it must have n-3 triangulating diagonals. Therefore, steps 4, 5, 6, 7 are to be performed at most $n+(n-3)$ times in the worst cases. That is, the running time of the algorithm is in $O(n^2)$. An optimal $\Theta(n^2)$ running time can be attained when the input polygonal region has a convex boundary, because adding a new vertex to the polygonal chain always produces a triangulating diagonal.

3.3.2. Triangulation Algorithm Using Steiner Points

As to the triangulation using Steiner-points, a set of non-overlapping triangular regions which cover the polygonal region are to be produced while some new vertices on the boundary are allowed during the processing and/or on the resulted decomposition. However, only 'triangulation' algorithms without Steiner points on the final decomposition are implemented to the mobile robot's navigation strategy.

(a) Algorithm. A triangulation algorithm with no Steiner points in the final decomposition and without pre-conditioning of the data structure is developed as follows:

Subject: Triangulation of Simple Polygonal Region Π by Sweeping
Input: Boundary of Π: $Bo(\Pi)=v_1v_2...v_{n-1}v_n$ in a counter-clockwise sequence
Output: $T(\Pi)_D=\{D(k) \mid k=1 \text{ to } n-3, D(k) \text{ is a diagonal}\}$
Algorithm:

1. $j\leftarrow 1$; $k\leftarrow 1$
2. $\Pi(1)\leftarrow\Pi$
3. **for** $i\leftarrow 1$ **to** $2n-5$
4. **while** $\Pi(i)$ is not a triangular region
5. **do** call algorithm (Partitioning Simple Polygonal Region $\Pi(i)$)
6. $\Pi(j+1)\leftarrow\Pi_1$; $\Pi(j+2)\leftarrow\Pi_2$
7. $D(k)\leftarrow D$
8. $j\leftarrow j+2$; $k\leftarrow k+1$
9. **next** i
10. **end**

Subject: Partitioning Simple Polygonal Region $\Pi(i)$ with $n(i)$ vertices
Input: Boundary of $\Pi(i)$: $Bo(\Pi(i))=v_1v_2...v_{n(i)-1}v_{n(i)}$ in a counter-clockwise sequence
Output: D is the diagonal; Π_1 & Π_2 that $\Pi(i)=\Pi_1\cup\Pi_2$
Algorithm:

11. examine convexity of $\Pi(i)$: let the first concave vertex examined (internal angle larger than $180°$) in order be v_b
12. **if** $v_b=\varnothing$: $\Pi(i)$ is a convex polygonal region
13. **then** $D\leftarrow S(v_1,v_{\lfloor n(i)/2\rfloor})$
14. $\Pi_1\leftarrow v_1v_2...v_{\lfloor n(i)/2\rfloor-1}v_{\lfloor n(i)/2\rfloor}$; $\Pi_2\leftarrow v_{\lfloor n(i)/2\rfloor}v_{\lfloor n(i)/2\rfloor+1}...v_{n(i)-1}v_{n(i)}$
15. **else** $v_b\neq\varnothing$: $\Pi(i)$ is a concave polygonal region
16. $X\leftarrow\infty$; $S[v_d,v_{d+1})\leftarrow\varnothing$
17. **for** $c\leftarrow 1$ **to** $n(i)$: find the first intersection X of ray $R[v_{b-1},v_b)$ with $Bo(\Pi(i))$
18. **while** $v_c\notin\{v_{b-1},v_b\}$
19. **do** $X(c)\leftarrow R[v_{b-1},v_b)\cap S[v_c,v_{c+1})$
20. **if** $S(v_b,X)\supset S(v_b,X(c))$
21. **then** $X\leftarrow X(c)$; $S[v_d,v_{d+1})\leftarrow S[v_c,v_{c+1})$
22. **else** $X\leftarrow X$; $S[v_d,v_{d+1})\leftarrow S[v_d,v_{d+1})$
23. **next** c

24. **if** $X=v_d$: X is a vertex v_d of $\Pi(i)$
25. **then** $D \leftarrow S(v_b, v_d)$
26. **if** $d>b$
27. **then** $\Pi_1 \leftarrow v_1 \ldots v_b v_d v_{d+1} \ldots v_{n(i)}$; $\Pi_2 \leftarrow v_b v_{b+1} \ldots v_{d-1} v_d$
28. **else** $\Pi_1 \leftarrow v_1 \ldots v_d v_b v_{b+1} \ldots v_{n(i)}$; $\Pi_2 \leftarrow v_d v_{d+1} \ldots v_{b-1} v_b$
29. **else** $X \in S(v_d, v_{d+1})$: X is a point on side $S(v_d, v_{d+1})$
30. $v_f \leftarrow v_{d+1}$
31. **for** $e \leftarrow 1$ **to** $n(i)$: find v_f from vertices contained in $\Delta v_b X v_{d+1}$ which makes $\angle v_f v_b X$ the minimum
32. **while** $v_e \notin \{v_b, v_{d+1}\}$
33. **do** $Y(e) \leftarrow v_e \cap \Delta v_b X v_{d+1}$
34. **if** $Y(e)=\varnothing$: v_f not contained in $\Delta v_b X v_{d+1}$
35. **then** $v_f \leftarrow v_f$
36. **else** $Y(e)=v_e$: v_e contained in $\Delta v_b X v_{d+1}$
37. **case** 1: $\angle v_f v_b X < \angle v_e v_b X \Rightarrow v_f \leftarrow v_f$
38. **case** 2: $\angle v_f v_b X > \angle v_e v_b X \Rightarrow v_f \leftarrow v_e$
39. **case** 3: $\angle v_f v_b X = \angle v_e v_b X$
40. **if** $S(v_b, v_f) \supset S(v_b, v_e)$
41. **then** $v_f \leftarrow v_e$
42. **else** $v_f \leftarrow v_f$
43. **next** e
44. $D \leftarrow S(v_b, v_f)$
45. **if** $f>b$
46. **then** $\Pi_1 \leftarrow v_1 \ldots v_b v_f v_{f+1} \ldots v_{n(i)}$; $\Pi_2 \leftarrow v_b v_{b+1} \ldots v_{f-1} v_f$
47. **else** $\Pi_1 \leftarrow v_1 \ldots v_f v_b v_{b+1} \ldots v_{n(i)}$; $\Pi_2 \leftarrow v_f v_{f+1} \ldots v_{b-1} v_b$
48. **Return**

The algorithm has two parts: a main program from steps 1 to 10 and a sub-routine from steps 11 to 48. By recursively calling the partitioning sub-routine $2n-5$ times in the main program at steps 3, 4, 5, the algorithm continuously divides the polygonal region by its diagonals until a triangulation is achieved. In other words, the algorithm will stop processing when no polygonal regions can be further partitioned. A maximum set of $n-3$ diagonals and $n-2$ triangular regions will be produced.

A set of polygonal regions organised as a binary tree are built up along with the progressing of the algorithm. The root of the binary tree is the input n-vertex polygonal region. When the partitioning sub-routine is performed, one diagonal and two child nodes are produced that each child node represents a polygonal region just attained (divided). In the binary tree, a node is a leaf if it stands for a triangular region. When a triangulation is completed, n-3 diagonals are required according to theorem 3.1 so that $2(n$-$3)$ nodes (polygonal regions), including leaf nodes (triangular regions) and non-leaf nodes (intermediate polygonal regions), are produced. Therefore, the node set of the binary tree totally has $2(n$-$3)$ nodes plus the root, or $2n$-5 nodes. This is why the partitioning sub-routine has to be called $2n$-5 times.

(b) Correctness. The correctness of the algorithm is based on the assumption that an arbitrary polygonal region, except triangular region, can be partitioned into two child polygonal regions by a diagonal. This assumption is obviously true for a convex polygonal region since any vertex-vertex segment is a diagonal of the polygonal region. To complete the correctness, the assumption also has to be verified for non-convex polygonal regions.

Theorem 3.5. For a concave polygonal region, there is at least a diagonal induced from each concave vertex to partition the polygonal region.

Proof: When a polygonal region is not convex as shown in Fig. 3.7, it has concave vertices. Let v_b be a concave vertex in counter clockwise order. Ray $R[v_{b-1},v_b)$ must be inward and intersect the boundary $B_o(\Pi)$ of the polygonal region. Let the first intersection of ray $R[v_{b-1},v_b)$ and $B_o(\Pi)$ be X located on side $S(v_d,v_{d+1})$. If no vertex is included in the triangular region $\Delta v_b X v_{d+1}$, segment $S(v_b,v_{d+1})$ is a diagonal. Otherwise, for all vertices $\{v_f\}$ contained in $\Delta v_b X v_{d+1}$, the vertex making angle $\angle v_f v_b X$ is the minimum that can be connected to v_b by a diagonal. Hence, there is at least one diagonal induced from the concave vertex v_b. Proof is completed. □

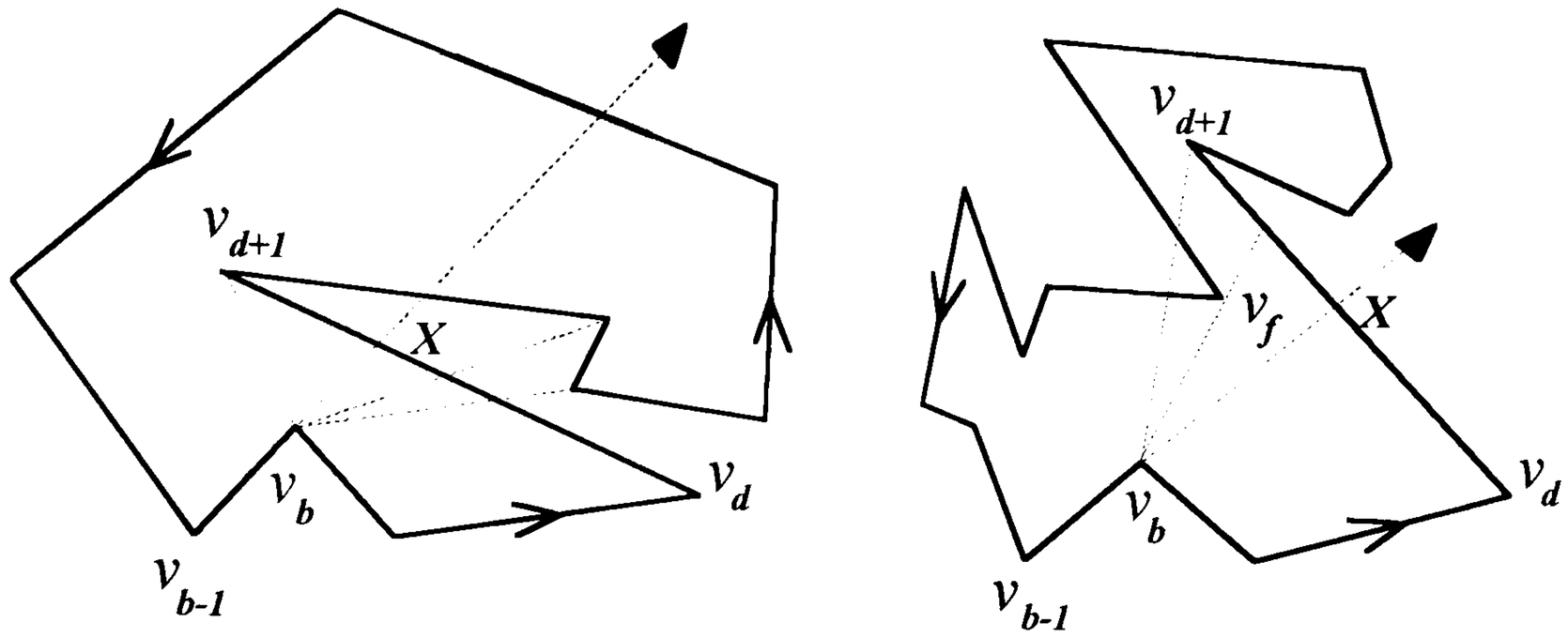

(a) diagonal: v_b & v_{d+1} (b) diagonal: v_b & v_f

Figure 3.7. Partitioning concave polygonal region

During the processing, the algorithm may emit an 'inward' ray from a concave vertex which may intersect the boundary of the polygonal region and cause some Steiner points. However, these Steiner points are only for intermediate use such that the output of the algorithm is a triangulation of the polygonal region.

(c) Complexity analysis. Regarding the complexity analysis of the algorithm when the input polygonal region has n vertices, the storage requirement is the summation of the sizes of all nodes in the binary tree. This can be estimated by multiplying the number of nodes with the upper bound of the node size. Since there are $2n-5$ nodes in the binary tree, each node representing a polygonal region with $O(n)$ vertices, the overall storage space required by the algorithm is a polynomial upper-bounded by $O(n^2)$.

As to the running time analysis, the total running time of the algorithm can be attained consequently if the running time of the sub-routine is computed. The input polygonal region $\Pi(i)$ to the partitioning sub-routine has $n(i)$ vertices, $Bo(\Pi(i))=v_1v_2...v_{n(i)-1}v_{n(i)}$ and $i=1$ to $2n-5$. At step 11, the convexity of $\Pi(i)$ with $n(i)$ vertices is examined to find a concave vertex v_b that $O(n(i))$ running time is required. Steps 12, 13, 14 are for handling convex polygonal regions and $O(1)$ running time is needed to link the diagonal $S(v_1,v_{\lfloor n(i)/2 \rfloor})$. Steps 15 to 47 are for handling concave polygonal regions. From steps 15

to 23, $\Theta(n(i))$ running time is taken to find the first intersection X between ray $R[v_{b-1},v_b)$ and $\mathrm{Bo}(\Pi(i))$. If X is a vertex of $\Pi(i)$, steps 24 to 28 will take $O(1)$ running time to connect a diagonal $S(v_b,v_d)$. Otherwise, X is on a side of $\Pi(i)$. In this case, $O(n(i))$ running time will be required by steps 29 to 43 to find the vertex v_f making angle $\angle v_f v_b X$, the minimum among vertices contained in $\Delta v_b X v_{d+1}$. Finally, steps 44 to 47 connect a diagonal $S(v_b,v_f)$ and take $O(1)$ running time. Step 48 returns the algorithm control back to the main program.

By summing up all individual steps, the running time required to divide a $n(i)$-vertex polygonal region into two components by the partitioning sub-routine from steps 11 to 48 is in $O(n(i))$. Since the partitioning sub-routine is called by the main program $2n-5$ times in step 3, the total running time of the algorithm is

$$\sum_{i=1}^{2n-5} O(n(i)).$$

In other words, the computational time required by the algorithm is upper-bounded by the summation of the upper bounds of all $O(n(i))$.

In the worst case, each $n(i)$, the number of vertices of polygonal region $\Pi(i)$, is in order $O(n)$. Therefore, the algorithm totally takes $O(n^2)$ running time in the worst case. The best result happens when the input polygonal region is convex. The running time of the algorithm is the running time for handling $n-3$ triangular regions, $n(i)=3$ for $i=n-1$ to $2n-5$, plus the running time for partitioning a series of $n-2$ polygonal regions whose vertex numbers are: $n(1)=n$, $n(2)\approx n/2$, $n(3)\approx n/2$, $n(4)\approx n/4$, $n(5)\approx n/4$, $n(6)\approx n/4$, $n(7)\approx n/4$, $n(8)\approx n/8$,..., $n(k)\approx n(\frac{1}{2})^{\lfloor \lg k \rfloor}$,.... That is, using this algorithm to triangulate a n-vertex convex polygonal region requires $O(N)$ running time:

$$N\approx 3(n-3)+n+n/2+n/2+n/4+n/4+n/4+n/4+n/8...$$

$$=O(n)+\lim_{n\to\infty}\sum_{k=1}^{n-2} n\left(\frac{1}{2}\right)^{\lfloor \lg k \rfloor} = O(n)+O(nlgn)=O(nlgn).$$

3.3.3. Feature

Algorithms for triangulating a simple polygonal region Π with and without Steiner points have been developed. Final partitioned triangular regions by the algorithms contain only original vertices of Π, even though there may be Steiner points produced on the boundary of Π during processing. There are also many up-to-date algorithms using other types of triangulating philosophy and of input/output format, such as first decomposing Π into monotone, trapezoid, convex, or star shaped elements, and then triangulating each elements recursively. Although the rate of growth of running time, storage space and the pre-conditioning of data structure of these algorithms are variable, numbers of triangular regions and triangulating diagonals produced are both finite in $\Theta(n)$. These triangulation algorithms are equally adoptable as a tool to triangulate a polygonal region with polygonal holes Π' provided that Π' has been transformed by a pre-processing step, the bridge-building operation, into an equivalent polygonal region. The bridge-building operation will be presented next.

3.4. TRIANGULATING POLYGONAL REGION WITH POLYGONAL HOLES

Although algorithms for triangulating or decomposing simple polygonal regions have been studied for a while, the triangulation of a polygonal region containing polygonal holes has not been fully explored yet. In this section, efforts have been made to define the problem first. Once the polygonal region with polygonal holes has been specified, its

triangulation can be defined in a way similar to that of a simple polygonal region. A computational algorithm for this triangulation is also developed.

3.4.1. Problem Formulation

A polygonal region with polygonal holes Π' is a planar object formed by superimposing a set $\mathbf{H}$ of disjoint closed simple polygons $\mathbf{P}_i$ (corresponding polygonal region Π_i, $1 \le i \le |\mathbf{H}| = h$) on a polygonal region Π (boundary $\mathbf{P}$), so that the overlapping regions, Π with Π_i's, can be treated as polygonal holes in Π. Obviously, Π' has the union of $\mathbf{P}$ and all polygons of $\mathbf{H}$ as its boundary, denoted by $\mathbf{P}'$. In this polygonal region with polygonal holes Π', $\mathbf{P}$ is called the outer boundary, and all $\mathbf{P}_i$'s of $\mathbf{H}$ together are called the inner boundary of Π'. The area between $\mathbf{P}$ and all polygons of $\mathbf{H}$ is the interior of $\mathbf{P}'$. The exterior of $\mathbf{P}'$ is the set of points lying outside $\mathbf{P}$ and in the interior of $\mathbf{P}_i$'s. Vertices (sides) of the polygonal region and the polygonal holes are all vertices (sides) of $\mathbf{P}'$.

$$\mathbf{P}'=\{P|P\in\mathbf{P} \vee P\in\mathbf{P}_i \;\; 1\le i\le h\}$$

$$In(\mathbf{P}')=In(\mathbf{P})-\mathbf{P}_i-In(\mathbf{P}_i),\ \mathbf{P}_i\in\mathbf{H}$$

$$\Pi'=\mathbf{P}'\cup In(\mathbf{P}')=\{P|P\in\Pi \wedge P\notin In(\mathbf{P}_i) \;\; 1\le i\le h\}$$

In terms of the planar triangulation and decomposition of a polygonal region with polygonal holes, all h polygonal holes are assumed to be rigid and can not be penetrated through by any diagonal of Π. Since the interior of $\mathbf{P}'$, $In(\mathbf{P}')$, is the area within $\mathbf{P}$ and outside all h polygons $\mathbf{P}_i$'s of $\mathbf{H}$, definition of the planar triangulation of a polygonal region with polygonal holes Π' needs some adjustment.

Definition 3.19. The triangulation of a polygonal region with polygonal holes Π' is to find a maximum set of non-intersecting diagonals, whose end points belong to the union of vertices of composing polygonal region and polygonal holes, that the interior of Π' is partitioned into non-overlapping triangular regions.

To triangulate a polygonal region with polygonal holes, a pre-processing step, called bridge-building operation, is introduced to transform the original polygonal region with polygonal holes into a region bounded by an equivalent simple polygon. The proposed bridge-building operation facilitates the triangulation of a polygonal region with polygonal holes so that general triangulation algorithms for simple polygonal regions can be directly applied. In addition, the bridge building operation also helps understanding features of the triangulated polygonal region with polygonal holes.

3.4.2. Bridge Building

In graph theory, a bridge of a connected graph is an edge whose removal disconnects the graph. The presented bridge-building operation is similarly defined. To perform the bridge-building operation on a polygonal region with polygonal holes Π', the boundary of Π' is treated as an embedded planar graph $G=(V,E)$ first. G is thus a disconnected planar graph that the outer boundary and the inner boundary formed by the polygonal holes are disjoint sub-graphs (isolated simple cycles) of G. Finding bridges for G in graph theory is to produce a collection of additional edges on elements of V so that G can be transformed into a connected planar graph G'. Similarly, the set of additional edges constructed in the corresponding graph G are also called the bridges of the polygonal region with polygonal holes Π', whose removal disconnects G' and transforms G' back to G. It is obvious that the two end vertices of a bridge belong to different cycle sub-graphs. In addition, each cycle sub-graph should have at least one bridge, otherwise, there are still isolated cycle sub-graphs left to be connected.

Theorem 3.6. All bridges built on a polygonal region with polygonal holes Π' to transform the corresponding planar graph G (boundary) must be diagonals of Π'.

Proof: Since a bridge constructed is an edge linking two vertices on two different cycle sub-graphs of the corresponding planar graph G, it must be an edge linking two vertices of Π'. If an edge produced by the bridge-building operation is not a diagonal of Π', it must cross the boundary (edges of G) and lie on the exterior of Π'. Consequently, the connected graph produced after such an operation is not a planar graph. This is a contradiction. Hence bridges must be diagonals of Π'. Proof is completed. □

When extracting the boundary from a polygonal region Π containing h polygonal holes to form the corresponding planar graph G, a set of $h+1$ disconnected simple cycles can be identified. Obviously, a set of h bridges are required minimally in the bridge-building operation since each of the h inner disconnected cycle sub-graphs has to be de-isolated by at least one bridge. After adding h bridges, all polygonal holes (inner boundary) are connected directly or indirectly to Π (outer boundary).

Definition 3.20. The bridge-building operation for a polygonal region with polygonal holes Π' is to find a minimum set of its diagonals which transform the corresponding planar graph G, formed by the boundary of Π', to a connected planar graph G'. The removal of these constructed diagonals disconnects G' and transform G' back to G.

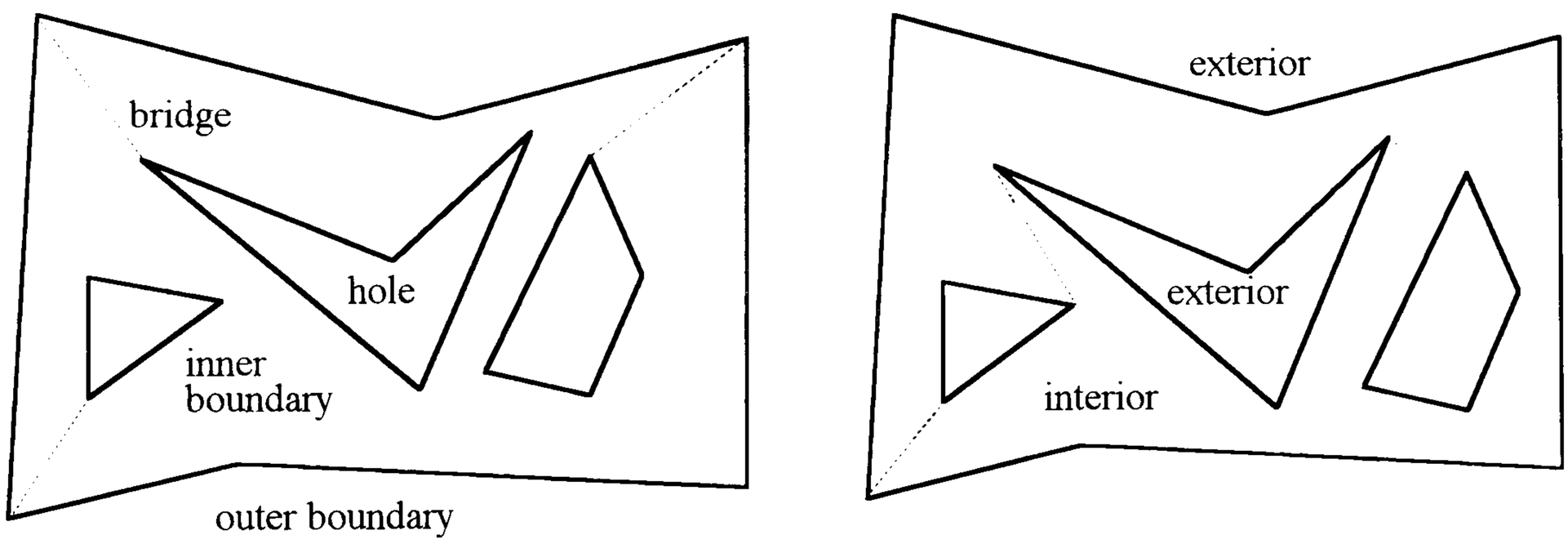

Figure 3.8. Bridge-building operation

Figure 3.8 shows two example ways of building bridges. The purpose of doing the bridge-building operation is to delete isolation of the cycle sub-graphs, each formed by the

inner boundary and the outer boundary of the polygonal region with polygonal holes, and produce an equivalent polygonal region.

3.4.3. Equivalent Polygonal Region

Once the bridge-building operation is performed on a polygonal region with polygonal holes Π' which contains *h* holes, totally *h* bridges are added to de-isolate the inner and the outer boundary. Each bridge is mounted on vertices of two distinct objects, and each polygonal hole is connected by at least one bridge.

Physically, the polygonal region with polygonal holes Π' and the bridges produced can be thought of as a traffic map. A bridge is a dual passage with two lanes each allowing traffic in one direction. A side of the boundary of Π' is a one-way passage, and vertices are junctions connecting one-way and dual passages. Let one start traversing from a point on the outer boundary of Π' in the counter-clockwise manner. Whenever a bridge-mounted vertex (entrance) is encountered, a left turn is taken to enter the 'left' lane of the bridge to leave for another polygonal object. A left turn is taken again when the other vertex (exit) of the bridge is reached. One then embarks on the new polygonal object and continues to traverse around the polygonal object along the boundary until a bridge-mounted vertex is come across. The bridge-crossing is performed again.

By always following the left-turn policy at every bridge-mounted vertices in a counter-clockwise traverse started from the outer boundary, every side and non-bridge vertex of Π' are traversed once, and every bridge and bridge-mounted vertex are passed twice, once in each direction. Finally the traversing converges to the original starting point. If each bridge-mounted vertex is treated as two regular vertices and each bridge is treated as two sides, one at the time encountered, the boundary of Π' and the bridges can be transformed (unfolded) to a corresponding equivalent simple polygon which satisfies definitions 3.9 and 3.10.

Example equivalent simple polygons caused by the bridge-building operations of Fig. 3.8 are illustrated in Fig. 3.9. These corresponding equivalent simple polygons of Π' are formed by 'unfolding' Π' from a bridge-mounted vertex, and consecutively doing so for all bridge-mounted vertices and bridges. Similar to the definition of a simple polygon, the union of an equivalent simple polygon with its interior is a called equivalent polygonal region of the original object Π'.

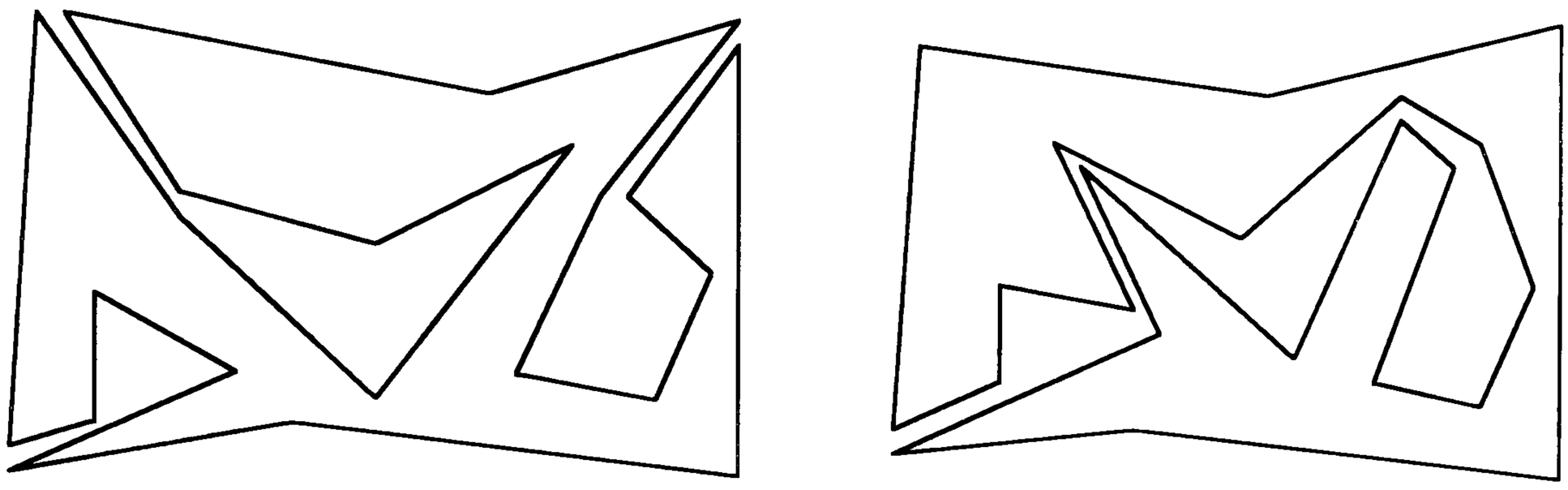

Figure 3.9. Equivalent simple polygons of Fig. 3.8

Theorem 3.7. If a polygonal region with polygonal holes Π' contains h holes and n vertices in total, any equivalent polygonal region of Π' has $n+2h$ vertices.

Proof: In the bridge-building operation, h bridges are added to 'break' and 'unfold' the boundary of Π'. Each bridge is accompanied by two new vertices, and $2h$ vertices in total are inserted into the origin object to form an equivalent simple polygon. Hence the boundary of Π' and the h added bridges can be transformed into an equivalent simple polygon with $n+2h$ vertices. The equivalent simple polygon has the same topology features as a simple polygon. Proof is completed. □

Since an equivalent simple polygon of a polygonal region with polygonal holes is equivalent to a simple polygon, it can be triangulated by regular triangulation algorithms according to theorems 3.1 and 3.2. The triangulation of a polygonal region with polygon holes can consequently be achieved by triangulating its equivalent polygonal region.

3.4.4. Bridge Building Algorithm

Algorithms solving the triangulation of a simple polygonal region have been developed in section 3.3. To triangulate a polygonal region with polygonal holes, the proposed idea is to produce an equivalent polygonal region by a bridge-building operation first. Then those previously developed or mentioned triangulation algorithms can be implemented to the equivalent polygonal region.

(a) Algorithm. A bridge building algorithm is listed as follows:

Subject: Bridge Building for Polygonal Region with Polygonal Holes Π'
Input:
Total vertex and hole number: n and h
Outer boundary of Π': $\mathbf{P}_0=v(0,1)v(0,2)\ldots v(0,n(0))$ in counter-clockwise order
Inner boundary: $\mathbf{P}_1=v(1,1)v(1,2)\ldots v(1,n(1))$, $\mathbf{P}_2=v(2,1)v(2,2)\ldots v(2,n(2))$,..., and

$\mathbf{P}_h=v(h,1)v(h,2)\ldots v(h,n(h))$, each hole in clockwise order, and $\sum_{i=0}^{h} n(i)= n$

Output: $T(\Pi')_B=\{B(k)|\ k=1$ to h, $B(k)$ is a bridge (diagonal)$\}$ and ESP: an equivalent simple polygon
Algorithm:

1. **for** $i\leftarrow 1$ **to** h: for all h holes
2. **do** $v_{minY}(i)\leftarrow$the vertex with the minimum Y co-ordinate among all vertices of $\mathbf{P}_i$
3. **next** i
4. **sort** h holes by their $v_{minY}(i)$: in increasing Y-co-ordinate order and in increasing X-co-ordinate order for equal minimum Y co-ordinates; re-arrange polygons $\mathbf{P}_1$, $\mathbf{P}_2$,..., $\mathbf{P}_h$ according to the order
5. ESP$(0)\leftarrow\mathbf{P}_0=v(0,1)v(0,2)\ldots v(0,n(0))$
6. **for** $i\leftarrow 1$ **to** h: for all h holes in order
7. **do** $q\leftarrow$the first intersection point of $R[v_{minY}(i),-\infty)\cap$ESP$(i-1)$: $R[v_{minY}(i),-\infty)$ is a ray emitting infinitely from $v_{minY}(i)$ along line Y=Y$(v_{minY}(i))$ towards left (X=$-\infty$); Y(q)=Y$(v_{minY}(i))$ and $q\in S[v_{i-1,j},v_{i-1,j+1})$
8. **if** $q=v_{i-1,j}$: q is a vertex of ESP$(i-1)$
9. **then** $B(i)\leftarrow S(q,v_{minY}(i))$
10. **else** $q\in S(v_{i-1,j},v_{i-1,j+1})$: q is on a side of ESP$(i-1)$

11. $v_b \leftarrow v_{i-1,j+1}$
12. **for** $k \leftarrow 1$ **to** n(ESP(i-1)): find v_b from vertices of ESP(i-1) contained in triangle $\Delta v_{minY}(i) q v_{i-1,j+1}$ making angle $\angle q v_{minY}(i) v_b$ the minimum
13. **while** $v_{i-1,k} \notin \{v_{i-1,j+1}\}$
14. **do** $p(k) \leftarrow v_{i-1,k} \cap \Delta v_{minY}(i) q v_{i-1,j+1}$
15. **if** $p(k)=\varnothing$: $v_{i-1,k}$ not contained in $\Delta v_{minY}(i) q v_{i-1,j+1}$
16. **then** $v_b \leftarrow v_b$
17. **else** $p(k)=v_{i-1,k}$: $v_{i-1,k}$ contained in $\Delta v_{minY}(i) q v_{i-1,j+1}$
18. **case** 1: $\angle q v_{minY}(i) v_b < \angle q v_{minY}(i) v_{i-1,k} \Rightarrow v_b \leftarrow v_b$
19. **case** 2: $\angle q v_{minY}(i) v_b > \angle q v_{minY}(i) v_{i-1,k} \Rightarrow v_b \leftarrow v_{i-1,k}$
20. **case** 3: $\angle q v_{minY}(i) v_b = \angle q v_{minY}(i) v_{i-1,k}$
21. **if** $S(v_{minY}(i), v_b) \supset S(v_{minY}(i), v_{i-1,k})$
22. **then** $v_b \leftarrow v_{i-1,k}$
23. **else** $v_b \leftarrow v_b$
24. **next** k
25. $B(i) \leftarrow S(v_{minY}(i), v_b)$
26. ESP(i) $\leftarrow$ ESP(i-1) $\cup B(i) \cup \mathbf{P}_i$: vertices in counter-clockwise order
27. **next** i
28. **end**

(c) Correctness. The correctness of the algorithm is based on the assumption that there is always a bridge induced from the minimum Y-co-ordinate vertex of each polygonal hole.

Theorem 3.8. For a polygonal region with polygonal holes Π' having a hole **H**, there is at least a diagonal (bridge) of Π' connecting the minimum Y-co-ordinate vertex v_{min} of **H** with a vertex of the outer boundary of Π' whose Y co-ordinate is less than v_{min}.

Proof: Let $R[v_{min},-\infty)$ be the ray emitting from v_{min} along line $Y=Y(v_{min})$ toward left infinitely ($X=-\infty$), as shown in Fig. 3.10. Since vertex v_{min} has the minimum Y-co-ordinate among all vertices of **H**, the internal angle of **H** at v_{min} must be convex and $R[v_{min},-\infty)$ intersects with no point of **H**. However, there must be a set of intersection points Q between $R[v_{min},-\infty)$ and the outer boundary of Π'. Let q be the nearest element of Q to v_{min}. If q is a vertex of the outer boundary of Π', segment $S(v_{min},q)$ is a diagonal of Π'. If q is not a vertex, q must locate on a side $S(v_i,v_{i+1})$ of the outer boundary of Π'.

When q traverses along $S(v_i,v_{i+1})$ toward v_{i+1}, segment $S(v_{min},q)$ sweeps across a triangular area $\Delta v_{min}qv_{i+1}$. If there is no other vertex lying inside $\Delta v_{min}qv_{i+1}$, $S(v_{min},v_{i+1})$ is a diagonal of Π'. Otherwise, segment $S(v_{min},v_k)$ is a diagonal where v_k is the first vertex encountered by the sweeping. Hence, v_{min} has at least one edge which is a diagonal of Π' and connects v_{min} to a vertex of the outer boundary of Π'. Proof is completed. □

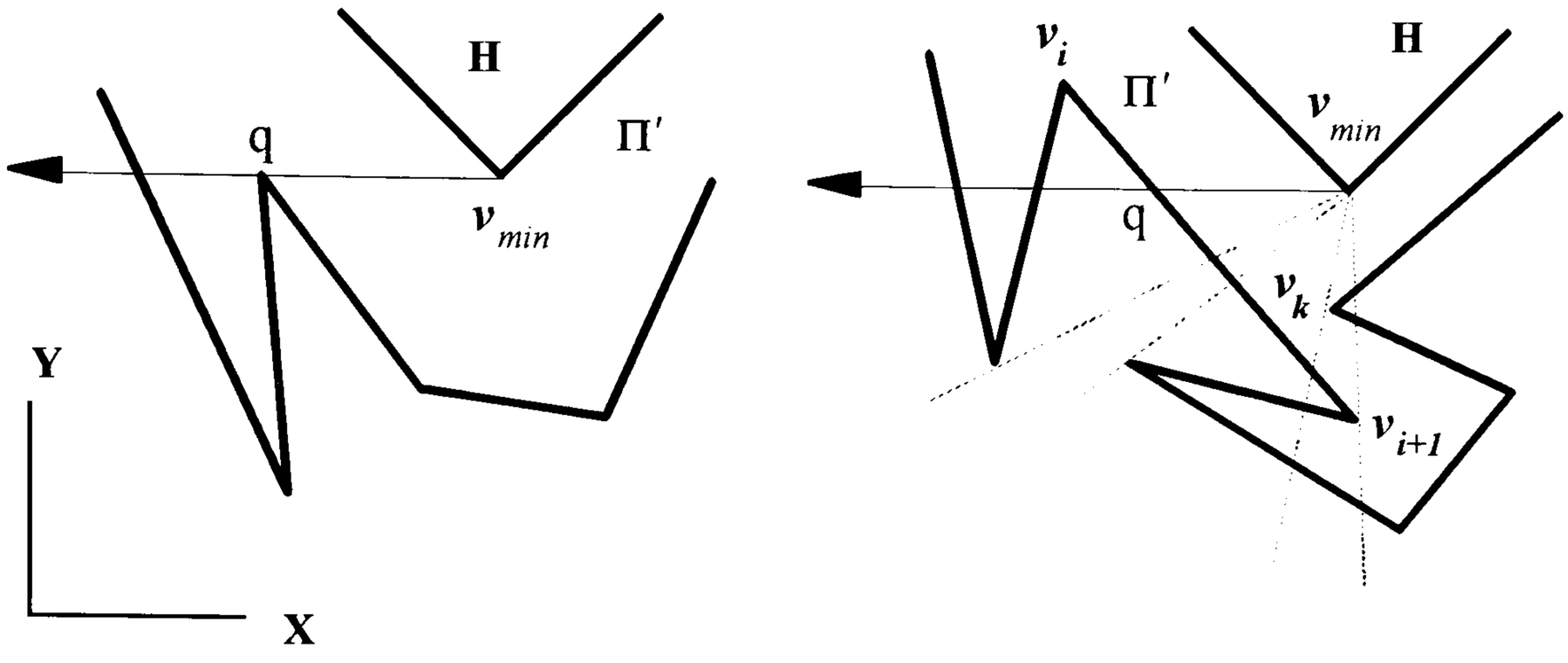

(a) q is a vertex

(b) q is on a side

Figure 3.10. Bridge building algorithm

In theorem 3.8, the case of a polygonal region containing one polygonal hole has been proved. For a general case, step 4 of the algorithm sorts h holes by their $v_{minY}(i)$ in increasing Y-co-ordinate order and in increasing X-co-ordinate order for $v_{minY}(i)$ vertices with equal minimum Y co-ordinates. That is, the bridge-building operation from steps 7 to 26 will be performed on the polygonal holes according to the order. The bridge-building operation is to find a vertex on the current equivalent simple polygon for the minimum Y-co-ordinate vertex of the currently handled polygonal hole to connect with. By recursively proceeding the bridge-building operation h times at step 6, the proposed algorithm can achieve the desired result.

The set of bridges produced are basically a sub-set of the visibility graph [3]. Thus the computational complexity of building bridges should have the similar features of that of constructing a visibility graph.

(c) Complexity analysis. As to the storage requirement, the algorithm has to keep a set of $\Theta(n)$ vertices representing the current equivalent simple polygon and a matrix of vertices of the polygonal region with polygonal holes. Since the matrix has $h+1$ rows (boundary), and each row has $O(n)$ columns (vertices), the total storage requirement is $O(hn)$.

As to the running time analysis, steps 1, 2, 3 are to find the minimum Y-co-ordinate vertex for each of the h polygonal holes, so that $\sum_{i=1}^{h} n(i)$, or $O(n)$, running time in total is required. Step 4 sorts the h polygonal holes and takes $\Theta(hlgh)$ running time by the merge sort algorithm, or $\Theta(h^2)$ running time by the insertion sort algorithm. Steps 6 to 27 are the main part of the algorithm which search for a diagonal (bridge) connecting the minimum Y-co-ordinate vertex of the currently handled polygonal hole and a vertex on the current equivalent simple polygon. Step 7 needs $n(\mathrm{ESP}(i-1))$ operations to find the first intersection q. The decision making steps 8, 9, 10 and the assignment step 11 all take $O(1)$ constant running time. Step 12 calls the inclusion-checking operation from 14 to 23 $n(\mathrm{ESP}(i-1))$ times, while each of the steps 13 to 23 takes $O(1)$ constant running time. Step 25 takes $O(1)$ running time and step 26 needs $O(n)$operations.

By summing up all the operations, $O(n)$ running time is required for each bridge-building operation from step 7 to step 26. Since the bridge building operation is called h times by step 6, or there are h bridges to be built, the running time from steps 6 to 27 is $O(hn)$. To sum up, the total running time of the bridge building algorithm is $O(hn)$.

3.4.5. Algorithm to Triangulate Polygonal Region with Polygonal Holes

The overall algorithm for triangulating a polygonal region with polygonal holes is finally a combination of the bridge-building algorithm and a triangulation algorithm:

Subject: Triangulation of Polygonal Region with Polygonal Holes Π'

Input:

Total vertex and hole number: n and h

Outer boundary of Π': $\mathbf{P}_0=v(0,1)v(0,2)\ldots v(0,n(0))$ in counter-clockwise order

Inner boundary: $\mathbf{P}_1=v(1,1)v(1,2)\ldots v(1,n(1))$, $\mathbf{P}_2=v(2,1)v(2,2)\ldots v(2,n(2))$,..., and

$\mathbf{P}_h=v(h,1)v(h,2)\ldots v(h,n(h))$, each hole in clockwise order, and $\sum_{i=0}^{h} n(i)= n$

Output:

Triangular regions: $T(\Pi')_T=\{\Delta(k)|\ k=1$ to $n+2h-2\}$

Triangulating diagonals: $T(\Pi')_D=\{D(k)|\ k=1$ to $n+3h-3\}$

Algorithm:

1. Building bridge for Π' to produce a set of bridges $T(\Pi')_B$ and an equivalent polygonal region Π''
2. Triangulating equivalent polygonal region Π''
3. $T(\Pi')_T=T(\Pi'')_T$
4. $T(\Pi')_D=T(\Pi'')_D\cup T(\Pi')_B$
5. **end**

3.4.6. Computational Complexity

The triangulation of a polygonal region with polygonal holes is divided into two sub-problems; bridge building and triangulating an equivalent polygonal region, which are solved one after the other successively. The computational complexity is thus the sum of the two individual algorithms. The bridge build algorithm takes $O(hn)$ running time and $O(hn)$ space to produce an equivalent polygonal region. The triangulating algorithm needs $O(n^2)$ running time and $O(n)$ space. Therefore, the algorithm developed to triangulate a polygonal region with polygonal holes totally requires $O(n^2)$ running time and $O(hn)$ storage space.

3.4.7. Feature

The triangulation of a polygonal region with polygonal holes can be done by the algorithm developed above. Some features of this triangulation such as numbers of triangular regions and triangulating diagonals can be specified.

The triangulation of a polygonal region with polygonal holes can be realised by building bridges on the object to transform it to an equivalent polygonal region, as previously discussed. Triangulating this equivalent polygonal region then produces a finite set of triangular regions and triangulating diagonals. The cardinality of the set will be shown to be a function whose arguments are equal to the overall vertex number and the hole number only. The cardinality function is independent of the shape complexity of each boundary and the ways of triangulation.

Theorem 3.9. Let Π' represent a polygonal region with polygonal holes. Suppose that Π' contains a set of h disjoint simple polygonal holes, and has total of n vertices on its boundary. Then Π' can be triangulated into $n+2h-2$ triangular regions by $n+3h-3$ triangulating diagonals.

Proof: An equivalent polygonal region of Π' can be constructed by building h bridges in the interior, with each of the h bridges brings two vertices (a bridge has two ends) to the corresponding equivalent simple polygon. Therefore, the equivalent polygonal region has $n+2h$ vertices. From theorem 3.1, this equivalent polygonal region can be triangulated into $n+2h-2$ triangular regions by $n+2h-3$ triangulating diagonals. Since the interior of Π' is equivalent to the interior of the equivalent polygonal region, Π' should equally have $|T(\Pi')_T|=n+2h-2$ triangular regions after being triangulated. As to the triangulating diagonals, the h edges constructed in the bridge-building operation are also diagonals of Π', and they should be included in the set of triangulating diagonals of Π'. Consequently, the number of triangulating diagonals of Π' is $|T(\Pi')_D|=(n+2h-3)+h=n+3h-3$. That is, Π' can be triangulated into $n+2h-2$ triangular regions by $n+3h-3$ triangulating diagonals, both functions using variables n and h only. Proof is completed. □

Theorem 3.10. The triangulation of a polygonal region with polygonal holes whose total vertex number is n has $\Theta(n)$ triangulating diagonals and $\Theta(n)$ triangular regions.

Proof: Let Π' be a polygonal region with polygonal holes containing h disjoint polygonal holes and having totally n vertices, the triangulation of Π' produces $|T(\Pi')_T|=n+2h-2$

triangular regions and $|T(\Pi')_D|=n+3h-3$ triangulating diagonals from theorem 3.9. Since the simplest form of Π' is a polygonal region containing one polygonal hole and the simplest polygon is a triangle, two inequalities $h\geq 1$ and $n\geq 3(h+1)\geq 6$ must hold. Inequalities $|T(\Pi')_T|=n+2h-2\geq n$ and $|T(\Pi')_D|=n+3h-3\geq n$ can be derived directly. $|T(\Pi')_T|$ $=n+2h-2\leq n+\frac{2}{3}(n-3)-2=\frac{5}{3}n-4\leq\frac{5}{3}n$. Since there exist positive constants $C_1=1$, $C_2=\frac{5}{3}$, and $n_o=6$ such that $0\leq C_1 n\leq|T(\Pi')_T|\leq C_2 n$ for all $n\geq n_o$, thus $|T(\Pi')_T|\in\Theta(n)$. Similarly, $|T(\Pi')_D|$ $=n+3h-3\leq n+(n-3)-3=2n-6\leq 2n$ can be derived. There exist positive constants $C_1=1$, $C_2=2$, and $n_o=6$ such that $0\leq C_1 n\leq|T(\Pi')_D|\leq C_2 n$ for all $n\geq n_o$, hence $|T(\Pi')_D|\in\Theta(n)$. Proof is completed. □

The triangulation of a polygonal region with polygonal holes ($h\geq 1$) produces a set of triangular regions and triangulating diagonals whose cardinality ($6\leq n\leq|T(\Pi')_T|=n+2h-2\leq \frac{5}{3}n-4$ and $6\leq n\leq|T(\Pi')_D|=n+3h-3\leq 2n-6$) is finite and asymptotically tight-bounded by $\Theta(n)$, where n is the total vertex number. The finite cardinality is one of the important features of the triangulation to be adopted by the mobile robot navigation strategy. Figure 3.11 illustrates the rate of growth of the cardinality.

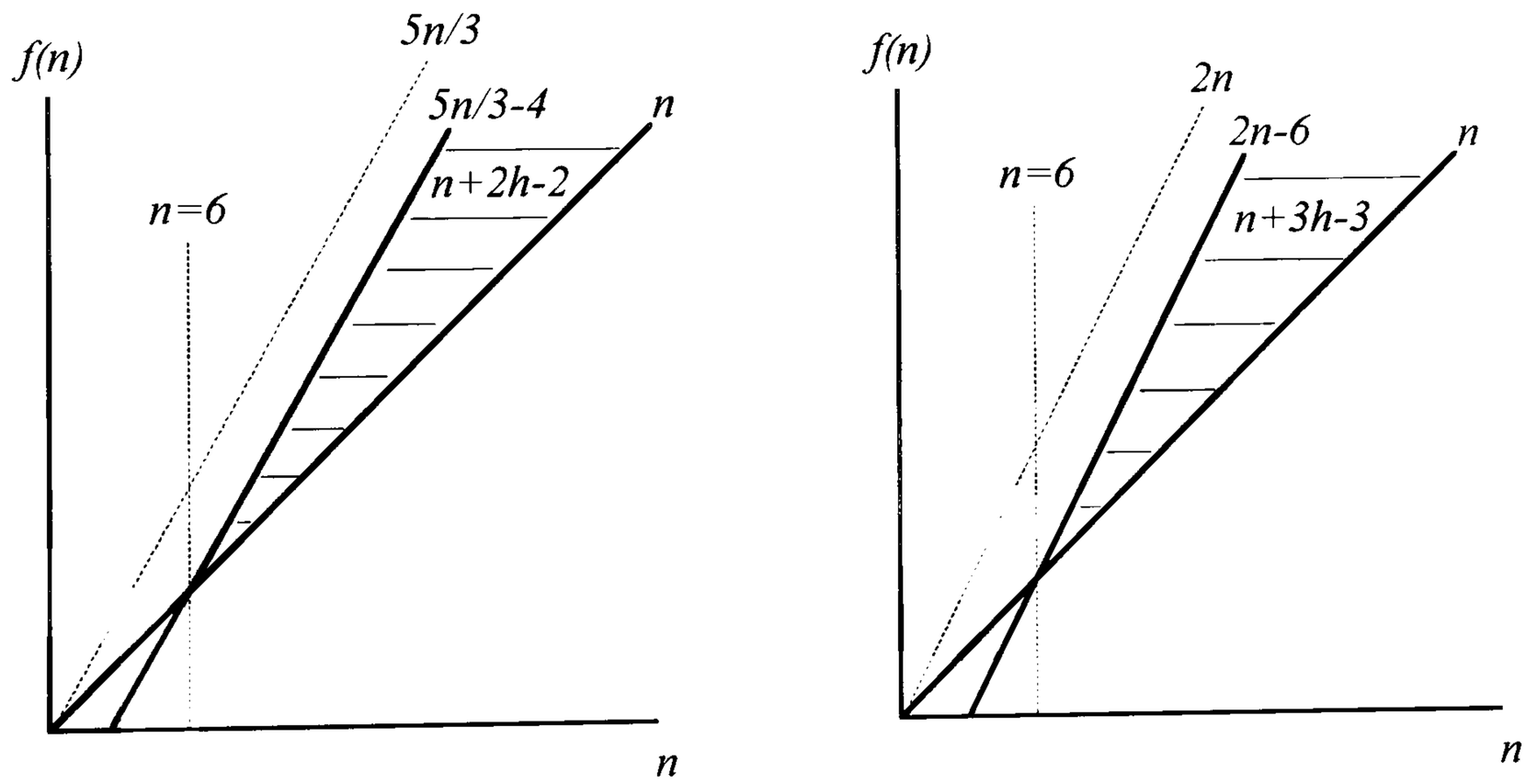

Figure 3.11(a) Rate of growth of triangular regions $\Theta(n)$
(b) Rate of growth of triangulating diagonals $\Theta(n)$

3.5. SUMMARY

A closed simple polygon in a plane is a piecewise-linear curve ending on itself, which is formed by a sequence of sides and vertices. The set of points in the plane enclosed by this polygon forms the interior of the polygon. The set of points surrounding the polygon forms its exterior. And the set of points on the polygon itself forms its boundary.

A triangulation of the region encompassed by a closed simple polygon $T(\Pi)$ is a set T of diagonals of the polygon that divide the polygonal region into disjoint (non-overlapping) triangular regions. In such a triangulation, no diagonals intersect (except at end vertices) and the set of diagonals is maximal. Every triangulation of a n-vertex polygon produces $|T(\Pi)_D|=n-3$ triangulating diagonals which divide the polygonal region into $|T(\Pi)_T|=n-2$ triangular regions. The numbers are both of order $\Theta(n)$.

For the triangulation of a polygonal region with polygonal holes $T(\Pi')$, when the input object has totally n vertices and contains h holes, h bridges are first constructed to de-isolate the inner boundary (polygonal holes) with the outer boundary. An equivalent polygonal region with $n+2h$ vertices is formed, whose features are equivalent to a polygonal region. The triangulation can then be performed on the equivalent polygonal region by the regular polygonal triangulation. The triangulation of a polygonal region with polygonal holes consequently produces a set of $|T(\Pi')_D|=n+3h-3$ triangulating diagonals, where the interior is decomposed into $|T(\Pi')_T|=n+2h-2$ triangular regions. The cardinality of the set is independent of the shape complexity of Π', and is $\Theta(n)$. The triangulation of a simple polygonal region is a special case of the triangulation of a polygonal region with polygonal holes whose contained hole set is $\varnothing$, or $h=0$.

Triangulation algorithms have been presented in this chapter, together with an indication of their computational complexity. In applications described in the following chapters, the algorithms will be used as a fundamental tool for the mobile robot navigation. Since triangles are easy to handle, a navigation strategy of this nature

simplifies tasks, such as testing for intersection, inclusion, etc., required by the spatial reasoning at the planning stage of the mobile robot navigation. It is likely that there will be advanced triangulation algorithms, approaching theoretical optimal triangulating performance, developed in the future. However, the overall computational complexity of navigating a mobile robot will also benefit from these up-to-date developments.

CHAPTER FOUR

PLANNING: SPATIAL REASONING AND ROUTE SEARCHING

This chapter theoretically deals with the planning aspect of the navigation problem faced by the developed flexible material transport system when its mobile robot agent is performing a delivery task. The target is to embody the mobile robot with a navigation planning capability in order to accomplish a given task specified by a start and goal spatial arrangement of the mobile robot. The mobile robot has to automatically decide a feasible route, and an associated operation scheme to move along the route. It should also have functions anticipating various contingencies, and must survive with limited sensing ability.

4.1. GENERAL DESCRIPTION

Generating collision-free motions of acceptable quality is one of the main concerns in robotics. A robot system typically has a manipulative mechanism with a fixed base, or a mobile mechanism, or a combination of the two operating in the three-dimensional Euclidean space. Whatever form it takes, the robot system is expected to move purposely

and safely in an often complex environment filled with obstacles. When mobile mechanisms are involved in the generation of collision-free motions, it is a navigation planning problem. During a navigational task, the entire mobile robot system must not collide with any obstacle, such as machines, other robot systems, or human workers, in the working environment. The purpose of the navigation planner is, therefore, to automatically develop feasible collision-free routes together with associated operation schemes for the mobile robot system to execute.

4.1.1. The Problem

The navigation planning problem for a mobile robot may be basically described as: Given the mobile robot a start posture S and a goal posture G, plan a route and associated operation scheme such that the mobile robot can move along the planned route from S to G using the operation scheme without crashing into any obstacle in the working environment. A posture usually describes the location and heading direction of the mobile robot with respect to a world model.

Inputs to the navigation planner include models of the mobile robot and working environment as well as requirements for the navigation. The model of the mobile robot consists of its geometrical descriptions, such as shape and dimensions, as well as kinematics and dynamics descriptions such as location and orientation, weight, and driving and steering capabilities and constraints. The model of the working environment contains complete geometrical or algebraic descriptions of the workplace for the mobile robot, e.g. features of walls, partitions, and contained furniture and machines. The navigational requirements consist of conditions for the solution navigation to meet. In the most common cases, the navigational requirements involve moving the mobile robot with the minimum required costs.

4.1.2. Related Techniques and Strategies

Planning navigation for a mobile robot has been one of the great fields in robotics for years. In general, researchers apply the problem solving methods and techniques in artificial intelligence to the navigation planning problem to find some compositions of states of the mobile robot, which transform a given initial world model into one that satisfies the intended goal conditions. Existing techniques and strategies are principally surveyed.

4.1.2.1. Configuration Space and Non-configuration Space Formulation

For a mobile robot, its features and working environment consist of a collection of objects, which are expressed in physical terms instead of being explicitly described by mathematical functions. To have the planning calculations performed on computers, transforming from the physical terms into attributes in a mathematical structure is necessary. The configuration space formulation [114][115] is a representational tool to formulate states for the robot motion planning problem.

(a) The philosophy of the configuration space formulation is to treat a mobile robot as a point in an appropriate space, the configuration space of the mobile robot. A configuration of a mobile robot is a specification of the position of every point in the mobile robot relative to a fixed reference frame [116]. The configuration space is, therefore, the union of all configurations of the mobile robot.

Physical concepts such as obstructions can also be represented in the configuration space as additional geometrical constructs. The original navigation planning problem for a mobile robot is consequently transformed into that of planning navigation for a point robot moving in the configuration space. Constructing the configuration space for a mobile robot with many degrees of freedom, and mapping physical concepts onto the

configuration space are expensive computational tasks. However, the complication is compensated by the simplicity of planning navigation for the corresponding point robot.

(b) There are also non-configuration space formulations [117] such as the generalised cone [118]. These formulations transform the physical features of the mobile robot and working environment into direct mathematical structures, using for example an algebraic formulation in the Euclidean co-ordinate system, without the configuration space treatment. A solution navigation can be planned in the mathematical structures in a straight forward manner. However, planning navigation in a straight manner does not imply simplicity. Many factors still need to be considered when planning navigation in these direct mathematical structures. The techniques used usually consist of functions for checking admissibility for the mobile robot, detecting collision with obstacles, and examining continuity of a route. Complicated computational operations are also required.

4.1.2.2. Graph and Field Searching Methods

Once a mathematical representation has been established, the navigation planning can be performed on computers. There are computational methods developed to solve the navigation planning problem in different mathematical representations. According to the ways of treating and searching on the mathematical representations, these methods may generally be classified into graph methods (or road map methods [119]) and field methods.

(a) A graph method solves the navigation planning problem by searching paths on a graph. First, it interprets the free working environment or configuration free space of a mobile robot into a graph. The free working environment or configuration free space is the union space which the mobile robot can safely occupy without overlapping with other objects. The interpretation is accomplished by extracting some distinctive features of the free working environment or configuration free space to form the nodes and edges of the

graph. Two nodes (edges) with the specifically defined spatial relationship are connected by an edge (intersect at a node) reflecting the spatial connectivity of their representing sub-sets of the free working environment or configuration free space. That is, the constructed graph topologically represents the free working environment or configuration free space. Well developed searching algorithms in graph theory [87][120], such as the A* algorithm [121] and the Dijkstra algorithm [122], are finally applied to the representative graph to find a solution graph path connecting the corresponding node elements of the start and goal. There are various ways of extracting spatial features from the free working environment or configuration free space to form a graph. Among them, some representative methods are the visibility graph [123], the Voronoi diagram [124], the free way [125], and the cell decomposition and connectivity graph [126].

(b) A field method deals with the navigation planning problem by a totally different philosophy. The general idea behind field methods is that the goal generates an attraction, which pulls the mobile robot towards the goal, and the obstruction produces a repulsion, which pushes the mobile robot away from the obstruction. Given a suitable field function, a total field value at every location spot of the mobile robot within the free working environment or configuration free space can be calculated. An overall artificial field with gradients towards the goal is then collectively generated. The free working environment or configuration free space is represented by a continuous field model. The negated gradient of the artificial field is treated as the tendency of movement. The navigation of the mobile robot towards the goal is, therefore, performed by always tracking the most descent gradient in the artificial field from the start. The potential field method [127], for example, depicts the free working environment of the mobile robot by a quadratic field function to construct the collision gradients. The potential grid method [128] decomposes the free working environment into fine regular grids such that each grid has an attribute expressing the inclination towards the goal.

4.1.2.3. Global and Local Planning Methods

Techniques solving the navigation planning problem for mobile robots may also be categorised into global and local planning methods. Each category includes provable (or non-heuristic) as well as heuristic methods, and each has its own advantages and difficulties.

(a) Some other names in literature [129] for global planning are the piano movers model, model-based approach, and motion planning with complete information. An important requirement in this category is that full information about the mobile robot and obstacles in the working environment is given in advance, so that the navigation planning becomes a one-time off-line operation. Geometrical information about the working environment is usually presented algebraically, e.g. obstacles are assumed to be polygonal. Global planning methods follow the paradigm of a human cognitive process which is in essence as follows: First, information necessary for the task is collected. A world model as accurate as possible is then built. And finally, a complete solution to the task is found. Only after that does the navigation executing begin. In other words, the navigation executing is seen as a pre-programmed rigid process with little information. Global planning methods could be described as act-after-thinking. The main advantages and disadvantages of global planning methods are all related to the requirement for complete information. In principle, most general planning cases can be handled, and optimal performance can be produced. In terms of applications, global planning methods are at their best in tightly structured environments such as a manufacturing factory. On the other hand, the computational bottleneck is the major weakness of global planning methods. Besides, the open-loop nature of global planning methods makes them brittle in an unstructured and time-changing environment where sensory feedback is essentially vital.

(b) Some other names for local planning are sensor-based motion planning, motion planning with incomplete information, and the South Pole Search model [130][131]. The main feature of local planning methods is that knowledge about the working environment and obstacles is partially known or unknown. This insufficiency is compensated by local on-line information from sensory feedback. Since no detailed model of the working environment is assumed, the navigation planning is done constantly, based on whatever partial information available at the planning moment. The paradigm of this cognitive process could be described as act-while-thinking. An obvious advantage of local planning methods is the capability of dealing with unstructured working environments as well as uncertainties. Since relatively little information is used at a single planning step, the computational resources required, such as memory, are low. On the negative side, having a local planning method with generality and completeness for all applications is elusive, and the global optimality is usually disregarded. Handling multi-dimensional cases and assuring convergence of achieving the destination are also difficult algorithmic issues. In addition, on-line real-time manipulation of sensory signals is a computational difficulty which normally affects the efficiency of, and costs more than, the planning process.

Although the existing navigation planning methods may be thus classified, the seeming incompatibility of the global and local models has not stopped researchers from attempting to combine their advantages while minimising their drawbacks [132][133]. For example, by using the techniques of the graph methods, based on the given, even incomplete, information about the working environment, the navigation planning can be reduced to a simpler problem of following a global physical road map. Once the physical road map has been computed off-line, it can be explored using the potential field techniques which locally quantify the road map. Generally speaking, carefully separating the planning task into sub-tasks requiring respectively global and local information is the crucial part of the development of successful global-local methods.

4.1.2.4. Gross and Fine Planning Methods

Another categor of navigation planning methods is subject to the way of dealing with the uncertainty issues. The use of terms gross and fine is sometimes confused with that of global and local. However, the distinction is described.

(a) Gross planning. In many planning cases, a mobile robot is assumed to be capable of perfectly controlling its mobility mechanism to exactly move along the routes generated by the navigation planner. This assumption is reasonable and realistic when the working environment is relatively uncluttered, and the destination does not have to be achieved too precisely. In these cases, the control uncertainty of the mobile robot can be taken into account by slightly growing the obstacles if such a consideration is necessary. Navigation towards the goal can then be performed rapidly within the free working environment or configuration free space. Methods based on the precise-control assumption, and having the motions planned and executed in such a quick manner, can be classified as the gross navigation.

(b) Fine planning. When the working environment is densely occupied by obstacles, a gross method which slightly grows the obstacles may result in discontinuity of the free working environment or configuration free space, so that collision-free routes to the destination are hindered by the overlapping of the grown obstacles. Moreover, even if the start and goal are within a connected space, executing the planned route may not allow the mobile robot to attain the goal since the passage is narrowly bounded. In such a case, sensing must be intensively incorporated into the navigation planning to properly command corrective motions. The navigation plan, therefore, should consist of a combination of motion commands and sensor readings, which interact to reduce uncertainties and to guide the mobile robot towards the destination with the desired

precision. Such a plan is usually called a motion strategy, and the motions thus produced are called the fine motions. A fine method directs a mobile robot by fine motions.

4.2. NAVIGATION PLANNING

Given a manufacturing environment, a mobile robot navigation strategy for flexible material transportation is developed. Complete knowledge about the spatial arrangement inside the manufacturing environment is presented beforehand for the planning. This prior knowledge can be provided by a user and a computer-aided design system, or obtained through sensing. To develop the strategy, specifications and fundamentals of the navigational task are clearly identified first.

4.2.1. Specifications and Notations

In the application, the mobile robot is the only object moving around in the manufacturing environment. The dynamic properties of the mobile robot are ignored, thus avoiding the temporal issues. Except the contact between the ground surface and wheels, motions are restricted to be non-contact, so that issues related to the mechanical interaction between two physical objects in contact can be disregarded. With these specifications, planning a physical navigation for the mobile robot is essentially transformed into a purely geometrical issue.

A rigid object is an object whose points are fixed with respect to each other. As the mobile robot is a single rigid cylindrical object, constrained to move on the ground surface, and the physical obstruction is caused by obstacles in the manufacturing environment, i.e. other rigid objects that may impede the movement of the robot, the geometrical planning issue can be further transformed to a two-dimensional problem by orthographic projection [134]. In the orthographic projection, all lines of projection are

parallel, and are perpendicular to the plane of projection. The projecting processes will be described next.

4.2.1.1. Orthographic Projection

Assume that there is a two-dimensional Euclidean co-ordinate system embedded in the level ground surface on which the mobile robot is navigating. The Euclidean plane formed is denoted by E, and treated as the orthographic projection plane. Let MR be the orthographic projection image of the mobile robot onto E, Fig. 4.1. Since the mobile robot is a single cylindrical rigid object whose centre axis (height) is perpendicular to the ground surface, MR is a circle with mobility in E. Let OB_0 represent the union image of the orthographic projection of the building of the manufacturing environment onto E. This union image is formed by projecting all parts of the environmental boundary (usually walls of the building), whose altitudes are lower than the height of the mobile robot, onto E. Further let WE be the continuous sub-set of E, bounded by the interior boundary of OB_0. WE is a simple polygonal region. The mobility of MR is thus constrained within WE.

Similarly, all parts of the polyhedral obstacles lower than the height of the mobile robot are projected onto E. These orthographic projection images, denoted by $OB_1,\ldots,OB_h$, are closed simple polygonal regions distributed in E. Since the overlapping images of obstacles or manufacturing environment can be merged into OB_0 or combined into one union image, all produced obstacle images OB_i's are assumed to be disjointed in WE. The collision-free working environment for MR, denoted by WEF, is thus

$$WEF = WE - \bigcup_{i=1}^{h} OBi \,.$$

As a result, the original physical navigation problem for the mobile robot in a manufacturing environment is transformed by the orthographic projection to that of

solving a two-dimensional geometrical issue. Figure 4.1 illustrates the orthographic projection.

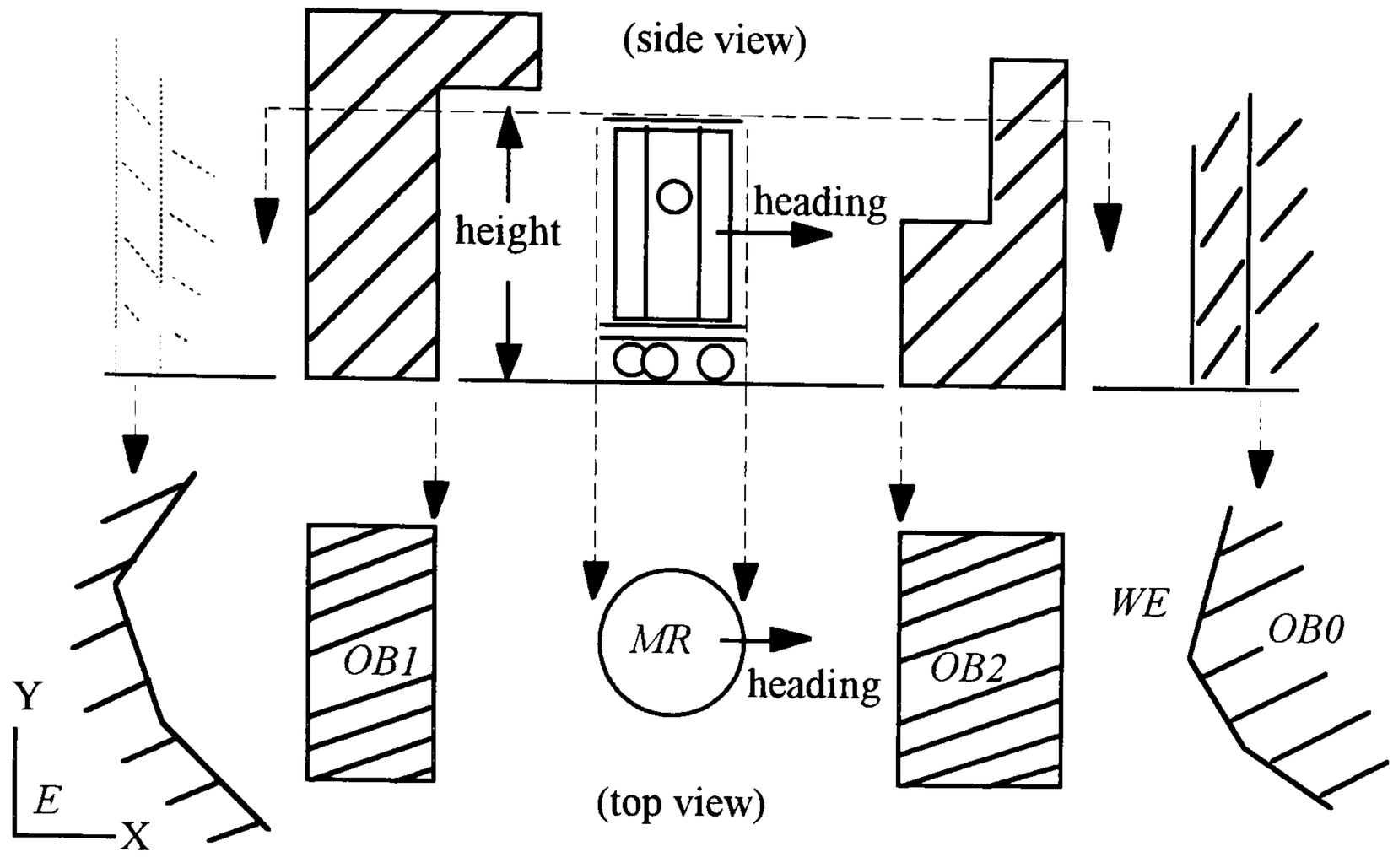

Figure 4.1. Orthographic projection

4.2.1.2. The Geometrical Issue

Since the prior knowledge about the mobile robot, manufacturing environment and obstacles are provided, both the geometry of *MR*, $OB_0,\ldots,OB_h$, and the spatial arrangement of $OB_1,\ldots,OB_h$ with respect to *WE* are known. The navigation of *MR* is only physically constrained by images $OB_0,\ldots,OB_h$ because the mobile robot has an omni-directional mobile mechanism. As described in chapter two, the omni-directional mobile mechanism has a translation (driving) motor and a rotation (steering) motor, which can be independently controlled to move forward and backward, and to revolve at a place about its centre axis. The mobile robot, therefore, is able to park at any location on the ground surface with any heading direction if there is no physical obstruction. In other words, every position and orientation of *MR* with respect to the frame of *E* can be achieved if there are no obstacle images *OBi*'s. A posture, expressing a location and heading direction of the mobile robot with respect to a world model, can be equally used to describe the

position and orientation of *MR* with respect to *E*. Since the mobile robot can always navigate from one posture to another with the omni-directional mobile mechanism, *MR* can be viewed as a free-flying object in the two-dimensional Euclidean plane *E*. However, the navigation between the two postures may be discrete.

The navigation planning problem is consequently re-stated as a two-dimensional geometrical issue: Given an admissible start posture ***S*** and goal posture ***G*** of *MR*, plan a collision-free route in *WE* from ***S*** to ***G***, generate an associated operation scheme which can be used to move *MR* along the route, and report failure if no such route or operation scheme exists. A route describes a trajectory of positions of the centre (the reference point) of *MR* with respect to *WE*. The associated operation scheme includes a continuous sequence of orientations of *MR* corresponding to every position along the route, which starts at the orientation of ***S*** and terminates at the orientation of ***G***. The developed navigation strategy deals with such a geometrical issue first. Once a route and associated operation scheme for *MR* are planned, the mobile robot will derive the required control profiles and operation schedules for its component systems, at the executing stage, to accomplish the plan. Several extensions of the navigation problem involving non-geometrical issues, such as the temporal and kinematics issues, will also be handled at the executing stage. By successfully performing the control profiles and operation schedules, *MR* can move its centre along the planned route such that no physical contact between *MR* and *OBi*'s will occur.

4.2.2. Inspiration and Observation

The development of the mobile robot navigation strategy is inspired from an observation of the navigational pattern of blind people. Having no visual ability, a blind person can access to a desired place in a familiar environment purposely and safely. Using simple aid tools such as a guide cane, he can move around in, for example, his own house or neighbourhood area independently without difficulty. A major explanation seems to be

that some topological maps are kept in mind, which record the corresponding floor layouts. To embody this navigational intelligence of blind people into the mobile robot, it would be helpful to construct a behaviour model of navigation through closely analysing the observation.

(a) Planning: global journey and local route. Take the scene of a blind person moving around in his house. General information about the interior layout of the house, such as the locations and dimensions of the furniture, contained in corridors and rooms, as well as their spatial arrangement is remembered. If then, for example, he wishes to move from the sitting room to the kitchen, he quickly reviews the layout map of the house in his memory to decide first a globally ideal journey. The chosen journey is only a preferable trend of movement, and includes a sequence of segments and passages consisting of, for example, the sitting room, corridor *A*, dinning room and kitchen. Then he begins to move locally in each segment of the decided journey.

In the first segment of the journey which is in the sitting room, he has to move along a safe route starting from his current location towards the first passage, door *A*, that interfaces the sitting room with corridor *A*, the second segment. Being familiar with the interior layout of the sitting room by remembering approximately the geometrical features of the furniture contained, he is likely to plan and then use a collision-free route which has large clearance spaces to the furniture or a short travelling distance. Although the collision-free route may be specified in different forms subject to the individuals and circumstances, it is always performed by a blind person through a sequence of movements and evaluations of locations and heading directions.

(b) Executing: sensing and motion co-ordinating. Without visual information, the sequence of movements and evaluations of locations and heading directions are normally accomplished by using aid tools and associated methods to attain the required surrounding

information and co-ordinated motions. For example, a guide cane is usually used to detect obstacles in front and check clearance when moving straight ahead, and to confirm space availability and sense heading directions when following a curve or making a turn. In order to move through a narrow passage, such as a door or crowded area, the guide cane is usually intensively used to co-ordinate motions. By mainly counting steps and turns made, and/or using a guide cane to help match the physical features of the surroundings with the recorded layout maps, the distance travelled can be estimated, and the localisation can be consequently achieved. Since the environment of the sitting room is basically static and known, the blind person can move towards door *A* purposely and smoothly along the planned collision-free route. Detecting unexpected obstructions and dynamic disturbances is also being carried out in real time while he is navigating in the first segment of the planned journey.

The same behaviour pattern of planning and executing is applied to the subsequent segments and passages of the globally ideal journey, i.e. corridor *A* and the dining room, until the kitchen, or the final segment, is achieved. To complete the entire navigation, a collision-free route in the kitchen is determined to approach the goal position. Getting closer to the goal position, the blind person slows down his movement gradually, and uses the aid tool more intensively to guide his motions. In other words, a compliant navigation behaviour is kept activating until the goal position is reached. The overall navigational task is accomplished through sequentially planning and executing the local route in every segment of the globally ideal journey.

(c) Handling unexpected obstruction. An unexpected obstruction is an object or event, which is not considered at the planning stage but encountered at the executing stage, always causes the discontinuity of the planned navigation. If no unexpected obstruction has been encountered, every local collision-free route within the globally ideal journey can be traversed safely, and the entire navigation from the sitting room to the kitchen can be

accomplished successfully by the described pattern. However, unexpected obstructions beyond the original plan, such as a re-located piece of furniture or a locked door, may happen when performing the planned navigation. In such a situation, the reactive behaviours have to be activated to handle the unexpected obstruction.

An unexpected obstruction generally causes problems at four levels of seriousness. The associated handling behaviours are accordingly different. At the first level, there are enough clearance spaces to bypass the unexpected obstruction, and the blind person can go around it through the clearance spaces to continue the original route. Secondly, the unexpected obstruction can be resolved in order to proceed on the original planned route, e.g. the obstruction moved to one side. At the third level, the unexpected obstruction can neither be bypassed through the clearance spaces nor be solved at the place. Since either the first or second approaches can handle the third situation, a re-planning process is necessary to produce a new route or journey from the obstructed position. For example, a new journey through door *B* via the living room and dining room to the kitchen may be generated and used. At the fourth level, the re-planning is not realisable either, the blind person can only wait until the unexpected obstruction is cleared automatically. He can also call for help and give up trying.

(d) Duplication of behaviour pattern. From the observations described, the main concern of the navigation is to arrive at the kitchen safely. The overall navigational task is accomplished only when the sequence of local routes in the globally ideal journey have been successfully planned and executed. Without the powerful and reliable visual ability, other considerations about cost requirements for the navigation, such as the time spent, are second any to the safety and completeness.

The behaviour pattern is finally modelled in Fig. 4.2.

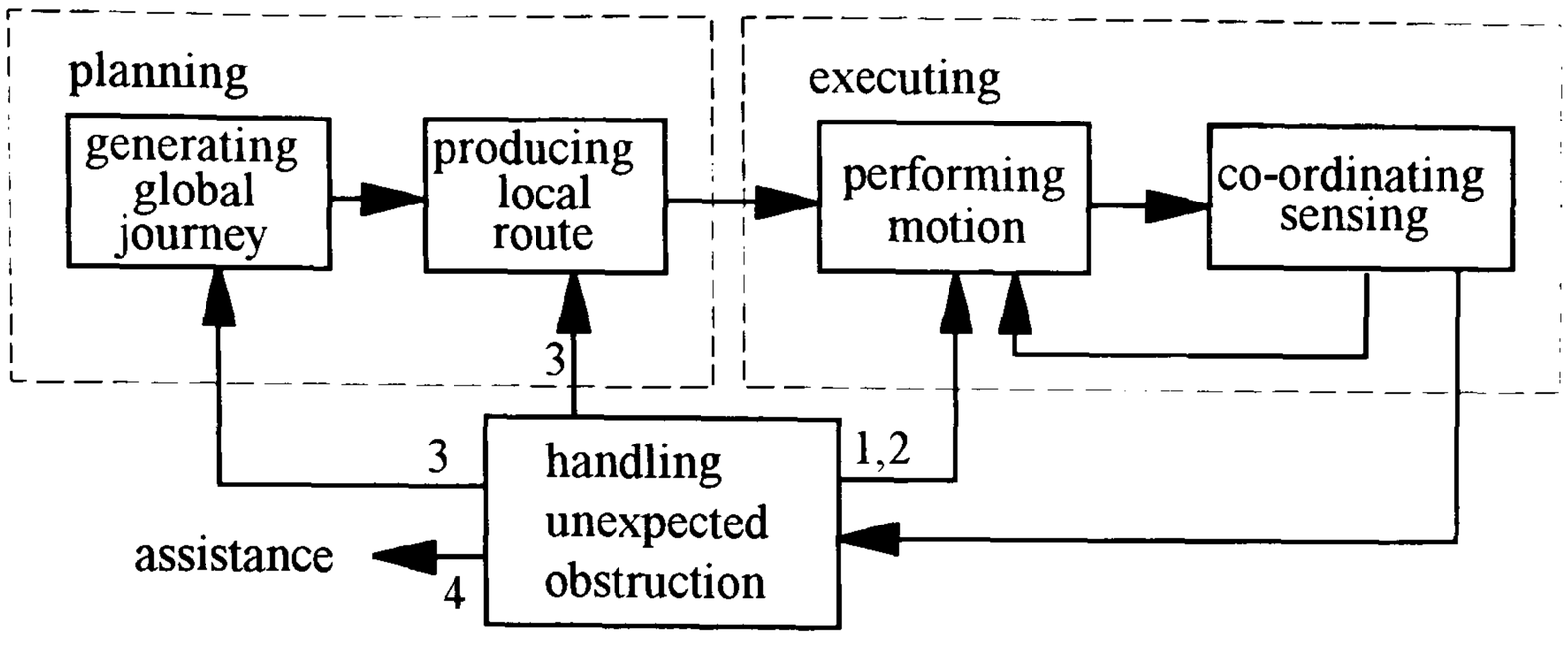

Figure 4.2. Navigation behaviour model

4.2.3. Triangulation Based Strategy

The development of the navigation strategy is to duplicate the kind of intelligence partly which could make the mobile robot resemble the behaviour pattern of the blind person moving around in a familiar environment. Since the mobile robot has a mechanism capable of moving forward and backward and turning at a place about its centre axis, as a human being does, the navigation pattern of the blind person can be a reasonable mobility model for the mobile robot. Therefore, the global journey planning, local route planning, unexpected obstruction handling, motion performing, and sensing co-ordination are all considered as major functions of the developed navigation strategy.

4.2.3.1. Considering Uncertainty at the Planning Stage

According to the survey in section 4.1.2, global navigation is performed when complete knowledge about the working environment is available; local navigation needs the on-line real-time surrounding information to be perceived, and intensively integrated into motion control; gross navigation in a loose environment is expected to be executed at a relatively high speed; and fine navigation with a low executing speed and high precision is required when the navigation is performed in a tight environment. Whatever type of navigation is performed, a fundamental difficulty for a mobile robot is that uncertainties

exist not only at the planning time but also executing time. A mobile robot is subject to the following kinds of uncertainties [38]:

(1) inaccuracy and errors in control,

(2) inaccuracy and errors in modelling, and

(3) inaccuracy and errors in sensing.

The navigation strategy is to find an accessible route and associated operation scheme at the planning stage, and to employ them at the executing stage. To successfully perform a navigational task, uncertainties must be taken into account at both stages. The objective is, therefore, to arrive at the goal even when the mobile robot is unable to perfectly execute the planned scheme along the planned route due to control, modelling and sensing inaccuracies and errors.

To minimise the effects of the imprecision in motion control, a mobile robot should navigate avoiding any physical contact with objects. Some clearance to objects has to be further assured, since the geometry of the mobile robot and working environment is likely to be imprecisely known (the model uncertainty). Besides, sensing is not perfect either and does not provide exact knowledge about the current situations of and around the mobile robot. This requires the best use of the equipped sensors as well as carefully filtering the perceived signals in order to attain as accurate as possible sensory data. This also requires the planner to generate proper routes and associated operation schemes along which the specific features or landmarks of the working environment can be made reliably identifiable by the equipped sensors. Furthermore, it is necessary for the mobile robot to anticipate knowledge that will only be available during the execution, and there should be functions to co-operate the knowledge to achieve the task. As a result, a single motion command is not enough; instead, a navigation strategy involving several motion commands and co-operating sensory input is required.

4.2.3.2. Process and Structure

Although the complete knowledge about the working environment is provided to the mobile robot in advance by the user through a computer aided design system in the flexible delivery applications, the developed navigation strategy attempts to combine the advantages of the global and the local planning while minimising their drawbacks. On the side of the global model, the algorithmic completeness is the aim. On the other side of the local model, the focus is on the computational efficiency. One way to increase the computational efficiency, but retain the algorithmic completeness, is to handle the navigational task by dividing it into sub-tasks requiring respectively global and local information and processing. This implies that only the interesting areas and characteristics of the working environment are recursively taken into deliberate consideration.

The method developed for the navigation planning can be classified as a graph method. It is a duplication of the behaviour pattern, discussed in section 4.2, for the mobile robot. Since the mobile robot can not manipulate geometrical objects directly, modelling the working environment as a mathematical structure in advance is required. The planning processes are structurally divided into spatial reasoning and route searching:

(a) Spatial reasoning. The spatial reasoning is based on partitioning the free space for the mobile robot into a finite set of triangular regions.

(a.1) Establishing numerical model. To deal with the spatial reasoning, the physical working environment is first interpreted as a group of attributes in a suitable mathematical structure recognisable to the computer of the mobile robot.

(a.2) Constructing triangulation graph. The numerical model is then transformed into a triangulation graph whose nodes and edges are extracted from the numerical model by specific transformation functions. The triangulation graph equally represents the topological continuity of the free space for the mobile robot.

(b) Route searching. Once the triangulation graph has been constructed, the corresponding nodes to the start and goal postures are identified. A graph-searching algorithm is then implemented to find a solution path connecting the two nodes.

(b.1) Global journey searching. The solution path on the triangulation graph is called a journey. The produced journey is not yet a physical route for the mobile robot to directly execute. It is only an isolated sub-set of the free space, representing a globally preferable movement trend of the mobile robot towards the goal.

(b.2.) Local route finding. Since the journey physically represents a sub-set of the free space for the mobile robot, the final route to be executed is generated within the journey. Due to the clearance space of the journey, alternative routes can be considered to handle unexpected obstacles and uncertainties.

The route produced is finally interpreted as an associated operation scheme which constitutes the performance of the mobile robot along the route. According to the operation scheme, motion and perception commands will be derived and carried out at the executing stage of the navigation strategy. Although the computational effort is huge when planning navigation for the mobile robot in a large and complicated working environment, the calculation is decreased by carefully and recursively identifying only the parts of the working environment required for global or local considerations.

4.3. SPATIAL REASONING

The spatial reasoning approach adopts the triangulation algorithms developed in chapter three. The configuration space of the mobile robot is identified first, and the physical obstruction mapped onto the configuration space to generate the configuration obstacles. The configuration free space is then partitioned into a continuous set of triangular regions. Specific functions are subsequently used to transform the

triangular regions into a triangulation graph. If the configuration free space of the mobile robot is connected, the triangulation graph is a connected graph. Finally, the start and goal postures of the mobile robot are retracted onto the triangulation graph according to the topological containment.

4.3.1. Establishing Numerical Model

When establishing a numerical model, the configuration space formulation is applied. The configuration free space of the mobile robot is obtained by shrinking the mobile robot to a point, and expanding the physical obstacles accordingly. The navigation problem is thus transformed to that of moving a point robot amongst the enlarged configuration obstacles.

4.3.1.1. Configuration Space of Mobile robot

Six parameters are minimally required to define the status of a free-flying single rigid object in a three-dimensional space; three for the position of a reference point on the object, and three for the orientation with respect to axes passing through the reference point. The mobile robot is a single rigid object with three identical wheels and a hard suspension. Since it is constrained to move on the level ground of the manufacturing environment, the vertical displacement to the ground surface is restricted. In addition, the mobile mechanism can rotate about its centre axis, which is perpendicular to the ground surface, and only one orientation is variable. That is, three constraint equations are generated to reduce the number of the status parameters of the mobile robot from six to three; two for position and one for orientation. The dimensions of the configuration space of the mobile robot are three. This theoretically supports the transformation of the navigation problem for the mobile robot to an equivalent geometrical problem for the projected images, as described in section 4.2.1.1, by using the orthographic projection to define the associated co-ordinate axes.

(a) Choosing reference. Due to the omni-directional mobility, the centre of *MR* is a perfect candidate for the reference point. The three-dimensional configuration space of *MR* is illustrated in Fig. 4.3. A Cartesian co-ordinate frame Fw is embedded in the level ground surface or the projection plane *E*. The origin and two axes are denoted by Ow, Xw and Yw respectively. Another Cartesian co-ordinate frame Fm is attached to *MR*. The origin of Fm, denoted by Om, is superimposed on the centre of *MR*, and the Xm axis is aligned with the heading direction of *MR*. Every point of *MR* has a pair of fixed co-ordinate attributes with respect to Fm, and Fm is a co-ordinate frame moving within Fw. A configuration of *MR* is hence a specification of Fm with respect to Fw.

(b) Configuration and posture. Since the centre of *MR* is identical with Om and the angle between Xm and Xw at any instant is equal to the heading direction of *MR*, a configuration of *MR* can also be equally described by the quantity of the corresponding posture of the mobile robot with respect to the working environment. For example, posture *1* in Fig. 4.3(a) is represented as a triple (a,b,α) where a and b determine the position of the centre of *MR* (origin Om of Fm) with respect to Fw, and α determines the heading of *MR* (orientation of the Xm axis) with respect to the Xw axis. Posture *1* corresponds to configuration *1* in Fig. 4.3(b).

(c) Configuration space. The configuration space of *MR*, denoted by *C*, is the union of all possible configurations of *MR*. The construction of the configuration space *C* of *MR* is a continuous mapping from the projection plane *E*:

$$E \rightarrow C: \boldsymbol{R^2} \rightarrow \boldsymbol{R^3}$$

A point in *E* can be mapped onto a vertical line in *C*. As illustrated in Fig. 4.3(b), a three-dimensional Euclidean frame Fc is embedded in the configuration space *C*, whose axes are denoted by Xc, Yc and Θ respectively. Practically, Xw, Yw and Ow of frame Fw can be

treated as Xc, Yc and Oc of frame Fc directly, and the Θ axis as the axis normal to plane *E* and passing through Ow.

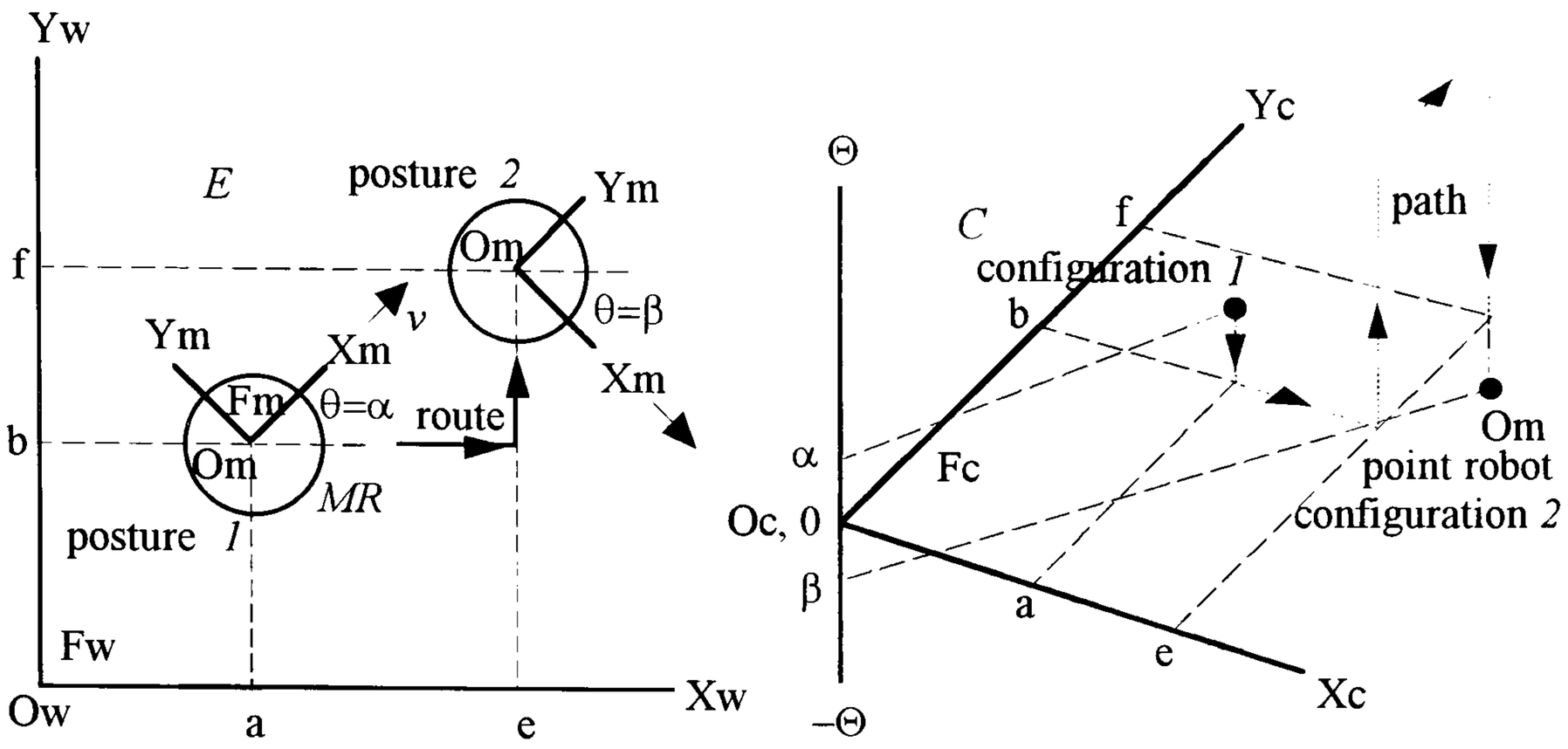

(a) Orthographic projection
Om overlaps with centre of *MR*
Xm aligns with heading of *MR*

(b) Configuration space
A path by discrete navigation

Figure 4.3. Establishing configuration space

Since the mobile robot has an omni-directional mobility mechanism, whose driving and steering motors are independently controlled to move forward and backward and revolve at a place about the centre axis, all configurations (postures of *MR*) in *C* are valid if there is no physical obstruction. The configuration space of *MR* is hence an open three-dimensional space. In other words, every two configurations are continuous in *C* since the two corresponding postures of *MR* can be connected by a route in *E*, although a discrete navigation mode may be required. A path between configurations *1* and *2* in the configuration space is illustrated in Fig. 4.3(b). The route on the ground surface *E* between postures *1* and *2*, as shown in Fig. 4.3(a), corresponds to the path, and the route is performed by the discrete navigation:

turn(-α), move(e-a), turn(+*90*°), move(f-b), and turn(-*90*°+β).

4.3.1.2. Mapping Obstacles onto Configuration Space

Since the mobile robot navigation is physically constrained by objects in the manufacturing environment, images *WE* and *OBi*'s have to be mapped onto the configuration space of *MR*. Let the sub-set of plane *E* occupied by *MR* at a configuration *c* be represented by *MR*(*c*). The configuration obstacle *COBi* in space *C* associated with an obstacle image *OBi* is a region defined by:

$$COBi=\{c\in C|MR(c)\cap OBi\neq\varnothing\},\ COBi\subset C,\ i\in[0,h].$$

The union of all configuration obstacles is called the configuration obstacle region:

$$\bigcup_{i=0}^{h} COBi=\{c\in C|MR(c)\cap\bigcup_{i=0}^{h} OBi\neq\varnothing\}.$$

The configuration free space *CF* is the sub-set of *C* excluding the configuration obstacle region:

$$CF=C-\bigcup_{i=0}^{h} COBi=\{c\in C|MR(c)\cap\bigcup_{i=0}^{h} OBi=\varnothing\}.$$

Since *MR* is constrained to move within *WE*, *CF* should be revised to:

$$CF=\{c\in C|MR(c)\subset WE\wedge MR(c)\cap\bigcup_{i=0}^{h} OBi=\varnothing\}.$$

The configuration free space can also be produced by mapping the collision-free working environment *WEF* onto the *C* space:

$$CF=\{c\in C|MR(c)\subset WEF,\ WEF=WE-\bigcup_{i=1}^{h} OBi\}.$$

A configuration in *CF* is a free configuration whose corresponding posture of the mobile robot is collision free.

In practice, the mapping is performed by the following equations:

$$\forall P\in MR$$

$$Xw(P)=Xw(Om)+(Xm(P)\cos\theta-Ym(P)\sin\theta)$$

$$Yw(P)=Yw(Om)+(Ym(P)\sin\theta+Ym(P)\cos\theta)$$

where P is a point of MR, θ is the heading of MR with respect to Fw, (Xw(Om),Yw(Om)) is the co-ordinates of the centre of MR (origin of Fm) with respect to Fw, and (Xw(P),Yw(P)) and (Xm(P),Ym(P)) represent the co-ordinates of point P with respect to Fw and Fm respectively. The geometrical symmetry of the mobile robot is considered in order to rapidly build the configuration free space for MR. Since MR is a circle and Om is at the centre of MR, the cross section of a configuration obstacle $COBi$ at a fixed orientation θ can be generated by enlarging the dimension of OBi with r units which is the radius of the mobile robot. Constructing $COBi$ is then accomplished by extending the cross section vertically along axis Θ subject to the imposed restriction on the heading of the mobile robot. In the application, the $[\pi,-\pi)$ interval of the steering angles is adopted. The configuration obstacle $COBi$ is hence a tower with 2π height in the three-dimensional configuration space. Figure 4.4 illustrates an example configuration obstacle, and its construction.

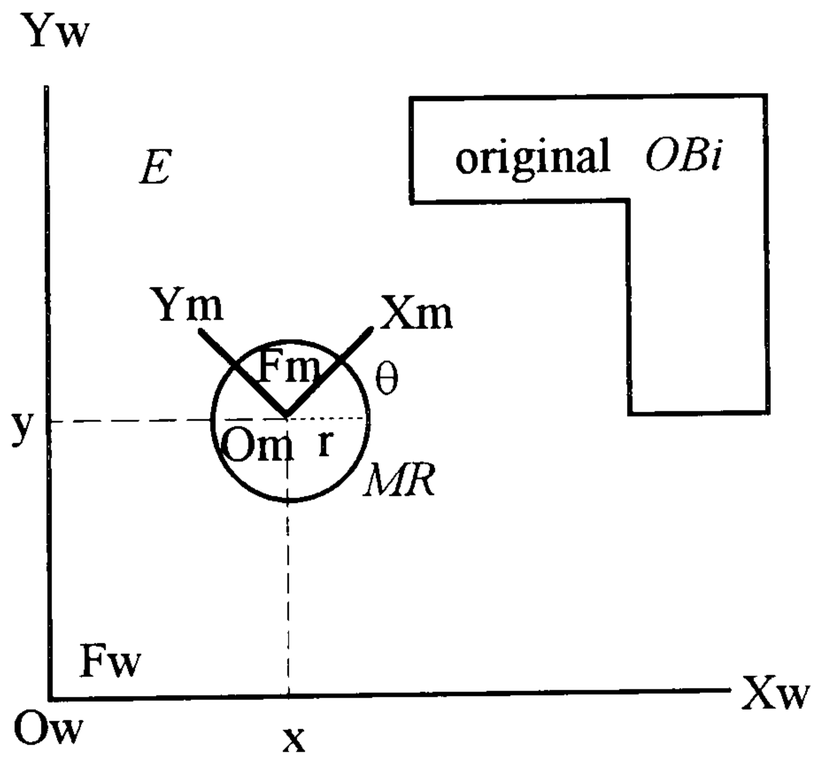

(a) Orthographic projection

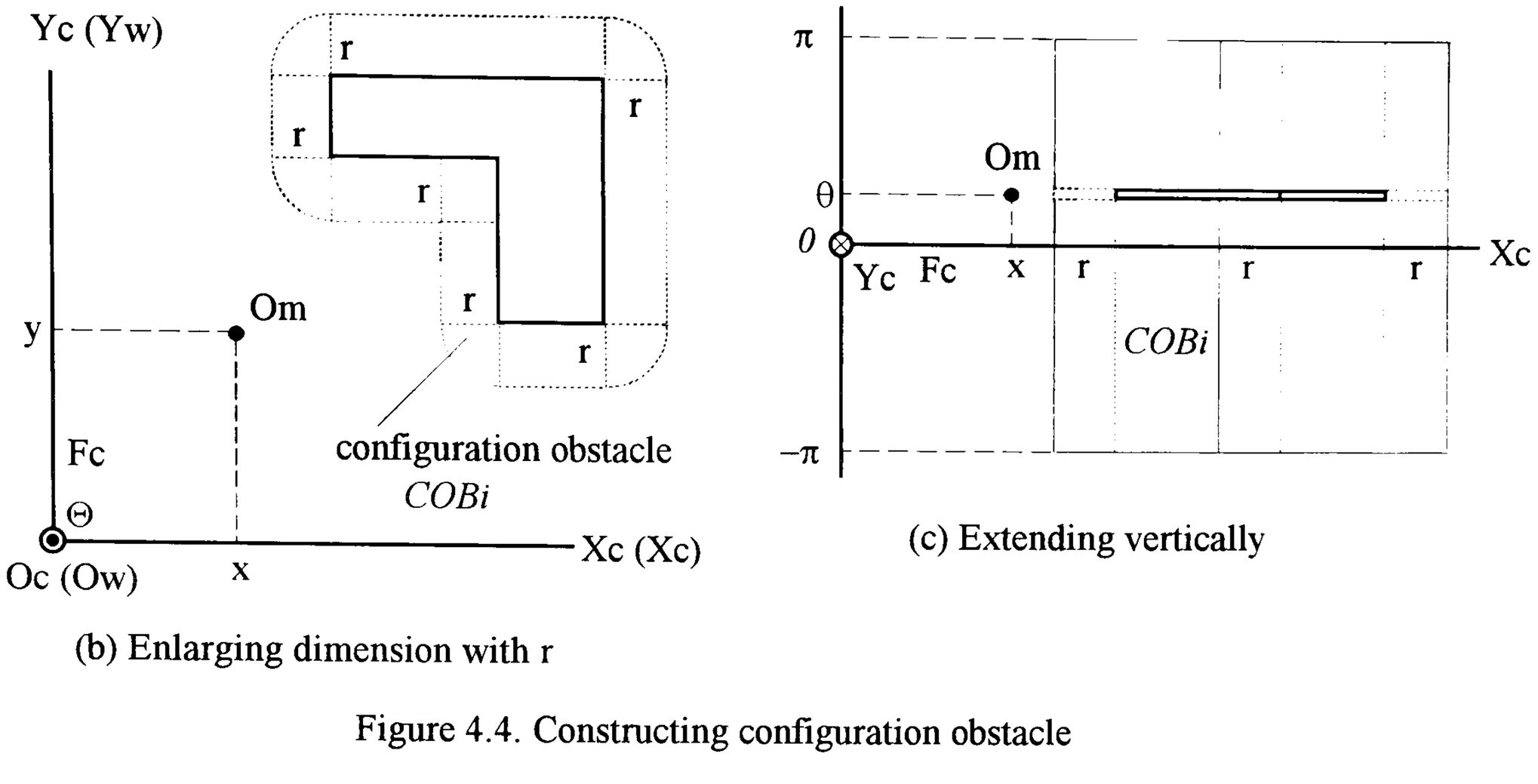

(b) Enlarging dimension with r

(c) Extending vertically

Figure 4.4. Constructing configuration obstacle

4.3.1.3. Polygonal Approximation

It has been learned from section 4.3.1.2 that a convex vertex of an obstacle image results in an arc surface when building the configuration obstacle for the mobile robot. Since directly dealing with arc surfaces is difficult and computationally expensive, most planning methods apply approximation approaches, such as [135], to the arc interpretation. An approximation approach capable of generating prism configuration obstacles is proposed to cut computational costs. The processes of the approach are illustrated in Fig. 4.5 and outlined as follows:

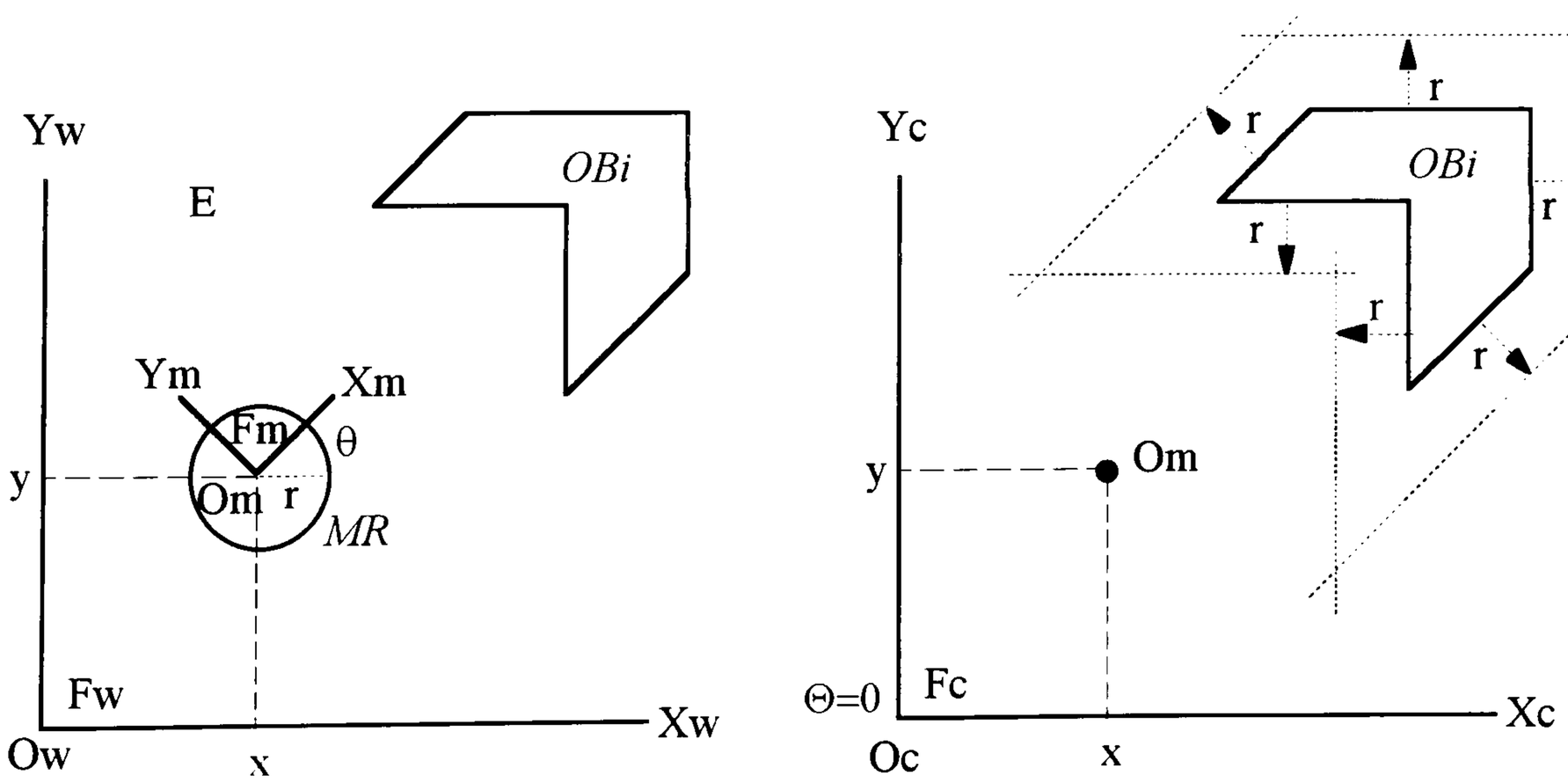

(a) Orthographic projection

(b) Enlarge by radius r

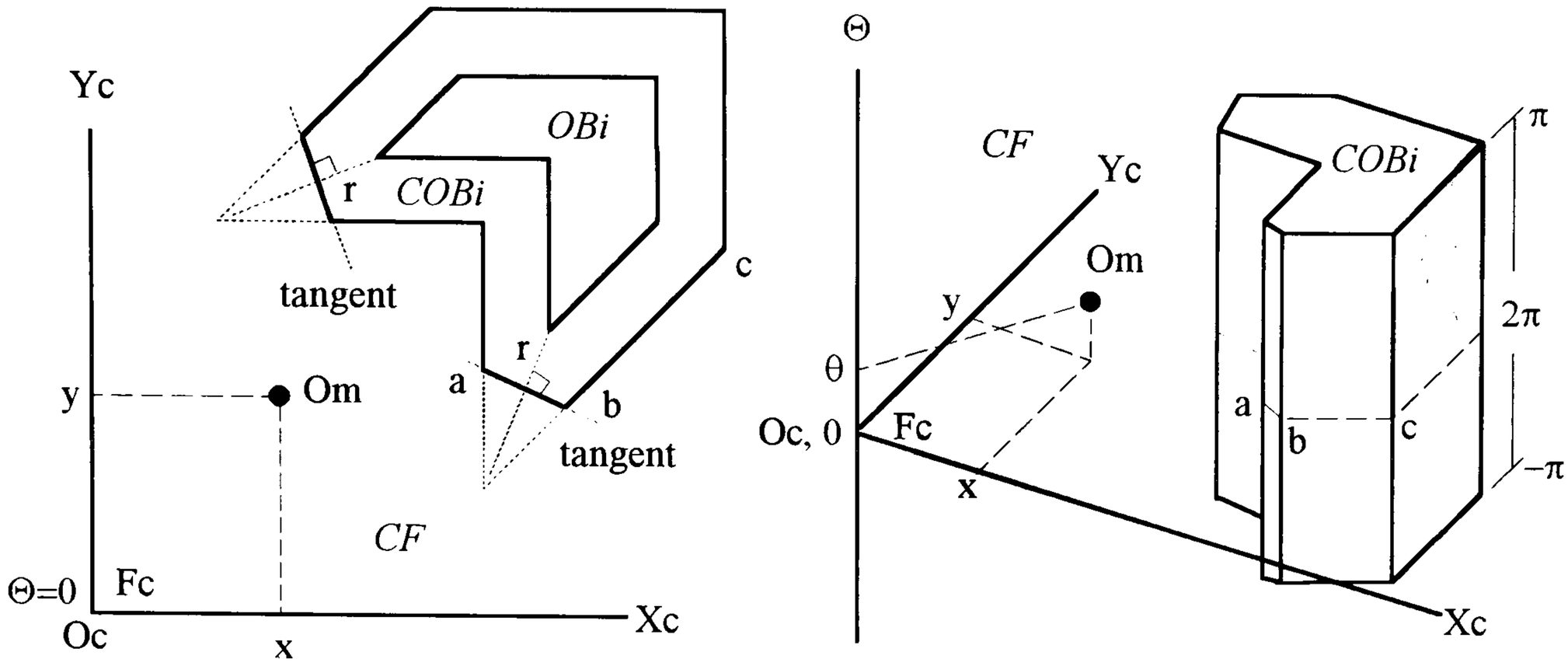

(c) Cut sharpness

(d) Extend vertically

Figure 4.5. Approximated configuration obstacle

(1) Place an obstacle image OB_i on the $\Theta=0$ plane of space C;

(2) Grow each side of OB_i outward in a direction normal to the side by r units to form a corresponding polygonal body at the $\Theta=0$ plane;

(3) Cut sharpness at every convex vertex of the grown polygonal body, whose internal angle is less than the assigned threshold, by drawing a tangent r units away from the vertex of OB_i and removing the sharpness part;

(4) Extend the new polygonal body vertically by module 2π units to the $\Theta=\pi$ and $\Theta=-\pi$ planes to form the approximated prism configuration obstacle COB_i.

As a result, the constructed configuration obstacles are prisms perpendicular to the Xc-Yc plane with the polygonal cross sections and 2π heights. Instead of using circular arcs to connect the corner points, new vertices are created at the intersection of the new sides and tangents. Although a limited space at the corner is sacrificed, the computational efficiency for constructing the configuration free space and the later route planning can be improved significantly. In addition, the configuration free space thus established has the

extra tolerance at the corner to account for the uncertainties of the mobile robot. The space sacrificed by the approximation approach can be reduced by increasing the threshold angle ($90°$ at present) at step **(3)** and recursively performing step **(3)**, but at the expense of the computational efficiency.

4.3.2. Constructing Triangulation Graph

The configuration space formulation is a mathematical representational tool to describe the states of the mobile robot in the environment. Once the mathematical model has been established, computational algorithms can be implemented on it to plan the navigation. The developed navigation strategy treats the mathematical representation as a graph, and searches on the graph to produce a journey for the mobile robot. To construct the graph, transforming the configuration space C into the attributes of the graph is necessary.

4.3.2.1. Triangulating Configuration Free Space

The graph transformation is based on decomposing the configuration free space of the mobile robot. Since the configuration obstacles established in space C are prisms perpendicular to the Xc-Yc plane, with approximate polygonal cross sections and 2π heights, the orthographic projection of the configuration free space CF onto the Xc-Yc plane is a polygonal region containing polygonal holes. Using the triangulation algorithms developed in chapter three, the orthographic projection of CF can be triangulated into a finite set of non-overlapping triangular regions:

(1) Equivalent simple polygon. The bridge-building operation is performed first to transform the orthographic projection of CF into an equivalent polygonal region.

(2) Triangulation. Once the equivalent polygonal region has been produced, it can be triangulated into a set of triangular regions.

Although the triangulation is performed on the orthographic projection of CF, each triangular region actually represents a prism, in the C space, normal to the Xc-Yc plane

and with a triangular cross section and 2π height. CF is thus decomposed into a collection of non-overlapping triangular prismatic spaces whose union is CF. This triangulation of CF is subsequently used as the spatial features of the configuration free space to form a graph, which is called the triangulation graph.

4.3.2.2. Triangulation Graph

To produce the nodes and edges of the triangulation graph $G_T=(N_T,E_T)$ from the triangulated CF, an implicit way of topological modelling is applied:

(a) Node. Modelling the node set N_T is done by extracting some distinctive spatial features of the triangulated configuration free space; each triangular prismatic space being abstractly interpreted as a node. The configuration free space is then represented by a set of nodes.

(b) Edge. The edge set E_T is a binary relation on N_T, which consists of unordered pairs of nodes. A pair of nodes whose representing triangular prismatic spaces are spatially adjacent are connected by a non-directed edge. Two triangular prismatic spaces are spatially adjacent if they share a common facet. The graph is accomplished by connecting edges in the node set, N_T.

The configuration free space of the mobile robot is finally modelled as a non-directed triangulation graph, associated with the triangulation of the orthographic projection of CF. Obviously, the triangulation graph being connected implies that the configuration free space is connected. Since the triangular prismatic spaces are convex, it is easy to find a free path connecting any two configurations in the same triangular prismatic space. That is, all configurations within a triangular prismatic space are qualitatively equivalent. For two configurations, each belonging to one of a pair of adjacent triangular prismatic spaces,

it is also easy to compute a free path connecting them by crossing the facet shared by the two adjacent spaces. In addition, due to the geometrical simplicity of the triangular prismatic spaces, the adjacency of any two triangular prismatic spaces is easy to examine, and the degree of every node of the non-directed triangulation graph is at most three.

Theorem 4.1. Given a collision-free working environment *WEF* with n vertices in total, the triangulation graph constructed is $G_T=(N_T,E_T)$. The node and edge sets of G_T, denoted by $|N_T|$ and $|E_T|$, are both of order $\Theta(n)$.

Proof: Since *WEF* has n vertices, *WEF* has k concave ($k \le n$) and $n-k$ convex vertices. At most the cut-sharpness is performed k times by the approach in section 4.3.1.3. Each operation produces two new vertices to replace the original one. The orthographic projection of the configuration free space *CF* thus produced is a polygonal region with polygonal holes, which has at most $n+k$ vertices in total. Since $n \le n+k \le 2n$, $n+k \in \Theta(n)$. Triangulating the $n+k$-vertex polygonal region with polygonal holes thus generates $\Theta(n)$ triangular regions and $\Theta(n)$ triangulating diagonals according to Theorem 3.10 of chapter three. Every triangulating region is represented by a node in N_T, and every triangulating diagonal corresponds to an edge in E_T. Therefore, $|N_T|$ and $|E_T|$ are both of order $\Theta(n)$. The proof is completed. □

As a result, the numbers of the nodes and edges of the triangulation graph are of the same order of complexity, and both are linear in the number of the vertices of *WEF*.

Figure 4.6 illustrates the processes of the implicit topological modelling and triangulation graph correspondingly constructed.

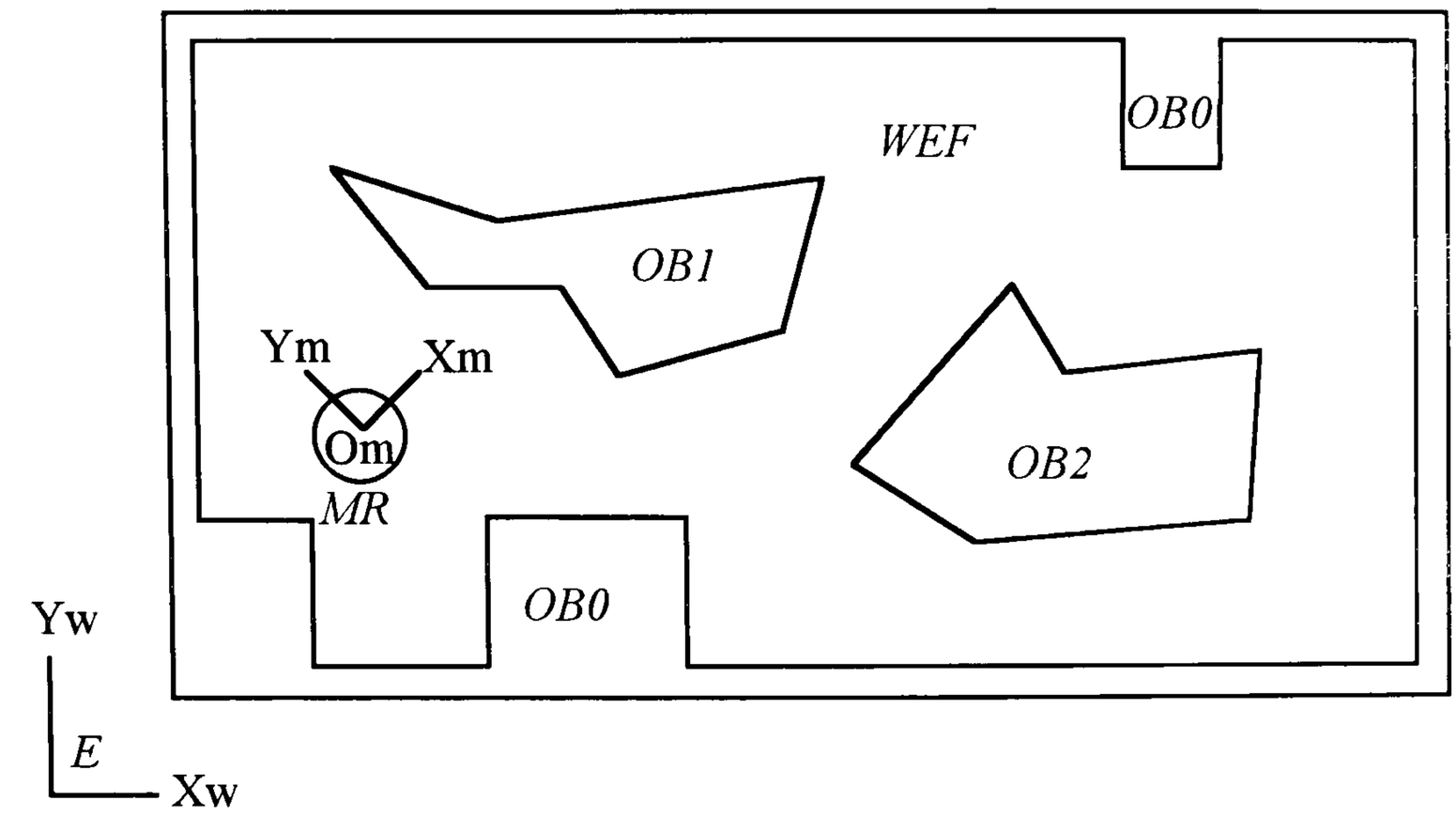

Figure 4.6(a) Orthographic projection of manufacturing environment

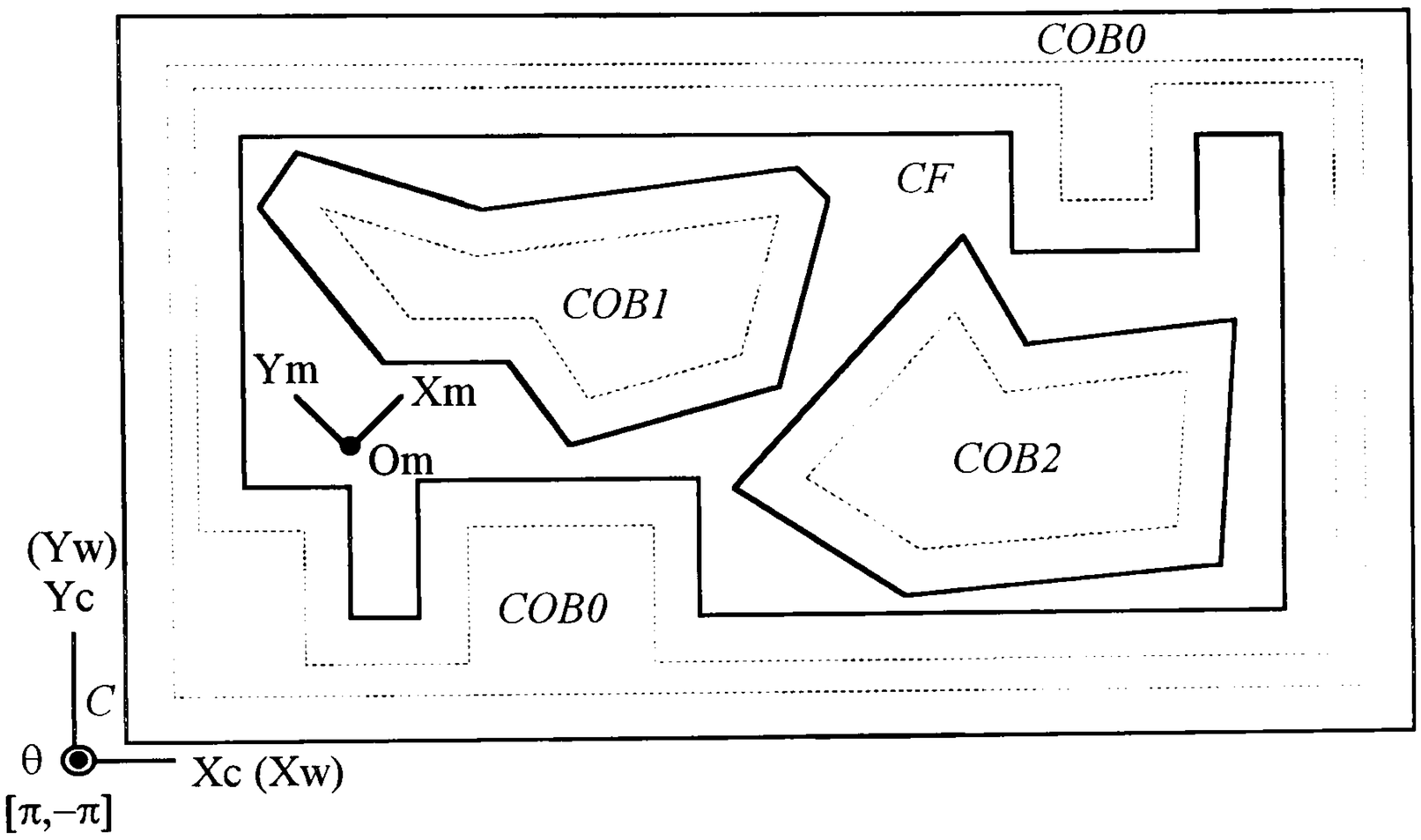

Figure 4.6(b) Orthographic projection of configuration space
n=29, h=2

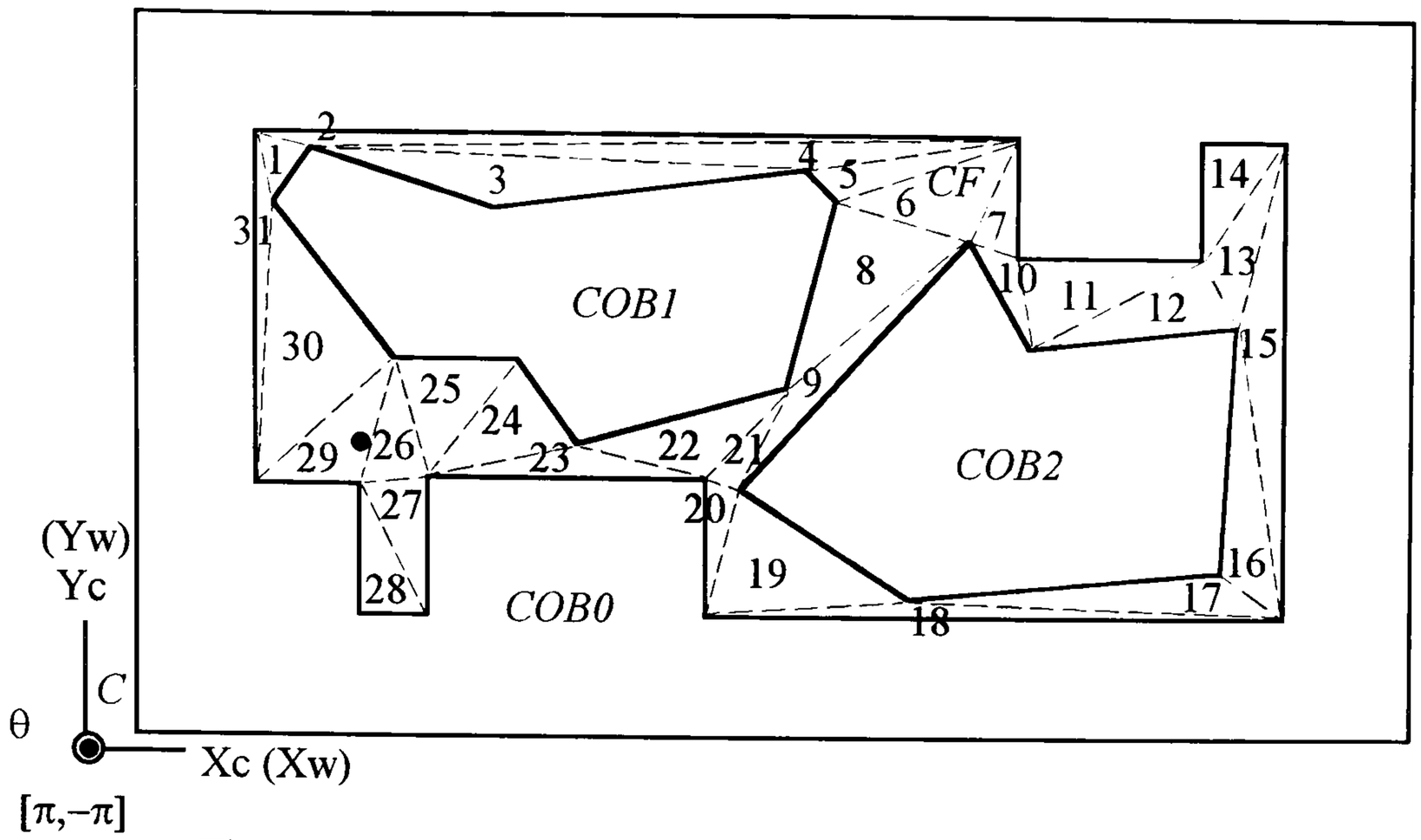

Figure 4.6(c) Triangulation of configuration free space
triangular regions: $n+2h-2$
triangulating diagonals: $n+3h-3$

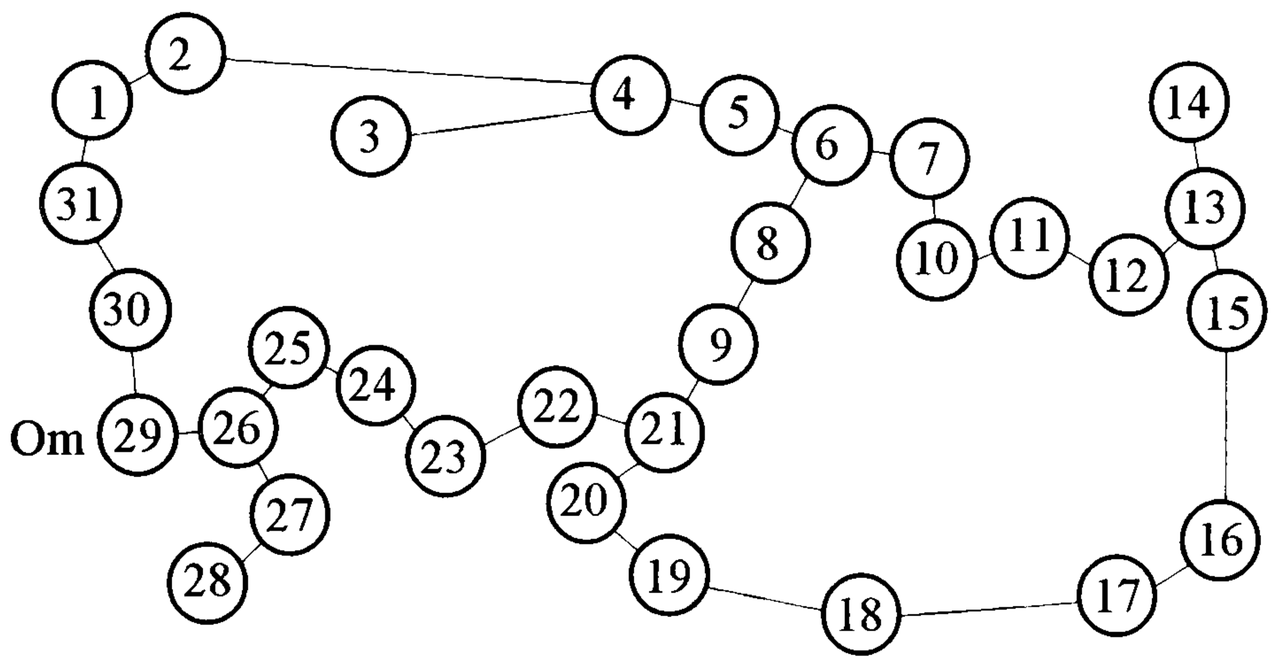

Figure 4.6(d) Associated triangulation graph

The produced triangulation graph G_T physically stands for the adjacent relationship among the triangular prismatic spaces resulted from the triangulation of CF. In other words, G_T consists of an implicit network of one-dimensional edges, reflecting the topological connectivity of the configuration free space. The edges could also be explicitly obtained by selecting a representative point (configuration) for every triangular prismatic space, and joining a physical path between the representative points of every pair of adjacent triangular prismatic spaces. However, the explicit triangulation graph is restrictive since it does not provide the useful information about the clearance space, and

alternative paths, for the mobile robot to deal with the kinematics/dynamics constraints and unexpected obstruction at the executing stage. The implicit triangulation graph is flexible, and the journey searching operation on it will be discussed next.

4.4. SEARCHING FOR GLOBAL JOURNEY

By transforming the configuration free space *CF* of the mobile robot to a non-directed triangulation graph $G_T=(N_T,E_T)$, the navigation planning has proceeded from finding a free path in the configuration space *C* to finding a path in *CF*, and finally to searching for a graph path on G_T. Well developed graph searching algorithms can be applied to the triangulation graph to generate a solution graph path connecting the nodes corresponding to the start and goal configurations (postures) of *MR*. To search for a solution graph path on the triangulation graph, the start and goal configurations of *MR* have to be retracted to the triangulation graph first. A weight function has to be defined to evaluate the weight of every node and edge of G_T so that the graph searching algorithms can be implemented to work on G_T. The solution graph path generated is called a journey, physically representing a globally preferable movement trend of the mobile robot towards the goal. A free path in *C* is finally produced in the journey, consisting of a series of local routes and the associated operation schemes.

4.4.1. Retraction by Point Containment

In the triangulation graph $G_T=(N_T,E_T)$, a node of N_T represents a collection of free configurations of *MR* in *C*, enclosed by the triangular prismatic space corresponding to the node. All configurations within the triangular prismatic space are qualitatively equivalent, and the corresponding collision-free postures of the mobile robot are also represented by the node. Retracting the start configuration (posture) ***S*** and goal configuration (posture) ***G*** to graph G_T is, therefore, equivalent to finding the nodes of G_T whose representing

triangular prismatic spaces contain $\boldsymbol{S}$ and $\boldsymbol{G}$. Such a problem can be solved by performing the point containment test on the orthographic projection of the triangulated configuration free space.

Given a test point and polygon in a plane, the point containment test is to determine whether the point is inside or outside the polygon [134]. In the application, the polygon to be tested is a triangular region. A point P is inside or on the boundary of a triangular region ΔIJK, $P \in \Delta IJK$, if and only if

$$\boldsymbol{A}(\Delta IJK)=\boldsymbol{A}(\Delta IJP)+\boldsymbol{A}(\Delta IPK)+\boldsymbol{A}(\Delta PJK).$$

Point P is outside ΔIJK, $P \notin \Delta IJK$, if and only if

$$\boldsymbol{A}(\Delta IJK)<\boldsymbol{A}(\Delta IJP)+\boldsymbol{A}(\Delta IPK)+\boldsymbol{A}(\Delta PJK).$$

In the equations, $\boldsymbol{A}(\Delta IJK)$ is the area of ΔIJK, computed by:

$$\boldsymbol{A}(\Delta IJK)=\frac{1}{2}\text{abs}\left(\begin{vmatrix} \text{X}(I) & \text{Y}(I) & 1 \\ \text{X}(J) & \text{Y}(J) & 1 \\ \text{X}(K) & \text{Y}(K) & 1 \end{vmatrix}\right),$$

where X(I) and Y(I) are the co-ordinates of point I with respect to the Euclidean frame embedded in the plane.

By comparing the projection images of configurations $\boldsymbol{S}$ and $\boldsymbol{G}$, on the Xc-Yc plane of the C space, with that of each of the triangular prismatic spaces, the triangular prismatic spaces containing $\boldsymbol{S}$ and $\boldsymbol{G}$ can be identified. The representing nodes are subsequently the start and goal nodes on the triangulation graph, denoted by N_s and N_g respectively.

4.4.2. Optimal Global Journey

Once the spatial reasoning has been completed, the implicit triangulation graph can be manipulated to search for the optimal solution graph path. The solution graph path generated is an ordered sequence of nodes and edges beginning from N_s, and terminating at N_g. Since the nodes represent a set of triangular prismatic spaces in CF, and the edges

represent the adjacency of these triangular prismatic spaces, the solution graph path spatially describes a channel of configuration free spaces containing the start and goal configurations. No explicitly physical route is planned directly from the triangulation graph, instead a global journey representing a connected subset of CF. The final collision-free navigation of the mobile robot, from postures $\boldsymbol{S}$ to $\boldsymbol{G}$, can be planned in the global journey as a path in the channel of configuration free space. To use graph searching algorithms, a weight function has to be defined to evaluate the triangulation graph.

4.4.2.1. Weighted Triangulation Graph

A weighted triangulation graph $G_T=(N_T,E_T)$ is a graph on which every edge has an associated weight, typically given by a weight function W: $E_T \rightarrow \boldsymbol{R}$ mapping the edges to real-valued weights:

$$\begin{cases} W(N_1,N_2) & \text{if } N_1,N_2 \in N_T \text{ and } E_{1,2}=(N_1,N_2)\in E_T \\ 0 & \text{otherwise} \end{cases}$$

The weight of a graph path $P_G=(N_0,N_1,\ldots,N_k)$ is the sum of the weights of its constituent edges:

$$W(P_G)=\sum_{i=1}^{k} W(Ni\text{-}1,Ni), \text{ where } Ni\in N_T \text{ and } (Ni\text{-}1,Ni)\in E_T \text{ for } i=1 \text{ to } k.$$

The optimal weight from N_1 to N_2 is defined by

$$\delta(N_1,N_2)=\begin{cases} \min\{W(P_G): N_1 \text{—} P_G \rightarrow N_2\} & \text{if there is a graph path } P_G \text{ from } N_1 \text{ to } N_2 \\ \infty & \text{otherwise} \end{cases}$$

A graph path with the optimal weight is the shortest graph path. The shortest graph path from the start node N_s to goal node N_g in the weighted triangulation graph is hence defined as a graph path P_G whose weight is optimal:

$$W(P_G)=\delta(N_s,N_g).$$

Obviously, there is no loop in the shortest graph path P_G from N_s to N_g, $P_G=(N_s,\ldots,N_g)$; otherwise, the generated optimal weight from N_s to N_g is not the optimal, and can be further reduced:

$$N_i,N_j\in\{N_s,\ldots N_g\}\Rightarrow N_i\neq N_j$$

Although the shortest graph path generated on the weighted triangulation graph is not the route to be directly executed by the mobile robot, it is still useful to have the optimal weight indicating the minimum costs for reference, that may be expected at the executing time. To determine the weight function for an edge between two adjacent nodes for this purpose, the physical contents of the edges have to be defined. In other words, the motion principles concerning how the mobile robot performs the navigation from one triangular prismatic space to an adjacent one should be realised.

4.4.2.2. Motion Principles

As described in chapter two, the mobile robot has a mechanism which can move forward and backward, and revolve at a place about the centre axis, and supports two navigation modes; continuous and discrete. In terms of realising the physical contents of the edges of the triangulation graph in order to define the weight function, the discrete navigation mode provides a better reference indication of costs, and is more essential, than the continuous mode.

In the discrete navigation mode, the moving and steering motions of the mobile robot are performed at different time intervals. That is, the translation distance and the angular displacement of *MR* between two configurations (postures) are considered independently. There is no change in the heading direction of the mobile robot while the translation motor is working:

$$\frac{d\theta}{d\,\mathrm{D}}=0\wedge\frac{d\mathrm{D}}{dt}\neq 0\ \therefore\ \omega=\frac{d\theta}{dt}=0\ \text{or}$$

moving straight $\therefore \frac{d\mathrm{Yc}}{d\mathrm{Xc}}=\frac{d\mathrm{Yw}}{d\mathrm{Xw}}=\tan\theta=\text{constant} \therefore \frac{d(\tan\theta)}{dt}=0 \therefore \omega=\frac{d\theta}{dt}=0$;

and vice versa, $v=\frac{d\mathrm{D}}{dt}=0$ while the rotation motor is working; where

$$(d\mathrm{D})^2=[(d\mathrm{Xc})^2+(d\mathrm{Yc})^2]=[(d\mathrm{Xw})^2+(d\mathrm{Yw})^2].$$

Figure 4.7 illustrates the motion schedule of the discrete navigation in Fig. 4.3, where the total performing time of the navigational task is divided into a series of time intervals.

Rotation displacement	$-\alpha$	*0*	+90	*0*	$-90+\beta$
Translation distance	*0*	e-a	*0*	f-b	*0*

beginning t1 t2 t3 t4 termination

(performing time)

Figure 4.7 Motion schedule of discrete navigation

Apart from the motion principles concerning the movement of *MR* using the discrete navigation mode, no slippage is assumed in the application. The kinematics constraint defining the no-slippage condition is

$$(d\mathrm{Xw})\sin\theta-(d\mathrm{Yw})\cos\theta=0.$$

Since $d\mathrm{Yw}=v\sin\theta=d\mathrm{Yc}$ and $d\mathrm{Xw}=v\cos\theta=d\mathrm{Xc}$, $(d\mathrm{Xc})\sin\theta-(d\mathrm{Yc})\cos\theta=0$.

In the above equations, v and ω are the instantaneous translation velocity and orientation velocity of the mobile robot respectively, t is the time, and all the other terms are subject to Fig. 4.3.

As a result, there are only horizontal and vertical movements while the point robot is moving in the configuration space by the discrete navigation mode. To resolve a path, produced in the configuration space, into a route and associated operation scheme, the horizontal parts of the path constitute the route, and the vertical parts the associated operation scheme. In other words, the route describing the trajectory of the centre of *MR* in *WE* consists of a sequence of straight-line segments in the *E* plane. The associated

operation scheme consists of a continuous sequence of orientations of *MR* along the route, which are constant along a straight-line segment, and change only at the intersection of two consecutive straight-line segments.

4.4.2.3. Graph Searching Algorithm

Before the weight function is defined, graph searching algorithms are discussed in order to realise how the weight function is applied in the algorithms. Given the weighted triangulation graph evaluated by the defined weight function, the graph searching algorithms are implemented on it to search for the optimal graph path. The graph searching algorithms can be outlined as follows:

(1) Put start node N_s on a list called OPEN and compute $f(N_s)$

(2) If OPEN is empty, exit with failure; otherwise continue.

(3) Remove from OPEN the node whose f value is the smallest and put it on a list called CLOSED. Call this node N_i. (Resolve ties for minimal f values arbitrarily, but always in favour of the goal node).

(4) If N_i is the goal node N_g, exit with the solution graph path obtained by tracing back through the pointers; if N_i is on CLOSED, go to **(2)**; otherwise continue.

(5) Expand node N_i by finding all of its successors. [If there are no successors, go immediately to **(2)**.] For each successor N_j, compute $f(N_j)$ by $f(N_j)=f(N_i)+W(N_i,N_j)$. Put these successors on OPEN, associating with them the f values just computed, and provide pointers back to N_i.

(6) Go to **(2)**.

In the steps outlined, the OPEN list contains a set of nodes to be The set of nodes and pointers, generated by the algorithms, forms a tree (the search tree) with the nodes on OPEN at the tips of the tree. The weight function $W(N_i,N_j)$ is used to define

the required cost from nodes N_i to N_j along the edge (N_i,N_j). Providing that the cost to achieve a node N_i is $f(N_i)$, the cost to achieve its successor node N_j through the edge (N_i,N_j) is $f(N_i)$ plus $W(N_i,N_j)$, and denoted by $f(N_j)$. The CLOSED list maintains a set of nodes whose final optimal weights from N_s have already been determined.

The Dijkstra algorithm [121][122] is a typical example of such a graph searching algorithm. The running time for the Dijkstra algorithm is $O(|V|^2+|E|)$ provided that the input graph has |V| nodes and |E| edges, and can be modified to $O((|V|+|E|)\lg|V|)$ [83]. Another example is the A* algorithm [121] which uses α heuristic function to improve the computational efficiency. It works by replacing the f function, $f(N_j)=f(N_i)+W(N_i,N_j)$ at step **(5)**, with a new one, $f(N_j)=g(N_j)+h(N_j,N_g)$. In the new f function, $g(N_j)$ is the actual cost from N_s to N_j produced by adding the weight $W(N_i,N_j)$ to the actual cost from N_s to N_i, denoted by $g(N_i)$, and $g(N_j)=g(N_i)+W(N_i,N_j)$. $h(N_j,N_g)$ is the heuristic function indicating an approximated cost from N_j to N_g. It has been theoretically shown that the A* algorithm is efficient as long as the heuristic function is a lower bound of the actual cost [121]. The A* algorithm becomes an ordinary one if the heuristic function is assigned to be zero. The Euclidean distance is usually used to define the heuristic function in the navigation planning.

4.4.2.4. Weight Function

Two free configurations are connected if and only if they are linked by a free path. In the configuration space C of MR, a free path between two connected free configurations $\boldsymbol{S}$ and $\boldsymbol{G}$ is a continuous map Pc: $[0,1]\rightarrow CF$, CF is the configuration free space with $Pc(0)=\boldsymbol{S}$ and $Pc(1)=\boldsymbol{G}$. Since Pc is produced using the discrete navigation mode, Pc should consist of a sequence of horizontal straight-line segments at different Θ planes of space C, and vertical straight-line segments connecting the horizontal segments. The final local route on plane E and the associated operation scheme, to be performed by MR (the mobile robot) at the executing stage, are then mapped from Pc. Obviously, the mapping

can be accomplished by using the orthographic projection of *Pc* onto plane *E* to produce the route. That is, the route is the projection image of *Pc* on *E*, which should be polygonal and zigzag shaped. In addition, the angle between two consecutive segments of the zigzag shaped route should be equal to the quantity of the corresponding vertical segment of *Pc*. The operation scheme is consequently produced. Figure 4.8 is an illustration.

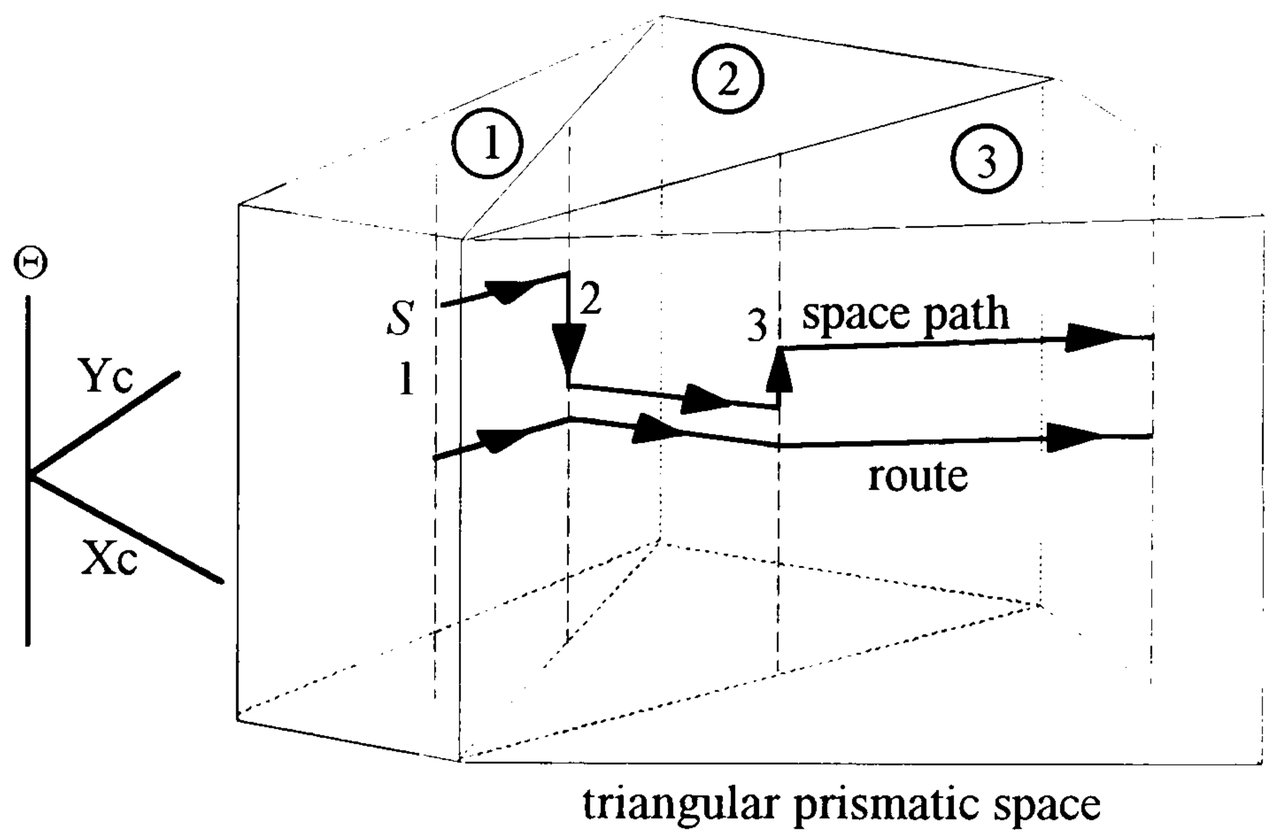

Figure 4.8 Space path vs. route and associated operation scheme

As already discussed, the path *Pc* between ***S*** and ***G*** is planned in the optimal journey, and the optimal journey is generated by searching on the triangulation graph according to the weight function defined. Since the optimal journey is a channel of configuration free space consisting of triangular prismatic spaces, one way to plan *Pc* in the spatial channel is to select representative configurations for the constituent triangular prismatic spaces, and to link every pair of adjacent configurations by a free path. Two configurations are adjacent if their representing triangular prismatic spaces are identical or adjacent. Once the selection is defined, the movement of the point robot from one node N_i to another N_j on the triangulation graph along the edge (N_i,N_j) is simply interpreted as the path linking the representative configurations for the adjacent triangular prismatic spaces. The weight $W(N_i,N_j)$ of an edge (N_i,N_j) can thus be defined to be the cost of the path

between the representative configurations. As a result, the definition of the weight function is highly related to the selection of the representative configurations for the triangular prismatic spaces.

The cost of a path can be interpreted as metrics in many forms, which is often used to represent time, distance, turn, energy, penalties, loss, or any other quantity that accumulate linearly along a navigation (space path) that one wishes to minimise. In the discrete navigation mode, a path in C is composed of a sequence of horizontal and vertical straight-line segments. A horizontal segment is a translation distance to be performed by the translation motor, and a vertical segment is an angular displacement to be carried out by the rotation motor. Since a path with short translation distances and few angular displacements is preferred, and the translation distance and angular displacement have different units, the time consumed is used to express the cost. The weight function can be derived consequently. If the maximum safe translation velocity and rotation velocity for the mobile robot are given, the time to navigate from one configuration to another is hence lower-bounded by:

$$\text{time} \approx \sum \frac{\text{translation distance}}{\text{translation velocity}} + \sum \frac{\text{rotation displacement}}{\text{rotation velocity}}.$$

As to the selection of the representative configurations for the triangular prismatic spaces, the central vertical segment of the facet shared by two spaces is selected to represent the triangular prismatic space to enter. It will be further discussed in section 4.5.

A weight function $W(N_i,N_j)$ has been defined to express the time cost required from nodes N_i to N_j along edge (N_i,N_j). The cost to achieve a node N_j, $f(N_j)$, is equal to $W(N_i,N_j)$ plus the cost required to achieve node N_i, if N_i is an ancestor of N_j and they are connected by edge (N_i,N_j). As in Fig. 4.8, the start configuration $\boldsymbol{S}$ is given by a triple (XS, YS, θS), and the representative configuration of node N_1 which contains $\boldsymbol{S}$ is a triple (X1, Y1, θ1). Since $N_s=N_1$, (X1, Y1, θ1)=(XS, YS, θS) and $f(N_s)=f(N_1)=0$;

$f(N_2)=f(N_1)+W(N_1,N_2)$, where

$$W(N_1,N_2)=\frac{\theta 2-\theta 1}{\omega_{safe}}+\frac{\sqrt{(X2-X1)^2+(Y2-Y1)^2}}{v_{safe}} \text{ and } \theta 2=\tan^{-1}\left(\frac{Y2-Y1}{X2-X1}\right);$$

$$f(N_3)=f(N_2)+W(N_2,N_3), \text{ where}$$

$$W(N_2,N_3)=\frac{\theta 3-\theta 2}{\omega_{safe}}+\frac{\sqrt{(X3-X2)^2+(Y3-Y2)^2}}{v_{safe}} \text{ and } \theta 3=\tan^{-1}\left(\frac{Y3-Y2}{X3-X2}\right).$$

Similarly, the cost to achieve a node is thus evaluated. Although the shortest graph path is just the optimal journey, and is not the route to be executed by the mobile robot, the optimal weight still indicates the performing time for reference, which is a lower bound of what may occur at the executing time if no unexpected obstruction is encountered.

4.4.2.5. Clearance of Solution Channel

The shortest graph path generated on the explicit triangulation graph is physically a spatial channel. This spatial channel represents a connected subset of the configuration free space containing the navigation solutions for the mobile robot from ***S*** to ***G***. Navigation along the graph path physically means that the mobile robot begins its journey from the start triangular prismatic space, passes consecutively through all constituent triangular prismatic spaces of the graph path, and terminates at the goal triangular prismatic space. Since every configuration in *CF* corresponds to a collision-free posture of *MR* in *WE*, a path produced in the spatial channel can always be mapped to a collision-free navigation for the mobile robot to perform in the manufacturing environment.

The final route and associated operation scheme applicable to the mobile robot will be planned inside the spatial channel according to the motion principles of the discrete navigation mode. Obviously, when the mobile robot performs a path thus produced in the optimal channel, some clearance to the obstacles can be assured. Due to the clearance, the continuous navigation mode consisting of curve routes can also be planned in the spatial channel.

4.5. FINDING LOCAL ROUTE AND OPERATION SCHEME

Once a solution graph path (the optimal journey) from the start to the goal node has been generated on the triangulation graph, a channel of configuration free space containing configurations S and G can be identified. The next task is to locally produce a feasible path connecting S and G in the spatial channel. This path can then be used to derive the route and associated operation scheme for the mobile robot. In addition, the function is developed of proposing alternative paths for the mobile robot to handle accidental happenings, such as avoiding collisions with unexpected obstacles.

4.5.1. Normal Case Using Central Line

Since the triangulation graph only represents the topological connectivity of the configuration free space, the generated graph path from the start to the goal node implicitly represents a channel of configuration free space, if such a graph path exists. This solution spatial channel not only contains configurations S and G but also provides various possibilities of linking S and G within it. However, a qualified free path, consisting of an ordered continuous combination of configurations from S to G within the channel, should satisfy the physical constraints on the mobility mechanism of the mobile robot. This ordered continuous combination of configurations from S to G should, in addition, satisfy the navigation mode and cost requirements.

The motion principles concerning the physical constraints on the mobility mechanism have been described in section 4.4.2.2, and the discrete navigation mode is used to produce a solution free path. As a result, the solution free path must consist of a sequence of horizontal straight-line segments at different Θ planes of the C space, and vertical straight-line segments connecting the horizontal segments. Also, the final local route and associated operation scheme, for the mobile robot to perform in the manufacturing

environment, can be produced from the orthographic projection image of the solution free path on plane E.

As to the cost requirements, a solution free path having a short travelling distance and few turns is preferred. Any path containing loops and identical configurations (position and orientation) should not be considered, and the mobile robot should not go to a posture more than once. Above all, the safety cost is the most important issue in the application. One easy way to take safety into account is to plan a free path with tolerance for errors and inaccuracies. This tolerance can be realised by keeping some relatively large clearance between the mobile robot and the obstacles, and making the best use of the on-board sensors, the impact of the uncertainties being relieved by the clearance, and corrected by the sensors.

To plan a path, the fact that the spatial channel is composed of a sequence of connected non-overlapping triangular prismatic spaces is considered. The central vertical segment of the facet interfaced between each pair of consecutive triangular prismatic spaces is used. The solution free path planned is the one that enables the point robot to start from $\boldsymbol{S}$, move upwards or downwards vertically to a suitable Θ plane, and move in the Θ plane towards the first central vertical segment in order to leave the first triangular prismatic space and enter the second. At the first central vertical segment, the point robot moves upwards or downwards vertically again, subject to the other central vertical segment of the facet interfaced between the second and third triangular prismatic spaces. These movements proceed sequentially until the point robot arrives at the last triangular prismatic space via the last central vertical segment. The point robot finally moves horizontally towards the configuration whose position components are equal to those of the goal configuration, and vertically to stop at $\boldsymbol{G}$.

Once the polygonal free path is produced, the route and associated operation scheme can be derived, by finding the orthographic projection image of the solution free path on plane E, or the Xw-Yw plane. The route is polygonal and zigzag shaped, consisting of

straight-line segments on plane E. The operation scheme along a straight-line segment of the route is constant, and equal to the angle of the straight-line segment with respect to the Xw axis. The operation scheme at an end point of a straight-line segment is in a transient state, the mobile robot changing its heading direction but not location. The sub-routine program is outlined as follows:

```
Finding route and operation scheme in spatial channel without unexpected obstruction
Sub-routine(Normal case)
CurrentC←S: Position(CurrentC)←Position(S): Orientation(CurrentC)←Orientation(S)
Ratio←0.5
DO
    IF NextFacet(CurrentC)=∅ THEN Position(NextC)←Position(G)
    ELSE Position(NextC)←Position(VerticalSegment(Ratio,NextFacet(CurrentC)))
    END IF
    Orientation(NextC)←Angle(Segment(Position(CurrentC),Position(NextC)),XwAxis)
    NextC←(Position(NextC),Orientation(NextC))
    OperationScheme←Orientation(NextC)-Orientation(CurrentC)
    Route←Segment(Position(CurrentC),Position(NextC))
    CurrentC←NextC
    IF Position(CurrentC)=Position(G)
    THEN OperationScheme=Orientation(G)-Orientation(CurrentC)
    STOP
    END IF
LOOP
```

Figure 4.9 illustrates a route and associated operation scheme found within the solution spatial channel. The clearance requirement is assured since the solution free path always keeps some distance from the boundary facets of the spatial channel (configuration obstacles). In addition, the route and operation scheme derived are specially suitable for the on-board ultrasonic sensors to attain reliable information, since the horizontal parts of the solution free path are always parallel with the boundary facets of the spatial channel.

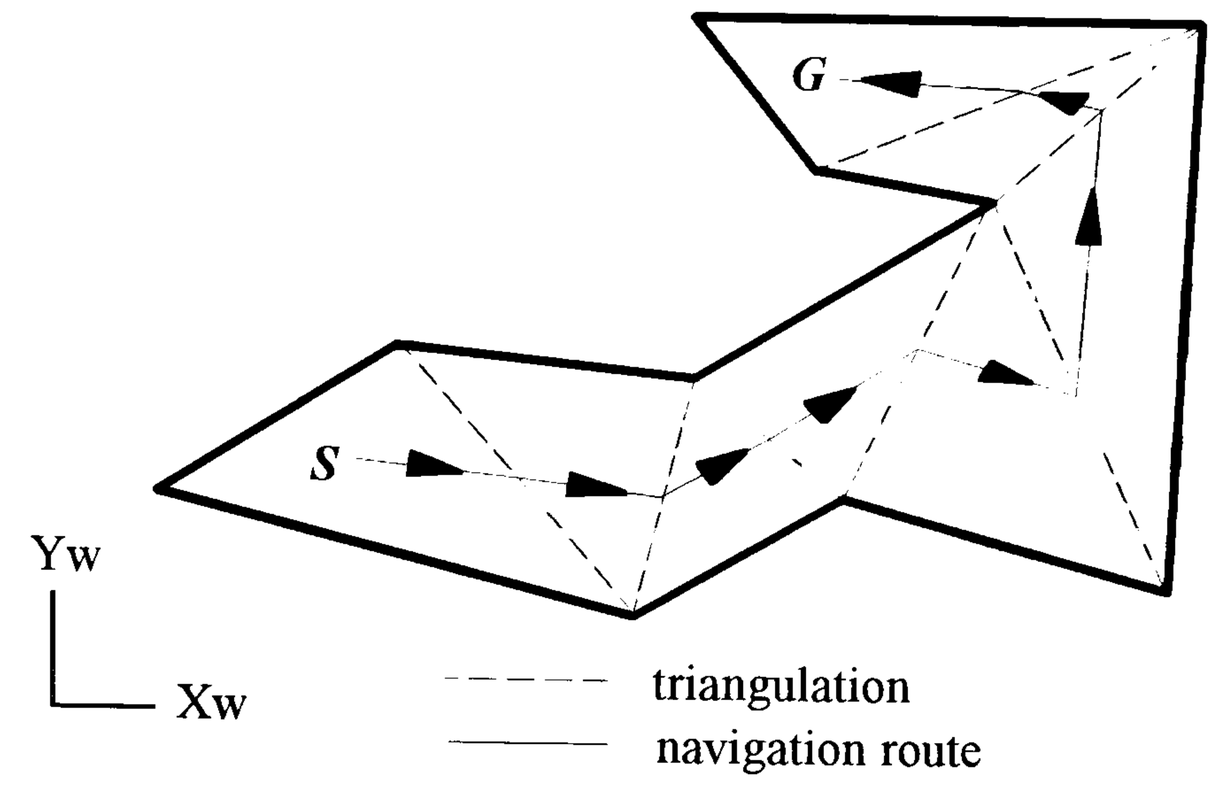

Figure 4.9 Projection image of solution channel
Local route and operation scheme

4.5.2. Handling Unexpected Obstruction

The central-line free path produced is a good safe solution, since the clearance provides the mobile robot with tolerance for control, model and sensing uncertainties. Also, the path supports the best use of the equipped ultrasonic sensors to perceive reliable feedback. However, when an unexpected obstruction, which interferes with the original global/local plan, is encountered, handling behaviours must be activated. These behaviours should propose alternative solutions, around the unexpected obstruction, to achieve the goal, and help build a reliable mobile robot planner.

4.5.2.1. Type of Unexpected Obstruction

As described in section 4.2.2, an unexpected obstruction is likely to cause problems at four levels of seriousness. In practice, the problems can also be classified into software, hardware and external state failures [136]:

(1) Software failures are used to indicate logic errors and bugs in the programs. It is assumed that the developed programs are logically correct, and the unexpected obstruction is only due to hardware or external state failure.

(2) Hardware failures include physical errors and system inaccuracies of the mobile robot, such as motor disability. It might not be possible to recover from a hardware failure.

However, it is reasonable to assume that a hardware failure of the mobile robot, in a manufacturing application, is detectable and correctable, and the mobile robot is able to continue functioning.

(3) External state failures describes the circumstance where the state of the world, assumed by the mobile robot, does not match that perceived by the equipped sensors. Although an external state failure is sometimes interrelated with hardware failures in practice, it is only used here to indicate an unexpected obstruction exclusive of the effects caused by hardware failures.

At the planning stage of the navigation strategy, the mobile robot only deals with unexpected obstacles classified as external state failures, and leaves hardware failures to be handled at the executing stage. The handling behaviours for an unexpected obstacle are hierarchically organised at the planning stage. The presence of an unexpected obstacle in the path of the mobile robot need not immediately invoke the planner to produce a new path to avoid the obstruction. Instead, the mobile robot waits in case the unexpected obstacle will be cleared. If this simple handling behaviour fails, the unexpected obstruction is propagated to a higher level of the handling behaviours. The handling behaviours developed are classified into local detouring and global re-planning.

4.5.2.2. Detouring

When the simple wait-and-see handling behaviour fails, the control is propagated to a higher level of the handling behaviours. At this level, the handler deals with the obstruction if the presence of the unexpected obstacle does not disconnect the planned spatial channel. The detouring handler is initiated to avoid the unexpected obstacle, by locally adjusting the original path in the spatial channel. Handling the unexpected obstacle at this level heavily relies on the perceiving ability of the mobile robot. Therefore, it is assumed that the equipped sensors are capable of reliably detecting or localising the

presence of the unexpected obstacle within a distance range in front of the mobile robot. Two detouring approaches are developed, tangent and triangulation.

(a) Tangent detouring. The general idea behind the tangent detouring approach is to navigate the mobile robot from its current posture along an adjusted path, which is tangent to the unexpected obstacle, to a posture on the interface facet between the current and next triangular prismatic spaces. Since the obstacle is unexpected, it is only detected when the mobile robot is moving along the planned path. When an unexpected obstacle is detected in front, the mobile robot stops navigation and finds its current (obstructed) posture. The sub-routine for normal cases, outlined in section 4.5.1, is interrupted, and the obstructed posture found is assigned to the variable Current$C$. Then, the next transient configuration, or the variable Next$C$ which is on the interface facet between the current and next triangular prismatic spaces, is the intersection of the interface facet with a straight-line path tangent to the unexpected obstacle.

The tangent detouring handler is outlined as follows, and the next transient configuration is produced by Sub-routine(Find Next$C$).

Finding route and operation scheme in spatial channel with unexpected obstruction
Sub-routine(Tangent detouring)
Current$C$←***S***: Position(Current$C$)←Position(***S***): Orientation(Current$C$)←Orientation(***S***)
DO
  Ratio←*0.5*
  IF NextFacet(Current$C$)=∅ **THEN** Position(Next$C$)←Position(***G***)
  ELSE Position(Next$C$)←Position(VerticalSegment(Ratio,NextFacet(Current$C$)))
  END IF
  Orientation(Next$C$)←Angle(Segment(Position(Current$C$),Position(Next$C$)),XwAxis)
  Next$C$←(Position(Next$C$),Orientation(Next$C$))
  IF Detectable(Next$C$)=No **THEN CALL** Sub-routine(Find Next$C$)
  END IF
  OperationScheme←Orientation(Next$C$)-Orientation(Current$C$)
  Route←Segment(Position(Current$C$),Position(Next$C$))
  Current$C$←Next$C$

IF Position(Current$C$)=Position(***G***)
THEN OperationScheme=Orientation(***G***)-Orientation(Current$C$)
STOP
END IF
LOOP

Sub-routine(Find Next$C$)
Next$C$'←Line(Position(Current$C$),Position(Tangentpoint(Obstacle)))∩
NextFacet(Current$C$)
Position(Next$C$)←Position(Next$C$')
Orientation(Next$C$)←Angle(Segment(Position(Current$C$),Position(Next$C$)),XwAxis)
RETURN

A tangent free path to avoid the unexpected obstacle is planned, and the physical contact between the mobile robot and the unexpected obstacle is minimised to be at the tangent point. Once the obstruction has been handled, the normal movement pattern (central line) is called again to restore the navigation in the spatial channel. Figure 4.10 illustrates an example.

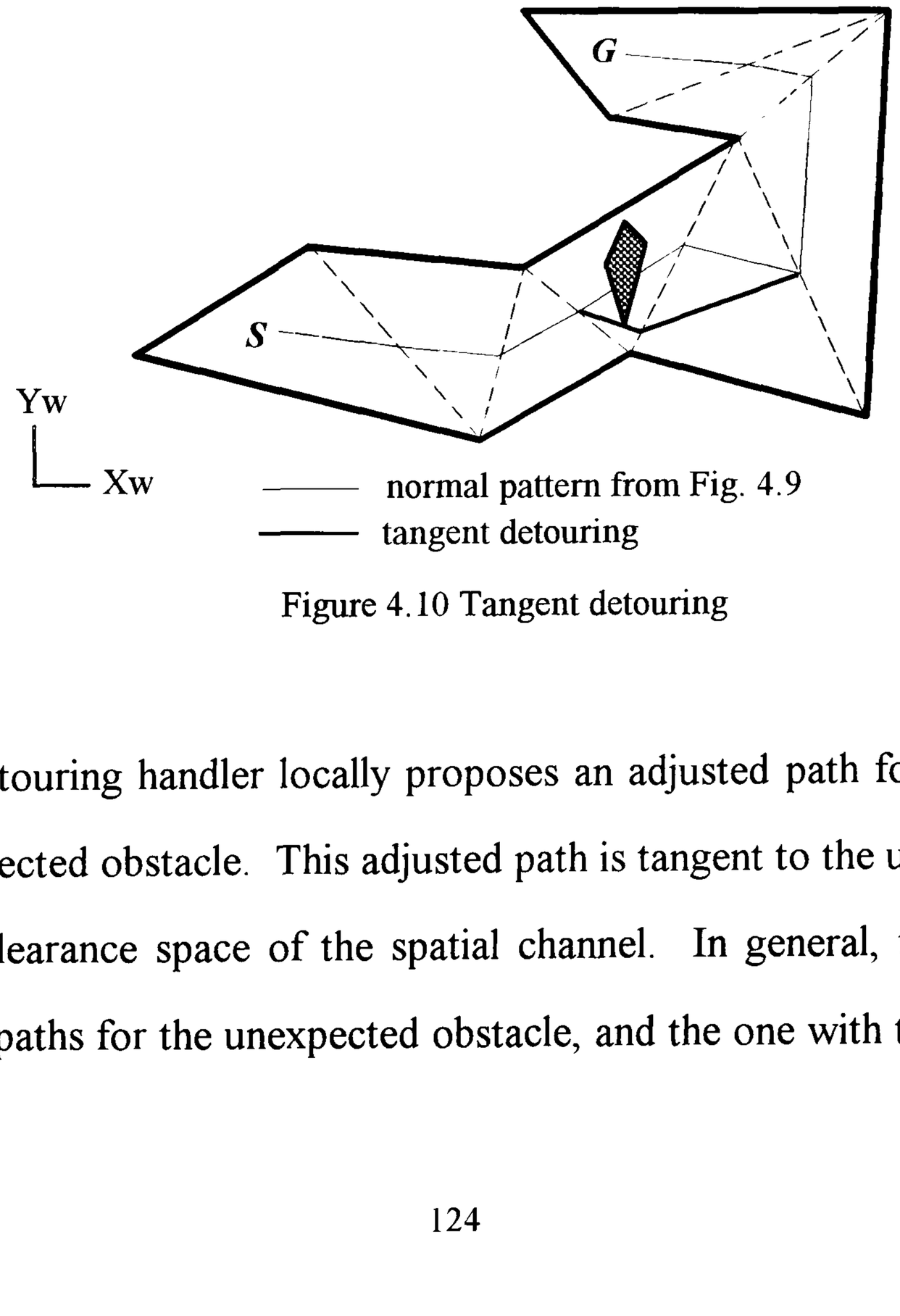

Figure 4.10 Tangent detouring

The tangent detouring handler locally proposes an adjusted path for the mobile robot to avoid the unexpected obstacle. This adjusted path is tangent to the unexpected obstacle and through the clearance space of the spatial channel. In general, there are two such tangent detouring paths for the unexpected obstacle, and the one with the shorter distance

is used. Since only information about the width of the unexpected obstacle is required, the tangent detouring approach is not computationally expensive. However, completeness is not assured.

(b) Triangulation detouring. The second detouring approach uses operations similar to the triangulation global planning approach, but in the local environment. It is based on further decomposing the free space of the obstructed (occupied) triangular prismatic spaces of the spatial channel into a set of smaller triangular prismatic spaces. A local triangulation graph can be formed consequently. Searching for the optimal graph path on this local triangulation graph generates a sub-local spatial channel within the obstructed triangular prismatic spaces. A detouring route and associated operation scheme avoiding the unexpected obstacle can be produced within the sub-local spatial channel, using the central-line method described in section 4.5.1. If the unexpected obstacle does not disconnect the spatial channel, the triangulation detouring approach is able to complete the handling task by finding a sub-local free path, to avoid the unexpected obstacle, through the clearance space of the spatial channel. The adjusted free path thus produced, or the route and associated operation scheme found, is illustrated in Fig. 4.11.

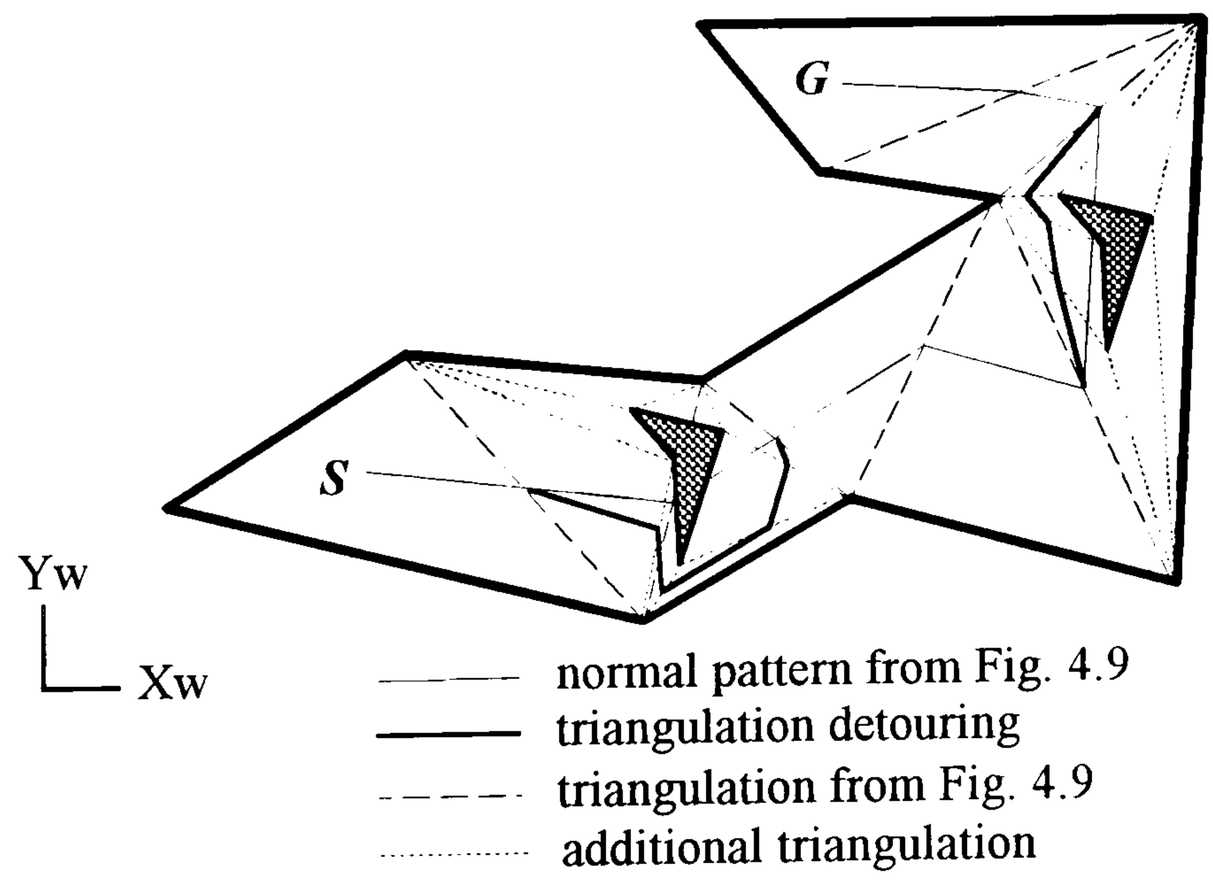

Figure 4.11 Triangulation detouring

The triangulation detouring approach is specially suitable for dealing with cases when the unexpected obstacle can be precisely detected. Completeness of handling the unexpected obstacle is assured, provided that the presence of the unexpected obstacle does not disconnect the spatial channel. Once the adjusted polygonal free path is produced, the route and associated operation scheme to avoid the unexpected obstacle can be generated consequently by mapping the orthographic projection image of the produced detouring path onto the E plane. However, the triangulation detouring approach is more expensive than the tangent detouring approach. Also, complete information about geometrical features of the unexpected obstacle is required.

Two detouring approaches to locally modify the original path, planned in the spatial channel, are developed to handle unexpected obstacles. When an unexpected obstacle is detected, and Sub-routine(Find Next$C$) of the tangent detouring approach can not produce a value for Next$C$, the triangulation detouring approach is initiated. Since handling unexpected obstacles by the detouring approaches requires the obstacle information be available at the handling instant, it is assumed that the equipped sensors are able to reliably detect and identify the presence and geometry of the unexpected obstacle within a distance range in front of the mobile robot. If this is not the case or the presence of the unexpected obstacle disconnects the spatial channel, the obstruction will be propagated to the highest level of the handling behaviours, described in the next section.

4.5.2.3. Updating Triangulation Graph and Re-planning

If a free path can not be produced in the spatial channel to locally avoid the unexpected obstacle by the previous detouring handlers, the obstruction is propagated to the global re-planning handler. This handler globally updates the triangulation graph, inserts the

unexpected obstacle into the database of the manufacturing environment, and re-initiates the planning processes. The handling behaviour is outlined as follows:

(1) Treat the current configuration, triangular prismatic space and node where the mobile robot is obstructed as the new start.

(2) Update the triangulation graph by masking the current triangular prismatic space in the spatial channel, and deleting the current node and associated edges from the triangulation graph.

(3) Search the updated triangulation graph from the new start to generate a new graph path to the goal node, and produce the corresponding solution spatial channel.

(4) Find a local route and associated operation scheme in the new solution channel.

(5) Update the database of the manufacturing environment by inserting the unexpected obstacles, if after several tries of step **(1)** to **(4)** the mobile robot still fails to achieve the goal.

(6) Construct a new triangulation graph based on the updated manufacturing environment, and re-do the spatial reasoning and path planning processes.

(7) Report failure and send a help message.

In the application, it is assumed that an unexpected obstruction is detected before the mobile robot performs the next segment of the route, i.e. the mobile robot has already revolved to the next heading direction, and the corresponding point robot is in a facet between two adjacent triangular prismatic spaces. Therefore, the current node and corresponding triangular prismatic space, in step **(2)**, are occupied by the unexpected obstacle. Given the updated triangulation graph, the re-planning handler globally generates a new graph path and the corresponding spatial channel in **(3)**, and locally produces a free path in **(4)**. If after several tries, each try being done on a triangulation graph update, the mobile robot still can not achieve the goal, the spatial reasoning

processes will be carried out again in **(5)**. A new triangulation graph is constructed, and the planning is performed again in **(6)**. Similarly, if after several tries, each try being done on an environmental datebase update, the mobile robot fails to achieve the goal, the program terminates with an appropriate message in **(7)**.

4.6. SUMMARY

In this chapter, a new approach for planning collision-free navigation for mobile robots in a manufacturing environment has been presented. This planning approach is based on triangulation from computational geometry. Since triangles are easy to handle, an approach of this nature simplifies the task of planning collision-free navigation.

A navigation planning task is divided for mobile robots into four sub-tasks:

(1) modelling the manufacturing environment as a group of numerical data in a suitable mathematical construction accessible to the computing system of the mobile robot;

(2) transforming the mathematical model to a graph;

(3) applying a graph searching algorithm to the graph to produce a solution graph path;

(4) interpreting the solution graph path as a navigation proposal for the mobile robot.

Given a mobile robot and manufacturing environment, the configuration free space of the mobile robot is constructed. The planning approach then models the configuration free space of the mobile robot as a connected set of triangular related cells, and builds a triangulation graph accordingly. This triangulation graph implicitly represents the topological connectivity of the configuration free space. If the start and goal configurations, denoted by S and G, are given in a connected sub-set of the configuration free space, a corresponding graph path can be produced on the triangulation graph, using an optimal graph searching algorithm. This solution graph path is a journey indicating a globally preferable movement trend of the mobile robot. Since the journey physically represents a spatial channel in the configuration free space, which contains S and G, there

are many free paths from S to G, available in the journey. A solution path connecting S and G with maximum clearance is locally planned in the journey channel, using the discrete navigation mode. The route and associated operation scheme for the mobile robot to navigate are finally derived from the path.

Due to the clearance advantage of the journey, the solution path is also adjustable to avoid unexpected obstacles. Handling behaviours capable of proposing alternative paths to avoid unexpected obstacles are developed, and organised in a hierarchical structure. When an unexpected obstacle has been encountered, the mobile robot waits for a moment in case the obstruction will be cleared automatically. Otherwise, the obstruction is propagated to a higher level of handler, which plans a tangent or triangulation detouring path in the journey, through the clearance space, to locally avoid the obstruction. At the highest level of the handlers, the triangulation graph and database for the manufacturing environment are updated, and a global re-planning process, including spatial reasoning and path searching, is carried out.

At the executing stage of the navigation strategy, the mobile robot will follow the planned route and operation scheme, as required by the motion and sensing commands, to perform the navigation in the manufacturing environment.

CHAPTER FIVE
EXECUTING: MOTION CO-ORDINATING AND SENSING

This chapter deals with the executing aspect of the navigation strategy. The proposals produced at the planning stage are to be implemented in practical scenes. The implementation is carried out in three steps:

(1) Computer. A graphical user interface tool is developed for the host personal computer to interactively communicate with the user through its visual display unit, by graphically demonstrating the planning procedure and results.

(2) Manipulative robot and camera. The planned navigation is simulated, using the MOVEMASTER-EX manipulative robot. The camera system (Data Translation Inc. and Prostab International Limited) is used to attain the initial environmental information.

(3) Mobile robot and ultrasonic sensors. The navigation planning approach is implemented in the B12 mobile robot, using six ultrasonic sensors for external sensing.

Whatever system is used for the implementation, motion co-ordinating and sensing mechanisms are two major subjects to be considered at the executing stage. Given a planned route and associated operation scheme, the motion co-ordinating mechanism is to compose and initiate appropriate motion instructions at appropriate moments, which can direct system behaviours to as accurately as possible perform the route and operation scheme. The sensing mechanism is to provide on-line navigation-related information for

the system to make decisions, performance corrections and further plans. However, the aim of the implementation is to prove the feasibility of the triangulation based navigation planning approach in manufacturing environments. Only minimum basic equipment is used for external sensing, so that the advantages of the planning approach can be verified.

Different systems use different types of mechanisms for motion co-ordinating and sensing. Therefore, the implementation techniques in the three steps are system specific, and are described individually.

5.1. GRAPHICAL USER INTERFACE

The flexible material transport system itself is not likely to understand a user-requested task. Therefore, a tool for graphical user interface is developed, which converts the user's input to the system's knowledge, and the system's responses to graphical displays for the user's convenience. The flexible material transport system, that waits for the user, is thus a collection of machinery (hardware) and programs (software) to be instructed or initiated. The functions of the graphical user interface tool may be partially achieved by using a commercial CAD/CAM package. A major task is to transform/transfer the database format, used in the CAD/CAM package, to a compatible set of the flexible material transport system [12]. However, the graphical user interface tool is developed in order to understand the internal communications mechanism among the component systems of the flexible material transport system.

The development of the graphical user interface tool is to put the user into direct and interactive communication with the flexible material transport system, through the visual display unit (screen) of the host personal computer. Using the tool, the user can interface with the flexible material transport system, operate every component system individually, and compose control programs off-line for automatic operations. The turnaround time

and costs for designing and re-designing layouts of a manufacturing environment, and finding and adjusting the system performance, can be reduced.

5.1.1. Software Structure

The graphical user interface tool supports two modes of interaction to operate the flexible material transport system, which are the direct and indirect modes. They are distinguished by whether the user or the navigation planner (planning approach) is in control of the system's behaviours.

(a) Direct interaction mode. In this mode, the tool has two functions:

(a.1) The user can create and edit an environmental layout. Geometrical features and spatial arrangement of the contained objects, which are to be avoided by the mobile robot, can be illustrated on-line on the computer screen.

(a.2) The flexible material transport system is to work under direct supervision of the user. No intelligent or decision making task is done by the system itself. All component systems of the flexible material transport system are at their standby states, waiting for instructions from the user. Only one instruction can be executed at a time since the host computer is a serial machine. All entered instructions are carried out sequentially, and each is responded immediately. Any response produced by the flexible material transport system is a result of the user's activities.

(b) Indirect interaction mode. On the other hand, the flexible material transport system is controlled by the navigation planner, based on the developed triangulation planning approach. In the indirect mode, there are also two functions:

(b.1) A function for computational graphical simulation is developed, in order to preview the planned navigation for the mobile robot in a given environmental layout. The computer is graphically simulating the navigation performance of the mobile robot on the

screen. This function enables the user to enter variable information, and to preview possible navigation results correspondingly. The user can also monitor the steps of the navigation planning approach as it progresses. As a result, much unnecessary trial-and-error implementation in practical scenes can be saved. Due to the rapid response of the computational graphical simulation function, an environmental layout can be designed, tested, and edited rapidly on the host computer through this function.

(b.2) The mobile robot can navigate to the goal posture itself without direct human interference, until any occurrence of non-recoverable errors. The navigation result, consisting of a sequence of "current" postures of the mobile robot, is on-line graphically displayed on the computer screen for the user's reference.

5.1.2. Techniques and Results

As described in chapter two, the hardware set-up of the flexible material transport system has been completed. The manipulative robot, camera vision system, and mobile robot with six ultrasonic sensors are connected to the host personal computer through the parallel cable, internal bus board, and serial cable respectively. The flexible material transport system is ready to operate without further hardware modification. To develop the graphical user interface tool, a major task required is to produce software for communications and control, which can drive each of the component systems and mechanisms from the host computer.

The software is produced using the Visual BASIC programming language. A 640 by 480 resolution is defined to the computer's visual display unit to construct the graphical environment for computational simulation. To prevent any disaster happening, the emergency buttons, provided by manufacturers of the component systems, are treated as the first priority interruption for all processing. When any emergency button of the component systems is pressed , the flexible material transport system is immediately

brought to a stop. A reset procedure is necessary to activate the flexible material transport system again.

5.1.2.1. Direct Interaction Mode

The direct interaction mode is developed for designing layouts of a manufacturing environment, testing system commands and reactions, and previewing operational procedures.

(a) To achieve the **(a.1)** function of section 5.1.1, a drawing program is produced, using the versatile graphic commands provided by the programming language. The drawing program can graphically display an environmental layout on the computer screen, by combining geometrical shapes, such as points, lines, rectangles, circles, arcs, and wedges, to form a variety of screen images. Since an environmental layout is designed by the user as a set of numerical data, the drawing program manipulates the data to produce a on-line clear and simple picture. The picture illustrates the set of numerical data, and thus the environmental layout. This function can communicate facts and ideas that would be abstractly difficult for the user to grasp from the equivalent set of numerical data.

(b) As to the **(a.2)** function of section 5.1.1, a specific communications program is produced, enabling the user to interactively instruct the flexible material transport system. The communications program is completed by knowing the format and protocol for data transmission among the component systems. Apart from the serial communications cable produced to connect the host computer and the mobile robot with six ultrasonic sensors, a communications setting of 9600 Baud Rate, 8 Data Bits, 1 Stop Bits, None Parity Check and Xon/Xoff Flow Control is required to transmit signals mutually. In addition, since a parallel communications cable has been produced to connect the manipulative robot with the host computer, no such serial communications setting is required. However, if serial

communications is used between the manipulative robot and host computer instead of parallel communications, 9600 Baud Rate, 7 Data Bits, 2 Stop Bits, Even Parity, Xon/Xoff Flow Control, and Enable Parity Check are assigned to meet the default configurations of the manipulative robot for serial communications.

Technically, every communications port of the host computer is managed as a random access file [67][69] in the communications program. In addition to the hardware cable configurations and the communications settings, interpretation sub-programs are also produced to convert the transmitted digital signals, complying with the ASCII code, and associated data protocols to languages or symbols understandable to the user. The communications program is invoked to function as a terminal emulation tool, which makes the host computer act as a full duplex operational terminal for the flexible material transport system, echoing all user entered instructions.

5.1.2.2. Indirect Interaction Mode

The indirect mode of interaction is based on the programs produced for the direct mode, and on the previously developed triangulation based navigation planning approach. The software begins by manipulating the input information about the environmental layout, in order to identify the free work space where the mobile robot can move freely. The free work space is then given to the planning approach, as a polygonal region with polygonal holes, to be processed.

(a) There are many situations in which understanding the performance of a dynamic system, without practically running the system in the real world, is required. For example, the real world version might perform too slowly, or yield potentially devastating consequences. In these situations, it is better to reason how the system would behave, than to observe its behaviours. The computational graphical simulation function, described in **(b.1)** of section 5.1.1, is for this purpose. This function is achieved by using a circular image, moving on

the visual display unit of the host computer, to perform the behaviours of the mobile robot. This circular image is controlled by an executing approach, simulating the executing mechanism of the mobile robot. By integrating the executing approach with the triangulation planning approach, the circular image can perform the planned route and associated operation scheme. In addition, all intermediate processes, including layout defining, free space constructing, bridge building, triangulating, triangulation graph searching, global journey generating, and local route and associated operation scheme producing, are displayed on the screen sequentially. Although the graphical simulation function is not able to replace the real implementation in the mobile robot, the function provides a useful tool for reasoning about possible consequences due to an input environmental layout. This function is an important design aid. Figure 5.1 illustrates a simulation example.

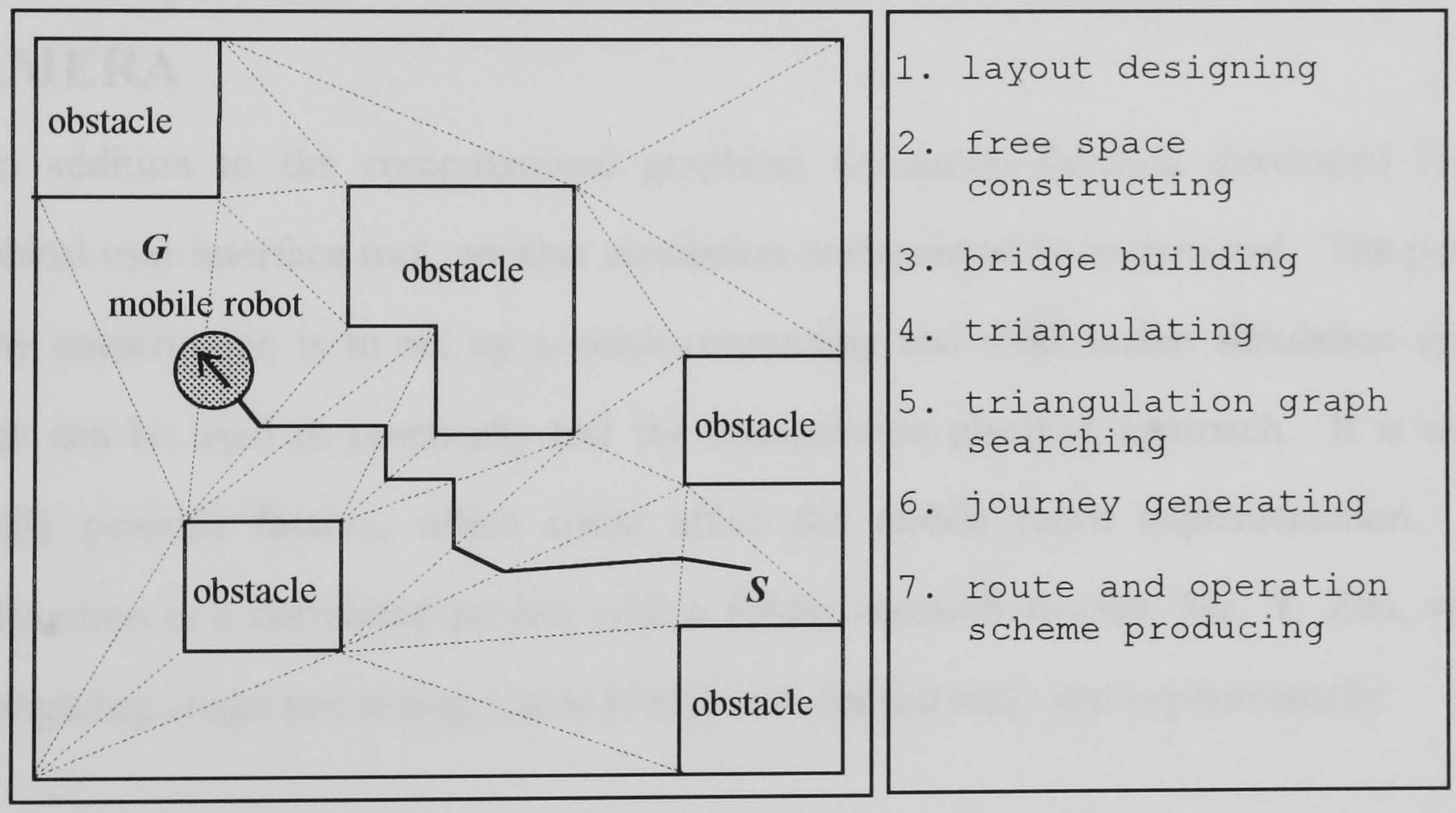

Figure 5.1. Graphical user interface

(b) The **(b.2)** function of section 5.1.1 is only invoked when the mobile robot itself is executing the navigation. Given a layout of a manufacturing environment, the mobile robot navigates along the planned route and associated operation scheme. Due to

uncertainties, the practical performance of the mobile robot is not likely to be identical to the theoretically planned navigation. By manipulating the information produced by on-board sensors, the "actual" postures of the mobile robot with respect to the defined world co-ordinate frame, at instants of sensor-triggering (sampling time), are calculated. These postures are graphically displayed on the screen. Since the sampling time is discrete, postures between two instants of sensor-triggering are linearly interpreted. As a result, the actual navigation performance of the mobile robot, in the given manufacturing environment, is illustrated. Although the displayed actual navigation result may not precisely describe the real performance of the mobile robot, due to uncertainties, sensor insufficiency and linear interpretation, the displayed result can still be a useful reference.

5.2. SIMULATION USING MANIPULATIVE ROBOT AND CAMERA

In addition to the computational graphical simulation function developed for the graphical user interface tool, another simulation environment is constructed. The purpose of the construction is to set up a quick-responding and small-scaled simulation system, which can be used to practically test the triangulation planning approach. It is also to identify possible factors, which could affect the mobile robot implementation. This construction is a correlated project with a fellow research student, Mr. Y. Zhu, who is investigating image processing issues [137], both theoretically and experimentally.

5.2.1. System Construction

The simulation system is constructed, using the manipulative robot and vision camera of the flexible material transport system. The working domain of the simulated manufacturing environment is defined by a camera stand. The base board of the camera stand represents the "floor" of a manufacturing environment. Several pieces of plastic

plate are placed on the base board to represent possible obstacles in a real manufacturing environment. The plastic plates have polygonal shapes and 2mm thickness, and are allocated according to a designed environmental layout.

The vision camera is fixed overhead, 70cm above and with its optical axis perpendicular to the base board, to cover the working domain. Images grabbed by the vision camera are processed to produce useful information about the environmental layout. This information is used as the input to the developed navigation planning approach. Output of the navigation planning approach is used to drive the manipulative robot. The manipulative robot is located along side the base board. A pencil is held by the gripper of the manipulative robot to draw the planned navigation trajectory on the base board. Figure 5.2 illustrates the constructed simulation environment.

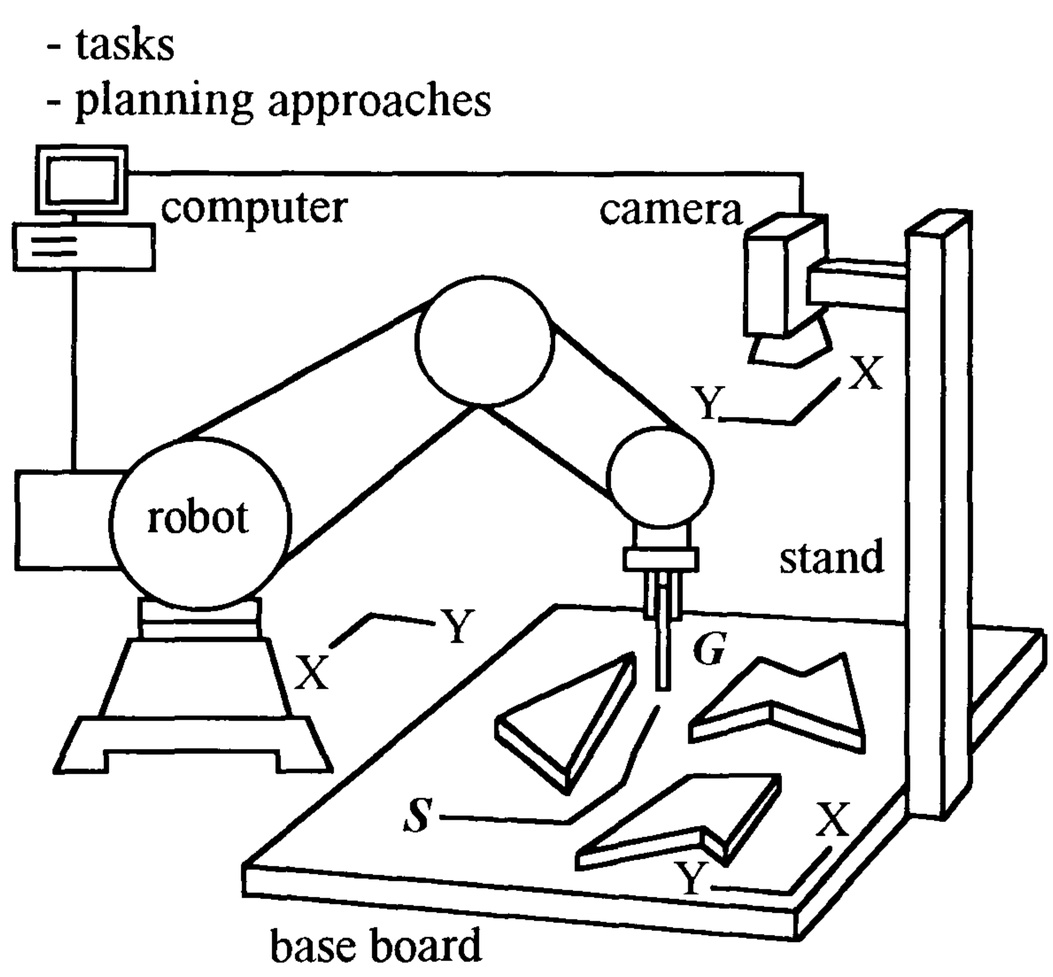

Figure 5.2. Simulation environment

5.2.2. Techniques and Results

Having constructed the simulation system, the triangulation based navigation planning approach is implemented. First, an image of the environmental layout is grabbed and processed by the vision camera to abstract useful information. Once the start and goal points have been assigned, the triangulation planning approach can produce a route and

associated operational scheme in the environmental layout. The route and associated operational scheme is finally performed by the MOVEMASTER-EX manipulative robot.

When using the simulation system to execute the planned result, three co-ordinate systems are involved:

(1) the co-ordinate system for planning navigation,

(2) the co-ordinate system for co-ordinating motion,

(3) the co-ordinate system for sensing.

The three co-ordinate systems are illustrated in Fig. 5.2. Since the simulation system has to work harmonically, data signals are transferred from the camera vision system to the navigation planner, and from the navigation planner to the manipulative robot. Data with respect to one co-ordinate frame have to be transformed to their equivalent values with respect to the other co-ordinate frame, before they are processed by the corresponding system. Transformation among the co-ordinate systems is required.

The co-ordinate system for planning navigation is defined by superimposing a Cartesian co-ordinate system on the working domain, or the base board of the camera stand. This co-ordinate frame is intuitively settled, complying with the right-hand rule and 1:1 scale rate, and has its origin at a corner of the base board. Data produced by the camera vision system have to be transformed into this co-ordinate system, in order to be exported to the navigation planning approach.

5.2.2.1. Motion Co-ordinating

The motion co-ordinating mechanism of the simulation system controls the manipulative robot to draw, using a pencil, in the simulated manufacturing environment, or on the base board. In other words, it is to find the necessary torque to actuate the joint motors at every instant of sampling time. Three levels of controllers [40] are included in the motion co-ordinating mechanism of the manipulative robot:

(1) Supervisor level controller. A supervisor is either a human user or the planning approach. The supervisor level controller provides instructions for the manipulative robot to perform the desired behaviours.

(2) Command level controller. The command level controller converts the instructions, from the supervisor level controller, to voltage values, which are used by the joint level controller.

(3) Joint level controller. The joint level controller manages angular movements of the robot joints, by using position servos for the joint motors.

The manipulative robot is a commercially off-the-shelf and ready-to-use industrial system. It has a control unit supporting the command level and joint level controllers for reliable performance. Therefore, the supervisor level controller is produced to complete the motion co-ordinating mechanism. The supervisor level controller is used mainly to convert the output from the triangulation based navigation planner to a combination of available robot motions. To draw on the base board smoothly, the gripper of the manipulative robot, which holds a pencil, is always kept perpendicular to the base board. However, some working space of the simulated manufacturing environment is sacrificed due to this restriction.

The manipulative robot has a manufacturer defined Cartesian co-ordinate system. Comparing it with the Cartesian co-ordinate system for planning navigation, the co-ordinate system for motion co-ordinating has the same unit scale. Since the manipulative robot is fixed along side the simulated manufacturing environment, making the two Cartesian co-ordinate systems parallel, the transformation between the two co-ordinate systems is constant.

To deal with the position repeatability and line-following difficulty, a number of intermediate points are introduced to all straight-line routes, in order to perform the planned discrete navigation. The more number of intermediate points, the smoother and closer the performance is to the planned discrete navigation. However, more executing

time is also required. In addition, a tolerance width, which is about 3mm and experimentally produced, is defined to the navigation route. Any gap, between obstacles in the simulated manufacturing environment, narrower than the tolerance width is assumed obstructed. Gaps are determined by the heights of the triangular regions, produced by the triangulation planning approach. Figure 5.3 illustrates the implementation techniques.

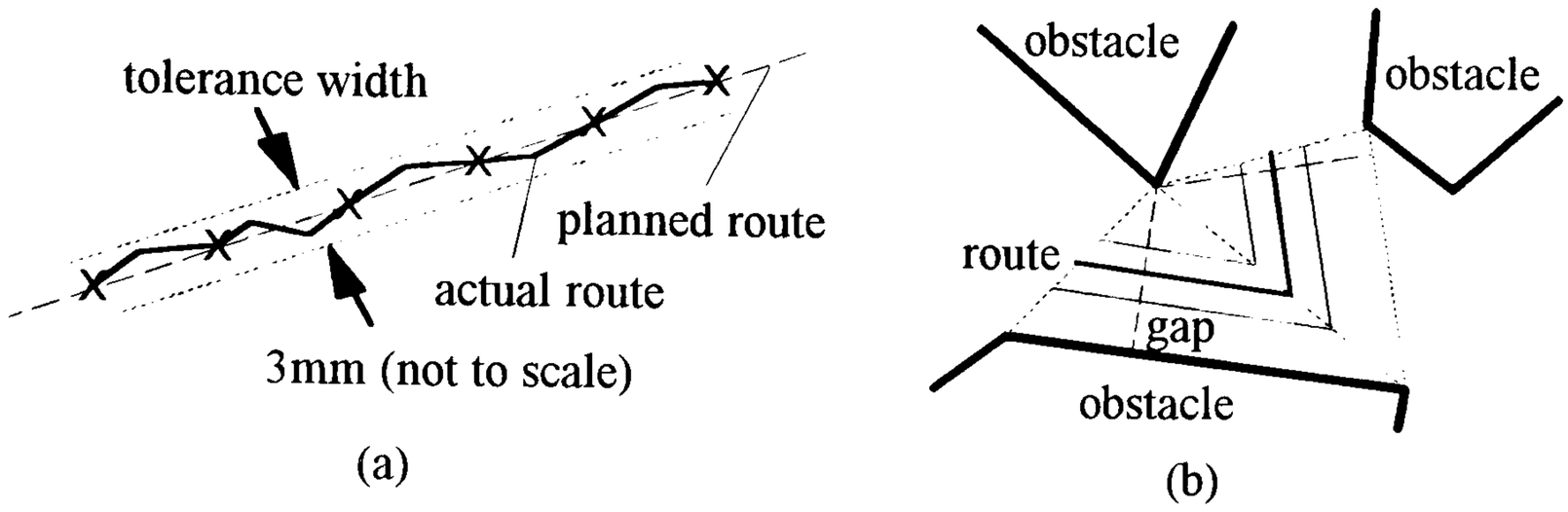

Figure 5.3. Intermediate points and tolerance width

5.2.2.2. Sensing

The vision system comprises a camera, processing boards, a monitor, and lighting equipment. The camera is placed above the simulated manufacturing environment. After taking an image of the environment, the camera returns a matrix of pixels. Each pixel represents a voltage proportional to the light level of its corresponding part in the image. Since the vision system is monochrome, the pixels are quantified by 8 bits of discrete grey levels, black through to white. Information about the environment is inferred by processing the pixel data. Understanding an image usually requires a sequence of complex processing and a large amount of computations. In addition, the processing must raise the quality of the raw data to the standard required by the navigation planner.

A grey-level representation of the matrix of pixels may not truly stand for the corresponding environmental image. This may be due to factors such as reflectance function, illumination, shadowing, electrical noise, visual noise, distortion, orientation of obstacles, etc. Since the simulation system is mainly to test the feasibility of the navigation

planning approach in practical scenes, attempts are made to technically eliminate problems caused by these factors.

Four lamps of the lighting equipment are positioned around the base board to provide sufficient light sources. Therefore, the simulation system has illumination bright enough to deal with the suffering from varying light condition and noise. The distortion effect is minimised, by excluding the boundary area of an image from processing, and setting the overhead camera to point perpendicularly downward to the base board.

The camera is fixed 70cm high above the working domain. Since the camera is fixed, the co-ordinate system for sensing can be calibrated to refer the co-ordinate system of the navigation planner. The two co-ordinate systems are parallel, and have the same directions but different unit scales. At 70cm height, the camera produces a 40cm by 40cm square of coverage on the base board. Since the co-ordinate system of the camera, or the resolution for processing an image, is a square of 512 pixel by 512 pixel, the transformation rate between the co-ordinate systems for sensing and navigation planning can be produced; 1cm=12.8pixels.

In addition, all obstacles in an environmental image are assumed to have zero heights, when the edge-detection processing is performed to identify obstacle boundaries. That is, it is assumed that environmental images are taken from an infinitely far distance. This orthographic projection assumption avoids the complexity of distinguishing three dimensional obstacles from a two dimensional image. However, information about an obstacle thus produced is slightly larger than the real one. The thin thickness of the plastic plates is to submerge the shadowing noise.

As to the effect of obstacle orientation, different positions and orientations of an obstacle on the base board may result in irregularity of obstacle edges in the corresponding pixel representations. This problem is handled by assuming that all obstacles in the working domain are polygons. When processing an environmental image, boundaries of obstacles are produced, by first identifying pixels with discontinuity in grey levels. Each

obstacle boundary consists of a connected set of pixels. By setting a width threshold, consecutive pixels within the width threshold are represented by a straight-line segment, which is tangent to these pixels. Boundary information about the 'polygonal' obstacles is finally produced. After processing, an obstacle may present a 6-gone at a position and orientation, but an 8-gone at another. Figure 5.4 illustrates an example. The information produced is the input to the navigation planner, if the camera image system provides the only environmental information.

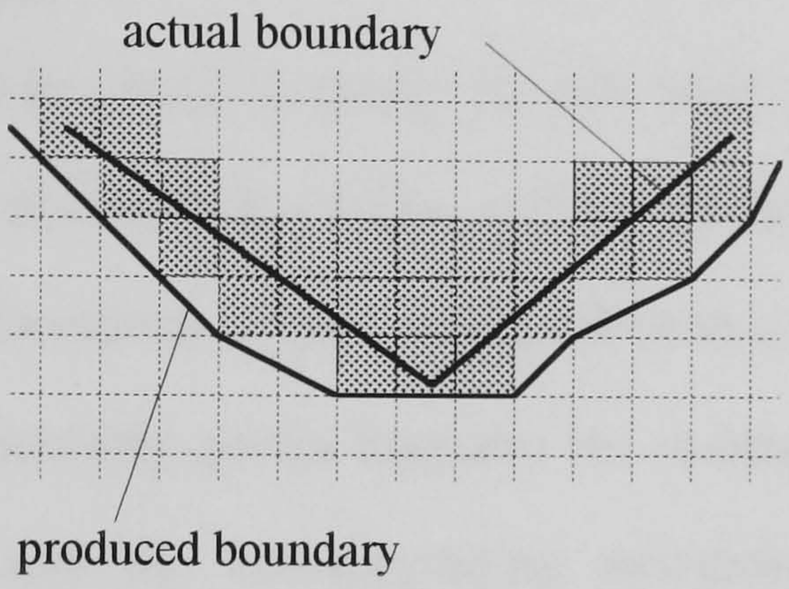

Figure 5.4. Pixel boundary

5.2.2.3. Results

A simulation system is accomplished, using the manipulative robot and the vision camera of the flexible material transport system. The camera scans the simulated manufacturing environment, and passes the produced obstacle information to the triangulation based navigation planner. A navigation is then planned for the manipulative robot to execute. The camera and manipulative robot being fixed, with respect to the camera stand, enables calibration of the three co-ordinate systems to be made. The zero-height obstacle model introduces a gross navigation effect, which slightly enlarges obstacles, and enhances clearance for the planned navigation.

The feasibility of the triangulation based planning approach, in a small-scaled simulated manufacturing environment, is verified. The simulation system also helps identifying possible factors, which could affect the mobile robot implementation. In addition,

hardware of the simulation system can be used to test other navigation planning approaches. However, expensive computational costs for processing vision images (approximately 1.5 minutes) are the main disadvantage of the simulation system. A real-time performance may be achieved by improving approaches, techniques, and hardware for processing vision images, which reduces the time required to update the input to the navigation planner.

5.2.3. Design and Simulation

The graphical user interface tool, running on the host personal computer, and the simulation system, using the manipulative robot and the vision camera, are both developed to model the navigation performance of the mobile robot in a manufacturing environment. Simulation represents a particularly useful function for reasoning about a possible spatial arrangement of obstacles, and the corresponding navigation results, that avoids the imprecision of intuition or prediction. Also, it provides a more practical formulation than mathematics for modelling the navigation planning approach.

In the development of the flexible material transport system, the two simulation functions are both regarded as important aid tools in designing layouts of a manufacturing environment. If simulation runs can conveniently test, or verify, the navigation processes of the mobile robot in a simulated environmental layout, then, in situations where the structural characteristics of the corresponding real manufacturing environment are user controlled, the simulation information can be used as a basis for judging and modifying the layout structure of the real manufacturing environment.

The design of a physical system is often accomplished by a cycle of activities [138], including phases that construct models, test behavioural consequences of the models by simulation, diagnose the causes for poor behaviour in terms of design weakness, and propose model changes. Ideally, a cycle of such activities should produce a system with the desired behavioural properties.

Similarly, designing structural layouts of a manufacturing environment is also an iterative procedure. Candidate layout designs are proposed first, according to the manufacturing target. Their implications for the mobile robot navigation are followed by simulation. Selection or modification on these candidates is then made, based on the simulation results. The design cycle is repeated until a layout design is decided, which has satisfactory simulation results of the mobile robot navigation. The designed environmental layout is finally employed to construct or re-locate the physical objects in the manufacturing environment. The design cycle is illustrated in Fig. 5.5. Using the two simulation tools to design a layout of a manufacturing environment, implementation costs and damages due to trial-and-error practices by navigating the mobile robot can be reduced.

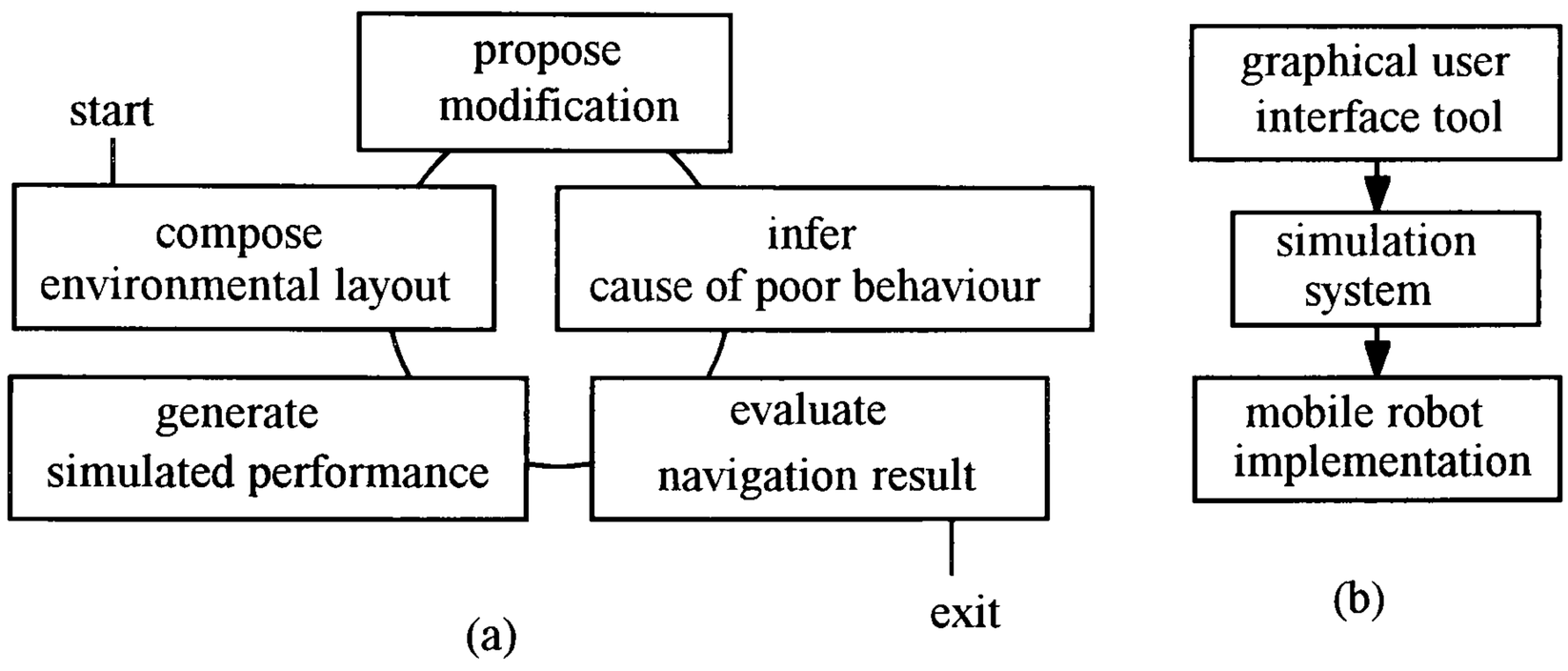

Figure 5.5. Design cycle

The final step is to implement the triangulation based navigation planning approach to the mobile robot. The manufacturing environment is constructed according to the designed layout and simulation results. In the implementation, the motion co-ordinating, sensing, and managing mechanisms are required to execute the planned navigation.

5.3. MOTION CO-ORDINATING FOR MOBILE ROBOT

To perform the planned navigation, the mobile robot must move itself from the start posture to the goal posture in a co-ordinated fashion, and along the prescribed route and associated operation scheme. Therefore, an important concern at the executing stage is to develop a motion co-ordinating mechanism, which can automatically compose a sequence of motions of the mobile robot. This sequence of motions is then converted to proper motor control profiles, used to drive the translation (wheeling) and rotation (steering) motors. In other words, the motion co-ordinating mechanism is to derive systematic motor control profiles for the mobile robot to execute the planned route and associated operation scheme.

5.3.1. Structure and Techniques

As described in chapter two, the mobile robot has a translation and a rotation servo loop. Each servo loop consists of a motor and an encoder, and can be independently operated in velocity, position, power, and limp modes, within a range of velocities and accelerations. As a result, the three wheel driving and three wheel steering mechanism gives the mobile robot an omni-directional travelling capability. Also, this synchronous mobile mechanism provides the robot system with two modes of navigation; discrete and continuous.

5.3.1.1. Structure

Whatever navigation mode is performed by the mobile robot, three levels of hierarchically organised controllers are used to construct the motion co-ordinating mechanism, as those of the simulation system in section 5.2.2.1.

(a) Motor level controller [43]. Two motor level controllers are at the lowest level of the motion co-ordinating mechanism; one for translation and the other for rotation. Each

consists of control circuits for managing a motor and an optical encoder, and forms a servo loop. The motor level controllers work by controlling state vectors of angular position and angular velocity for the motors, and integrating signals from the optical encoders.

(b) Command level controller. The command level controller converts the motion instructions, from the supervisor level controller, to voltage values. The voltage values are used by the motor level controllers to drive the two servo loops. The command level controller also produces an encoder count for each of the servo loops through accumulating encoder signals, captured by the corresponding motor level controller.

(c) Supervisor level controller. The supervisor level controller describes the route and associated operation scheme, produced by the navigation planning approach, as a set of motion instructions of the mobile robot. It also informs the navigation planning approach the current posture and failure performance of the mobile robot. Using the produced motion instructions, the mobile robot can perform the planned navigation.

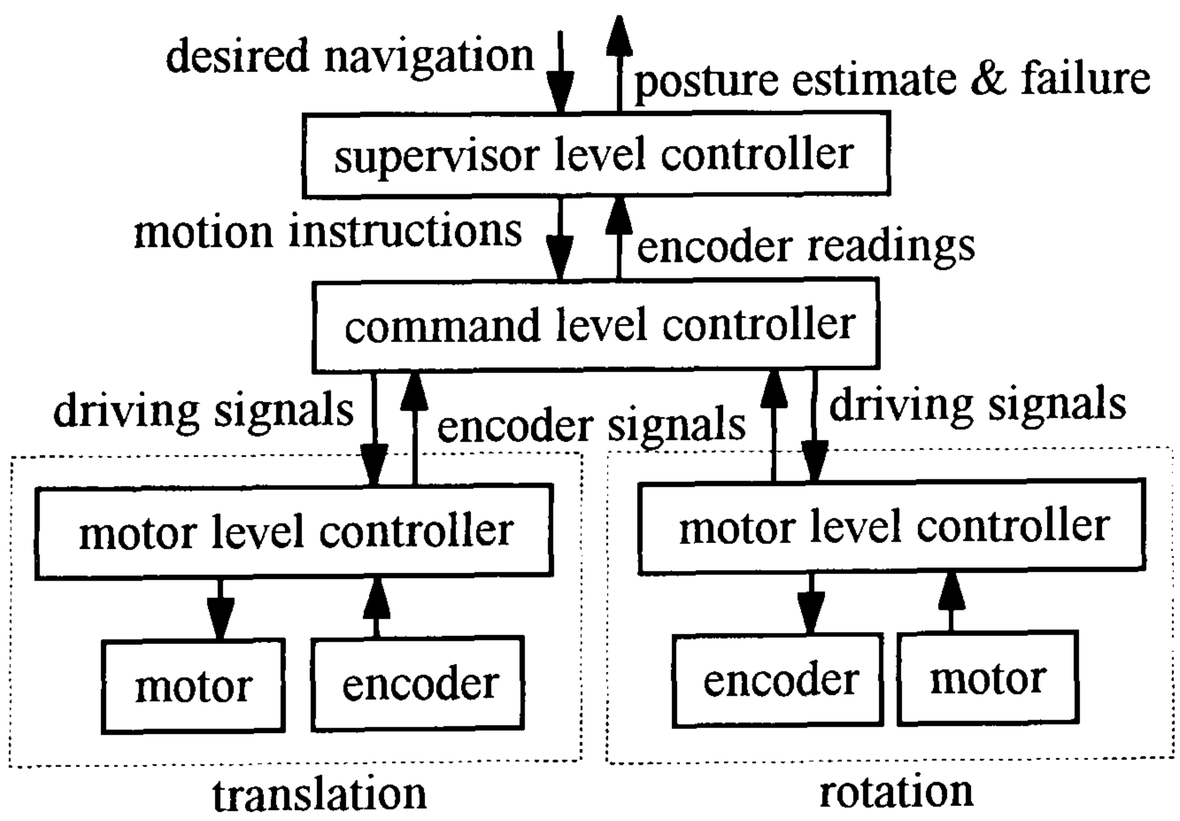

Figure 5.6 Motion co-ordinating mechanism

Figure 5.6 illustrates the hierarchical structure of the motion co-ordinating mechanism. The control unit of the B12 mobile robot has the functions of the motor level controllers. Also, a manufacturer-defined operation system is pre-loaded in the mobile robot. This operation system consists of a set of control commands for the two servo loops, and can be used to function as the command level controller of the mobile robot. Therefore, the supervisor level controller is produced to complete the motion co-ordinating mechanism.

5.3.1.2. Techniques

A major concern for the development of the supervisor level controller is to achieve a prescribed navigation, which is expressed in the co-ordinate system of the navigation planning approach, or of the manufacturing environment. Two principal functions are included in the supervisor lever controller; to perform the prescribed navigation and to make posture estimates with respect to the manufacturing environment while navigating.

(a)Performing prescribed navigation. Methods enabling the mobile robot to perform the two modes of navigation are developed. Technically, discrete and continuous navigation can be accomplished by the following control methods:

(a.1) The discrete navigation mode is achieved, if the translation and rotation servo loops are sequentially controlled in a scheduled order. The overall navigation is divided into a sequence of performance intervals. Each performance interval is formulated by executing velocity, acceleration, displacement, and time of either the translation or rotation servo loops. One motor is only initiated, when the other stops. Therefore, the mobile robot can move forward and backward, or revolve on its central axis, but not together in the same performance interval. In this mode, a navigation trajectory of the mobile robot is presented as a sequence of move-stop-revolve movements. Given the geometrical parameters of a prescribed discrete navigation, time parameters are used by the supervisor level controller to compose the velocity and acceleration functions for the performance

intervals, and to co-ordinate the translation and rotation motors. A desired discrete navigation can always be described as a sequence of motion instructions of the mobile robot.

(a.2) The continuous navigation mode is achieved by simultaneously controlling the two servo loops of the mobile robot. A curve navigation trajectory is presented by the mobile robot in the continuous navigation mode. To perform a prescribed continuous navigation, a set of translation and rotation motions of the mobile robot are carefully combined, in order to match the performed trajectory with mathematical features of the prescribed curve route. The combination is a result of complicated and precise computations. Time-based parameters are used to control the translation and rotation motors. However, translation-displacement based parameters are considered for controlling the rotation motor, if the given curve route is characterised by a curvature function. That is, the rotation motor is controlled by the travelling distance of the mobile robot. The general expression for curvature of a curve route is $K=d\Theta/dS$, where S is the route-length (travelling distance) variable, and Θ is the angle of the tangent to the route (the heading direction of the mobile robot since its centre of rotation is following the route). An arbitrarily prescribed curve route may not be feasible due to kinematics constraints of the mobile robot.

(b) Making posture estimate. To perform a prescribed navigation, expressed in the co-ordinate system of the planning approach, the supervisor level controller has to make posture estimates of the mobile robot, with respect to the manufacturing environment. The posture-estimation is done by a dead reckoning method, mainly using readings from the two optical encoders. Assuming that at time t_0, the mobile robot is at an initial posture (X_0, Y_0, Θ_0), with respect to the manufacturing environment. In the triple, (X_0, Y_0) is the position of the revolving axis (centre of rotation), and Θ_0 the heading direction, of the

mobile robot. This dead reckoning method makes posture estimates for the two navigation modes by the following approaches:

(b.1) In the discrete navigation mode, the translation and rotation servo loops are sequentially controlled in a scheduled order. One motor is only initiated when the other motor stops. When the mobile robot is performing a discrete navigation, the overall performing time is divided into n time intervals ($t_0,t_1,t_2,\ldots,t_n$), and each time interval equivalently represents a performance interval as illustrated in Fig. 5.7. During a time interval Δt_i, $\Delta t_i=t_i-t_{i-1}$ and $1\le i\le n$, either the translation or the rotation servo loop is working. Since a time instant t_j ($0\le j\le n$), dividing the performing time, is also a sensor sampling time, encoder readings of the translation and rotation servo loops at t_j are fetched. Therefore, S_j and ϕ_j, respectively representing the translation and rotation positions at t_j, can be produced from the encoder readings.

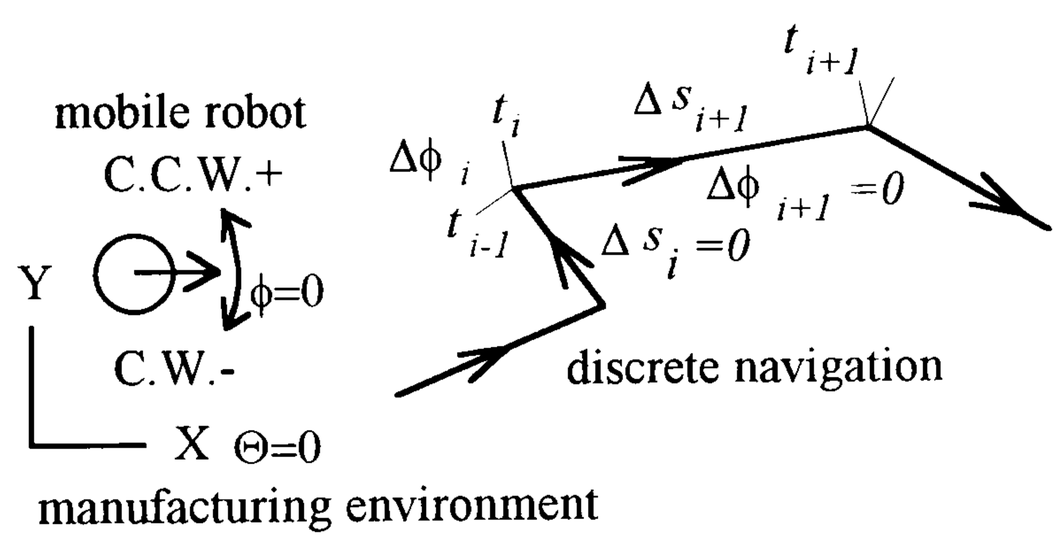

Figure 5.7. Time interval and discrete navigation

Let ($S_0,S_1,S_2,\ldots,S_n$) and ($\phi_0,\phi_1,\phi_2,\ldots,\phi_n$) be the position intervals for translation and rotation respectively, corresponding to ($t_0,t_1,t_2,\ldots,t_n$), $\phi_0=\Theta_0$. Furthermore, let (X_i,Y_i,Θ_i) be the posture estimate of the mobile robot with respect to the manufacturing environment, at a sampling time t_i, $t_i\in\{t_0,t_1,t_2,\ldots,t_n\}$. ($X_i,Y_i,\Theta_i$) can be produced by the following equations:

$$\Theta_i=\Theta_0+\sum_{k=1}^{i}\ \Delta\phi_k=\phi_0+\sum_{k=1}^{i}\ \Delta\phi_k=\phi_i$$

$$X_i=X_0+\sum_{k=1}^{i}(\Delta S_k\times\cos\Theta_{k-1})=X_0+\sum_{k=1}^{i}(\Delta S_k\times\cos(\Theta_0+\sum_{j=1}^{k-1}\Delta\phi_j))$$

$$Y_i=Y_0+\sum_{k=1}^{i}(\Delta S_k\times\sin\Theta_{k-1})=Y_0+\sum_{k=1}^{i}(\Delta S_k\times\sin(\Theta_0+\sum_{j=1}^{k-1}\Delta\phi_j))$$

where $\Delta\phi_k=\phi_k-\phi_{k-1}$ and $\Delta S_k=S_k-S_{k-1}$.

Similarly, at an arbitrary time instance t_l, $t_{i-1}<t_l<t_i$ and $t_i\in\{t_1,t_2,\ldots,t_n\}$, the posture estimate (X_l,Y_l,Θ_l) is:

$$\Theta_l=\Theta_{i-1}+\Delta\phi_l=\phi_l$$

$$X_l=X_{i-1}+\Delta S_l\times\cos\Theta_{i-1}$$

$$Y_l=Y_{i-1}+\Delta S_l\times\sin\Theta_{i-1}$$

where $\Delta\phi_l=\phi_l-\phi_{i-1}$ and $\Delta S_l=S_l-S_{i-1}$ respectively represent the displacements of rotation and translation from t_{i-1} to t_l.

(b.2) The continuous navigation mode is to simultaneously control the two servo loops of the mobile robot. It is also formulated from the velocity, acceleration, displacement and time inputs to the translation and rotation servo loops. Let v_i, ω_i, ϕ_i and S_i respectively represent the instantaneous translation velocity, rotation velocity, heading direction and travelling distance of the mobile robot at time t_i. Let (X_i,Y_i,Θ_i) be the posture estimate of the mobile robot with respect to the manufacturing environment at t_i. (X_i,Y_i,Θ_i) can be theoretically calculated by the following equations:

$$\Theta_0=\phi_0$$

$$\Theta_i=\Theta_0+\Delta\phi=\Theta_0+\int_{t_0}^{t_i}\omega dt=\phi_i \text{ or}$$

$$\Theta_i=\Theta_0+\int_{s_0}^{s_i}Kds \text{ and } S_i=S_0+\int_{t_0}^{t_i}vdt$$

where K is a curvature function. The variations of X and Y at the neighbourhood of time t_i are ΔX_i and ΔY_i respectively:

$$\Delta X_i=v_i\cos\Theta_i\Delta t$$

$$\Delta Y_i=v_i\sin\Theta_i\Delta t$$

Therefore, the X and Y positions of the mobile robot with respect to the manufacturing environment at time t_i are:

$$X_i = X_0 + \int_{t_0}^{t_i} v\cos\Theta dt$$

$$Y_i = Y_0 + \int_{t_0}^{t_i} v\sin\Theta dt$$

The dead reckoning method uses encoder readings to make posture estimates of the mobile robot. Practically, fetching and processing encoder readings takes time, and the time intervals between sampling instants have to be considered. In other words, when the mobile robot is performing a continuous navigation, an interpretation model of the curve route, between two sampling instants, has to be used instead of the theoretical model. As a result, the following equations are proposed to make practical posture estimates in a continuous navigation:

$$\Theta_i = \phi_i$$

$$X_i = X_{i-1} + \Delta S_i \cos((\phi_i + \phi_{i-1})/2)$$

$$Y_i = Y_{i-1} + \Delta S_i \sin((\phi_i + \phi_{i-1})/2)$$

if t_i and t_{i-1} are the current and previous sampling instants, and $\Delta S_i = S_i - S_{i-1}$. Obviously, the proposed equations use a heuristic model for the continuous navigation mode, and the mobile robot can only make approximate posture estimates. However, this interpretation model provides a practical means for localising the mobile robot in continuous navigation. Figure 5.8 illustrates an example of continuous navigation.

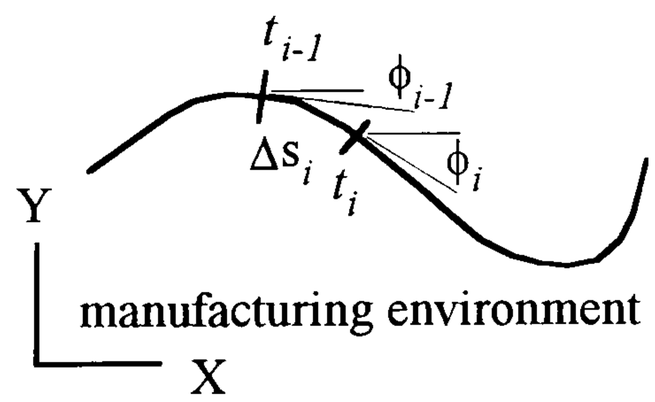

Figure 5.8. Continuous navigation

The dead reckoning method, using readings from the optical encoders, is very economical to implement. However, making posture estimates by this method is recognised to be prone to modelling errors, and noises from encoder quantization and floor roughness. The mobile robot requires other methods to make posture estimates, as a supplement to the dead reckoning method, at least on an occasional basis.

5.3.2. Physical Features

In order to develop the motion co-ordinating mechanism, physical features of the control unit of the mobile robot (the command and motor level controllers of the motion co-ordinating mechanism) have to be realised.

There are incremental optical encoders mounted on both the translation and rotation motors, providing dead reckoning and feedback control for the mobile robot. Each optical encoder provides 500 counts per motor revolution. Since the control unit zeros the encoder counters at every system reset, angular positions of the motors can be measured cumulatively from the reset moment. By using constant time intervals, and consistently checking the variations of angular position and angular velocity over the time intervals, the control unit can maintain the motors at the desired angular velocity and angular acceleration respectively.

The motion commands and parameters, provided by the manufacturer, are motor based and in hexadecimal notation. Therefore, they have to be converted into the notation which is recognisable to the supervisor level controller.

5.3.2.1. Translation

To transmit work from the translation motor to the wheels, three gear sets are available to drive the mobile robot; $7\frac{1}{3}:1$ for light loads and high speed, 11:1 for medium loads and medium speed, and 14:1 for heavy loads and slow speed. The gear sets serve for work

transmission as well as speed reduction. Each ratio is a speed reduction rate, representing the number of revolutionsof the translation motor per wheel revolution.

Given a gear set, the travelling distance of the mobile robot, D, can be calculated by the following equations:

$$D=2\times\pi\times R\times Rev._w=2\times\pi\times R\times(Rev._m\div Rate)=2\times\pi\times R\times(Count\div 500\div Rate)$$

where R, Rev.w, Rev.m, Rate, Count and 500 respectively represent the wheel radius (4.15cm), number of revolution of the wheels, number of revolution of the translation motor, reduction rate, counts of the translation optical encoder, and encoder counts per motor revolution. For example, the three reduction rates, 14:1, 11:1 and $7\frac{1}{3}$:1, enable the mobile robot to travel 1000cm by 268267, 210302 and 139882 counts (decimal) of the translation optical encoder. In addition, an encoder count in decimal notation has to be converted to a corresponding value in hexadecimal notation, before it is used to command the mobile robot. Table 5.1 is a conversion table for translation distance versus encoder count. At present, the 11:1 gear set is used, enabling the mobile robot to travel approximately 26cm for every 11 motor revolutions.

gear set	**14:1**	**14:1**	**11:1**	**11:1**	$7\frac{1}{3}$**:1**	$7\frac{1}{3}$**:1**
count distance	**(dec.)**	**(hex.)**	**(dec.)**	**(hex.)**	**(dec.)**	**(hex.)**
1cm	268	10C	210	D2	140	8C
10cm	2683	A7B	2103	837	1399	577
100cm	26827	68CB	21030	5226	13988	36A4
1000cm	268267	417EB	210302	3357E	139882	2226A

Table 5.1. Distance travelled versus encoder count

5.3.2.2. Rotation

As to the transmission system employed by the rotation motor, a 236.4:1 reduction ratio is provided. Every 236.4 revolutions of the rotation motor the mobile robot revolves 360 degrees about its central axis. Therefore, there are

$$236.4\times500=118200 \text{ encoder counts (decimal)}$$

for every 360 degrees of change of the heading direction. In other words, there are

$$118200\div360=328\frac{1}{3} \text{ encoder counts (decimal)}$$

per degree of change of the heading direction.

Similarly, an encoder count in decimal notation has to be converted to a corresponding value in hexadecimal notation, before it is used to instruct the mobile robot. Table 5.2 is a conversion table for rotation displacement versus encoder count.

degree	**dec.**	**hex**	**degree**	**dec.**	**hex.**	**degree**	**dec.**	**hex.**
10	3283	CD3	130	42683	A6BB	250	82083	140A3
20	6567	19A7	140	45967	B38F	260	85367	14D77
30	9850	267A	150	49250	C062	270	88650	15A4A
40	13133	334D	160	52533	CD35	280	91933	1671D
50	16417	4021	170	55817	DA09	290	95217	173F1
60	19700	4CF4	180	59100	E6DC	300	98500	180C4
70	22983	59C7	190	62383	F3AF	310	101783	18D97
80	26267	669B	200	65667	10083	320	105067	19A6B
90	29550	736E	210	68950	10D56	330	108350	1A73E
100	32833	8041	220	72233	11A29	340	111633	1B411
110	36117	8D15	230	75517	126FD	350	114917	1C0E5
120	39400	99E8	240	78800	133D0	360	118200	1CDB8

Table 5.2. Heading change versus encoder count

5.3.2.3. Motor Control Profiles

Another important physical feature is how the command and motor level controllers instruct the mobile robot. That is, the motor control profiles for translation and rotation have to be understood. This feature is realised, through analysing experimental results, and using the following kinetics equations, for constant translational and rotational accelerations:

$$v=v_o+at,\ s=v_ot+0.5at^2,\ v^2=v_o^2+2as$$

$$\omega=\omega_o+\alpha t,\ \theta=\omega_o t+0.5\alpha t^2,\ \omega^2=\omega_o^2+2\alpha\theta$$

where v_o, ω_o, v, ω, s, θ, a, α, and t respectively, represent the initial translation velocity, initial rotation velocity, current translation velocity, current rotation velocity, translation displacement, rotation displacement, translation acceleration, rotation acceleration, and time. Experimental results are produced by recording the motor states, when the mobile robot is performing a given translation displacement, using assigned translation velocities and accelerations. The same experiments are applied to the rotation motor.

Experimental results show that the motor control profiles are acceleration symmetrical. In other words, when the acceleration values are given, the deceleration values are equally assigned automatically. Two experimental examples are illustrated in Fig. 5.9, that acceleration and velocity profiles over time are produced.

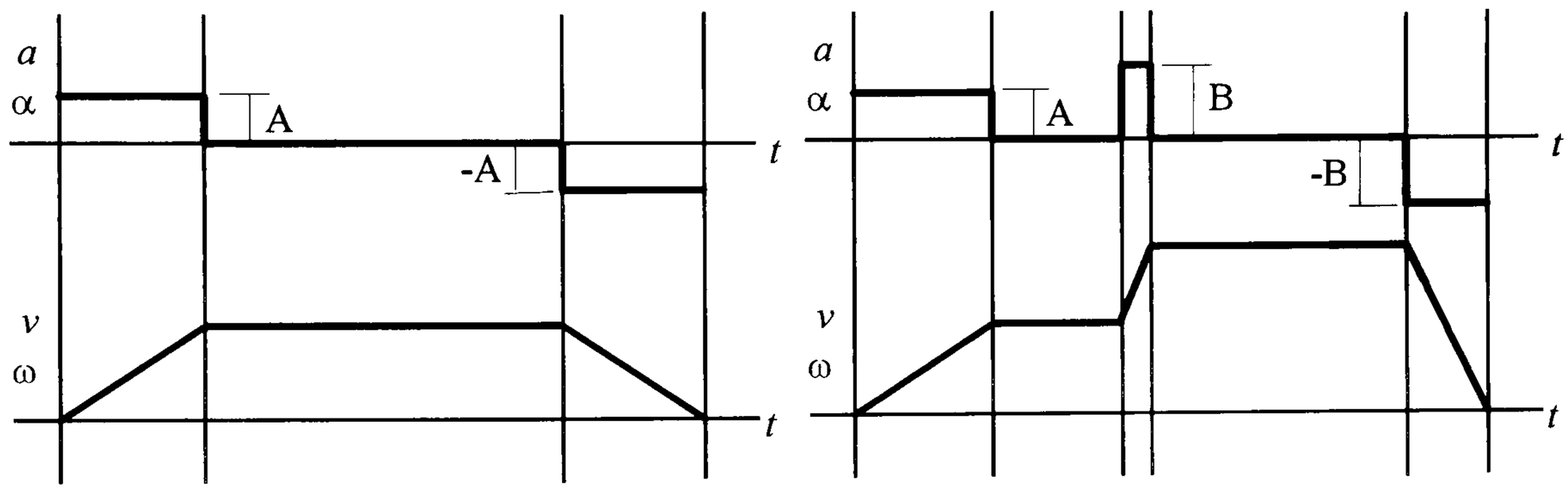

Figure 5.9. Motor control profiles

5.3.3. Characteristics

The motion co-ordinating mechanism of the mobile robot has three levels of controllers. Each of the two motor level controllers, including an optical encoder and a motor, provides an independent servo loop for translation or rotation. The command level controller delivers motion instructions to the motor level controllers, and produces information about the motor level controllers for the supervisor level controller. Therefore, it is possible to make posture estimates as the mobile robot moves, by the

supervisor level controller, using the dead reckoning method and encoder readings from the motor level controllers.

Although both discrete and continuous navigation modes are discussed, the discrete navigation mode is considered in the implementation. This is because an arbitrarily planned path in the configuration space may not be executed by the mobile robot. For example, as the mobile robot can not change its heading direction while it is moving along a straight route, the "shortest" path between the two configurations, Fig. 5.10(a), can not be performed. Also, a constant-curvature route may not be feasible due to the kinematic constraints of the mobile robot. For example, the circular curve route in Fig. 5.10(b) can not be practically followed, since the rotation motor has an accelerating-decelerating procedure. Besides, making an accurate estimate of postures along a continuous navigation is in practice a difficult issue. Using the dead reckoning method and shaft encoders alone, the posture-estimating is prone to modelling errors and noises from encoder quantization intervals. Therefore, the route and operation scheme, locally proposed by the triangulation based planning approach in the globally produced spatial channel (journey), is a discrete navigation. The planned discrete navigation is always able to be executed by the mobile robot directly.

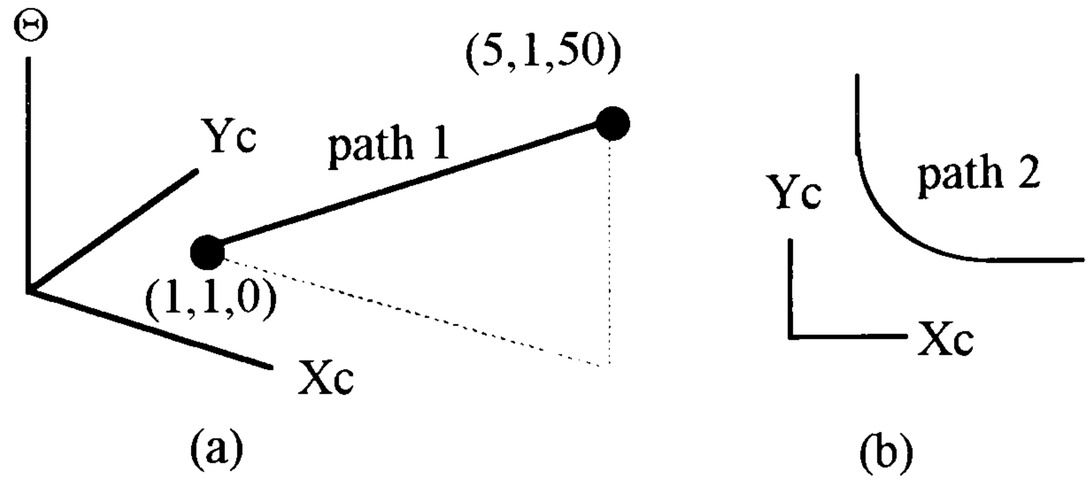

Figure 5.10. Unfeasible paths

5.4. EXTERNAL SENSING BY ULTRASONIC SENSORS

A mobile robot can navigate in three types of working environment according to the a priori knowledge the mobile robot has about its working environment;

(1) structured: a complete model is supplied,

(2) less structured: the working environment is partially known,

(3) unstructured: no a priori knowledge is given.

An external sensing ability can benefit a mobile robot in navigating safely in a structured environment, and is necessary to extend its navigational capability to a less structured or unstructured environment. In general, the external sensing ability of a mobile robot provides environmental information to both the planning and executing stages of the navigation strategy. At the planning stage, a model of the working environment can be provided through the external sensing ability. The more complete the environmental model is, the more precise navigation a mobile robot can plan. At the executing stage, a mobile robot is capable of doing close-loop navigation and dealing with uncertainties by integrating the external sensing ability with its motion co-ordinating mechanism. The newly attained information is also helpful to update the knowledge of a mobile robot about its current state and the working environment. The updated knowledge can be used to detect obstruction or errors.

In the project, the mobile robot is navigating within a constructed manufacturing environment, and a complete environmental model is supplied. Therefore, the concern is to develop a sensing mechanism for the mobile robot, which can monitor and assist the navigation. Two principal functions are included in the sensing mechanism: making posture estimates and detecting objects.

When the mobile robot is performing a navigational task, it must have some ways of finding its postures with respect to the manufacturing environment. Implementing a sensing mechanism that uses artificial beacons, fixed in the manufacturing environment, together with beacon-detecting sensors may provide accurate and reliable measurements

of beacon locations. Postures of the mobile robot with respect to the detected beacons, and thus to the manufacturing environment, can be derived from the measurements [139].

The beacon methods may provide a straightforward procedure. However, it is normally expensive to equip the manufacturing environment with beacons, covering the whole working site. Besides, modification costs and flexibility sacrifice have to be considered. Techniques, using naturally occurring structures of the manufacturing environment as beacons, and being capable of achieving comparable performance to the artificial beacon methods without modifying the manufacturing environment, are preferred.

In addition to the dead reckoning method using the two optical encoders, which has been incorporated into the motion co-ordinating mechanism, a sensing mechanism, using six ultrasonic sensors, is developed. Its purpose is to help the mobile robot to cope with uncertainties and to detect unexpected obstacles. Ultrasonic sensors have unique properties which make them extremely useful for mobile robot navigation. The transducers are safe and cheap, and physically robust and reliable. They can scan a wide variety of objects since most solids in manufacturing environments are good ultrasound reflectors. Also, data about range estimates are easy to extract from sensor signals. These properties are very useful for detecting objects, and are difficult to obtain by other sensing methods.

5.4.1. Structure of Sensing Mechanism

Hardware of the ultrasonic sensing mechanism consists of six transmit/receive transducers and circuits, and a dedicating timing, driving and interfacing circuitry. The control software is hierarchically structured, including the following three levels of controllers:

(a) Transducer level controller. There are six transducer level controllers. Each manages an ultrasonic transducer and a transmit/receive circuit. The transducers are

Polaroid grade electrostatic instruments [140], converting acoustic waves into voltage signals, and vice versa. Technical specifications, frequency range, and beam pattern for these transducers can be found in [141][142]. A description of the acoustic beam pattern is illustrated in Fig. 5.11, where the horizontal axis is the azimuth angle with respect to the transducer axis, in degrees, and the vertical axis shows acoustic intensity in dB relative to the on-axis level.

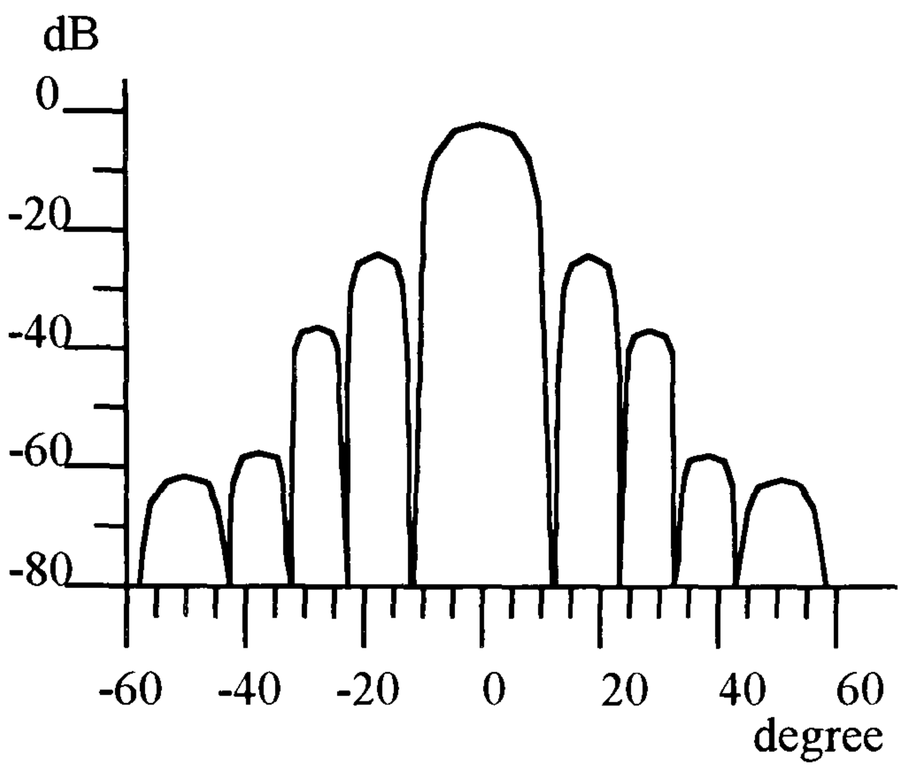

Figure 5.11. Beam pattern [140]

Figure 5.11 also indicates that the transducer has a central acoustic lobe whose beam width is 12 degrees between the -6dB points, at 50kHz [140]. This indication agrees well with our experimental results. However, the beam width is not very meaningful for interpreting Polaroid sensor data [33], and should be used only as a rough measure of probability of reception of an echo from a smooth surface [141]. In addition, the beam patterns of the transducers are not symmetrical [33], and vary from transducer to transducer. These effects are significant for the side-lobes. The differences in the surface area, texture, orientation, and size of an object will all affect the echo signal strength.

(b) Command level controller. The command level controller has a dedicated timing, driving and interfacing circuitry, which interacts with the six transducer level controllers. Operating theory behind the command level controller for detecting objects is based on the

propagation of acoustic waves. The speed of sound in air depends on the ambient temperature, humidity, and pressure. If this speed is measured or calculated, the distance travelled by an acoustic wave can be determined by measuring the elapsed time, or the time of flight of the acoustic wave. Practically, the command level controller initiates the transducer level controllers. The ultrasonic transducers, each embodying a transmitter and a receiver, transmit acoustic signals into space. Upon encountering an object, reflections, or echoes, may be detected by the ultrasonic transducers acting as receivers. Each transducer has a dedicated timing counter. A pulse reading is produced when amplitude of an echo, received by a transducer, exceeds a pre-set threshold level. The time of flight corresponding to the pulse reading is obtained, and is stored in the counter. If a detected echo signal does not exceed the threshold value, no pulse reading is registered in the counter. In this case, an arbitrary range value, such as zero or some large value, may be produced. The minimum distance at which an object can be detected is determined by the required duration of the blanking. Experimental results have shown that reliable readings can be obtained as close as 10cm. In addition, the command level controller has a manufacturer-defined operation system for controlling the circuitry. This operation system supports a set of control commands, which use two letter mnemonic commands and can be divided into status and action commands. A status command either changes a control parameter on the G96 Sonar Board [143], or returns a response regarding current states of the sensors. A action command causes a transducer driver to emit acoustic signals. Parameters following or responding to the control commands are in hexadecimal notation.

(c) Supervisor level controller. The supervisor level controller manages operations of the ultrasonic sensors at the highest level of the sensing mechanism. Programs are produced to initiate the transducers through the driving function of the command level controller. Once range, or time of flight, values are obtained, they are interpreted by the

supervisor level controller to corresponding values in distance notation. The command level controller operates on the first echo received, whose amplitude exceeds the pre-set threshold value. Therefore, multiple reflections from the same object are filtered, since these occur later than the first qualified reflection. As a result, a produced time of flight value is assumed to represent the distance from the transducer to the nearest reflecting point on an object within the transducer range. However, this assumption does not work well in some cases, which will be discussed in section 5.4.2. Similarly, signals that return to the receiver by bouncing off the floor and ceiling can be also ignored, allowing the use of a two dimensional model. To interpret a range value, a time of flight dot is placed at the transducer range along the line-of-sight [144][145][146] of the transducer, or the central axis of the acoustic beam.

A manufacturing environment is a constructed work space whose internal conditions can be maintained at some states. Our manufacturing environment for the mobile robot implementation is maintained, on average, at 25 degrees Celsius and 17% humidity. Therefore, a table for converting transducer readings from hexadecimal notation, to decimal notation, and to distance notation is experimentally produced, Table 5.3. The conversion table can also be theoretically produced, in that a reading count represents the number of 3.2552 microsecond cycles [143] for the echo to return, and the sound speed is $20.05\sqrt{25+273.16}$ metres per second [14]. However, Table 5.3 is used for data interpretation in the implementation. If a reading is between two sampling instances, it is linearly interpreted.

Ultrasonic sensors provide a safe, convenient and inexpensive means for determining proximity of objects. Since information produced by the ultrasonic sensing mechanism can be used quantitatively and qualitatively, the ultrasonic sensing mechanism constructs a useful function for implementing the planned navigation to the mobile robot. However, the main task, or problem, with the ultrasonic sensing mechanism is that the produced

ranging measurements require reliable geometrical interpretation to obtain meaningful environmental information.

cm	hex.	dec.	cm	hex.	dec.	cm	hex.	dec.	cm	hex.	dec.
0	0000	0	60	0449	1097	115	0819	2073	170	0BED	3053
10	00CC	204	65	04A0	1184	120	0875	2165	175	0C50	3152
15	0126	294	70	04FB	1275	125	08CF	2255	180	0CA7	3239
20	017A	378	75	0553	1363	130	0925	2341	185	0D03	3331
25	01D6	470	80	05B1	1457	135	097F	2431	190	0D5B	3419
30	022C	556	85	0609	1545	140	09DA	2522	195	0DB1	3505
35	0288	648	90	0661	1633	145	0A32	2610	200	0E10	3600
40	02E2	738	95	06BB	1723	150	0A8C	2700	205	0E6B	3691
45	033A	826	100	0714	1812	155	0AE0	2784			
50	0393	915	105	076F	1903	160	0B3E	2878			
55	03ED	1005	110	07BA	1978	165	0B94	2964			

Table 5.3 Range distance versus ultrasonic sensor reading

5.4.2. Physical Features and Experimental Results

In order to interpret the ranging data, provided by the ultrasonic sensing mechanism, to meaningful environmental information, three principal assumptions have been made [33][58][141][144][145][146] as previously described:

(1) A ranging data is produced by a reflecting point (dot) on an object.

(2) A reflecting point is at the central axis of the transducer, which produces the data.

(3) A reflecting point is the nearest point of the object to the transducer in the range.

However, experimental results show that these assumptions may not reliably explain the ranging data in some applications. These applications are analysed in order to propose guidelines for implementing the ultrasonic sensing mechanism, which can avoid causing the same problems and wrong interpretation.

5.4.2.1. Physical Features

When the ultrasonic sensing mechanism is initiated to detect an object within a transducer range, four situations may occur as illustrated in Fig. 5.12. In situations (a) and (c), ranging data, produced by the ultrasonic sensing mechanism, quantitatively and

qualitatively represent the existence of the object in a correct manner. In situation (d), no object exists but a ranging value is returned. Apart from the sensor hardware failure, the ranging value is usually caused by receiving an echo from another transducer. This problem can be technically solved by firing transducers sequentially, and hence a transducer can avoid being affected by others. In situation (b), the sensing mechanism can not quantitatively or qualitatively detect the existence of the target object correctly within a transducer range. This situation usually causes serious problems.

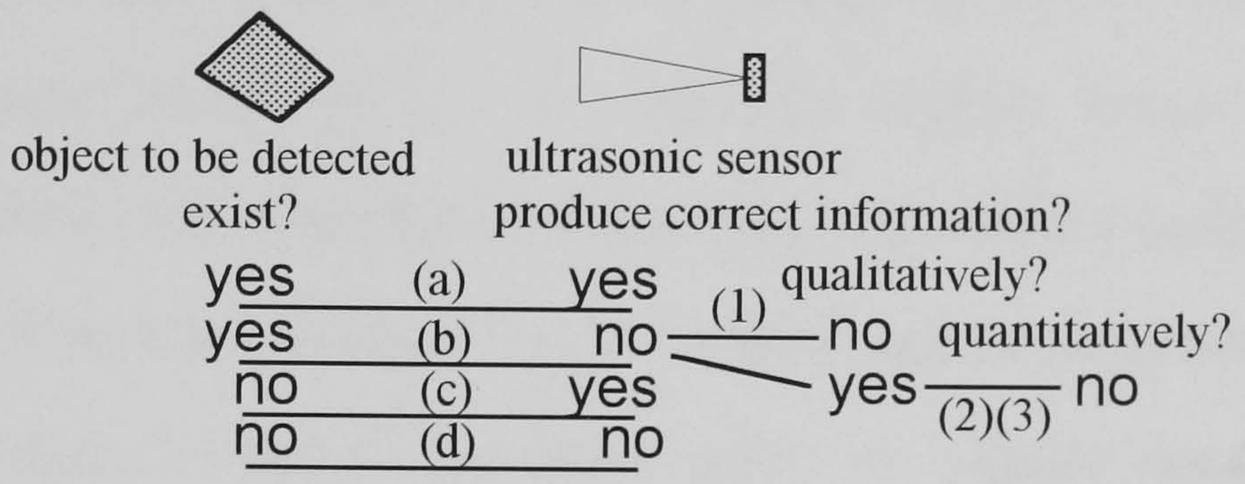

Figure 5.12. Situations using ultrasonic sensor

In situation (b), the sensing mechanism produces wrong environmental interpretation and causes problems. The problems may be classified into three types, Fig. 5.12:

(1) No reflection echo has been detected.

(2) The produced ranging distance is longer than the real one.

(3) The produced ranging distance is shorter than the real one.

Problem **(3)** is normally caused by the same reason as situation (d). Since situation (d) has been technically handled, problem **(3)** can be solved. As to problems **(1)** and **(2)**, theoretical analysis provides good explanations for the phenomena.

The ultrasonic sensing mechanism uses the pulse-echo ranging principle, that a short acoustic wave train is emitted from a transducer first. The ranging distance to an object is produced by measuring the time difference between the transmission of a pulse and reception of its echo. If an acoustic wave train is transmitted towards an object, but no reflection echo is detected, there are two possible reasons. First, energy of the acoustic

waves may be absorbed or diffused by the surface area and texture of the target object. Therefore, there is no echo, or no echo amplitude is large enough to be detected by the receiver circuit of the transducer. Second, the waves are reflected away from the receiver by an object surface which is not perpendicular to the transducer axis. The theoretical explanations behind this are discussed below.

There are certain object configurations, which cause an acoustic sensor to fail to detect an object. Take an object with a specular surface for example. A specular surface is one with roughness less than 5% of the acoustic wavelength [147], or 13mils (13/1000 inch) for 50kHz ultrasonic waves [141]. If a specular surface forms an angle with the transducer axis, which is greater than a critical value, the emitted acoustic wave train will be reflected away from the transducer by the surface, and no echo will be received. The critical value is equal to half of the beam width, or angular resolution [33], of the transducer. The principles are illustrated in Fig. 5.13.

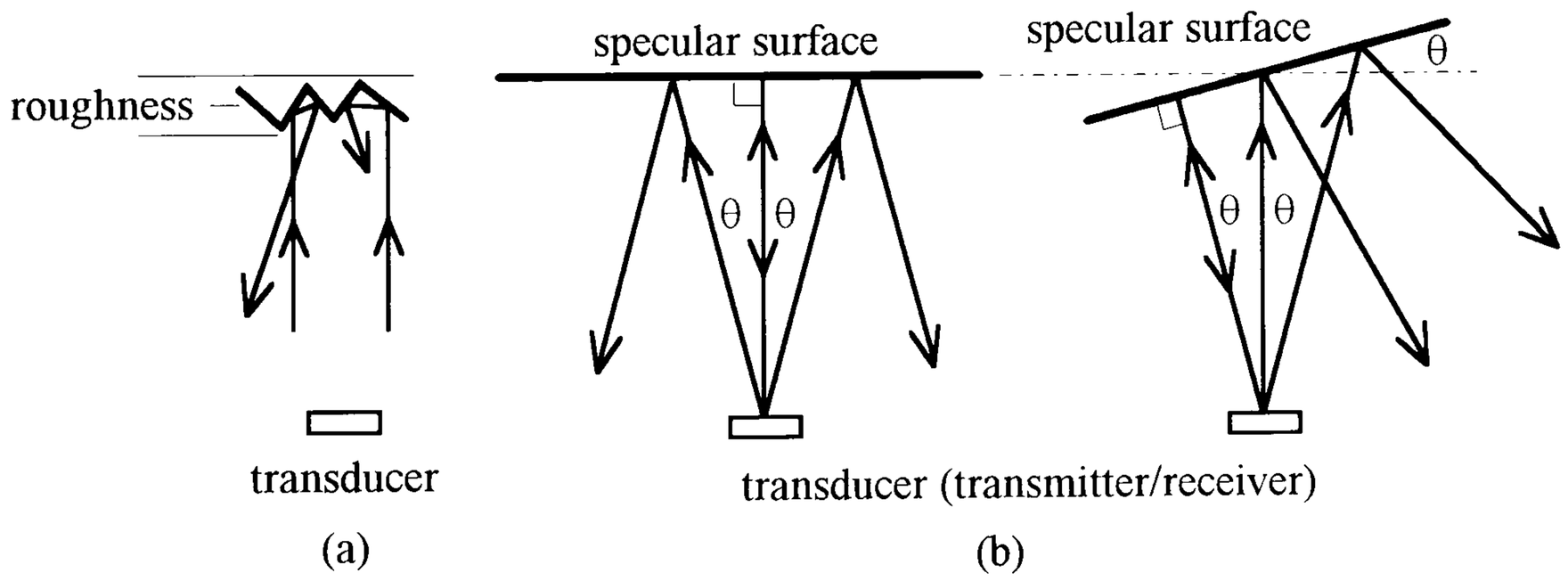

Figure 5.13. (a) Diffusion (b) Angular resolution

Six degrees is half of the beam width (central lobe), or angular resolution, of a Polaroid transducer, corresponding to a 50% drop in pressure amplitude from on-axis response [141]. However, experimental results show that the effective angular resolution of the ultrasonic sensing mechanism in the manufacturing environment is generally between 20 to 25 degrees. In this case, side lobes and objects with non-specular surfaces are the main

reasons for reflection echoes. Since the sensing mechanism is operated to attain surrounding information about nearby objects, detectable reflection echoes are likely to be received at that (20°-25°) angular resolution. Due to these physical features, it is only possible to detect an object with specular surfaces over the critical angle in the manufacturing environment, if complementary sensing systems, based on principles other than acoustics, are used.

Apart from the problem of no reflection echo, problem **(1)**, large distance readings may be produced in some applications, which do not correspond to obvious objects within the transducer range, problem **(2)**. This problem is the result of multiple reflections. Due to the physical features discussed before, the problem of multiple reflections can occur when an acoustic wave train is diverted away by an oblique surface of the target object. If the diverted acoustic wave train encounters other objects, and a reflection echo is detected by the receiver, the ranging distance thus produced for the target object is larger than the real one. Figure 5.14 illustrates the case.

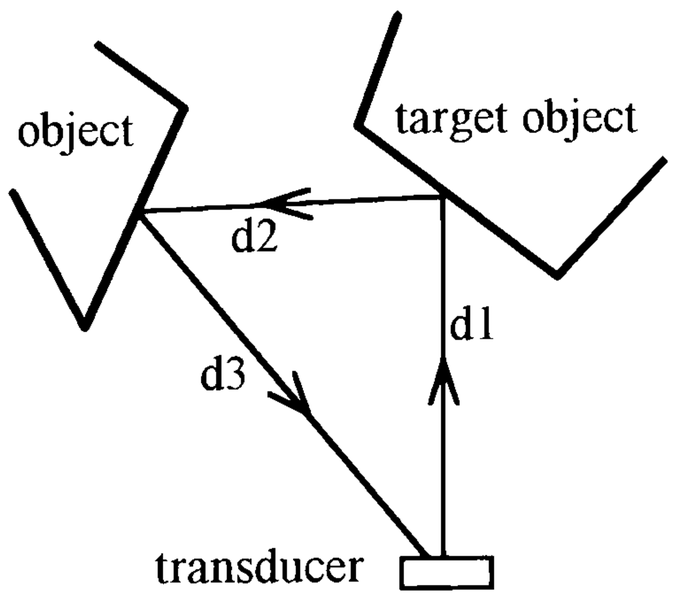

distance readings = (d1+d2+d3)/2

Figure 5.14. Multiple reflections

Finally, when aiming an ultrasonic sensor perpendicularly at an object surface, or directly at an object corner, there are clear and accurate readings produced, which are visible over a range of angles. Both convex and concave corners produce the same phenomenon [145][146]. Although ultrasonic sensors can produce accurate ranging

measurements in these cases, they typically have poor angular resolutions. This makes it hard to determine which characteristic of the working environment is being observed. Also, the physical features combine to make the interpretation of ranging data, produced by the ultrasonic sensing mechanism, very difficult. A reliable filtering strategy, or application guidelines, for effective data interpretation is required.

5.4.2.2. Results

Using the ultrasonic sensing mechanism to scan and build a local map, which can correctly represent the surrounding environment, turns out to be surprisingly difficult. The main source of difficulty is the relatively long wavelength of sound in the usable frequency range (7mm at 50kHz). This makes a transducer of a reasonable size (a few centimetres) to produce beam patterns with significant side-lobes (side lobes frequently produce detectable echoes), and to be diffraction-limited to an extremely poor angular resolution [148]. This lack of angular resolution makes an ultrasonic sensor very difficult, in many applications, to reliably produce ranging information about objects in its working environment.

The long wavelength also implies that objects with specular surfaces have to be carefully handled. Such a surface may reflect an ultrasonic wave train away from the transducer entirely, or bounce it back from an unexpected direction after multiple reflections. Unfortunately, these unexpected ranging data, caused by multiple reflections, are common, especially in artificial environments. Figure 5.15 illustrates an example environmental map, corresponding to a corner of the Mechanical Engineering robotics laboratory, produced by the ultrasonic sensing mechanism.

In summary, a number of features, inherent to the ultrasonic sensing mechanism, are:

(1) The timing circuitry limits the ranging precision.

(2) Detection sensitivity of an ultrasonic sensor varies with the angle of the reflecting object to the transducer axis.

(3) Sensor beams can be diverted away from transducers, and given unexpected distance readings, due to multiple reflections or specular reflections.

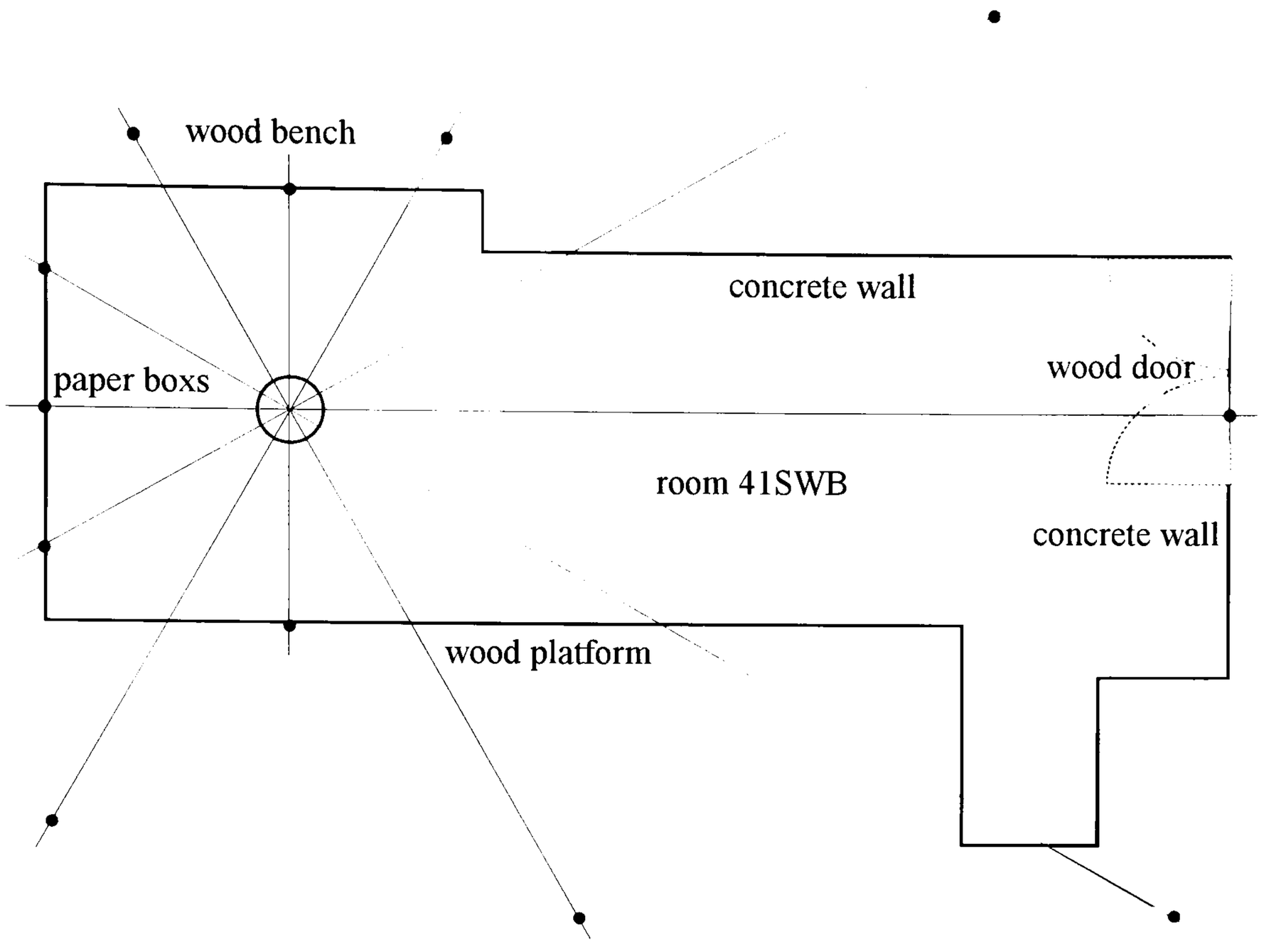

Figure 5.15. Example environmental map with 30 degree sampling intervals

5.4.3. Geometrical Arrangement and Applying Techniques

According to the experimental results summarised in section 5.4.2, some techniques are used for the ultrasonic sensing mechanism to aid the mobile robot navigation in practical scenes. When aiming an ultrasonic sensor directly and perpendicular at an object surface, clear and accurate information can be produced. Otherwise, a target object may not be detected correctly. As a result, ranging data produced by the ultrasonic sensing mechanism does not always correspond to an object at that range. A filter for effectively and correctly interpreting ranging data is required. Due to the low speed of sound, the sampling rate has to be kept low. In addition, it is necessary to pause operations of the ultrasonic sensing mechanism for about one second between supplying power to the driver

boards and the first transducer triggering. This pause allows the transducer driver circuitry to charge and stabilise.

As to the implementation of the ultrasonic sensing mechanism to the mobile robot navigation, if the six ultrasonic sensors are properly mounted on the mobile robot, reliable ranging information can be obtained. Since every route of the navigation, proposed by the triangulation based planning algorithm, is parallel to a boundary side of the solution channel, the six ultrasonic sensors are arranged in a ring, considering their physical features, in order to make the best use of the sensors. Figure 5.16 illustrates the geometrical arrangement of the six ultrasonic sensors.

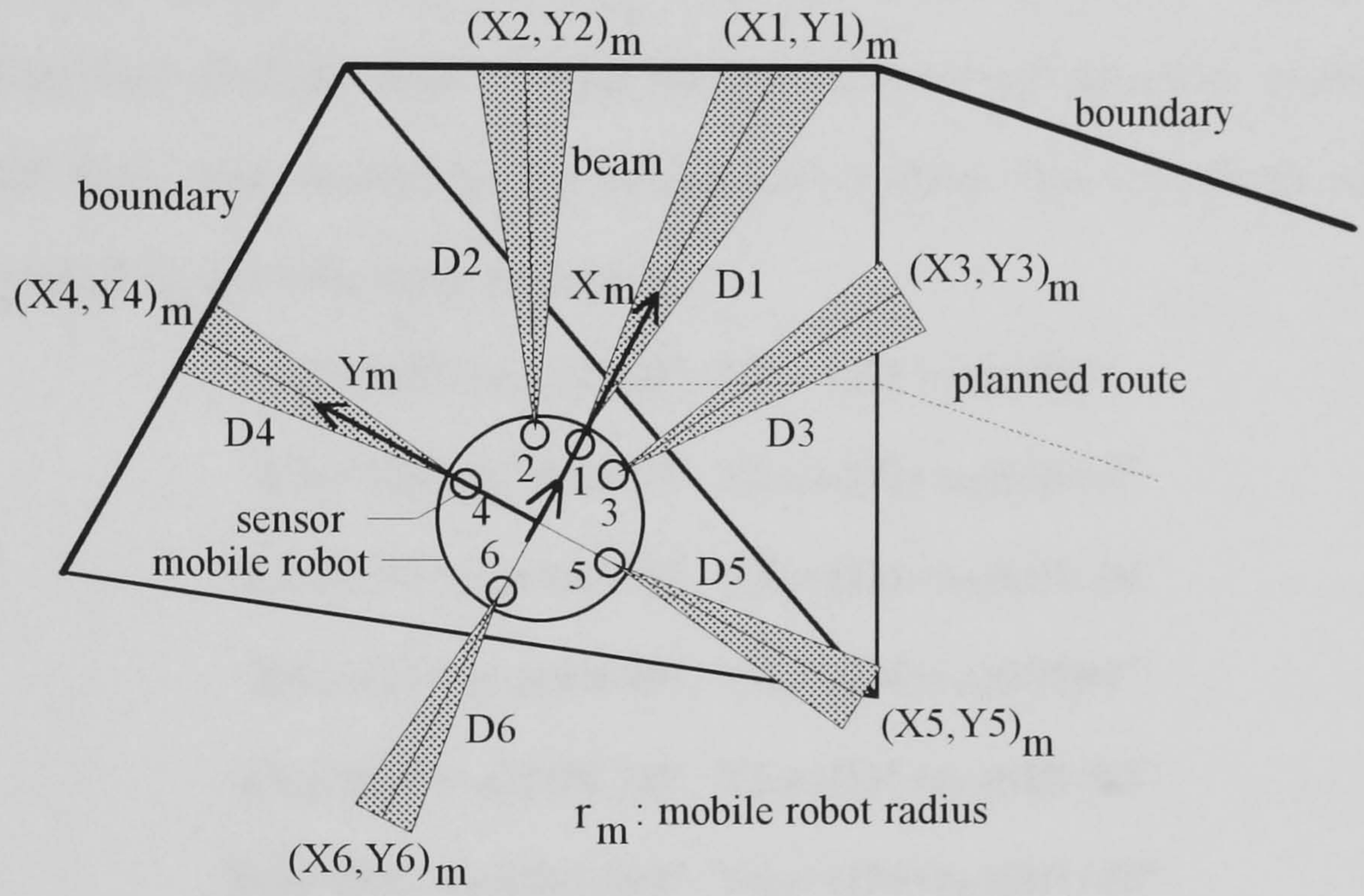

Figure 5.16. Geometrical arrangement of six ultrasonic sensors

The axes of the front three sensors, 1, 2 and 3, lie in the same horizontal plane at 30 degrees of azimuth intervals. They are for detecting unexpected objects in front, or measuring clearance space ahead. Two sensors, 4 and 5, are equipped on both sides of the mobile robot to monitor the navigational performance. When the mobile robot is performing the planned navigation, sensor 4 is routinely triggered to collect ranging data from the left side. This distance information can be used to tell whether the mobile robot

is moving along the planned routes precisely. Since the probing beam (transducer axis) of sensor 4 is always perpendicular to the heading direction of the mobile robot, the probing beam is normal to a boundary side of the solution channel. Reliable ranging data can be produced. If control errors of the motion co-ordinating mechanism are considered (less than ±0.5 degree in rotation and ±0.5cm in translation), the incident angle of the probing beam is nearly perpendicular. Reliable ranging data can still be produced. Therefore, readings produced by sensor 4 can reliably represent the left-side clearance between the mobile robot and a boundary side. Similarly, sensor 5 is used to monitor the navigational performance from the right side. Sensor 6 is used when the mobile robot has to reverse.

Ranging data, produced by the ultrasonic sensing mechanism, are used to map corresponding time-of-flight dots. Under the geometrical arrangement, position of these time-of-flight dots, with respect to the co-ordinate system, X_m-Y_m, of the mobile robot, can be calculated by the following equations:

$$X1_m=(D1+r_m)\cos 0^\circ,\ Y1_m=(D1+r_m)\sin 0^\circ$$

$$X2_m=(D2+r_m)\cos 30^\circ,\ Y2_m=(D2+r_m)\sin 30^\circ$$

$$X3_m=(D3+r_m)\cos -30^\circ,\ Y3_m=(D3+r_m)\sin -30^\circ$$

$$X4_m=(D4+r_m)\cos 90^\circ,\ Y4_m=(D4+r_m)\sin 90^\circ$$

$$X5_m=(D5+r_m)\cos -90^\circ,\ Y5_m=(D5+r_m)\sin -90^\circ$$

$$X6_m=(D6+r_m)\cos 180^\circ,\ Y6_m=(D6+r_m)\sin 180^\circ$$

where the notation is also illustrated in Fig 5.16.

Ultrasonic sensors provide a low-cost, safe and convenient means for distance measurement. Proximity information about "natural" beacons can be used qualitatively or quantitatively. However, since the reliability of the produced data depends highly on the angle between the probing beam of a transducer and the target object surface, an interpretation filter which can discard unreliable data is important. A geometrical arrangement is proposed for this purpose. Also, integrating the motion co-ordinating and sensing mechanisms in a co-operative fashion is vital to the mobile robot navigation.

5.5. IMPLEMENTATION

This section describes the implementation of the triangulation based planning approach to the mobile robot. The target is to embody the mobile robot with an executing capability, which can manage the motion co-ordinating and sensing mechanisms to achieve the proposed discrete navigation, specified by a route and associated operation scheme of the mobile robot.

5.5.1. Managing Mechanism

In order for the mobile robot to smoothly execute a navigation, co-operatively integrating the navigation planning, motion co-ordinating and sensing mechanisms is important [48]. Since the three mechanisms have been individually discussed and developed, a managing mechanism is developed for the integration purpose. This managing mechanism is functionally similar to the two used in the graphical user interface tool and the manipulator simulation system, section 5.1 and 5.2, but operates a different motion co-ordinating mechanism (mobile robot vs. computer screen vs. manipulative robot) and sensors (optical encoders and ultrasonic sensors vs. human operator vs. vision camera).

During navigation, the managing mechanism continuously receives on-line sensory information, which comes from the ultrasonic sensing mechanism and the optical encoders of the motion co-ordinating mechanism. As a result, the managing mechanism has to filter and integrate the sensory information. Figure 5.17 illustrates the implementation structure.

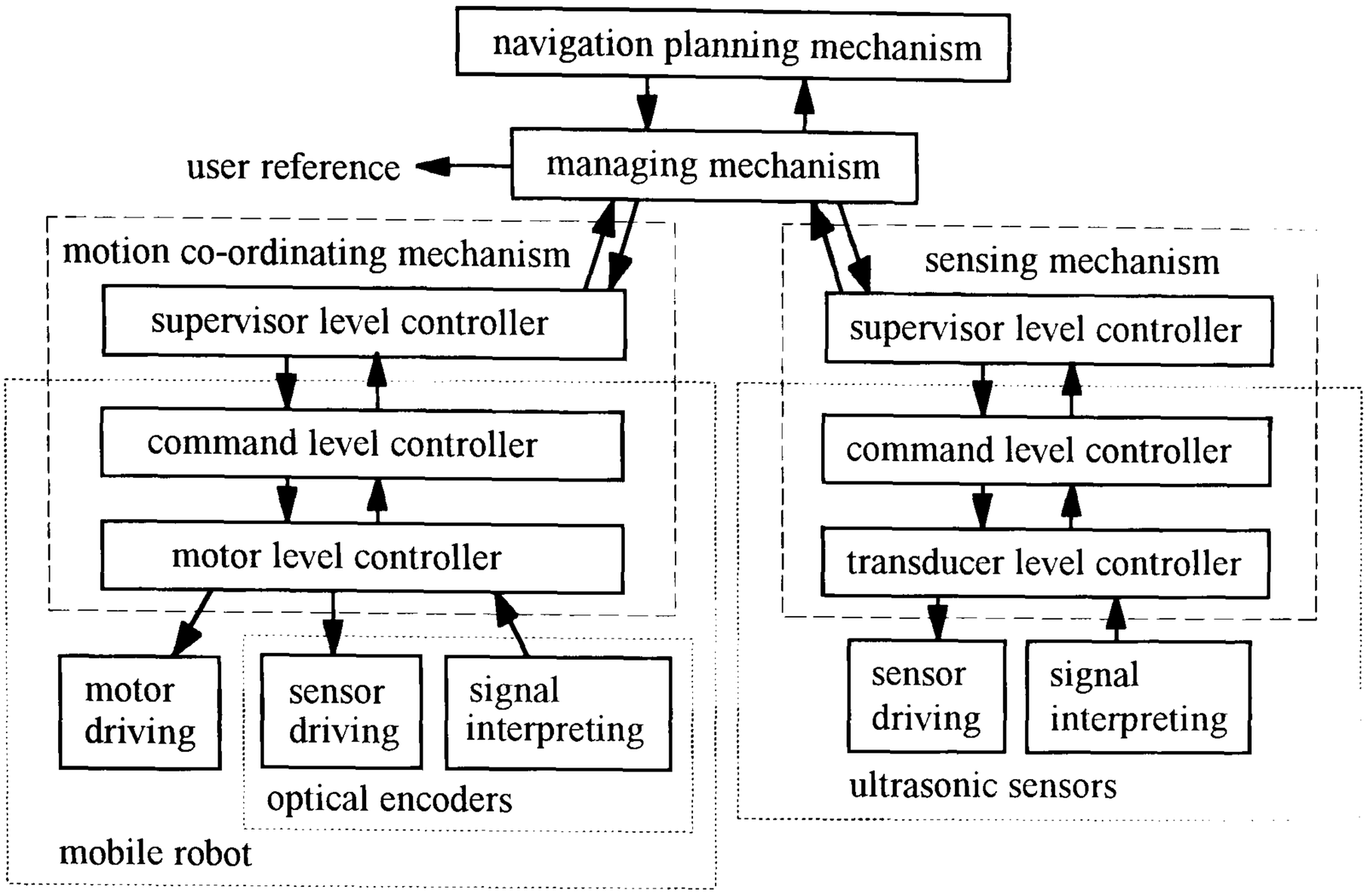

Figure 5.17. Managing mechanism

5.5.1.1. Management of Sensory Information

The acquisition of sensory information, by the motion co-ordinating mechanism (optical encoders) or the sensing mechanism (ultrasonic transducers), is individually interpreted. Each mechanism produces sensory information of a specific module. The two information modules are both exported to the managing mechanism to construct a common environmental representation in the co-ordinate system of the navigation planner. Due to the intrinsic limitations of the qualitatively different sensing devices, it is essential to integrate information coming from these sensors. Specific assertions provided by the information modules are correlated to each other in the managing mechanism.

In general, sensory information can be used by a mobile robot for four purposes:

(1) obtaining a priori information about the environment for the initial planning [57],

(2) localisation by matching against the build-in or constructed map [49][149],

(3) correction of the position and orientation errors [50][150][151],

(4) detection of potential obstruction and minimisation of the effects [47][51][152].

In the applications, the working domain is a manufacturing environment, and a priori information about the manufacturing environment is given to the mobile robot, through the graphical user interface tool. A manufacturing environment, such as a factory or warehouse, normally has a fairly well known construction. A manufacturing environment is also likely to be traversed repeatedly by the mobile robot. Therefore, it is reasonable to build a priori environmental map as a guide to navigation. Both on-line sensory information and map information are essential for effective navigation.

(a) Localisation and correction. To achieve a navigation, the mobile robot has understandings of its surroundings and postures, by acquiring and manipulating a model of the manufacturing environment. This model is based on the given environmental map, and assertions composed from the various sensors, and reflects the sensory data obtained and hypotheses proposed so far. Local information is continuously collected for localisation through a sequence of activities, including generation of expectations, natural landmark (boundary sides) recognition, and matching of newly acquired information against the stored environmental map. Localisation of the mobile robot is mainly by the dead reckoning method and optical encoders, which deduce postures of the mobile robot from the velocity history of the motion co-ordinating mechanism. Expectations along the navigation are generated, which include knowledge about clearance ahead and aside with respect to the postures. However, errors encountered by the dead reckoning method and optical encoders are cumulative. The mobile robot that navigates in this way alone will eventually lose track of its postures. This is handled by periodically re-establishing absolute postures, using the ultrasonic sensing mechanism and generated expectations. The motion co-ordinating and ultrasonic sensing mechanisms can be connected by the following equations:

$$X_w = X_i + (X_m \cos\Theta_i - Y_m \sin\Theta_i)$$

$$Y_w = Y_i + (X_m \sin\Theta_i + Y_m \cos\Theta_i)$$

where (X_i, Y_i, Θ_i) is the posture of the mobile robot at the time instant t_i, (X_m, Y_m) the position of one of the six time-of-flight dots with respect to the mobile robot, and (X_w, Y_w) the position of the time of flight dot with respect to the co-ordinate system of the manufacturing environment, Fig. 5.18(a).

Although the mobile robot can reliably navigate, an error in rotation can cause a significant offset displacement after a long translation distance. The rotation error has been experimentally showed to be small (less than $\pm 0.5°$), but happening often and randomly. If posture (X_i, Y_i, Θ_i) is produced by the dead reckoning method and optical encoders, section 5.3.1.2, the produced (X_w, Y_w) position will be different to the expected (X_w, Y_w) position. Since a route segment of the planned discrete navigation is always parallel to a boundary side (or nearly parallel if the rotation error is considered), the two side ultrasonic sensors can reliably produce ranging information. By comparing the ranging information with the expected distance, posture correction is made. Figure 5.18(b) illustrates the method.

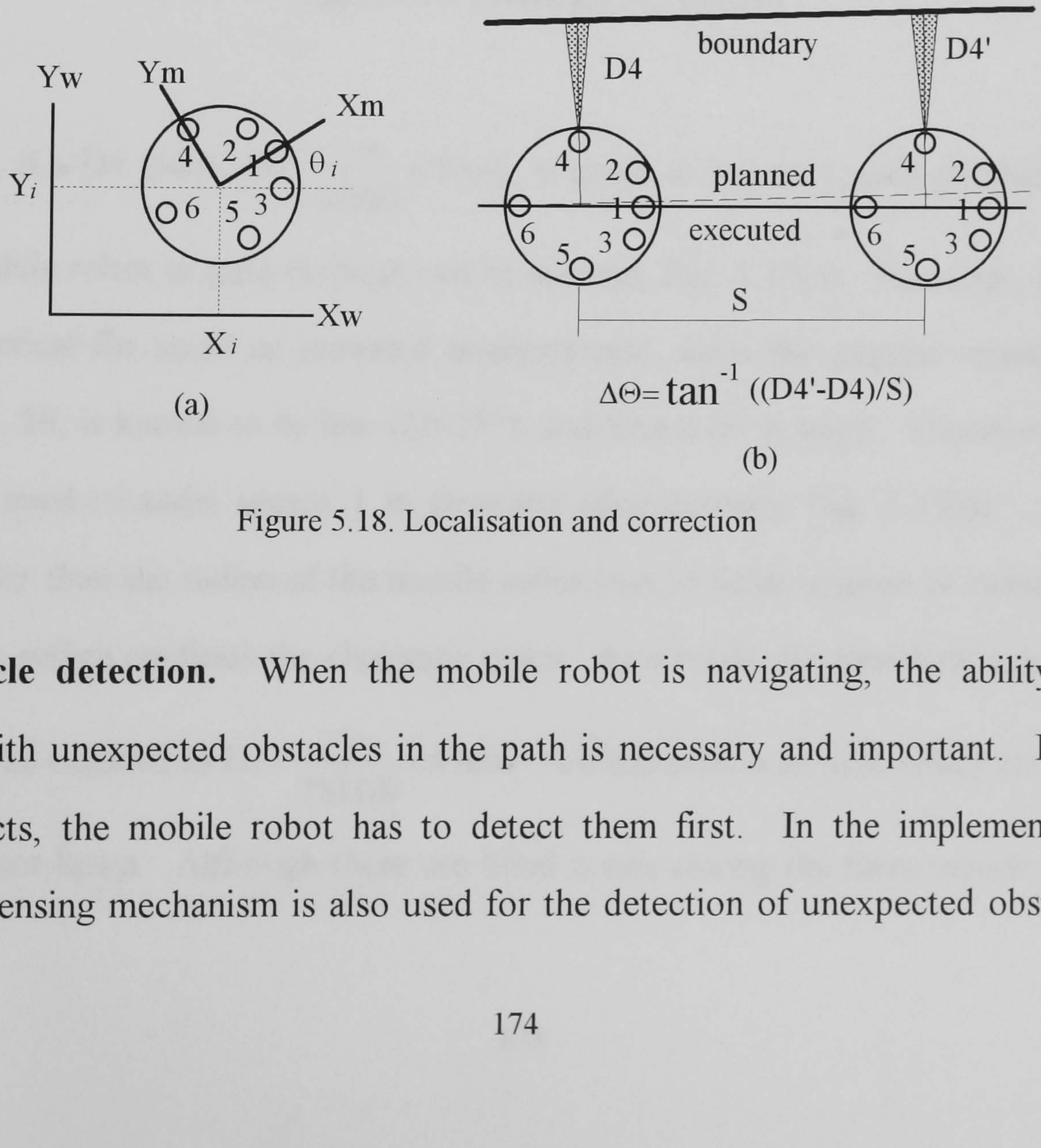

Figure 5.18. Localisation and correction

(b) Obstacle detection. When the mobile robot is navigating, the ability to avoid colliding with unexpected obstacles in the path is necessary and important. In order to avoid objects, the mobile robot has to detect them first. In the implementation, the ultrasonic sensing mechanism is also used for the detection of unexpected obstacles. An

obstacle is viewed as a solid object, which extends vertically from the ground surface to a height more than the altitude of the sensor ring (about 30cm). Detection is defined as a discontinuous state variation in one of the six ultrasonic sensors due to the acquisition of sensed data relating to an obstacle. The front three sensors, 1, 2 and 3, are mainly for detecting unexpected obstacles ahead, acting as sensor bumpers. Since thresholds can be assigned to the front three sensors, a safety strategy for the mobile robot is produced. Figure 5.19 illustrates the safety strategy.

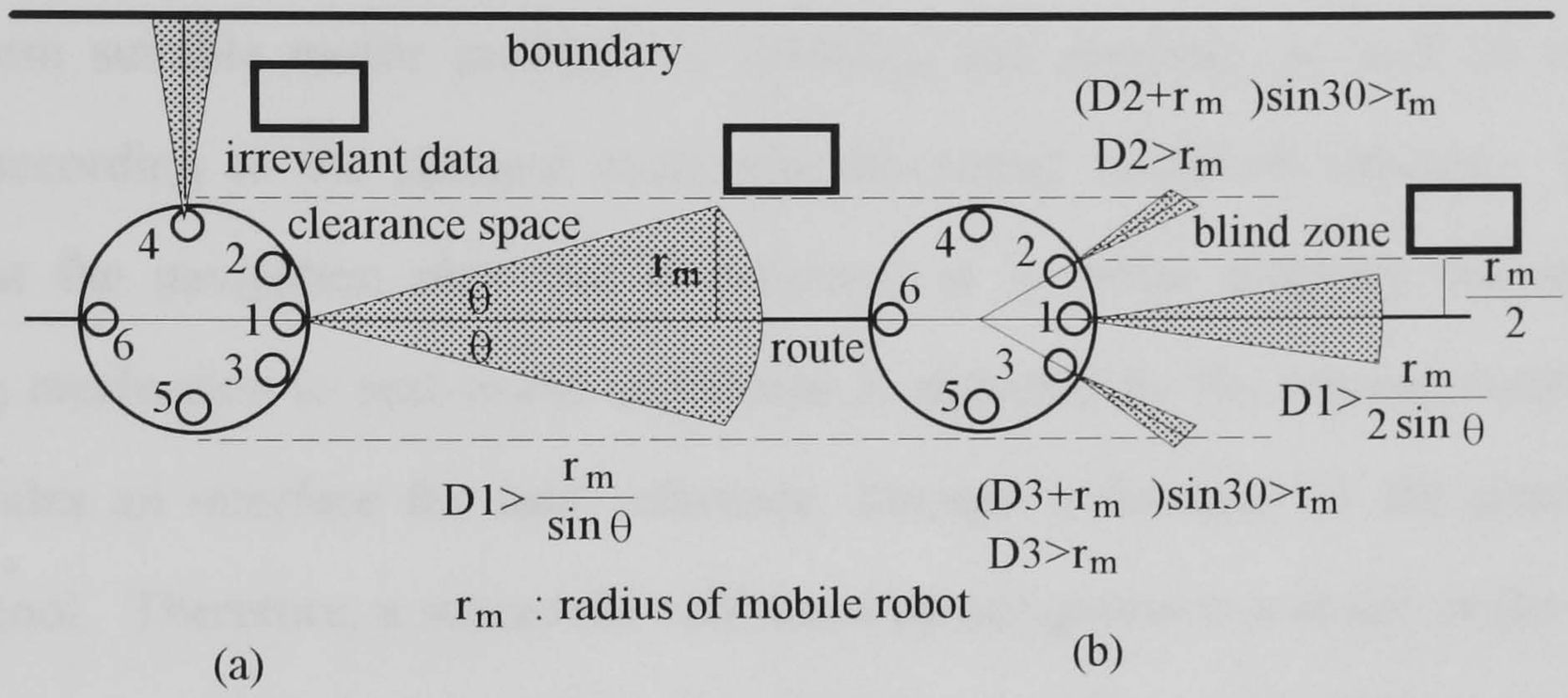

Figure 5.19. Thresholds for clearance

Ideally, if a D1 value, D1>$\frac{r_m}{\sin\theta}$≈90cm, is given to sensor 1, enough clearance space for the mobile robot to pass through can be assured, Fig. 5.19(a). However, this strategy is not practical for small or crowded environments, since the angular resolution of the transducer, 2θ, is known to be low (20-25°), and hence D1 is large. Therefore, sensors 2 and 3 are used to assist sensor 1 in crowded environments, Fig. 5.19(b). A threshold value greater than the radius of the mobile robot (r_m≈15.5cm) is given to sensors 2 and 3, D2, D3>r_m, which confirms the clearance space. As a result, the threshold value, assigned to D1, can be reduced to D1>$\frac{r_m}{2\sin\theta}$≈45cm. A blind zone is an area which is not covered by any sensor beam. Although there are blind zones among the three sensor ranges, the

$D1 > \frac{r_m}{2\sin\theta}$ assignment can assure that an unexpected obstacle, which is within a blind zone of the clearance space, will be detected by sensor 2 or 3 before collision. Any discontinuous state variation of the two side sensors, 4 and 5, which is irrelevant to the expectations for boundary edges, is ignored.

5.5.1.2. Management of Activities

The goal of the navigation strategy at the executing stage is to automatically compose and perform suitable motor profiles for wheeling and steering, as well as to activate sensors, according to the planned route and associated operation scheme. This stage carries out the navigation plan that is exported to it, while adapting the motion co-ordinating mechanism to real-world conditions as detected by the sensing mechanism. It also provides an interface for user reference, through a function of the graphical user interface tool. Therefore, a successful collision free navigation is a result of the managing mechanism co-operatively integrating the planning, sensing, and motion co-ordinating mechanisms to move the mobile robot between two admissible postures.

The managing mechanism is responsible for the scheduling of activities of the mechanisms, and for combining plan driven (actions) and sensory data driven (reactions) activities in an integrated manner to achieve coherent behaviours. These activities are mainly for two purposes: maintaining navigation and handling unexpected obstacles.

(a) Maintaining navigation. To achieve the prescribed discrete navigation, the motion co-ordinating mechanism is requested to provide a sequence of motor actions first. These motor actions describe the performance of the mobile robot along the navigation. The mobile robot is then initiated to perform the motor actions. During the performance, the posture estimates for the mobile robot, with respect to the environmental map, are mainly based on the velocity history of wheeling and steering, and subject to readings from the

optical encoders. These posture estimates are provided to the managing mechanism to deduce expectations for locality information, according to the given environment map. Since the ultrasonic sensing mechanism is consistently initiated to monitor the navigation performance, ranging data acquired are also given to the managing mechanism for posture modification. By matching the acquired information against the expectations, deviations from the route are calculated according to section 5.5.1.1.

To maintain the mobile robot along the desired navigation, a compliance control is performed by selectively providing corrective compensation torques to both motors. In addition to adjusting for the navigation, the deviation information is also used to update the knowledge about the current posture of the mobile robot with respect to the given environmental map. However, the execution speed at present is low since delay time is required for the sensor information to be received and processed.

(b) Handling unexpected obstacle. In the discrete navigation, the mobile robot acquires information about clearance ahead, and reacts to the data perceived, while it is moving. This is done by using the front three ultrasonic sensors and the safety strategy, proposed in section 5.5.1.1. If the safety strategy has been satisfied, that no unexpected obstacle has been detected, the managing mechanism assumes that the mobile robot can navigate safely forwards. Otherwise, unexpected obstacles have been detected, and the managing mechanism asks the motion co-ordinating mechanism to immediately bring the mobile robot to stop.

If an unexpected obstacle is detected by sensor 1, which is at S distance away, the deceleration, a, will be assigned to a value according to $\frac{v}{2a}<S$, where v is the instantaneous velocity at the sampling time. Similarly, if an unexpected obstacle is

detected by sensor 2 or 3, which is at S distance away, the deceleration, a, will be assigned to a value according to $\frac{v^2}{2a} < \frac{\sqrt{3}}{2} S$.

Once the mobile robot stops, the managing mechanism will export the unexpected obstruction message and posture information to the planning mechanism to plan a diverted or new navigation, and direct the navigation plan executing again.

5.5.2. Implementation Results

A general task for the flexible material transport system is to safely deliver materials from one location to another within a manufacturing environment. The mobile robot navigation is fundamental. Presented is the implementation results of the triangulation based navigation planning approach, using a B12 three-wheel omni-directional mobile robot and six Polaroid ultrasonic sensors.

To initiate a navigational task, a job description (goal posture) as well as an environmental map (obstacle information) are given to the planning mechanism through the graphical user interface tool. A discrete navigation is planned, which consists of a route and associated operation schemes. This navigation plan is interpreted, by the motion co-ordinating mechanism, to a sequence of motion commands of the mobile robot. The sensing mechanism, operating a ring of ultrasonic sensors, produces surrounding information for the detection of unexpected collisions and modification of navigational behaviours. The managing mechanism routinely integrates the sensing and motion co-ordinating mechanisms to monitor and correct the navigation performance, while the mobile robot is carrying out the planned discrete navigation.

In the implementation, the ultrasonic sensing mechanism performs two functions. First, it provides a means for safe encoder-based movement. Range readings from the three forward sensors are subjected to the safety strategy, so that the mobile robot navigation is sensitive only to unexpected obstacles located in the path. When an unexpected obstacle

is detected, the mobile robot brings itself to stop. The second function of the ultrasonic sensing mechanism is to maintain clearance between the mobile robot and the environmental boundary. Since the environmental map is given, clearance expectations along the planned discrete navigation can be produced. By matching the ranging data from the two side sensors against the produced expectations, posture errors can be supplied to the motion co-ordinating mechanism, which then steers and drives the mobile robot with compensations.

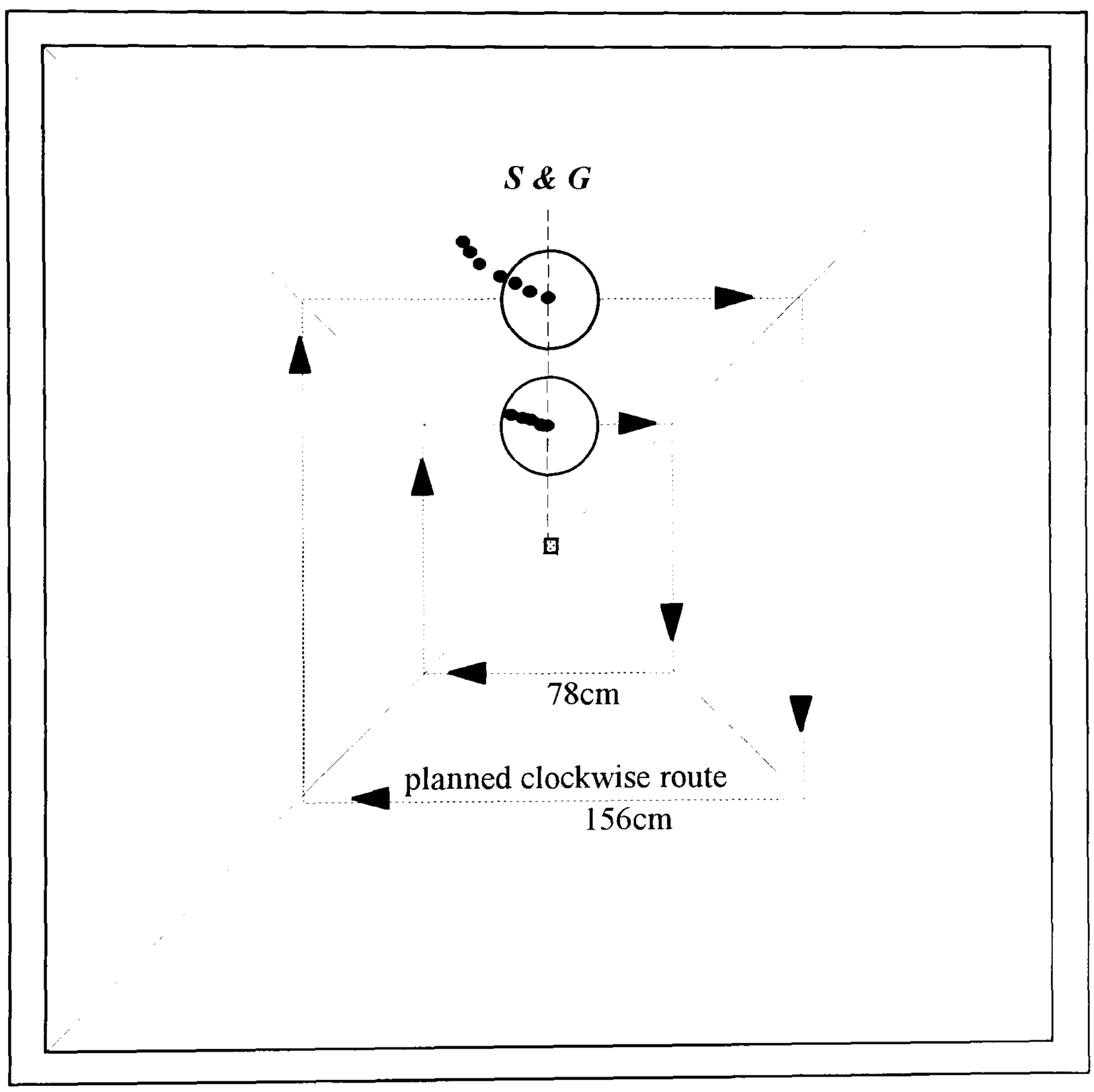

Figure 5.20. Optical encoders only

Figure 5.20 illustrates experimental examples when the mobile robot is performing navigation without integrating the ultrasonic sensing mechanism. A "point" obstacle is assumed at the centre of the platform. Two discrete navigational tasks, requiring the mobile robot to move along two square routes (78cm × 78cm and 156cm × 156cm) and terminate at the start postures, are assigned. The terminating positions of the mobile robot after several discrete navigational cycles are distributed as illustrated in the figure. Since the motion repeatability of the mobile robot in this manufacturing environment has been experimentally shown to be randomly within ±0.5cm and ±0.5 degree, the navigation results can be analytically explained in Figure 5.21(a). From the start position, S, errors are cumulative in turning at the four corners before reaching the goal position, G. Should all the errors be positive and of maximum value then the total error, SG, for the case of the 156cm square route, can be estimated to be around 11.2cm for a cycle run, Fig 5.21(b).

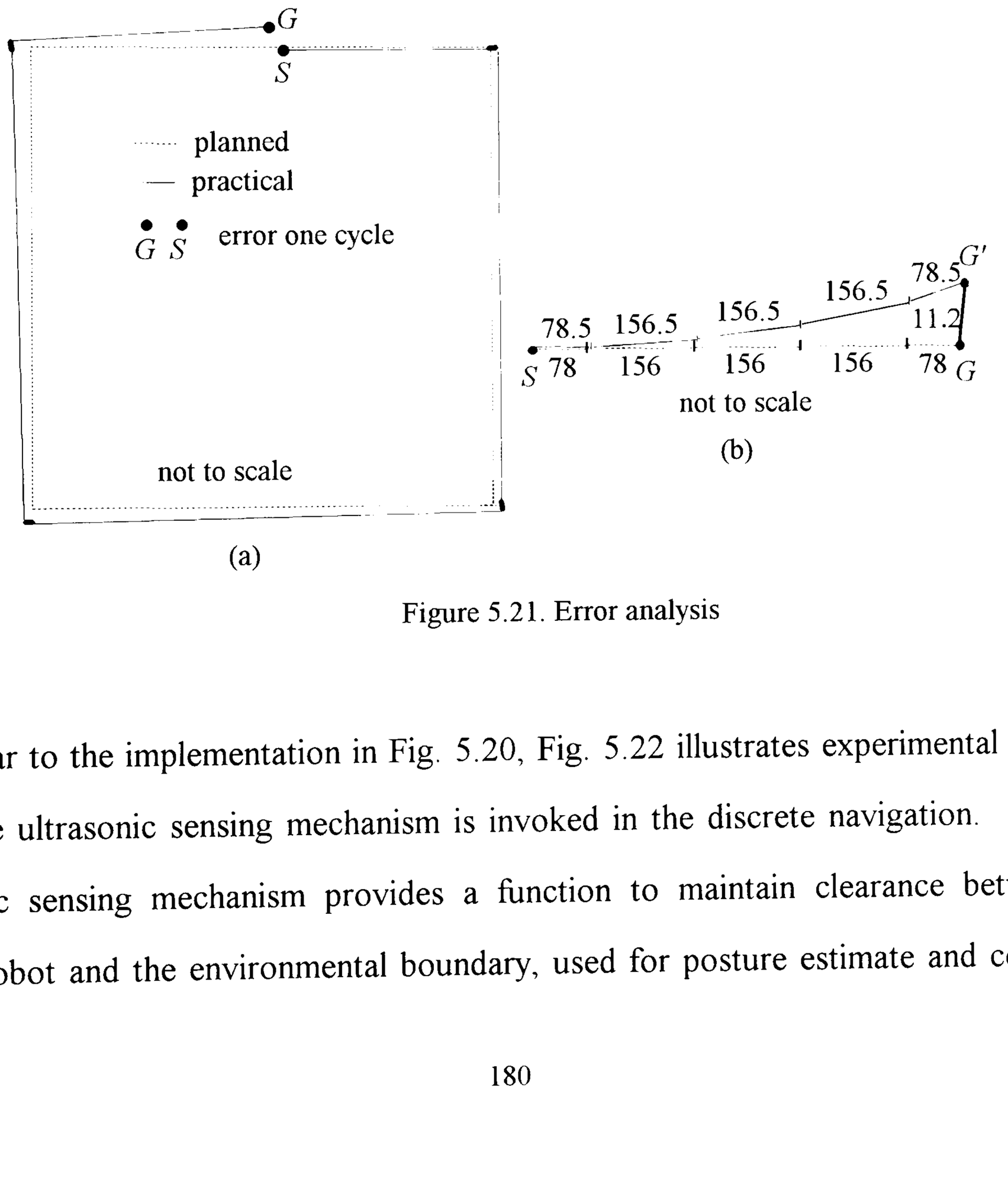

Figure 5.21. Error analysis

Similar to the implementation in Fig. 5.20, Fig. 5.22 illustrates experimental examples when the ultrasonic sensing mechanism is invoked in the discrete navigation. Since the ultrasonic sensing mechanism provides a function to maintain clearance between the mobile robot and the environmental boundary, used for posture estimate and correction,

the lateral and longitudinal deviation is improved, compared with Fig. 5.20. The lateral deviation stops growing "out" after several runs of discrete navigation, which is subject to the reliability tolerance (5cm in the example) defined to the ultrasonic sensing mechanism. The longitudinal deviation also reduces since a compensation scheme (2.5cm for a cycle run) is applied.

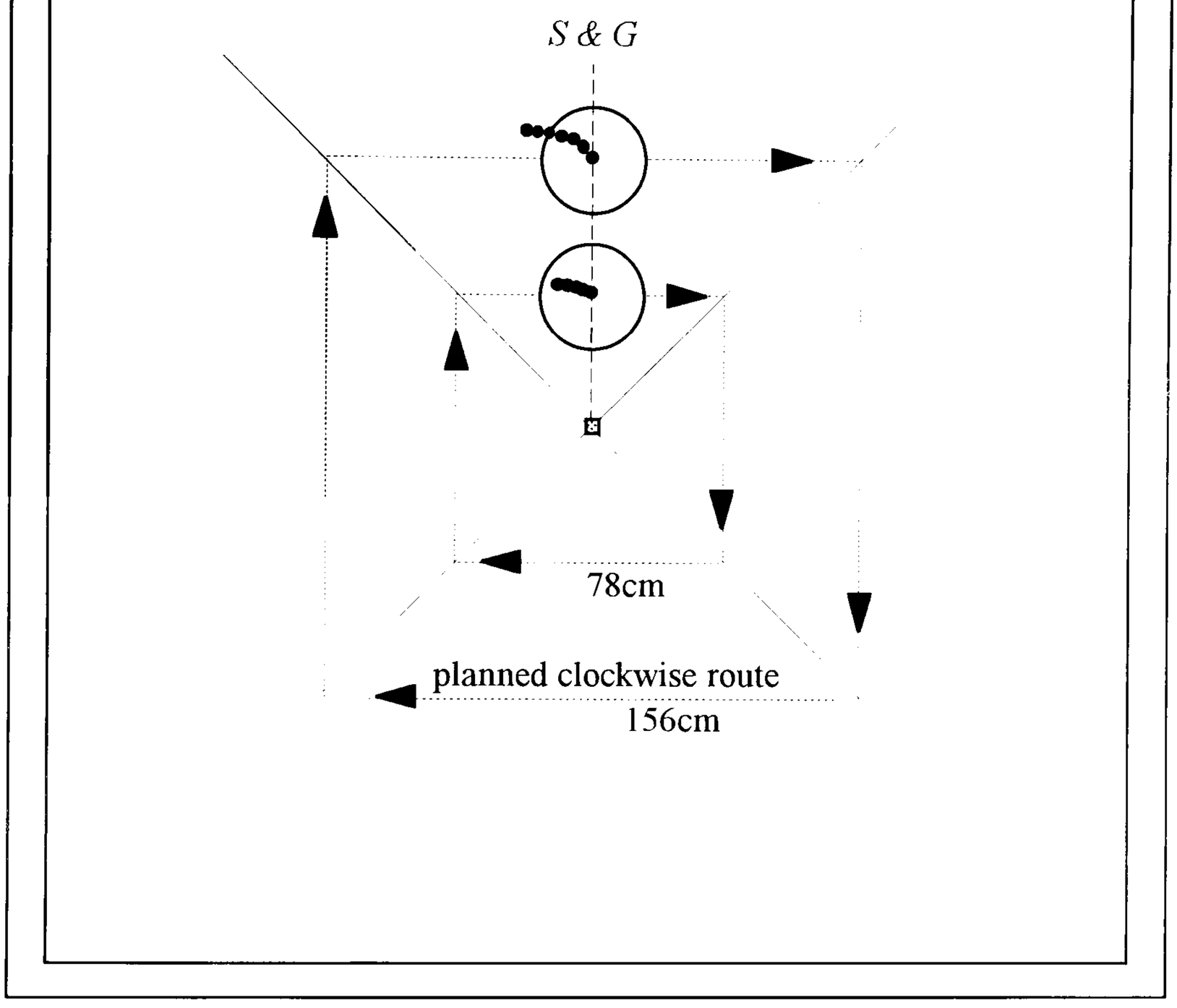

• location distribution

..... planned discrete navigation

Figure 5.22. Optical encoders & ultrasonic sensors

Finally, Fig. 5.23 illustrates two discrete navigation experimental examples within a layout of the manufacturing environment. In example 1, *S1* to *G1*, the mobile robot navigates to the goal without collision. In example 2, *S2* to *G2*, an unexpected obstacle, located in the path after the mobile robot starts the discrete navigation, is detected by one

(left-hand) of the three forward ultrasonic sensors (readings do not match the clearance expectations). The mobile robot then brings itself to stop.

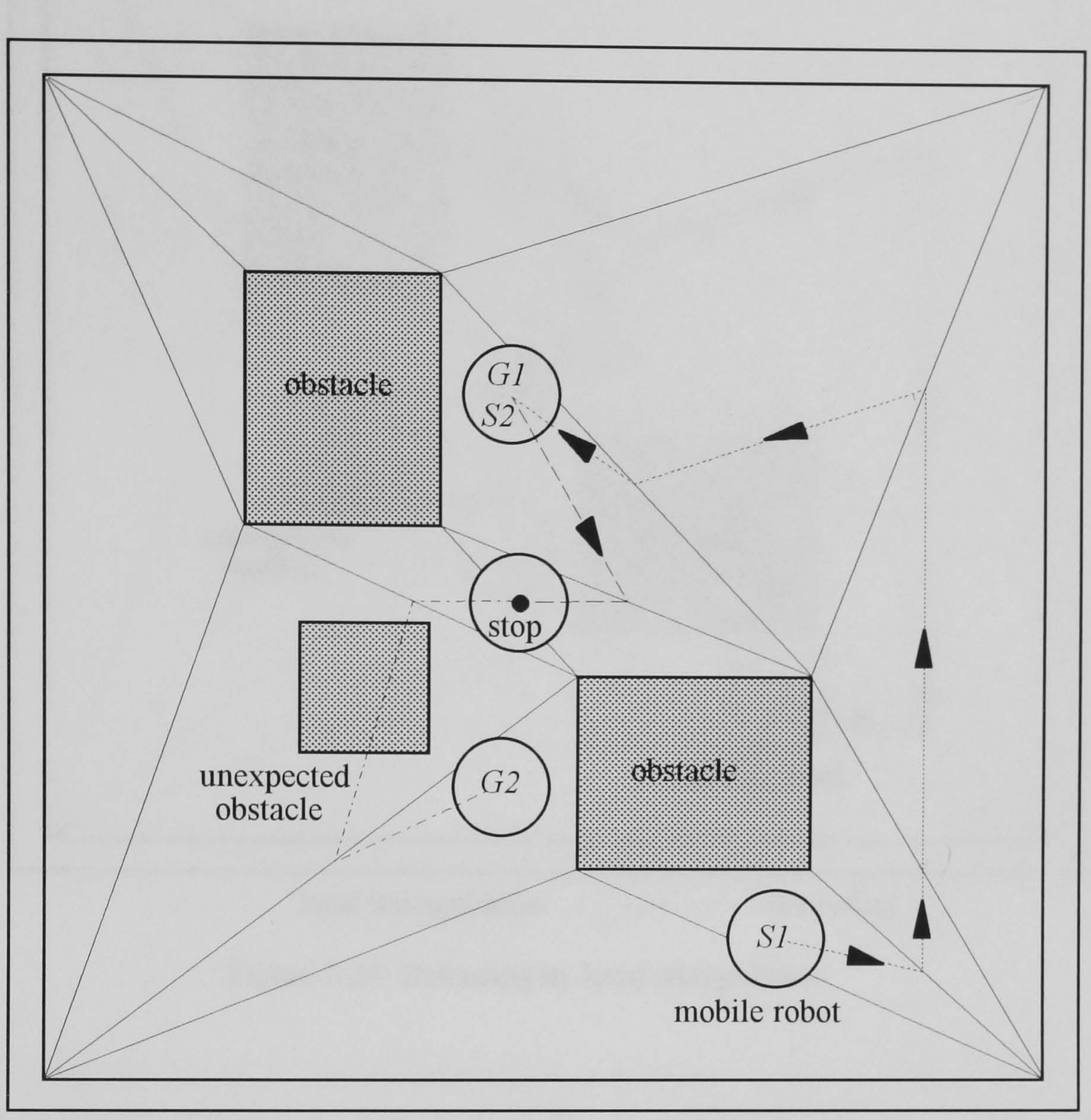

Figure 5.23. Navigation examples

The ultrasonic sensors are not, at present, sufficiently developed to enable the extent of the unexpected obstacle to be determined. When this is possible then from the stop position further local triangulation might produce a safe navigation to the goal position *G2*. Figure 5.24 illustrates the case.

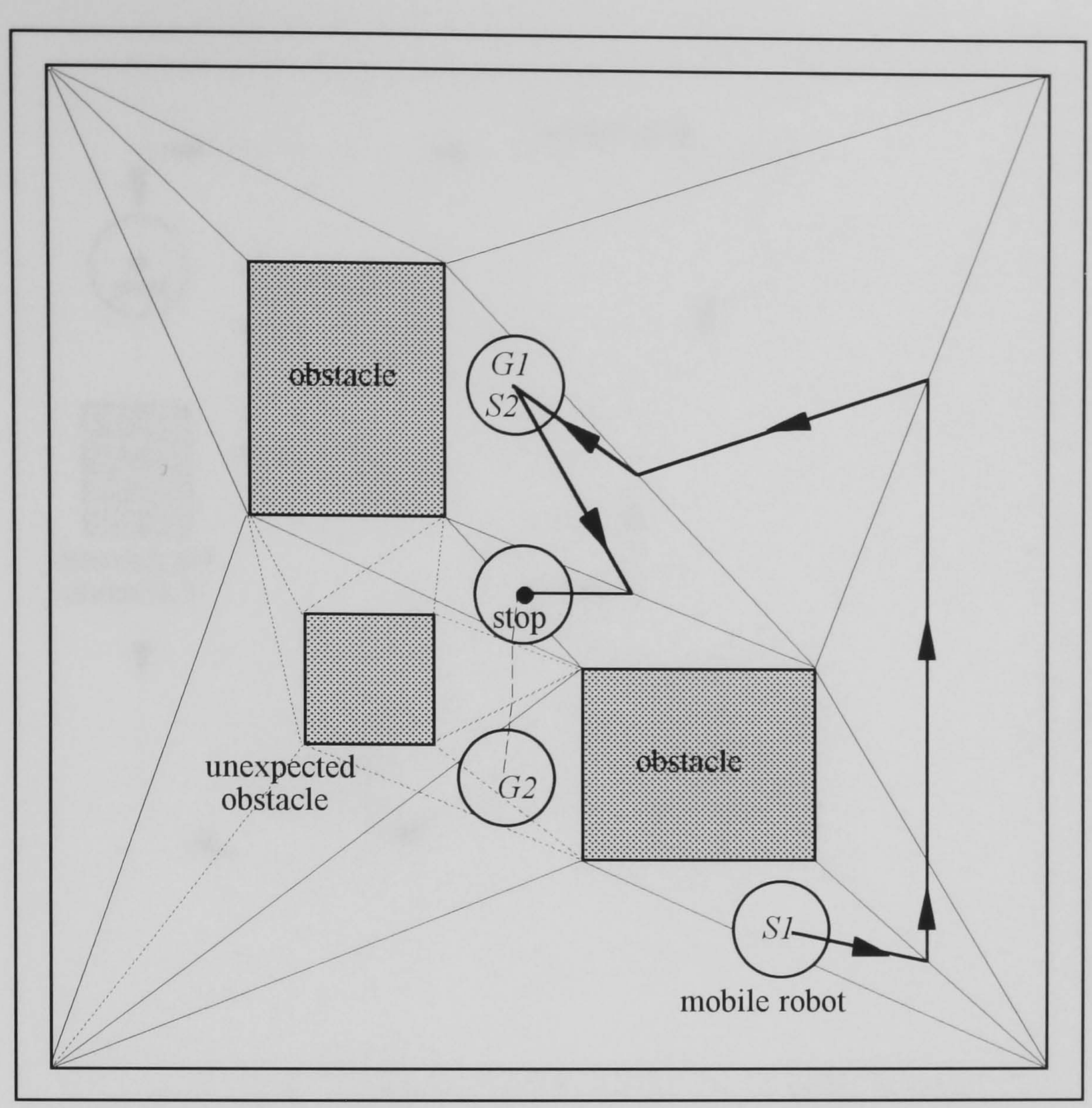

Figure 5.24. Detouring by local triangulation

Since the extent of the unexpected obstacle, except its existence, is not understood in the implementation, the mobile robot plans another navigation, Fig. 5.25, from the stop position to *G2*. This new navigation is produced, based on the same triangulation.

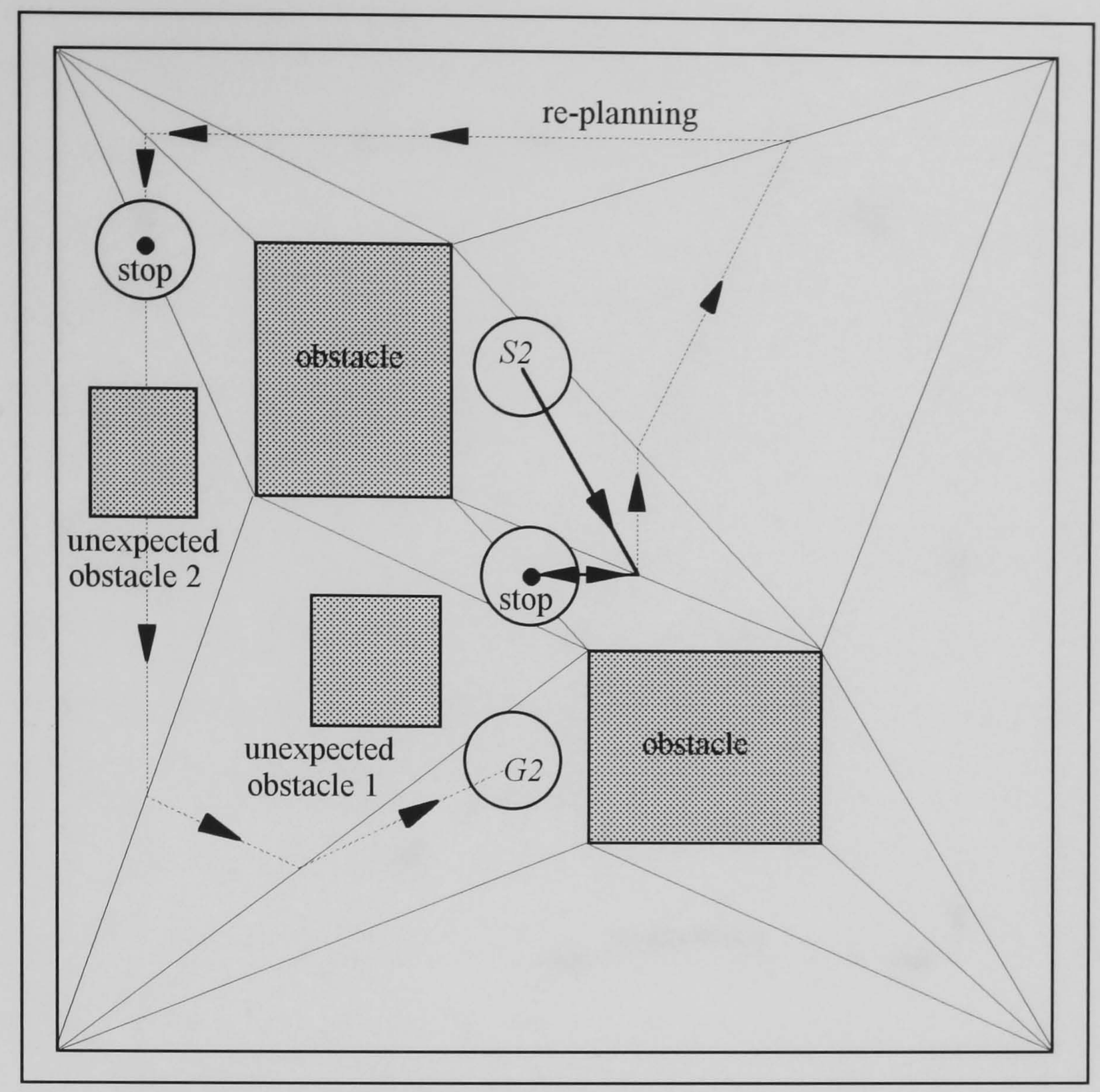

Figure 5.25. Re-planning

Should there be another unexpected obstacle obstructing the executing of the new navigation, another re-planning will be carried out. Figure 5.26 illustrates the example. At present, three attempts are considered in the navigation strategy to handle unexpected obstacles. Otherwise, a warning message will be activated, calling for help. However, additional attempts could be added at the expense of cumulative errors, and posture calibration and adjustment will be required for a successful navigation.

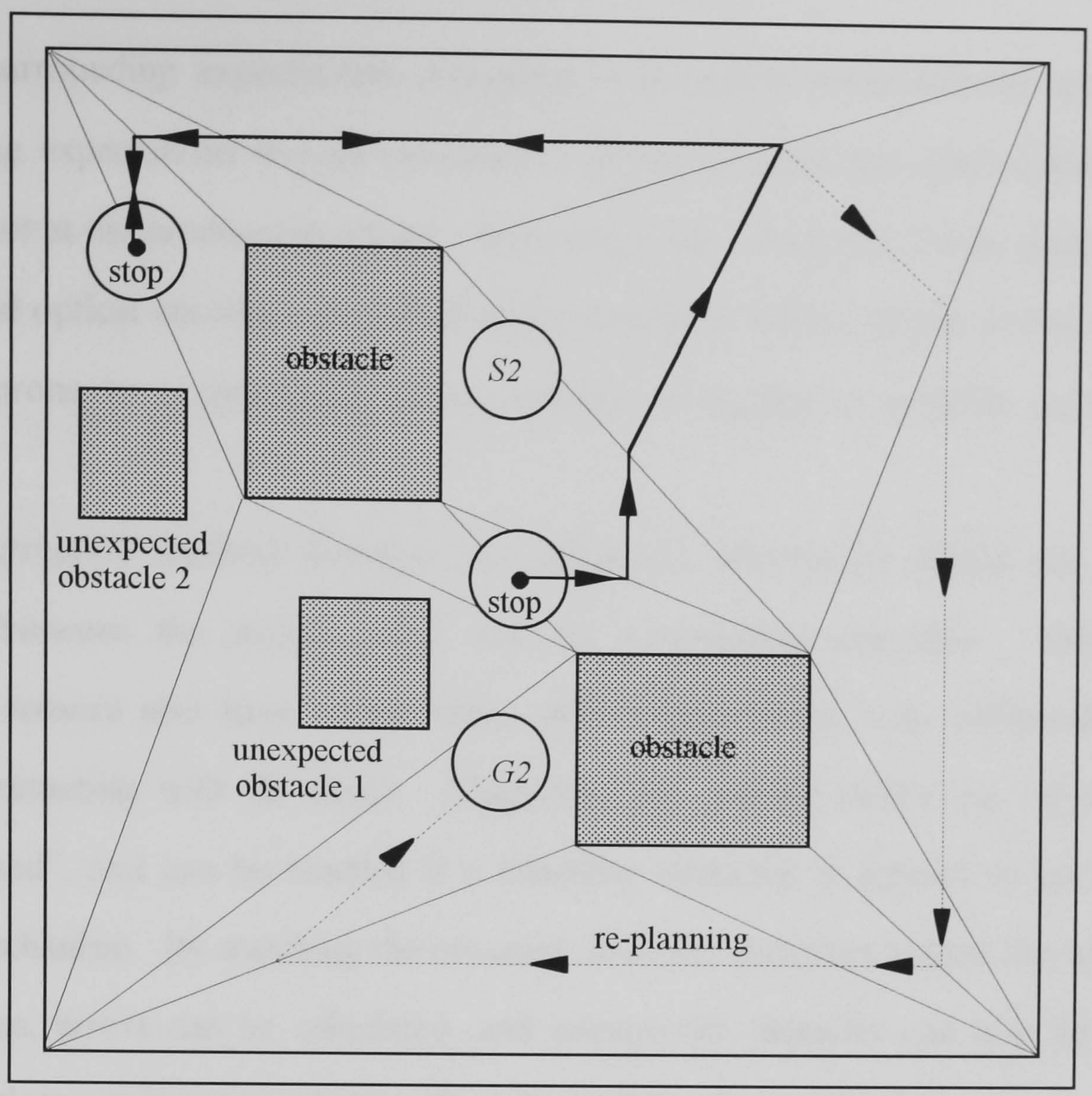

Figure 5.26. Re-planning

Thus the feasibility is shown of applying the triangulation based navigation planning approach to a mobile robot within a manufacturing environment.

5.6. SUMMARY

At the executing stage, two motors of the mobile robot are co-operatively managed to perform the planned navigation. The optical encoders and ultrasonic sensors are used to provide navigation-related information. This information is necessary for making decisions, performance corrections and further plans.

Posture estimates of the mobile robot along the navigation route are produced by the dead reckoning method and optical encoders. These posture estimates are used to

generate surrounding expectations according to the given environmental map. These surrounding expectations include information about the front and side clearance of the mobile robot at the produced postures. Since the posture estimates by the dead reckoning method and optical encoders are based on the kinematic history of the mobile robot, and are thus prone to accumulated errors, making as regular as possible corrections is necessary.

The correction method activates the ultrasonic sensors to obtain the clearance distances between the mobile robot and the surrounding obstacles. Although the ultrasonic sensors also have uncertainties, each measurement is an independent event, directly interacting with an object. Therefore, the sensory errors are "absolute" but "accumulated", and can be handled if a reliability tolerance is defined to the ultrasonic sensing mechanism. By matching the obtained clearance distances against the surrounding expectations, errors can be calculated, and unexpected obstacles can also be detected. Compensations are then provided to adjust the mobile robot navigation.

The feasibility of the triangulation based navigation strategy has been verified by three steps of practical implementation, using the computational graphical simulation, manipulative robot, and mobile robot. Since the developed strategy does not use artificial beacons or physical guidance, the navigational tasks the mobile robot can perform are flexible. In other words, costs for re-initiating delivery tasks, given a new manufacturing environment or production plan, are low.

CHAPTER SIX

DISCUSSIONS, CONCLUSIONS AND FUTURE DEVELOPMENT

Principal tasks of the flexible material transportation include delivering documents or parts within a constructed (known) work place such as a warehouse, factory or office. This constructed work place normally consists of stationary boundary walls (building structure), and temporarily fixed but removable objects such as space partitions, working benches and tooling machines. Once a new production plan is given, a new interior layout of the work place, or a new manufacturing procedure, will be designed correspondingly. The temporarily fixed but removable objects may consequently be re-located. The delivery system has to be re-initiated as soon as possible for the new production plan. In addition, the less system adjustment and associated modification costs the better.

At present, goods conveyors are widely used in industries for material transportation, and floor-buried cable-guided vehicles are used in many instances. These systems have advantages for mass production. However, due to their inherent physical constraints, it is difficult to modify the delivery routes and re-initiate them for flexible production. They are too rigid and restrictive to satisfy the required flexibility. Constructing a flexible

material transport system which contains functions for mobility, manipulation, perception and automated control, and can deliver materials freely according to a given production plan, is a desired solution to the problem. A mobile robot project, aiming at developing a navigation strategy for a flexible material transportation system in a manufacturing environment, is the accomplished objective of this work.

6.1. DISCUSSIONS

A flexible material transport system is constructed, consisting of off-the-shelf systems, and software for communications and control. A navigation strategy is developed for the mobility agent of the flexible material transport system, including triangulation based planning and executing approaches. This navigation strategy produces collision-free delivery in an efficient and flexible manner, and can handle unexpected obstacles and emergencies.

6.1.1. Project Features

The ultimate goal of studying robotics is to produce universal human like behaviours. As a contribution towards this, the mobile robot project is focused on the flexible material transportation for factory automation. The purpose is to enable a mobile robot to navigate itself freely, safely and efficiently from one location to another. Features of the mobile robot project are:

(a) The mobile robot navigates in a manufacturing, indoor and constructed environment. This feature makes it easier to model the working place, to attain surrounding information and communications, and to plan navigation. The types of problems that may be encountered are also constrained. However, the mobile robot may not continue its current

navigation due to unexpected obstacles. In these cases, the mobile robot reports failure, or determines its location and then plans another navigation to achieve the destination.

(b) The mobile robot functions with minimum impact on the manufacturing environment. That is, the mobile robot can navigate between the current inhabitants in the environment, and avoid obstructions, without causing danger to itself, other machines, and buildings. This also implies that the mobile robot is self-contained, and the manufacturing environment is not equipped with external guidance mechanisms, such as embedded wires (or painted stripes) in the floor or sensory beacons on the walls that can be followed. All perceiving and guiding functions are performed by the on-board equipment.

(c) Efforts have been devoted to developing a system which can autonomously plan, perceive, and co-ordinate actions. The mobile robot project has two functional parts, hardware (the flexible material transport system) and software (the triangulation based navigation strategy), together with four development principles:

(c.1) modularity: integrating general-purpose off-the-shelf systems and devices;

(c.2) expandability: capable of adding components for future expansion;

(c.3) flexibility: rapidly adjustable to different applications;

(c.4) feasibility: applicable to practical scenes.

6.1.2. The Flexible Material Transport System

A working flexible material transport system, which consists of a mobile robot, an articulated robot, ultrasonic sensors, a vision camera, and a personal computer, has been constructed as a research test bed. Its hardware structure is principally divided into an operational unit and a processing unit. To function, the system also needs on-board power and input information.

The operational unit acts on the environment, and reacting to the signals provided by the processing unit. The processing unit performs data-processing functions that supply output signals after manipulating the input information. The input information may fall into three categories;

(1) instructions and objectives defining the task to be carried out, given by users through the developed graphical user interface tool;

(2) measurements concerning the states of the operational unit, provided by the equipped internal encoders;

(3) observations on the environment from the ultrasonic sensors and camera vision system.

The input information is coherently managed by the processing unit to generate instructing signals for the operational unit. Figures 6.1(a) and (b) illustrate the hardware structure of the flexible material transport system, and Plates 6.1 (a) and (b) show two different views of the system.

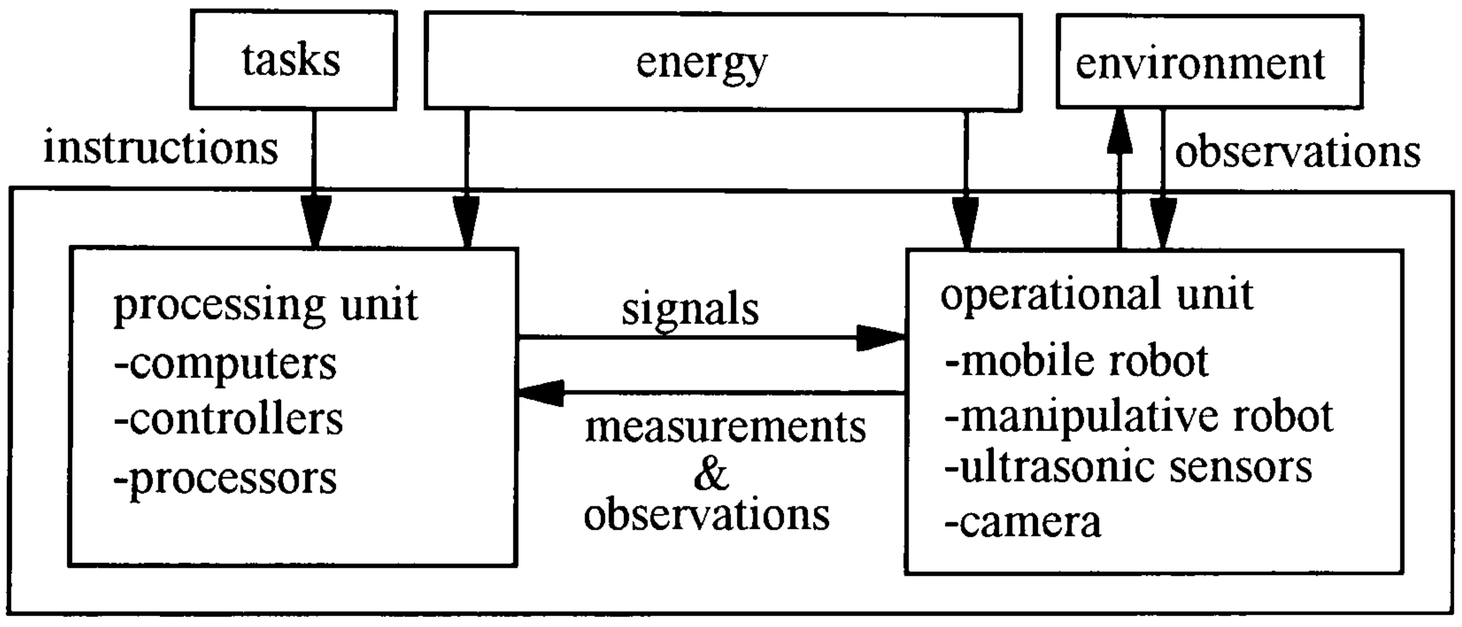

(a)

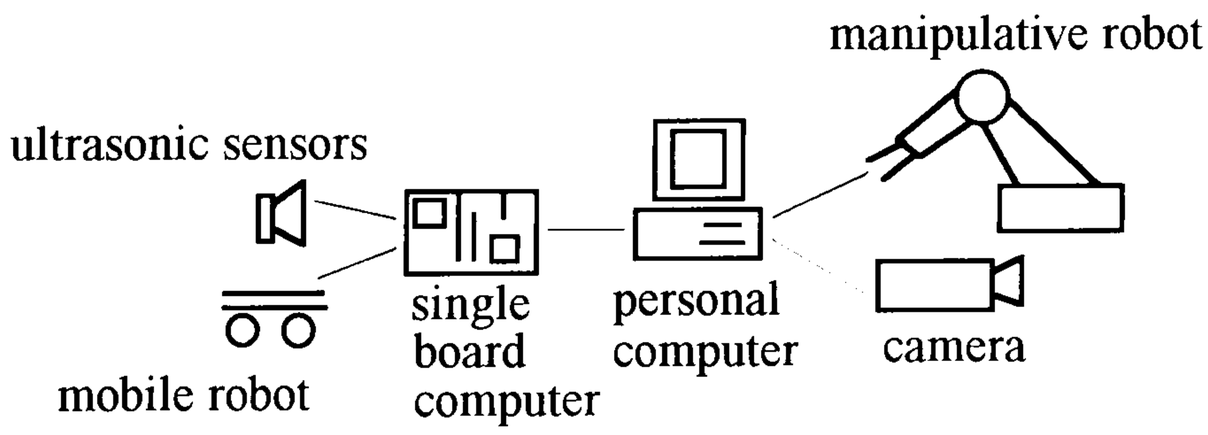

(b)

Figure 6.1. Flexible Material Transport System

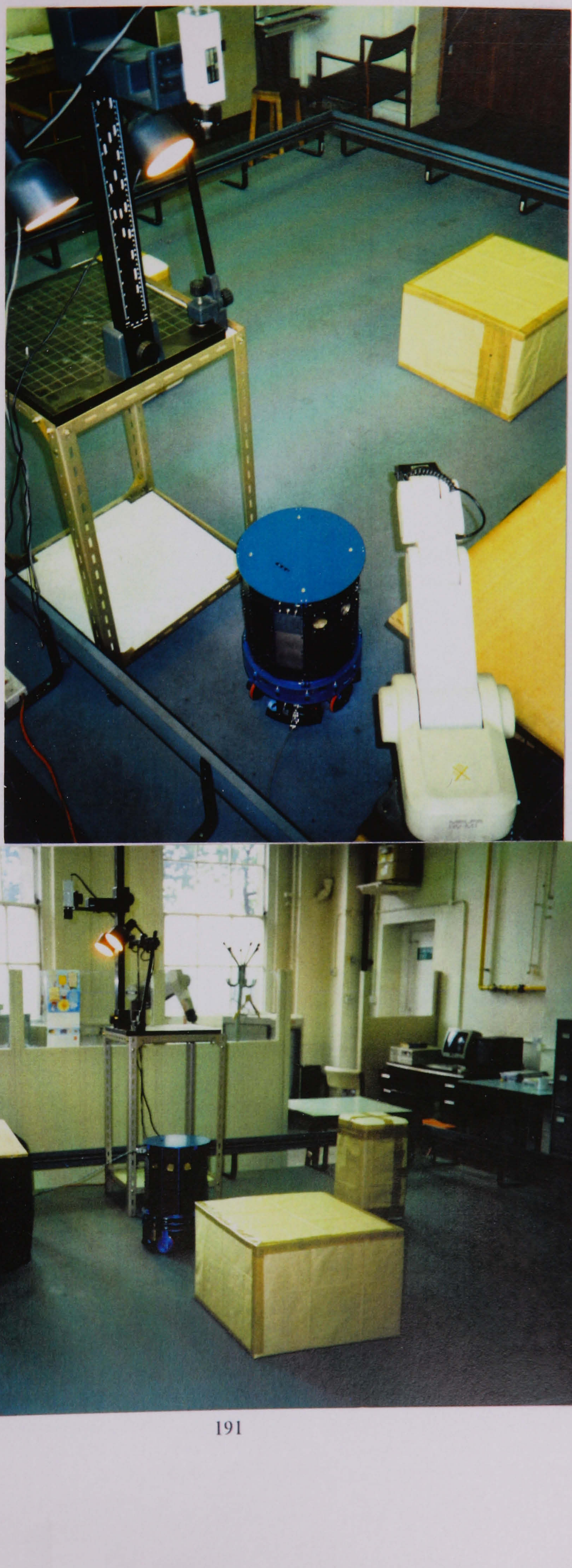

Plates 6.1 (a) & (b)
The Flexible Material Transport System

6.1.3. The Triangulation Based Navigation Strategy

A new navigation strategy for mobile robots in a manufacturing environment has been developed. This strategy works at two stages, planning and executing, and is based on triangulation approaches. The planning stage is to generate a collision-free navigational route. System behaviours are then co-ordinated, at the executing stage, to perform the planned navigational route.

The planning stage of the navigation strategy is sequentially divided into a global journey planning step and a local route planning step. The global journey planning step carries out operations for spatial reasoning and graph mapping. A triangulated model of the free space is employed to construct a triangulation graph. A node of the triangulation graph represents a triangular partition of the free space, and an edge represents the topological connectivity of two triangular partitions (nodes). Searching the triangulation graph will produce a solution graph path. This solution graph path is actually a space channel bounded by physical objects, which represents a global journey (trend) for a mobile robot towards the given destination. A variety of navigational routes for the mobile robot to follow are included in the solution space channel. The final navigational route is then locally determined according to physical criteria, which contain cost requirement, robot kinematic constraints, and unexpected obstruction.

The local route planning step only works on the space channel produced by the global journey planning step. Since the space channel is a sub-set of the overall free space of the mobile robot, searching efforts irrelevant to the final navigational route can be saved. In addition, a navigational route planned by the triangulation based strategy is always within the free space of the mobile robot, and, thus, collision free.

The executing stage of the navigation strategy is to manage operations of motion co-ordinating and sensing. Since the final navigational route to be followed is designed to keep clearance distances to obstacles and to be parallel to the environment boundary, ultrasonic sensors can be integrated to generate reliable observations for monitoring the

navigation. Executing programs for performing the planned navigational route in the computational graphical simulation environment, or using the manipulative robot have also been developed.

The advantages of the navigation strategy are summarised as follows:

(a) Efficiency. The planning efficiency of a navigation strategy depends on the chosen environment representation and route searching approaches. For navigation strategies using graphs, the efficiency is described by the computational complexity for constructing and searching the graphs. Given a manufacturing environment with n vertices in total, the developed navigation strategy takes $O(n^2)$ running time to produce a triangulation graph with $O(n)$ nodes and $O(n)$ edges. The visibility graph has $O(n)$ nodes and $O(n^2)$ edges, and requires $O(n^2)$ computation cost to form [73][114][119][123]. The Voronoi diagram is another useful environmental representation, taking $O(n^2)$ running time to construct, and has a network of linear and parabolic line segments of $O(n\lg n)$ data size [119][124]. The approximate cell decomposition produces connectivity graphs, with cell-resolution dependent computation costs, but leads to loss of completeness [75][119][126]. Comparing with these existing approaches, the developed navigation strategy provides a solution of similar efficiency.

(b) Simplicity. When planning a navigation, the larger and more complicated the manufacturing environment is, the more computational effort is required. The global journey planning stage works on the currently available environmental information to produce a spatial channel (a journey), which merely indicates a preferable movement trend of the mobile robot. Since the local route planning stage only concentrates on the produced spatial channel, a much smaller space of interest rather than the whole manufacturing environment is manipulated. A solution navigation is then locally planned within the journey, subject to local criteria, and on-line knowledge update about the

neighbouring environment. As a result, calculations that are irrelevant to the solution navigation are saved, in addition to the structural simplicity (small data size) of the triangulation graph.

(c) Clearance. Since the produced journey, or solution channel, is a subset of the free space, it accommodates clearance distances to the environmental boundary. Due to this clearance, the final navigation to be performed can be flexibly planned locally in the journey according to the navigation mode, sensors equipped, and cost requirement. Once a navigation is planned, it is adjustable to avoid unexpected obstacles through the clearance space. The mobile robot performance can be monitored through using on-board ultrasonic sensors to maintain the clearance space. Impact on the manufacturing environment, caused by the executing uncertainties, can be decreased. In addition, continuous navigations (curve routes) can be planned in the journey.

6.1.4. Experiments

The feasibility of the triangulation based navigation strategy has been demonstrated and verified by three steps of practical implementation, using a computational graphical simulation tool, a manipulative robot, and a mobile robot:

(a) A graphical simulation environment has been developed on a personal computer. It is a useful and convenient tool for a user to preview and examine the navigational performance of the mobile robot in a possible interior layout, when designing or renewing the manufacturing environment.

(b) A practical scene is imitated by incorporating a manipulative robot with a vision camera system to draw the planned paths on a board, clustered with toy blocks. This work enables a user to investigate the candidate environmental layout designed at the **(a)**

step, and to do fine adjustments before the candidate design is finally applied to the manufacturing environment.

(c) Implementation of the navigation strategy is completed by using a mobile robot with ultrasonic sensors on board. As the developed triangulation based navigation strategy always provides clearance space for uncertainty and error correction, collision-free performance is produced by the mobile robot.

6.2. CONCLUSIONS

Presented in this thesis is the design and construction of a mobile robot system, which is able to perform flexible material transportation tasks in a manufacturing environment. An attempt to actually implement a working system with imprecise control, capable of functioning in an environment with uncertainties, is also represented. Although the difficulties of autonomous system operation are still not completely understood, the research efforts have given some insight into what the problems really are.

This research project has produced a simple and flexible navigation strategy for mobile robots working within a manufacturing environment, and has investigated the implementation issues. Three major parts of the project are concluded as following:

(a) System. A flexible material transport system with a centralised control structure has been constructed for manufacturing applications. To be capable of autonomous operations, this system requires functions for manipulation, mobility, perception, and intelligence. Therefore, off-the-shelf systems, including a manipulative robot, a mobile robot, ultrasonic sensors, a compass, a camera, a single board computer, and a personal computer, are put together, as component systems, for the purpose. Since signals have to be exchanged frequently and smoothly among these component systems, and different

systems have different interface configurations, cables and control programs for communications are produced. To achieve the centralised control mode, the personal computer is used to manage the other component systems. Since all intelligent processing tasks are performed by the personal computer, software which can drive and supervise the component systems from the personal computer is also composed. Hence the flexible material transport system is ready to be operated by the developed navigation strategy.

(b) Navigation strategy. A common feature for mobile robots and navigation problems is that uncertainties and errors exist, which accumulate along with the working time. Therefore, clearance spaces for navigation to tolerate control, modelling, and operational uncertainties, and sensors and sensing methods to detect errors and unexpected obstacles are two required features for a working strategy to accomplish a safe navigation. A new triangulation based navigation strategy has been developed for mobile robots to perform navigational tasks for flexible material transportation. Given a mobile robot and a manufacturing environment, this strategy can plan a feasible and collision-free navigation, and direct the mobile robot to safely execute the navigation. The strategy also has functions anticipating various contingencies, and can survive with limited sensing ability. At the planning stage of the strategy, triangulation approaches are used to model the free space of the environment as a graph. Since triangles are easy to handle, a graph model of this feature has a simple structure, and is easy to manipulate. The solution navigation planned by searching on the graph is safe and collision free, because clearance spaces for uncertainty tolerance are considered. Handlers for unexpected obstacles are also developed to use the clearance spaces. In addition, searching efficiency is provided due to the simplicity of the graph structure. At the executing stage of the strategy, the two motors of the mobile mechanism are co-operatively managed to perform the planned navigation. The optical encoders and ultrasonic sensors are used to provide on-line navigation-related information, which is necessary for decision making, performance

correcting, and further planning. Posture estimates of the mobile robot, and thus the surrounding expectations, along the navigation are produced. By matching the surrounding expectations against the clearance distances between the mobile robot and the surrounding obstacles, obtained by the ultrasonic sensors, errors as well as unexpected obstacles can be detected. Compensations are then provided to adjust the mobile robot navigation. Since the developed strategy does not use artificial beacons or external equipment for guidance, the navigational tasks the mobile robot can perform are flexible.

(c) Implementation. Practical implementations and demonstrations have been conducted to verify the feasibility of the developed navigation strategy, using a computational graphical simulation, a manipulative robot with camera, and a mobile robot with six ultrasonic sensors as tools. In the computational simulation, users can input and renew information of a manufacturing environment, and communicate with the flexible material transport system, through the developed graphical user interface tool. The planning operations of the strategy as well as the solution navigation can be illustrated on a computer screen. The implementation using a manipulative robot with camera is to set up a quick-responding and small-scaled simulation system. Information about the working environment, produced by a camera, is given to the navigation strategy. A solution path is planned, which is then plotted on a board by a manipulative robot. This implementation shows that the developed navigation strategy works well with an automatic information provider, the camera. In the implementation using a mobile robot and six ultrasonic sensors, uncertainties have been recognised as an important factor to the navigation safety. Optimality is only meaningful when collisions and damages can be avoided. The implementation shows that the solution navigation planned by the developed strategy is error tolerant due to the clearance feature. In addition, the navigation strategy, based on the ultrasonic sensors working on the clearance feature, can effectively reduce the errors.

The thesis describes contributions to an on-going mobile robot project. The system is not yet a perfectly integrated autonomous system, and does not perform all the tasks that its hardware is designed and integrated to do. However, significant progress has been made given the time and monetary constraints. Further developments are issued.

6.3. FUTURE DEVELOPMENT

The developed mobile robot system, though is able to perform autonomous navigation, is confined to the flexible material transportation in a manufacturing environment. Therefore, future research efforts will be focused on improving the system towards stand-alone, and extending the system applicability to other applications.

6.3.1. System Improvement

One of the ultimate goals of robotics is to create an autonomous system that can perform tasks independently for hours without outside assistance. Such an unattended autonomous system will accept and execute high-level descriptions of tasks without further human intervention. In general, an autonomous system needs four principle functions; mobility, manipulation, perception, and intelligence. Since the constructed flexible material transport system is a working system, already consisting of component systems for the four functions, the hardware improvement will be carried out in two ways:

(a) System integration. Currently the manipulative robot and the vision camera system of the flexible material transport system are installed aside a docking site. A mobile robot system having an onboard manipulator to acquire and retrieve objects will be an economic solution to loading and unloading materials instead of setting systems for every docking sites. In addition, equipping the vision camera system on the mobile robot to make it

capable of visual tracking and visual detection will be helpful for controlling system behaviours. Therefore, the first step of improvement will be to integrate the present component systems into a compact form. Then, the module functions for manipulation, perception, and intelligence will be available on the mobility platform to achieve mobile robot operations autonomously.

(b) Advanced Perception. After the system integration, the mobile robot system will have optical encoders, ultrasonic sensors, and a vision camera on board for assessing tasks, environment and related interface interactions. Different types of sensory information will have to be handled.

(b.1) The raw data obtained by the three different types of sensors have to be processed by the corresponding pattern recognition functions before use. A considerable amount of work will have to be done, such as in [153], to make these sensing functions more reliable and efficient.

(b.2) Equipping the mobile robot system with more sensors implies that more information about the environment can be obtained, and sensory data fusion is important. Sensory data fusion approaches filtering conflict or superfluous information will be investigated.

(b.3) Independently building maps of the real world for navigation planning may not be necessary at present, since the environmental maps are provided by users. However, a representation of the environment autonomously determinable in a period of time by the mobile robot system, capable of being integrated into the navigation, will increase the safety, as suggested in [154]. Much work will have to be done to develop techniques to construct environmental maps from the raw sensory data.

(b.4) A low-cost and reliable self-localisation strategy is the key to many unsolved problems in mobile robotics. Once a map building function is available, investigations into a feasible and robust self-localisation method will be carried out.

6.3.2. Further Applications

A flexible material transport system and a working navigation strategy for its mobile robot have been developed to handle material delivery in a manufacturing environment. Further implementations will be to employ the developed system to other applications.

(a) Continuous navigation. It seems to be more natural for a mobile robot system to perform continuous navigation than discrete navigation. This research subject is attracting attentions in the mobile robotics community. When directing a mobile robot system to perform continuous navigation, three physical factors, the driving capability, the steering capability and the centre of gravity of the mobile robot system, will have to be intensively considered. These considerations will be vital to maintain navigation stability. Since the developed navigation strategy preserves clearance spaces to the environmental boundary, continuous navigation can be planned using the clearance advantage.

(b) Moving obstacles. In the basic application, all obstacles are assumed to be fixed. Also, there is only one mobile robot, made of a rigid object, navigating in the manufacturing environment. However, the navigation problem can easily be made complicate in dynamic environments. One extension of the problem consists of including moving obstacles in the environment. Another one allows multiple mobile robots to operate within the same environment; each being a potential obstacle to others. Since unexpected obstacle handlers have been proposed, efforts will focus on extending the unexpected obstacle handlers to these problems.

LIST OF PUBLICATIONS

Parts of the research project have been presented and published in the following conferences and associated proceedings. The present work has benefited by helpful feedback and comments from other researchers in this field.

(1) The International Conference on Automation, Robotics, and Computer Vision, ICARCV'92, Singapore, September 1992: Implementation of Robot Collision-Free Path Planning in a Maze Using the Triangulation Algorithm;

(2) The IEEE International Workshop on Emerging Technologies and Factory Automation, EFTA'92, Australia, August 1992: An Algorithm for Robot Path Planning with Obstacle Avoidance Using Triangulated Model;

(3) The IEEE/RSJ International Conference on Intelligent Robotics and Systems - Intelligent Robots for Flexibility, IROS'93, Japan, July 1993 Japan: Space Representation and Map Building - a Triangulation Model to Path Planning with Obstacle Avoidance;

(4) The International Conference on Advanced Mechatronics - Great Advancement of Intelligent Machines, ICAM'93, Japan, August 1993: Implementation of the Triangulation Algorithm to Robot Path Planning Problem;

(5) The ASME European Joint Conference on Engineering Systems Design and Analysis, ESDA'94, United Kingdom, July 1994: Extended Triangulation Algorithm for Robot Path Planning with Obstacle Avoidance.

APPENDIX A

MOVEMASTER-EX MANIPULATIVE ROBOT

The MOVEMASTER-EX manipulative robot, manufactured by Mitsubishi company, is a vertical articulated link structure comprising five revolute joints. Physically, it has 19kgf of weight, up to 1.2kgf of lift capacity, and 1000mm/sec of maximum path velocity measuring at the wrist tool surface [39]. Nomenclature of this manipulative robot is illustrated in Fig. A.1.

A.1. Mechanism

The manipulative robot has five DC electrical servo motors which are powered from an ordinary 240-voltage electrical socket through an internal adapter in the control unit. Motors for J1, J2 and J3 produce 30W of output, motors for J4 and J5 yield 11W, and there are relay cards handling in/out signals from the control unit to motor circuitry [39]. The upper arm and fore arm are rigid with 250mm and 160mm of length respectively. All five joint movements are rotary. Joints J1 and J5 are directly driven by motors, while timing belts are used to transmit mechanical power to joints J2, J3 and J4, from the corresponding motors. Limit switches and brakes are equipped to define the work envelop of the manipulative robot. The end effector is a DC servo motor driven gripper

with two rigid fingers. Its opening/closing stroke range is from 0mm to 60mm. This 600gf weighted gripper has a grip capability of up to 3.5kgf [39]. Table A.1 is a brief summary of the robot specifications.

Joint	Limit Switch	Brake	Timing Belt	Specifications (from Origin reference configuration)
J1	Yes	No	Direct Drive	±150° (max. 120°/sec)
J2	Yes	Yes	Yes	+100°, -30° (max. 72°/sec)
J3	Yes	Yes	Yes	-110° (max. 109°/sec)
J4	Yes	No	Yes	±90° (max. 100°/sec)
J5	Yes	No	Direct Drive	±180° (max. 163°/sec)

Table A.1 Specifications of MOVEMASTER-EX

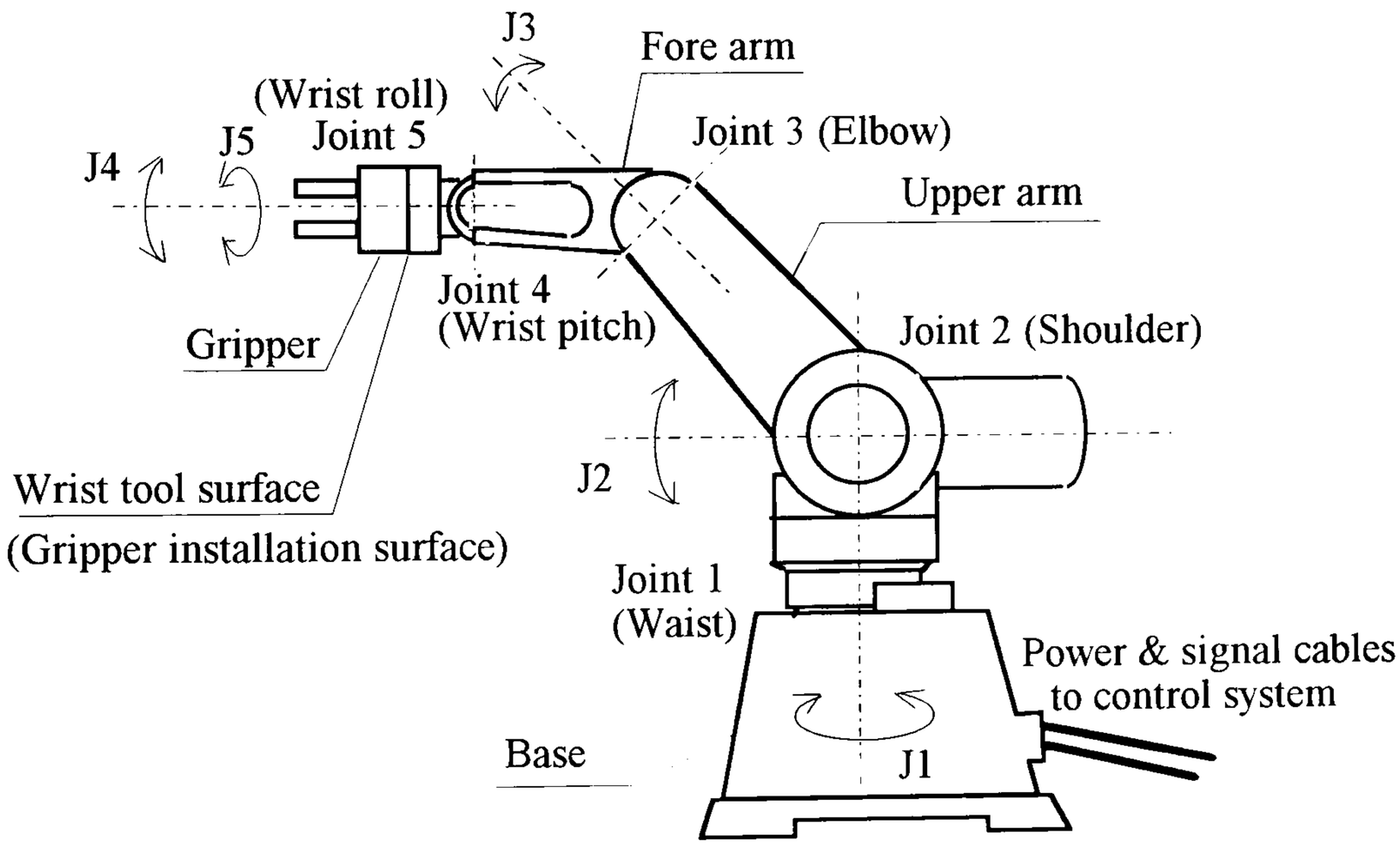

Figure A.1.(a) Robot articulation [39]

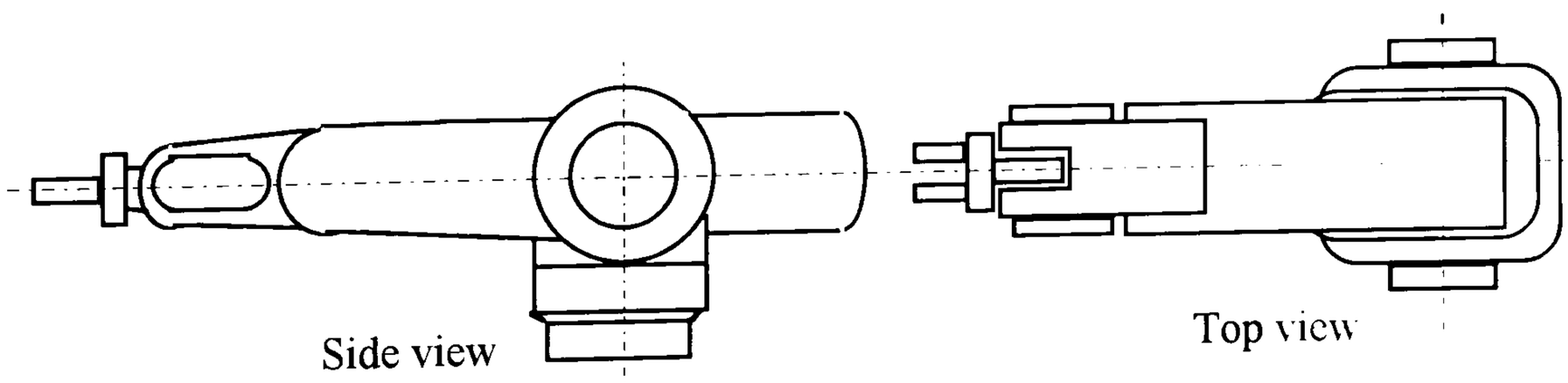

Figure A.1.(b) Reference configuration (Origin) [39]

A.2. Control Unit

The MOVEMASTER-EX manipulative robot has a dedicated control computer, the Drive Unit, functioning as power adapter, motor amplifier, motion controller and monitor, and signal input/output interface, to support the robot's mechanism.

A motor pulse encoder system, instead of hardware (optical) encoders, is equipped for position detection and motion control of the robot mechanism. In addition to ROM memory accommodating the operational system, battery-backed static RAMs are used for data storage; 629 positions and 2048 program steps can be recorded for programming [39]. Also, there is a built-in EPROM writer for EPROM recording. The input/output module of the Drive Unit supports one parallel interface (Centronics standard), one serial interface (EIA-RS232C standard), one teaching box input port and one motor signal output port for interface with peripheral systems and the robot mechanism. The emergency stop action can be initiated by pressing the emergency button on the Drive Unit, or on the teaching box.

As to the operational software, the Drive Unit uses the PTP (Point-To-Point) position control approach, with the linear interpolation on the articulated movements to manage joint motions, enabling the robot mechanism to move in either articulated or Cartesian patterns [39]. The Drive Unit can be programmed through the teaching box (MDI, Manual Data Input) or an external computer. The lead-through programming, using the teaching box, can be accomplished by playing back recorded positions and operational processes. The operational software has a set of programming languages with BASIC-like structure and syntax. Using these 63 commands, designed to control five joints and one additional axis (gripper), off-line programming can be achieved from an external computer, via the serial/parallel interface. All parameters required by the commands can be directly entered in the form of millimetre or degree [39]. Ten steps of speed, up to 1000mm/sec of path velocity at the wrist tool surface, can be set to run the robot [39].

APPENDIX B

B12 MOBILE ROBOT

The mobile robot used is a B12 mobile robot manufactured by Real World Interface Inc. It is a cylindrical, three-wheeled and self-contained platform with motors, power amplifiers, batteries, optical encoders, microprocessor-based control boards, and supporting operational software. Dimensionally, the mobile robot is 17.15cm (6.75 inches) in height and 30.48cm (12 inches) in diameter [19]. It is structurally rigid with an aluminium frame, and 11.35kgf (25 pounds) in total weight [19].

B.1. Mechanism

The mobile robot has two DC motors, each independently functioning as the translation (driving) actuator and the rotation (steering) actuator. Both motors provide 1.13Nm of torque enabling the mobile robot to carry loads of up to 20kgf [19]. Four on-board re-chargeable lead-acid batteries, providing 144 watt hours of electrical power, are also able to support additional devices, such as computers and sensors, with 12-voltage power through the 24-pin connector on the top surface of the mobile robot [19].

The mobile robot has a three-wheeled synchronous mobile mechanism. Through the specially designed transmission apparatus, the translation motor and the rotation motor can independently drive and steer the mobile robot. The three wheels remain parallel at all

times, even during the steering. The parts of the mobile robot that interact with the ground are three identical wheels whose treads are made of moulded polyurethane [19]. They are pivoted with rigid suspensions to the robot's body frame, measuring 4.15cm radii. For measuring movement, the mobile robot has two incremental optical shaft encoders mounted on the shafts of the motors. Each optical shaft encoders provides 500 counts per motor revolution [19].

The three-wheeled driving and three-wheeled steering mechanism gives the mobile robot stable traction and an omni-directional moving capability. Figure B.1 illustrates the driving mechanism.

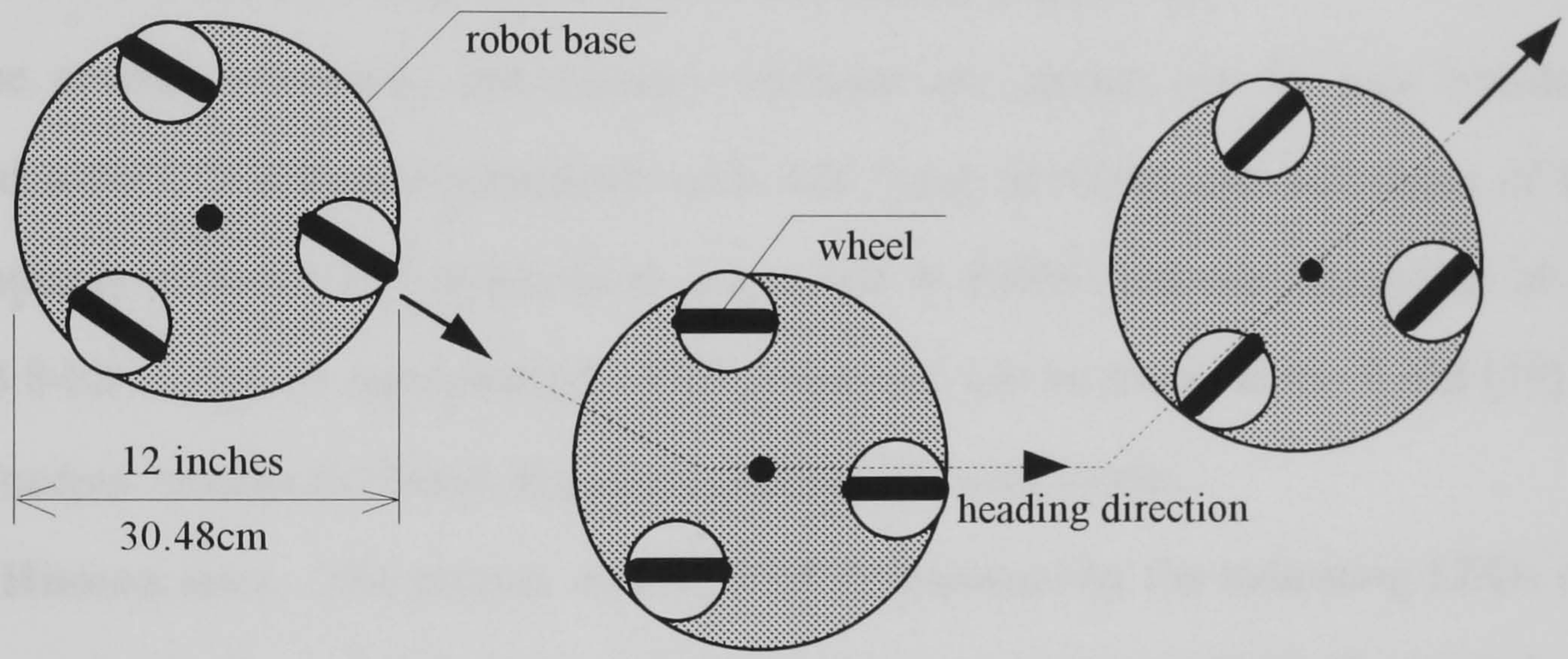

Figure B.1. Synchronous mobile mechanism offering omni-directional movement

B.2. Control Unit

The control unit of the mobile robot has six control boards including power amplifier module, encoder module, central processing module, memory module and input/output module. The control unit also monitors electrical current levels of the batteries and motors. This current-monitoring function can be used as a kind of bumper sensor. A set of motion/position control commands are provided by the manufacturer for off-line programming.

(a) Circuitry. The power amplifier module has two similar pulse-width modulator boards. Each board contains servo amplifier and current monitoring circuitry, and manages the servo-drive current to one motor. The encoder module is accomplished by two encoder drive boards. Each shaft encoder has its own drive board to manage operations, and produces feedback counting signals. Since both encoder drive boards zero their counters in every system reset, the angular positions of the motors can be cumulatively measured from the reset moment. Motor velocity and acceleration are derived by constantly checking the first and second differentiation of the angular position (position and velocity changes over a stable time base) respectively.

The central processing and memory modules are carried out by two boards built around a NEC78310 microprocessor with 32k bytes of ROM and 32k bytes of RAM. Operational software and instructions are stored in ROM, and user programs of up to 32768 8-bit words, or approximately 550 commands, can be stored in the RAM [19]. The input/output module facilitates the system interface in two modes:

(a.1) Human user. The present control level is displayed by the indicating LEDs on the front panel. In case of non-recoverable errors, error messages will be illuminated on the 'Status' LED using the international Morse codes. An exclusive input port accepting signals from a remote emergency switch has the first interruption priority. Pressing the emergency switch will disconnect both translation and rotation motors to the batteries, and also immobilise the mobile robot with brakes.

(a.2) Serial communications. The mobile robot interfaces with external systems only through its serial communications port with 4kb receive buffer, 2kb transmit buffer, and two connectors. This serial communications port is partially compatible with the EIA-RS232C standard, but has a different configuration in that it does not provide the handshaking signals for Data Carrier Detect, Data Terminal Ready, Data Set Ready, and Clear To Send. The two connectors are logically wired in parallel, and will cause data

collisions if they are used simultaneously. The 9-pin sub-miniature D connector is on the front panel, and the 24-pin double row 0.1-inch connector is on the top surface of the mobile robot.

(b) Operational software. The motion/position control commands use two alphabetic mnemonic characters, and can be classified as status and action commands. A status command either returns an internal status of the mobile robot, such as elapsed time, present motor angular position, battery condition, or assigns a velocity or acceleration value to the mobile robot. An action command causes the mobile robot to move, limp or halt. Each of the translation and the rotation servo loops can be independently operated in velocity, position, power or limp modes. Parameters responding to or required by control commands are in hexadecimal notations, and extra conversion programs are necessary to translate the particular parameters into meaningful values (metre, second, etc.) for user debugging and programming. The default value is zero if no parameter is entered after a command.

APPENDIX C

COMPUTERS

In the design of the flexible material transport system, all calculations of intelligent activities, such as supervising, decision making, planning, modelling, scheduling, module co-ordinating, monitoring, exception handling, are carried out by a host personal computer. A single board computer is equipped on the mobile robot to deal with general operations on the remote moving platform. This single board computer connects the control units of the mobile robot and the ultrasonic sensor system through a passive back plane (a system bus board).

C.1. Host Computer

The host computer, from ELONEX Inc., is based on a standard architecture designed by IBM Inc. The mother board has an Intel 80386SX-16Mhz microprocessor and 1MB of random access memory. The adapter for the visual display unit supports a VGA colour monitor. The use of the VGA monitor provides an animation environment for the developed graphical user interface tool with resolutions of 640 by 480. As to system interface and external signal transmission, the personal computer has two serial communications ports, with 9-pin sub-miniature D connectors, supporting the EIA-RS232C configurations [71][72]. It also has one parallel communications port with a 25-

pin sub-miniature D connector (IEC-625, International Electrotechnical Commission), supporting the IEEE-488 GPIB (General Purpose Interface Bus) configurations [155][156]. Operational software running on this personal computer is the MS-DOS (Microsoft Disk Operating System) and the Microsoft WINDOWS.

C.2. Single Board Computer

The applied single board computer is a Gespac MPL-4080 single board computer [66], manufactured by MPL AG Elektronikunternehmen and based on a Motorola 68HC000-8MHz microprocessor. This single board computer has 1024 bits of EEPROM allowing the storage of useful operating parameters [66]. The 512kb RAM is backed up by an on-board lithium battery [66]. For input/output extension, the single board computer supports two programmable serial ports and a G-64 bus interface. At the software level, a low-level software tool, Xbug [157], is contained in the monitor ROM for developing and debugging programs. At present, the single board computer is installed on the mobile robot for instructing ultrasonic perception and mobility performance through the G-64 bus interface.

C.3. Miscellaneous

A GESBUS-8M bus board, manufactured by GESPAC S.A. [158], is used to connect the control board of the ultrasonic sensors and the interface board of the mobile robot with the MPL-4080 single board computer. This bus board supports the G-64 bus configuration, and has eight slots accepting Euroboard expansion cards [26]. It caters for 8-bit or 16-bit processors (sixteen individual data lines are provided), and permits asynchronous as well as synchronous data transfer [26]. The eight expansion slots apply the DIN41612 form-C 96-pin connectors.

A DC to DC adapter is included to supply the bus board and other accessories with 5-volt power at 8 amps. Power to this adapter is provided by the batteries on the mobile

robot through the 24-pin connector and the mobile robot interface board. The mobile robot interface board, also supporting the G-64 configuration, is plugged into the GESBUS-8M bus board to manage power from the mobile robot and organise serial communications with other systems.

REFERENCES

[1] Robotics and Automated Manufacturing; Richard C. Dorf; Reston Publishing Company Inc. 1983
[2] Economic Indicators; The Economist 1993, 1994, 1995; The Economist Publications
[3] Fortune International 1993, 1994, 1995; TIME Inc.
[4] RIA Robotics Glossary; Robotic Industries Association
[5] Robotics and Automated Manufacturing; D. Sharon, J. Harstein, G. Yantian; World ORT Union. Pitman Publishing 1987
[6] Robotics: Introduction, Programming, and Projects; James L. Fuller; Macmillan Publishing Company 1991
[7] Fundamentals of Industrial Robots and Robotics; Rex Miller; PWS-KENT Publishing Company 1988
[8] Industrial robotics; Bernard Hodges; Butterworth-Heinemann Newnes Ltd. 1992
[9] Robotics and Automated Systems; Robert L. Hoekstra; South-Western Publishing Co. 1986
[10] Assembly with Robots; Tony Owen; Kogan Page Ltd. 1985
[11] Fundamentals of Robot Technology; D. J. Todd; Kogan Page Ltd. 1986
[12] A Supervisory System for Free Ranging Automated Guided Vehicles; Chung-Shing Wang; PhD Thesis 1991, Imperial College, University of London
[13] A Free Ranging AGV; G. Drunk; International Journal of Machine Tools and Manufacture, Volume 28, Number 3, 1988, Page 263-272
[14] Fundamentals of Robotics Engineering; Harry H. Poole; Van Nostrand Reinhold Co. Ltd. 1989
[15] Mobile Robots: Inspiration to Implementation; Joseph L. Jones, Anita M. Flynn; A. K. Peters Ltd. 1993
[16] Robotics Japan: New Technology Japan, Special Edition 1991 & Robotics Japan: Robot Technology-Past, Present and Future; Machinery and Technology Department; Japan External Trade Organisation (JETRO) 1991
[17] Robotics in Service; Joseph F. Engelberger; Kogan Page Ltd. 1989
[18] A Mobile Automaton: An Application of Artificial Intelligence Techniques; Niles J. Nilsson; Proceedings of the International Joint Conference on Artificial Intelligence, U.S.A. 1969
[19] B12 Operational Manual; Real World Interface Inc.
[20] Popular Science 1992, 1993, 1994, 1995; Times Mirror Magazines, Inc.
[21] Robot Technology-Modelling and Control, Volume 1; Phillippe Coiffet; Kogan Page Ltd. 1983
[22] Computer and Interfacing: Connection to the Real World; Martin Cripps; Edward Arnold Inc. & Hodder & Stoughton Ltd. 1989
[23] Microcomputers and Their Interfacing; R. C. Holland; Pergamon Press Ltd. 1984
[24] Computers and Microprocessors-Components and Systems; A. C. Downton; Van Nostrand Reinhold (UK) Co. Ltd. 1988
[25] Microprocessor Systems: Interfacing and Applications; Robert J. Bibbero, David M. Stern; John Wiley and Sons Inc. 1982
[26] Bus-Based Industrial Process Control; Michael Tooley; Heinemann Newnes Ltd. 1988
[27] The RS-232 Solution-How to Use Your Serial Port; Joe Campbell; SYBEX Inc. 1989
[28] Robots and Telechirs; M. W. Thring; Ellis Horwood Ltd. 1983
[29] Intelligent Robotics Control; George N. Saridis; IEEE Transactions on Automatic Control, Volume AC-28, Number 8, August 1983, Page 547-557
[30] Computing Techniques for Robots; Igor Aleksander; Kogan Page Ltd. 1985
[31] Robot Rover Visual Navigation; Hans P. Moravec; University Microfilms International Research Press 1980
[32] A New Method of Vehicle Position Measurement by Using Laser Beam Tracking; T. Tsumura, N. Fujiwara, M. Hashimoto, T. Tang; Advanced Robotics, Volume 2, Number 2, 1987, Page 121-135
[33] Directed Sonar Sensing for Mobile Robot Navigation; John J. Leonard, Hugh F. Durrant-Whyte; Kluwer Academic Publishers 1992
[34] Visual Navigation: Constructing and Utilizing Simple Maps of an Indoor Environment; Karen Beth Sarachik (Master Thesis, March 1989); AI-TR 1113, Technical Report 1113, Artificial Intelligence Laboratory, Massachusettes Institute of Technology

[35] MARVEL: A System for Recognising World Locations with Stereo Vision; David J. Braunegg (PhD Thesis, June 1990); AI-TR 1229, Technical Report 1229, Artificial Intelligence Laboratory. Massachusettes Institute of Technology
[36] Robot Builder's Bonanza: 99 Inexpensive Robotics Projects; Gordon McComb; TAB Books, McGraw-Hill Inc. 1987
[37] A Colony Architecture for an Artificial Creature; Jonathan Connell (PhD Thesis, August 1989); AI-TR 1151, Technical Report 1551, Artificial Intelligence Laboratory, Massachusettes Institute of Technology
[38] Error Detection and Recovery for Robot Motion Planning with Uncertainty; Bruce Randall Donald (PhD Thesis, June 1987); AI-TR 982, Technical Report 982, Artificial Intelligence Laboratory. Massachusettes Institute of Technology
[39] MOVEMASTER-EX Instruction Manual: Industrial Micro-robot System Model RV-M1; MITSUBISHI Co., Ltd.
[40] Making Complex Machinery Move: Automatic Programming and Motion Planning; David A. Sanders; Research Studies Press Ltd. 1993
[41] PUMA Instruction Manual; Stäubli Unimation Inc.
[42] Efficient Kinematic Transformations for the PUMA 560 Robot; S. Elgazzar; IEEE Journal of Robotics and Automation, 1985 September, Volume RA-1, Number 3, Page 142-151
[43] Coordination of Action and Perception in a Surveillance Robot; James L. Crowley; IEEE Expert, Winter, 1987, Page 32-43
[44] An Efficient Algorithm for One-Step Planar Compliant Motion Planning with Uncertainty; Amy J. Briggs; Algorithmica, Volume 8, Number 3, 1992, Page 195-208
[45] Robust Compliant Motion for Manipulators, Part I: The Fundamental Concepts of Compliant Motion; H. Kazerooni, T. B. Sheridan, P. K. Houpt; IEEE Journal of Robotics and Automation, Volume RA-2, Number 2, June 1986, Page 83-92
[46] Animal Sonar Systems; R. G. Busnel, J. F. Fish; Plenum Press 1980
[47] A Bat-like Sonar System for Obstacle Localisation; Billur Barshan, Roman Kuc; IEEE Transactions on Systems, Man, And Cybernetics, Volume 22, Number 4, July/August 1992, Page 636-646
[48] Incorporating Range Sensing in the Robot Navigation Functions; Vladimir Lumelsky, Tim Skewis; IEEE Transactions on Systems, Man, and Cybernetics, Volume 20, Number 5, September/October 1990, Page 1058-1069
[49] Sensor-Based Self-localisation for Wheeled Mobile Robot; A. Curran, K. J. Kyrikopoulos; Proceedings of 1993 IEEE Internal Conference on Robotics and Automation, U.S.A., Page 8-13
[50] Sonar-Based Real-World Mapping and Navigation; Alberto Elfes; IEEE Journal of Robotics and Automation, Volume RA-3, Number 3, June 1987, Page 249-265
[51] Obstacle Avoidance with Ultrasonic Sensors; J. Borenstein, Y. Koren; IEEE Journal of Robotics and Automation, Volume 4, Number 2, April 1988, Page 213-217
[52] A Kalman Filter Approach to Sensor-Based Robot Control; D. G. Johnson, J. J. Hill, IEEE Journal of Robotics and Automation, Volume RA-1, Number 3, September 1985, Page 159-162
[53] Laserrader and Sonar Based World Modelling and Motion Control for Fast Obstacle Avoidance of the Autonomous Mobile Robot *MOBOT-IV*; Markus Buchberger, Klaus-Werner Jörg, Ewald von Puttkamer; Proceedings of 1993 IEEE International Conference on Robotics and Automation, May 2-6, 1993, U.S.A., Page 534-540
[54] Ultrasonic Sensing for Mobile Robot to Recognise an Environment-Measuring the Normal Line of Walls; Y. Nagashima, S. Yuta; IROS'92 Proceedings of the 1992 IEEE/RSJ International Conference on Intelligent Robots and Systems, July 7-10, 1992, U.S.A., Page 805-812
[55] Ultrasonic Sensor Information Sheets; Polaroid Inc.
[56] Tri-aural Perception on a Mobile Robot; H. Peremans, J. Van Campenhout; Proceedings of 1993 IEEE International Conference on Robotics and Automation, May 2-6, 1993, U.S.A., Page 265-270
[57] Map Building for a Mobile Robot from Sensory Data; Minoru Asada; IEEE Transactions on Systems, Man, and Cybernetics, Volume 20, Number 6, November/December 1990, Page 1326-1336
[58] Mobile Robot Localisation Using Sonar; Michael Drumheller; IEEE Transactions on Pattern Analysis and Machine Intelligence, Volume PAMI-9, Number 2, March 1987, Page 325-332

[59] Sonarbased Outdoor Vehicle Navigation and Collision Avoidance; D. Langer, C. Thorpe; IROS'92 Proceedings of the 1992 IEEE/RSJ International Conference on Intelligent Robots and Systems, July 7-10, 1992, U.S.A., Page 1445-1450
[60] Toward Autonomous Driving: The CMU Navlab Part I-Perception; Charles Thorpe, Martial Hebert, Takeo Kanade, Steven Shafer; IEEE Expert, August 1991
[61] A Camera Space Control System for an Automated Forklift; R. K. Miller, D. G. Stewart, H. Brockman, S. B. Skaar; IEEE Transactions on Robotics and Automation, Volume 10, Number 5, October 1994, Page 710-716
[62] MARVEL: A System that Recognises World Locations with Stereo Vision; David J. Braunegg; IEEE Transactions on Robotics and Automation, Volume 9, Number 3, June 1993, Page 303-308
[63] Vision Camera Operational Manual; Data Translation Inc.
[64] Structured Control for Autonomous Robots; Reid G. Simmons; IEEE Transactions on Robotics and Automation, Volume 10, Number 1, February 1994, Page 34-43
[65] A Control Architecture for an Advanced Fault-Tolerant Robot System; Andreas Hormann, Wolfgang Meir, Jan Schloen; Robotics and Autonomous Systems, 7(1991), Page 211-225
[66] MPL-4080 Computer Information Sheet; MPL AG Elektronikunternehmen
[67] Running Visual Basic for Windows: a Hands-On Introduction to Programming for Windows; Ross P. Nelson; Microsoft Press 1993
[68] GW-BASIC Operating System User's Guide and Reference; Microsoft Corporation 1987
[69] Microsoft Quick BASIC: programmer's quick reference; Kris A. Jamsa; Microsoft Press 1989
[70] Absolute Beginner's Guide to Programming; Greg Perry; Sams Publishing Ltd. 1993
[71] Complete Guide to RS232 and Parallel Connections: A Step-by-step Approach to Connecting Computers, Printers, Terminals, and Modems; Martin D. Seyer; Prentice-Hall Inc. 1988
[72] RS-232 Made Easy: Connecting Computers, Printers, Terminals, and Modems; Martin D. Seyer; Prentice-Hall Ins. 1991
[73] Path Planning for Mobile Robot; Christos Alexopoulos, Paul M. Griffin; IEEE Transactions on Systems, Man, and Cybernetics, Volume 22, Number 2, March/April 1992, Page 318-322
[74] Shortest Paths for Line Segments; Christian Icking, Günter Rote, Emo Welzl, Chee Yap; Algorithmica, Volume 10, Number 2/3/4, August/September/October 1993, Page 182-200
[75] Shortest Path Planning in Discretized Workspaces Using Dominance Relation; Sungtaeg Jun, Kang G. Shin; IEEE Transactions on Robotics and Automation, Volume 7, Number 3, June 1991, Page 342-350
[76] Continuous Steering-Function Control of Robot Carts; Winston L. Nelson; IEEE Transactions on Industrial Electronics, Volume 36, Number 3, August 1989, Page 330-337
[77] Blanche-An Experiment in Guidance and Navigation of an Autonomous Robot; Ingermar J. Cox; IEEE Transactions on Robotics and Automation, Volume 7, Number 2, April 1991, Page 193-204
[78] A New Family of Omnidirectional and Holonomic Wheeled Platform for Mobile Robot; Franois G. Pin, Stephen M. Killough; IEEE Transactions on Robotics and Automation, Volume 10, Number 4, August 1994, Page 480-489
[79] A Motion Planning for Nonholonomic Mobile Robot; Jean-Paul Laumond, Paul E. Jacobs, Michel Taïx, Richard M. Murray; IEEE Transactions on Robotics and Automation, Volume 10, Number 5, October 1994, Page 577-593
[80] A Robust Layered Control System for a Mobile Robot; Rodney A. Brooks; IEEE Journal of Robotics and Automation; Volume RA-2, Number 1, March 1986, Page 14-23
[81] Robot Motion Planning: A Distributed Representation Approach; Jerome Barraquand, Jean-Claud Latombe; The International Journal of Robotics Research, Volume 10, Number 6, December 1991, Page 51-72
[82] Algorithmic: The Spirit of Computing; David Harel; Addison-Wesley Publishing Company 1987
[83] Introduction to Algorithms; Thomas H. Cormen, Charles E. Leiserson, Ronald L. Rivest; The Massachusetts Institute of Technology Press 1990
[84] Algorithms and Automatic Computing Machines; B. A. Trakhtenbrot (translated and adapted from Russian by Jerome Kristian, James D. McCawley); D. C. Heath Inc. 1963
[85] Computational Geometry-An Introduction; Franco P. Preparata, Michael Ian Shamos; Springer-Verlag New York Inc. 1985

[86] Computational Geometry-A Survey; D. T. Lee, Franco P. Preparata; IEEE Transactions on Computers, Volume C-33, Number 12, December 1984, Page 1072-1101
[87] Introduction to Graph Theory; Robin James Wilson; Longman Group Ltd. 1979
[88] Euclidean Geometry and Convexity; Bussell V. Benson; McGraw-Hill New York Inc. 1966
[89] Elementary Topology: A Combinatorial and Algebraic Approach; Donald W. Blackett; Academic Press Ltd. 1982
[90] Convex Figures and Polyhedra; L. A. Liusternik (translated from Russian by T. Jefferson Smith); Dover Publication Inc. New York 1963
[91] From Geometry to Topology; H. Graham Flegg; The English Universities Press Ltd. 1974
[92] Decomposing a polygon into its convex parts; B. Chazelle, D. Dobkin; Proceedings of the 11th Symposium on Theory of Computing (Atlanta, Ga, U.S.A., April 30-May 2); ACM New York 1979, Page 38-48
[93] Algorithms and Complexity; Herbert S. Wilf; Prentice-Hall London Ltd. 1986
[94] Computer Algorithms: Introduction to Design and Analysis; Sara Baase; Addison-Wesley Inc. 1988
[95] Decomposing A Polygon into Simpler Components; J. Mark Keil; SIAM Journal on Computing, Volume 14, Number 4, November 1985, Page 799-817
[96] Convex Decomposition of Simple Polygons; S. B. Tor, A. E. Middleditch; ACM Transactions on Graphics, Volume 3, Number 4, October 1984, Page 244-265
[97] Decomposition of Polygons into Convex Sets; Bruce Schachter; IEEE Transactions on Computers, Volume C-27, Number 11, November 1978, Page 1078-1082
[98] On Decomposing Polygons into Uniformly Monotone Parts; Robin Liu, Simeon Ntafos; Information Processing Letters, 27(1988) Page 85-89, 29 February 1988
[99] An O(logn) Time Parallel Algorithm for Triangulating a Set of Points in the Plane; Cao An Wang, Yung H. Tsin; Information Processing Letters, 25(1987) Page 55-60, 20 April 1987
[100] New Results for the Minimum Weight Triangulation Problem; L. S. Heath, S. V. Pemmaraju; Algorithmica, Volume 12, Number 6, 1994, Page 533-552
[101] Triangulation and Shape-Complexity; Bernard Chazelle, Janet Incerpi; ACM Transactions on Graphics, Volume 3, Number 2, April 1984, Page 135-152
[102] A Linear Time Algorithm for Triangulating a Point-Visible Polygon; T. C. Woo, S. Y. Shin; ACM Transactions on Graphics, Volume 4, Number 1, January 1985, Page 60-70
[103] Optimal Search in Planar Subdivisions; D. G. Kirkpatrick; SIAM Journal on Computing, Volume 12, Number 1, February 1983, Page 28-35
[104] Triangulating Simple Polygons and Equivalent Problems; Alain Fournier, Delfin Y. Montuno; ACM Transactions on Graphics, Volume 3, Number 2, April 1984, Page 153-174
[105] Triangulating a Simple Polygon; Michael R. Garey, David S, Johnson, Franco P. Preparata, Robert E. Tarjan; Information Processing Letters, Volume 7 Number 4, Page 175-179, June 1978
[106] An O(nloglogn)-Time Algorithm for Triangulating A Simple polygon; Robert E. Tarjan, Christopher J. VanWyk; SIAM Journal on Computing, Volume 17, Number 1, February 1988, Page 143-178
[107] An Efficient Algorithm for Decomposing a Polygon into Star-Shaped Polygons; D. Avis, G. T. Toussaint; Pattern Recognition, Volume 13, Number 6, 1981, Page 395-398
[108] A Simple and Fast Incremental Randomized Algorithm for Computing Trapezoidal Decompositions and for Triangulating Polygons; Raimund Seidel; Computational Geometry: Theory and Applications, 1(1991), Page 51-64
[109] Convex Decomposition of Polyhedra and Robustness; Chanderjit L. Bajaj, Tamal K. Dey; SIAM Journal on Computing, Volume 21, Number 2, April 1992, Page 339-364
[110] A Triangulation Algorithm from Arbitrary Shaped Multiple Planar Contours; A. B. Ekoule, F. C. Peyrin, C. L. Odet; ACM Transactions on Graphics, Volume 10, Number 2, April 1991, Page 182-199
[111] Shading of Regionson Vector Display Devices; D. T. Lee; ACM Computer Graphics Volume 15, Number 3, July 1981, Page 34-44
[112] Decomposition of Polygons into Simpler Components: Feature Generation for Syntactic Pattern Recognition; Hou-Yuan F. Feng, Theodosios Pavlidis; IEEE Transactions on Computers, Volume C-24, Number 6, June 1975, Page 636-650

[113] A Survey of Motion Planning and Related Geometric Algorithms; J. T. Schwartz, M. Sharir; Artificial Intelligence, 37(1988), Page 157-169
[114] An Algorithm for Planning Collision-Free Paths Among Polyhedral Obstacles; Tomas Lozano-Perez, Michael A. Wesley; Communications of the ACM, Volume 22, Number 10. October 1979, Page 560-570
[115] Spatial Planning: A Configuration Space Approach; Tomas Lozano-Perez; IEEE Transactions on Computers, Volume C-32, Number 2, February 1983, Page 108-120
[116] A Subdivision Algorithm in Configuration Space for Findpath with Rotation; Rodney A. Brooks, Tomas Lozano-Perez; IEEE Transactions on Systems, Man, and Cybernetics, Volume SMC-15. Number 2, March/April 1985, Page 224-233
[117] A Novel Representation for Planning 3-D Collision-Free Paths; Susan Bonner, Robert B. Kelley; IEEE Transactions on Systems, Man, and Cybernetics, Volume 20, Number 6, November/December 1990, Page 1337-1351
[118] Solving the Find-Path Problem by Good Representation of Free Space; Rodney A. Brooks; IEEE Transactions on Systems, Man, and Cybernetics, Volume SMC-13, Number 3, March/April 1983, Page 190-197
[119] Robot Motion Planning; Jean-Claude Latombe; Kluwer Academic Publishers 1993
[120] Graphs and Their Uses; Oystein Ore; Random House 1963
[121] Principles of Artificial Intelligence; Nils J. Nilsson; Springer-Verlag Inc. 1982
[122] Finding the Shortest Route Using Cases, Knowledge, and Dijkstra's Algorithm; Bing Liu, Siew-Hwee Choo, Shee-Ling Lok, Sing-Meng Leong, Soo-Chee Lee, Foong-Ping Poon, Hwee-Har Tan; IEEE Expert, October 1994, Page 7-11
[123] Computation of the Tangent Graph of Polygonal Obstacles by Moving-Line Processing; Yun-Hui Liu; Suguru Arimoto; IEEE Transactions on Robotics and Automation, December 1994, Volume 10, Number 6, Page 823-830
[124] Motion Planning in a Plane Using Generalised Voronoi Diagrams; Osamu Takahashi, R. J. Schilling; IEEE Transactions on Robotics and Automation, Volume 5, Number 2, April 1989, Page 143-150
[125] Motion Planning for an Autonomous Vehicle, Proceedings of the IEEE International Conference on Robotics and Automation, Page 529-533
[126] Navigation of a Car-Like Mobile Robot Using a Decomposition of the Environment in Convex Cells; Hubert A. Vasseur, François G. Pin, Jack R. Taylor; Proceedings of the 1991 IEEE International Conference on Robotics and Automation, Page 1496-1502
[127] A Potential Field Approach to Path Planning; Yong K. Hwang, Narendra Ahuja; IEEE Transactions on Robotics and Automation, Volume 8, Number 1, February 1992, Page 23-32
[128] Real-Time Robot Motion Planning Using Rasterizing Computer Graphics Hardware; Jed Lengyle, Mark Reichert, Bruce R. Donald, Donald P. Greenberg; Computer Graphics, Volume 24, Number 4, August 1990, P327-335
[129] On the "Piano Movers'" Problem I. The Case of a Two-Dimensional Rigid Polygonal Body Moving Amidst Polygonal Barriers; Jacob T. Schwartz, Micha Sharir; Communications on Pure and Applied Mathematics, VolumeXXXVI, P345-398 (1983)
[130] Simulation and Animation of Sensor-Driven Robots; ChuXin Chen, Mohan M. Trivedi, Clint R. Bidlack; IEEE Transactions on Robotics and Automation, Volume 10, Number 5, October 1994, Page 684-704
[131] Introduction to the Special Section on Perception-Based Real-World Navigation; Bir Bhanu, Olivier Faugeras, Banavar Sridhar, Charles E. Thorpe; IEEE Transactions on Robotics and Automation, Volume 10, Number 6, December 1994, Page 725-727
[132] Navigation Templates: Mediating Qualitative Guidance and Quantitative Control in Mobile Robots; Marc G. Slack; IEEE Transactions on Systems, Man, and Cybernetics, Volume 23, Number 2, March/April 1993, Page 452-466
[133] An Integrated Architecture for Robot Motion Planning and Control in the Presence of Obstacles with Unknown Trajectories; R. Spence, S. Hutchinson; IEEE Transactions on Systems, Man, and Cybernetics, Volumn 25, Number 1, January 1995, Page 100-110

[134] Computer Graphics: An Introduction to the Mathematics and Geometry; Michael E. Mortenson; Heinemann Newnes Ltd. 1989
[135] An Obstacle Avoidance Algorithm for an Autonomous Land Vehicle; T. S. Chang, K. Qiu, J. J. Nitao; International Journal of Robotics and Automation, Volume 2, Number 1, 1987, Page 21-25
[136] Exception Handling in Robotics; Ingemar J. Cox, Narain H. Gehani; Computer, March 1989, Page 43-49
[137] Optimal Polygonal Approximation of Digitized Curves; Y Zhu, L. D. Seneviratne, S. W. E. Earles; International Workshop on Image Analysis and Synthesis, Graz, Austria, June 1993
[138] An object-oriented Language for Constructing Simulations; David McArthur, Henry Sowizral; 7th International Joint Conference on Artificial Intelligence, IJCAI-81, 24-28 August 1981, University of British Columbia, Vancouver, B.C. Canada, Page 800-809
[139] A Beacon Navigation Method for Autonomous Vehicles; Clare D. McGillem, Theodore S. Rappaport; IEEE Transactions on Vehicular Technology, Volume 38, Number 3, August 1989, Page 132-139
[140] The Polaroid Ultrasonic Ranging System; C. Biber, S. Ellin, E. Sheck, J. Stempeck; 67th Audio Engineering Society Convention, New York, October 1980; Reprinted in Polaroid Ultrasonic Ranging System handbook
[141] The Sonar Ring: Obstacle Detection for a Mobile Robot; Scott A. Walter; Proceedings of the 1987 IEEE International Conference on Robotics and Automation, Page 1574-1579
[142] Ultrasonic Range Finders; Polaroid Corporation, Cambridge, MA, 1982
[143] G96 Sonar Board Guide to Operations, version 1.1, Real World Interface, Inc.
[144] Physically Based Simulation Model for Acoustic Sensor Robot Navigation; Roman Kuc, M. W. Siegel; IEEE Transactions on Pattern Analysis and Machine Intelligence, Volume PAMI-9, Number 6, November 1987, Page 766-778
[145] Differentiating Sonar Reflections from Corners and Planes by Employing an Intelligent Sensor; Billur Barshan, Roman Kuc; IEEE Transactions on Pattern Analysis and Machine Intelligence, Volume 12, Number 6, June 1990, Page 560-569
[146] A Spatial Sampling Criterion for Sonar Obstacle Detection; Roman Kuc; IEEE Transactions on Pattern Analysis and Machine Intelligence, Volume 12, Number 7, July 1990, Page 686-690
[147] Ultrasonics; B. Carlin; McGraw Hill New York Inc. 1960
[148] Sonar Localisation for Mobile Robots: A Model-Based Approach; Bill Trigge, Stephen Cameron; IEEE International Workshop on Emerging Technologies and Factory Automation-Technology for the Intelligent Factory, ETFA'92, August 11-14, 1992, Melbourne, Australia, Page 387-392
[149] Optimal Estimation of Position and Heading for Mobile Robots Using Ultrasonic Beacons and Dead-reckoning; Lindsay Kleeman; Proceedings of the 1992 IEEE International Conference on Robotics and Automation, Page 2582-2587
[150] A Physically Based Navigation Strategy for Sonar-Guided Vehicles; Roman Kuc, Victor Brian Viard; The International Journal of Robotics Research, Volume 10, Number 2, April 1991, Page 75-87
[151] ROBNAV: A Range-Based Robot Navigation and Obstacle Avoidance Algorithm; David F. Cahn, Stephen R. Phillips; IEEE Transactions on Systems, Man, and Cybernetics, September 1975, Page 544-551
[152] Feature Extraction Techniques for Recognising Solid Objects with an Ultrasonic Sensor; M. K. Brown; IEEE Journal of Robotics and Automation, 1985 December, Volume RA-1, Number 4, Page 191-205
[153] Border Detection of the Object Segmented by the Pyramid Linking Method; Z. Tomori; IEEE Transactions on Systems, Man, and Cybernetics, Volumn 25, Number 1, January 1995, Page 176-181
[154] Evidential Reasoning for Building Environment Maps; A. P. Tirumalai, B. G. Schunck, R. C. Jain; IEEE Transactions on Systems, Man, and Cybernetics, Volumn 25, Number 1, January 1995, Page 10-20
[155] PET/CBM and the IEEE 488 Bus (GPIB); Eugene Fisher, C. W. Jensen; Osborne/McGraw-Hill Inc. 1982
[156] Computer Controlled Testing and Instrumentation: An Introduction to the IEC-625: IEEE-488 Bus; Martin Colloms; Pentech Ltd. London 1983
[157] XBug Information Sheet; Real World Interface Inc.
[158] GESBUS-8M Bus Board Information Sheet; GESPAC S. A.